PREPARATION, CHARACTERIZATION OF BIMETALLIC NANOPARTICLES SOAKED ON POLY-IONIC RESINS AND THEIR CATALYTIC APPLICATIONS

A Thesis submitted to the University of North Bengal

For the Award of

Doctor of Philosophy

in

Chemistry

By

Debasish Sengupta

GUIDE

Prof. Basudeb Basu

Department of Chemistry
University of North Bengal
December-2014

DEDICATED TO MY PARENTS

DECLARATION

I declare that the thesis entitled "**PREPARATION, CHARACTERIZATION OF BIMETALLIC NANOPARTICLES SOAKED ON POLY-IONIC RESINS AND THEIR CATALYTIC APPLICATIONS**" has been prepared by me under the guidance of Dr. Basudeb Basu, Professor of Chemistry, University of North Bengal. No part of this thesis has formed the basis for the award of any degree or fellowship previously.

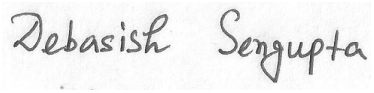

Debasish Sengupta
Department of Chemistry
University of North Bengal
Darjeeling-734013
West Bengal
India

DATE: 19.12.2014

UNIVERSITY OF NORTH BENGAL

Dr. B. BASU
Professor of Chemistry
DEPARTMENT OF CHEMISTRY
North Bengal University,
Darjeeling – 734 013
India

Phone: +91 353 2776 381
Fax: +91 353 2699 001
Cell: +91 9434428477
Email: basu_nbu@hotmail.com

CERTIFICATE

I certify that Debasish Sengupta has prepared the thesis entitled "**PREPARATION, CHARACTERIZATION OF BIMETALLIC NANOPARTICLES SOAKED ON POLY-IONIC RESINS AND THEIR CATALYTIC APPLICATIONS**", for the award of Ph.D. degree of the University of North Bengal, under my guidance. He has carried out the work at the Department of Chemistry, University of North Bengal.

Dr. Basudeb Basu
Professor of Chemistry
Department of Chemistry
University of North Bengal
Darjeeling-734013
West Bengal
India

DATE: 19.12.2014

ACKNOWLEDGEMENT

There are a number of people that I would like to acknowledge for their help, support and guidance in last four years.

First and foremost, I would like to express my deep and sincere gratitude to my supervisor Dr. Basudeb Basu, Professor, Department of Chemistry, University of North Bengal, Darjeeling, for his invaluable ideas, guidance and encouragement during the entire period of my research work.

I wish to express my warm and sincere thanks to Dr. Goutam De, Chief Scientist & Head, Nano-Structured Materials Division, CSIR-CGCRI, Kolkata, for his assistance and support during my research work.

I offer my special thanks to Jony Saha and Koushik Bhowmik from CSIR-CGCRI, Kolkata, for their valuable contribution in my scientific work.

I would like to thank my laboratory colleagues, Babli di, Kinkar da, Sujit da and Samir for their help and co-oparation. I convey my special thanks to Sumanta da for his encouragement and support.

Furthermore, I would like to express my earnest respect and thanks to the entire faculty, staff members and all research scholars of this department for their valuable suggestion and co-operation.

I would like to thank IACS, Kolkata, for providing the HR-TEM and HRMS facilities.

I would like to express my thanks to CSIR, New Delhi, for awarding me Junior and Senior Research Fellowship, University of North Bengal for providing the infrastructural facilities and DST, New Delhi.

It is hard to put my gratitude for my papents and sister. Their endless love, understanding and support, made everything seem possible.

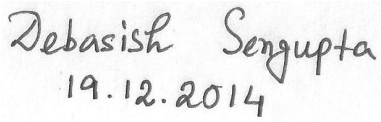

Debasish Sengupta

ABSTRACT

The fields of catalysis and nanoscience have been inextricably linked to each other for quite some time. Several inorganic or organic materials like mesoporous silica, zeolites, charcoal, graphene oxides as well as organic polymers have been used either to promote surface-mediated reactions or to immobilize metal nanoparticles for catalytic performance. Both mono- and bi-metallic nanoparticles (NPs) embedded with heterogeneous supports exhibit improved catalytic activity and find applications in several industrial processes. Development of more active, versatile and recyclable catalysts has remained the contemporary challenges in this field of chemistry and catalysis. The present thesis entitled "PREPARATION, CHARACTERIZATION OF BIMETALLIC NANOPARTICLES SOAKED ON POLY-IONIC RESINS AND THEIR CATALYTIC APPLICATIONS" has made some efforts to demonstrate new heterogeneous surface-promoted reactions as well as to develop mono- and bi-metallic nanocomposites mainly based on poly-ionic resins and graphene-based carbonaceous materials. These two different heterogeneous supports, either free or embedded with metals, have been utilized in diverse C−C, C−S and S−S bond-forming reactions. The thesis is divided into eight chapters.

Chapter I summarizes a brief review on heterogeneous catalysis, nanocomposites and their catalytic applications.

Chapter II describes the use poly-ionic resin hydroxide (Amberlyst® A-26(OH)), as an efficient heterogeneous base for the preparation of organic disulfides from alkyl and acyl methyl thiocyanates. Further extension of this protocol has been tested using two different organyl thiocyanates to prepare unsymmetrical disulfides. The present protocol shows the advantage of using the heterogeneous base Amberlyst A-26(OH) over some existing homogeneous bases (NaOH, NH_3, K_2CO_3). The recyclability was also checked.

Chapter III delineates a simple procedure for the preparation of poly-ionic amberlite resins embedded with CuO NPs (referred to as CuO@ARF). The as synthesized heterogeneous catalyst CuO@ARF was characterized and successfully applied in C−S cross–coupling reaction under ligand–free and 'on–water' conditions. Low loading of the catalyst, recyclability without leaching and chemoselectivity between aromatic halides are notable features. Further application of the chemoselectivity has been demonstrated in the synthesis of bioactive heterocyclic scaffold phenothiazine.

Chapter IV deals with the bi-metallic nanocomposite material. Cationic and macroporous amberlite resins with formate ($HCOO^-$) as the counter anion (ARF) have been used to prepare a new class of heterogeneous Pd/Cu bimetallic composite nanoparticles (NPs) (Pd/Cu–ARF). The physicochemical characteristics of Pd/Cu−ARF revealed fairly uniform distributions of composite NPs of average size~4.9 nm. The nanocomposite material (Pd/Cu ARF) exhibited high catalytic activity in the Sonogashira cross–coupling reaction between aryl iodide and terminal alkynes. Heterogeneity of the catalytic activity was evidenced from different tests (hot-filtration and catalyst-poisoning) and the recycling ability of the catalyst was examined for five consecutive runs without any significant loss of activity.

Chapter V describes further use of the Pd/Cu bimetallic composite nanoparticles (Pd/Cu ARF) in other cross–coupling reactions like Suzuki–Miyaura and Mizoroki–Heck reactions. The bi-metallic nanocomposite material was much effective as compared to monometallic Pd–ARF catalyst, as prepared in this laboratory previously. The catalyst was also recyclable for seven consecutive runs with excellent conversions.

Chapter VI depicts successful application of graphene oxide (GO) as the metal-free carbocatalysts for (i) sequential dehydration–hydrothiolation reaction from a mixture of secondary aryl alcohols and thiols in toluene and (ii) chemoselective thioacetalization of aldehyde under mild, solvent-free and aerobic conditions.

Chapter VII demonstrates the catalytic activity of Ni(0) nanoparticles supported with reduced graphene oxide (Ni/RGO) in Kumada–Corriu cross–coupling reaction. A detail study of the catalysis was performed by varying the haloarenes and Grignard reagents. Interestingly, this catalyst was found to be equally active for the oxidative addition to the sp^2 C−F bond. The recyclability of the catalyst was examined for six consecutive runs without significant loss of activity. Finally the recovered Ni/RGO was characterized by X-ray diffraction (XRD) and Raman spectroscopy and found to be unaltered.

Chapter VIII describes the use of Ni/RGO nanocomposite in C−S cross–coupling reaction. The catalyst was found to be recyclable for six consecutive runs, as examined.

PREFACE

Ion-exchange materials are insoluble substances containing loosely held ions which are able to be exchanged with other ions in solutions which come in contact with them and normally obtained as beads of 1-2 mm diameter. The most typical ion-exchange resins are based on cross-linked polystyrene. Ion-exchange resins are widely used in different separation, purification and decontamination process. This heterogeneous material has been utilized in different organic transformations too. On the other hand, graphene belongs to a new class of carbon nanomaterials, and graphene oxide (GO) possessses a range of reactive oxygen functional groups that render it to be a good candidate for use in the several organic transformations.

The present research work represents the multidisciplinary branches of material chemistry, nanocatalysis and green chemistry. This dissertation begins with a brief review on heterogeneous catalysis by metal nanocomposites followed by the application of poly-ionic resin hydroxide in disulfide bond-forming reactions. The next chapters of the thesis deal with poly-ionic resin-supported mono- and bi-metallic nanocatalysts preparation, characterization and catalytic applications in diverse cross–coupling reactions. The last three chapters describe applications of graphene oxide (GO) as the 'carbocatalyst' in different organic transformations, and finally a Ni/RGO nanocomposite has been shown to be a highly efficient heterogeneous catalyst for the Kumada–Corriu and C−S cross–coupling reactions.

TABLE OF CONTENTS

LIST OF TABLES

LIST OF SCHEMES

LIST OF FIGURES

.

LIST OF APPENDICES

APPENDIX A:

List of Publications

1. "An efficient metal-free synthesis of organic disulfides from thiocyanates using poly-ionic resin hydroxide in aqueous medium" **Debasish Sengupta** and Basudeb Basu, ***Tetrahedron Lett***., **2013**, *18*, 2277–2281.
2. "An efficient heterogeneous catalyst (CuO@ARF) for on–water C−S coupling reaction: an application to the synthesis of phenothiazine structural scaffold" **Debasish Sengupta** and Basudeb Basu, ***Organic and Medicinal Chemistry Letters***, **Accepted**.
3. "Pd/Cu bimetallic nanoparticles embedded in macroporous ion-exchange resins: an excellent heterogeneous catalyst for the Sonogashira reaction" **Debasish Sengupta**, Jony Saha, Goutam De and Basudeb Basu, ***J. Mater. Chem. A***, **2014**, *2*, 3986–3992.
4. "Graphene oxide as a carbocatalyst: the first example of a one-pot sequential dehydration–hydrothiolation of secondary aryl alcohols" Basudeb Basu, Samir Kundu and **Debasish Sengupta**, ***RSC Adv***., **2013**, *3*, 22130–22134.
5. "Graphene Oxide (GO)–catalyzed chemoselective thioacetalization of aldehydes under solvent-free conditions" Babli Roy, **Debasish Sengupta** and Basudeb Basu, ***Tetrahedron Lett.***, **2014**, 55, 6596–6600.
6. "Reduced graphene oxide supported Ni nanoparticles: a high performance reusable heterogeneous catalyst for Kumada–Corriu cross-coupling reactions" Koushik Bhowmik, **Debasish Sengupta**, Basudeb Basu and Goutam De, ***RSC Adv***., **2014**, *4*, 35442–35448.
7. "In Quest of ''Stereoselective Switch'' for On-Water Hydrothiolation of Terminal Alkynes Using Different Additives and Green Synthesis of Vicinal Dithioethers" Basudeb Basu, Kinkar Biswas, Samir Kundu and **Debasish Sengupta**, ***Org. Chem. Int***., doi:10.1155/2014/358932.

APPENDIX B:

- **Oral Presentation** in the One-day Seminar in Chemistry organized by the **Chemical Research Society of India** NBU Local Chapter in collaboration with Department of Chemistry, University of North Bengal, held at of University of North Bengal on September 12, 2014.

Poster Presention

- Pd/Cu bimetallic nanoparticles soaked on poly-ionic resins: an excellent heterogeneous catalyst for Suzuki-Miyaura and Heck coupling reactions, **Debasish Sengupta**, Babli Roy, Samir Kundu and Basudeb Basu, *National Seminar on Frontiers in Chemistry 2014* held at University of North Bengal, Darjeeling, March 11, 2014.

- Heterogeneous Bimetallic Nano Particles (NPS): Preparation Characterization and Application in catalysis, **Debasish Sengupta**, Samir Kundu, Susmita Paul and Basudeb Basu*, *National Seminar on Frontiers in Chemistry 2013* held at University of North Bengal, Darjeeling, February 28, 2013.

ABBREVIATION

ARF	Amberlite resin formate	NMP	*N*-Methylpyrrolidone
Bu	Butyl	nm	nanometer
CNT	Carbon nanotube	NMR	Nuclear Magnetic Resonance
^{o}C	Degree Celsius	PEG	Polyethylene glycol
d	Doublets	ppm	parts per milllion
dd	Doublet of a doublet	PVP	Polyvinylpyrrolidone
DVB	Divinylbenzene	PS	Polystyrene
DMF	Dimethyl formamide	RT	Room temperature
DMSO	Dimethyl sulfoxide	SAED	Selected area electron diffraction
EDX	Energy Dispersive X-ray	SBA	Santa Barbara Airport
GO	Graphene oxide	SDS	Sodium dodecyl sulfate
HMT	Hexamethylenetetramine	SEM	Scanning Electron Microscopy
HRTEM	High Resolution Transmission Electron Microscopy	s	singlet
h	Hours	t	triplate
LDHs	Layered Double Hydroxides	TBAF	Tetrabutylammonium fluoride
MCM	Mobil Company of Matter	TBAB	Tetrabutylammonium bromide
min	minute	TEG	Tetraethylene glycol
mol%	mol percent	TEM	Transmission Electron Microscopy
mg	milligram	THF	Tetrahydrofuran
MHz	mega hertz	XRD	X-ray Diffraction
NPs	Nanoparticles		

CHAPTER I

A review on heterogeneous catalysis, metal nanocomposites and catalytic applications

I.1. Catalysis

Catalysis represents a new way to meet the challenges of energy and sustainability which are becoming the main concerns of the universal vision on societal challenges and world economy. Catalysis occupies an important place in chemistry; it lies at the heart of numerous chemical protocols, from research laboratories to the chemical industry. A variety of products, such as medicines, fine chemicals, polymers, fibers, fuels, paints, lubricants, and many other value-added products, would not be feasible in the absence of catalysts. Catalysis can be broadly divided into two branches, homogeneous and heterogeneous.

I.1.1. Homogeneous Catalysis

In a homogeneous catalysis, the catalyst is in the same phase as the reactants.[1] Homogeneous catalysts have several advantages such as high selectivity, better yield, and easy optimization of catalytic systems by modification of ligand and metals. In spite of their several advantages and applications, many homogeneous catalytic systems have not been commercialized because of the difficulty encountered in extrication the catalyst from the ultimate reaction product. Even when it is possible to separate the catalyst from the reaction mixture, trace amounts of catalyst are likely to remain in the final product.

I.1.2. Heterogeneous Catalysis

To overcome the problems of isolation and separation in homogeneous catalysis, chemists and engineers have investigated a wide range of strategies and the use of heterogeneous catalyst systems appears to be the superlative logical solution.[2] A vast majority of the industrial heterogeneous catalysts are high-surface area solids onto which an active component is dispersed or attached. Grafting can be achieved by covalent binding or by simple adsorption of the active catalytic molecules. The performance of heterogeneous catalysts is determined by exposed surface area.

I.1.3. Nanocatalysis

Most of heterogeneous catalytic processes take place at the active surface sites of the bulk catalyst. Therefore, it is apparent that the smaller the size the higher the surface area and activity. Since the end of the 1990s, and with the development of nanosciences, nanocatalysis has clearly emerged as a domain at the interface between homogeneous and heterogeneous catalysis, which offer unique solutions to answer the demanding conditions for catalyst improvement.[3]

Nanoparticles refer to materials with their extensions in all three dimensions smaller than 100

nm. Metal nanoparticles display unique properties on optical, electronic and chemical behavior which is quite different from bulk metal materials due to quantum size effect, surface effect and others effects.[4]

Transition metal nanoparticles as good catalysts for organic synthesis have attracted much attention over the past decade.[5] Metal nanoparticles (M-NPs) considered for catalytic process can be generated by (i) chemical reduction of a metal salt, (ii) thermal, photochemical, or sonochemical decomposition of a metal(0) complex, (iii) hydrogenation of a coordinating olefinic moiety, and (iv) vapour phase deposition.

Metal NPs without any solid support has rarely been applied in cross–coupling reactions. In such cases NPs becomes much larger in size because of aggregation and precipitation of the catalysts was observed.[6] The separation of the products and the recycling of the catalyst are not straightforward. Therefore to prevent nanocatalysts from aggregating, NPs are widely supported on some supporting materials and recycled by simple filtration. Transition metal nanoparticles can be either adsorbed on inorganic support or chemically bonded to polymeric support.

I.2. Heterogeneous Supports, Metal Nanocomposites and Catalytic Applications

The support usually has an impact on the activity of the catalytic system. Particle size, surface area, pore structure, and acid-base properties are important parameters of the support. The use of the appropriate support is therefore critical to obtain NPs of a suitable size to form highly active catalysts but also to stabilise the surface, so leaching is minimized. Popular supporting materials include mesoporous silica, alumina, zeolite, metal oxides, metal hydroxides, poly-ionic resins, carbon nanotube, graphene oxide and organic polymers.[7]

According to IUPAC notation, porous materials can be classified into microporous materials, mesoporous materials and macroporous materials according to their size. Microporous materials have pore diameters less than 2 nm; the mesoporous materials have pore diameters within the range of 2 – 50 nm and the macroporous materials have pore diameter greater than 50 nm.

I.2.1 Ordered Mesoporous Silica

MCM-41 and SBA-15 are two most representative example of ordered mesoporous material, extensively used in heterogeneous catalysis.

MCM-41

MCM-41, the simplest mesoporous molecular sieve, has been extensively studied.[8] Hexagonally packed mesoporous molecular sieves (designated MCM-41) are of great interest

to catalysis because their large and uniform pore sizes (20-100 Å) allow sterically hindered molecules facile diffusion to their internal active sites. Direct amidation of fatty acids with long-chain amines was successfully performed by using MCM-41.[9]

Since palladium-grafted mesoporous MCM-41 material designated as Pd-TMS11 was synthesized by Ying et al. in 1998.[10a] This heterogeneous material exequtes excellent activity for Heck reaction.

In 2005 Molnar et. al. have synthesized Pd–MCM–41 composite material by doing slight modification over MCM-41.[10b] The as synthesized catalyst was used in ligand-free Heck coupling reaction and also be recycled for 20 times without any activation treatment (Scheme I.1).

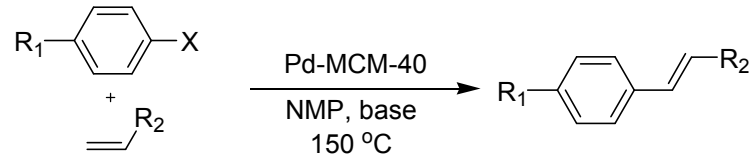

X = I, Br
R_1 = H, Cl, Br, OMe, Ac
R_2 = Ph, COOMe

Scheme I.1. Heck coupling using Pd-MCM-40.

SBA-15

SBA-15 is the most important hexagonal mesoporous material after MCM-41, which was first reported by Zhao et. al. at the university of California, Santa Barbara.[11]

Mesoporous SBA-15 was used as the heterogeneous support since its well-defined, large pore opening provided easy access for large substrate molecules. Shi and co-workers reported the use of a thin Pd NP layer on the pore channel surface of a mesoporous silica SBA-15, obtained through impregnation with a solution of [$Pd(OAc)_2$] in THF followed by ‘‘in situ’’ reduction. The heterogeneous material was highly efficient for Heck coupling.[12]

After that in 2007 Gao and co-workers have reported a simple one-step method to synthesise palladium nanoparticles in highly ordered mesoporous channels of SBA-15, which has a pore size in the range of 5–10 nm with a large specific surface area and a highly ordered pore structure.[13] The authors have indicated that the loading amount of palladium nanoparticles in SBA-15 can be adjusted using different amounts of palladium salts and can also be controlled easily. The resulting nanocomposites exhibit a highly catalytic activity and reused ability at least after five recycles without ligand for both the Suzuki and Heck coupling reactions (Scheme I.2).

Suzuki coupling reaction

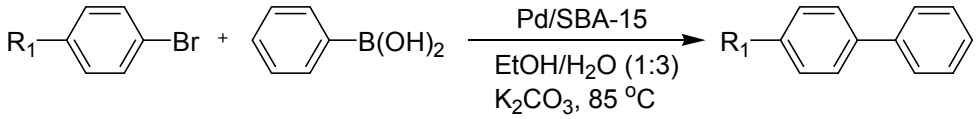

R_1	Pd (mol%)	t (h)	yield (%)
4-MeCO	0.2	5	99
4-MeO	0.2	10	85
H	0.2	10	88

Heck coupling reaction

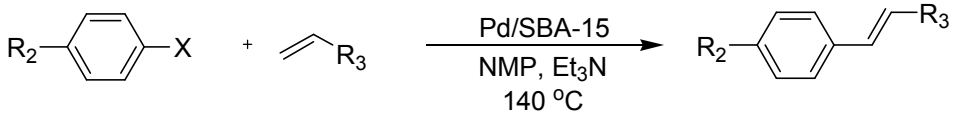

R_2	X	R_3	Pd (mol%)	t (h)	yield (%)
H	I	COOMe	0.04	1	99
H	I	Ph	0.04	3	99 (trans:cis = 84:16)
CH_3CO	Br	COOMe	0.2	4	95
CH_3CO	Br	Ph	0.2	8	90

Scheme I.2. Suzuki cross–coupling reactions catalysed by Pd/SBA-15 nanoparticles.

Amorphous Silica

In 2004, silica-stabilised Pd nanoclusters (2–5 nm) were prepared by Park and co-workers from a mixture of $[Pd(PPh_3)_4]$ in tetraethylene glycol and tetramethoxysilane through hydrolysis.[14] The resulting material exhibited good activity in the Heck, Suzuki, Sonogashira and Stille reactions at 0.75 mol% catalyst loading (Scheme I.3).

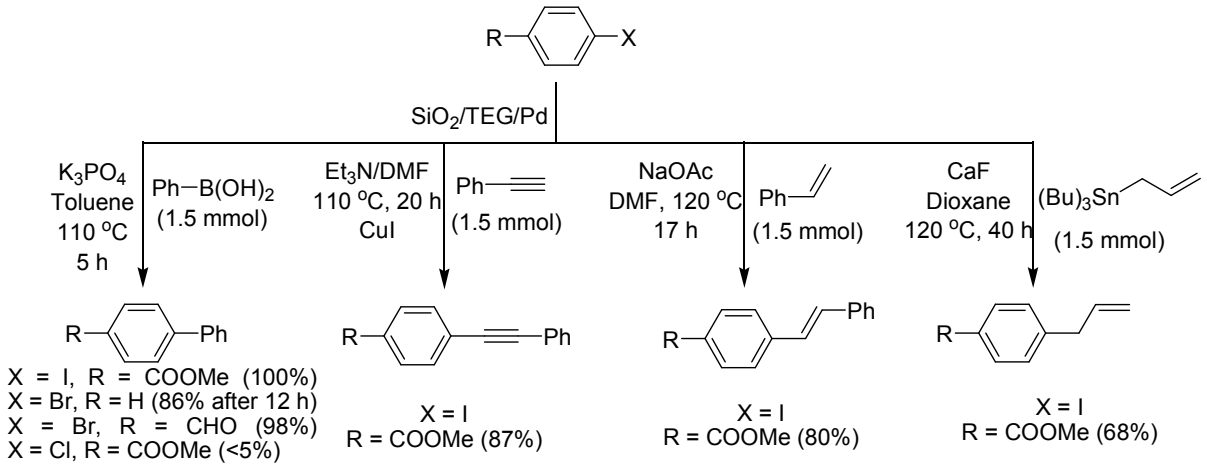

Scheme I.3. Silica supported Pd catalyst in Suzuki, Sonogashira, Heck, and Stille reaction.

In past years an improved and eco-friendly procedure has been developed to generate meso-porous silica (particle size 325 mesh) supported palladium nanoparticles ($Pd@SiO_2$) from our laboratory.[15] This sustainable heterogeneous Pd catalyst was used for phosphine-free Suzuki–

Miyaura and Heck coupling reactions with excellent turnover number and turnover frequency (Scheme I.4). Pd@SiO_2 was recyclable for four consecutive run in Suzuki–Miyaura cross–coupling reaction between 4-iodotoluene and phenylboronic acid.

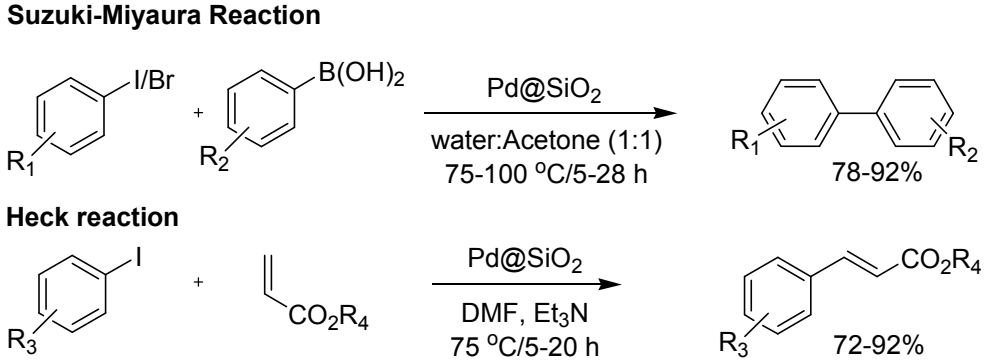

Scheme I.4. Pd@SiO_2 catalyzed Suzuki–Miyaura and Heck reaction.

Bimetallic nanoparticles also been investigated in many fields of science. Very recently Tang group was synthesized Au-Pd bimetallic nanocrystals in silica nanorattles.[16] Suzuki cross–coupling reactions are chosen as model reactions to evaluate the catalytic ability of these nanocatalysts (Scheme I.5). Notably, the alloy Au–Pd@SiO_2 with the lowest Pd content shows the highest catalytic activity and selectivity both for iodobenzene and bromobenzene.

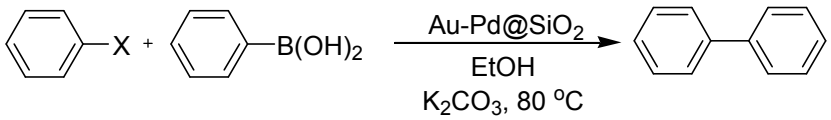

Scheme I.5. Scheme illustrating the Suzuki cross–coupling reaction using Au–Pd@SiO_2 as a catalyst.

I.2.2. Zeolites

Zeolites have a crystal structure which is constructed from TO_4 tetrahedra, where T is either Si or Al. Each structure type is given a unique framework code as shown in Table I.1.

Zeolites are well-defined porous materials can be used as supports for Pd as such or in a modified manner. Pd(II) on basic zeolites was reported in the Suzuki–Miyaura coupling of bromobenzene with phenylboronic acid in toluene.[17a] No leaching was observed, and the solid catalyst could be reused after washing with water. Only a minor decrease in the catalytic activity was observed. Pd(II)-NaY zeolite or Pd(0)-NaY zeolite performed very well in Suzuki reactions of aryl bromides without the addition of a ligand.[17b,c] The catalysts exhibited excellent activity with K_2CO_3 or Na_2CO_3 as base at room temperature allowing high yields to be achieved after short reaction times. However, they were less useful for aryl chlorides.

I.2.3. Metal Oxides

Different metal oxides have been used in nanocatalysis.

Table I.1. Zeolite ring sizes and codes.

Zeolite	Number of tetrahedral in ring	Framework Code
Sodalite	4	SOD
Zeolite-A	8	LTA
Erionite-A	8	ERI
ZSM-5	10	MFI
Fauzasite	12	FAU
Mordenite	12 and 8	MOR
Zeolite-L	12	LTL

I.2.3.1. MgO

Highly basic nanocrystalline magnesium oxide (MgO)-stabilised palladium NPs were prepared by counter ion stabilisation of $PdCl_4^{2-}$ with nanocrystalline MgO followed by reduction.[18] This catalyst was found to be very active in the Suzuki cross–coupling of aryl bromides and iodides with several arylboronic acids in pure water at room temperature (Scheme I.6).

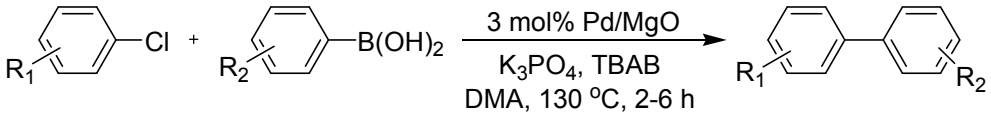

Scheme I.6. Suzuki cross–coupling reactions catalysed by PdNPs/MgO.

I.2.3.2. ZnO

ZnO-supported Pd, Pd-Ag, Pd-Cu, and Pd-Ni catalysts (Pd-M/ZnO) were prepared in $MeOH/H_2O$ mixture (4/1, v/v-%) by γ- irradiation at room temperature.[19] The catalytic efficiency of Pd and Pd-M/ZnO species was studied in Suzuki reaction (Scheme I.7). The catalytic activity was decreased in the order Pd-Ag/ZnO > Pd-Cu/ZnO > Pd-Ni/ZnO > Pd/ZnO. The Pd-Ag/ZnO was recycled successfully up to five consecutives but gradual decrease in catalytic activity was monitored.

I.2.3.3. CeO_2

Recently, cerium oxide (CeO_2) has been extensively used as heterogeneous catalysts for organic reactions.[20] One recent publication has exhibits Pd/CeO_2 system behaves as an effici-

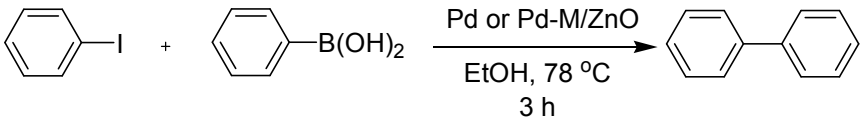

Pd-Ag/ZnO>Pd-Cu/ZnO>Pd-Ni>ZnO>Pd/ZnO

Scheme I.7. ZnO supported bimetallic catalyst in Suzuki reaction.

ent percatalyst for Suzuki–Miyaura reaction at room temperature. Author has demonstrated that a homo generous mechanism takes place most probably through a release/re-deposition process.

I.2.3.4. TiO_2

Zhong and their group have described a novel route to load palladium NPs on the surface of hydroxyl-group-rich titania precursor. Pd nanoparticles are formed by in-situ reduction of Pd(II) by Sn(II); the latter is linked to the surface of TiO_2 precursors through inorganic grafting (Figure I.1).[21] TiO_2 precursor-Pd exhibits high catalytic activity for Suzuki cross–coupling reaction (Scheme I.8).

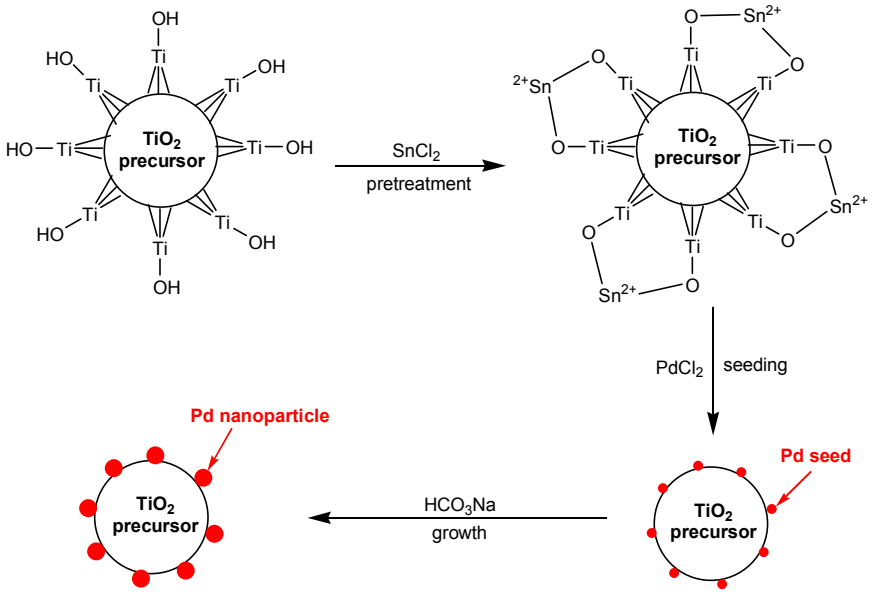

Figure I.1. Schematic process for loading Pd nanoparticles onto the surface of TiO_2 precursor.

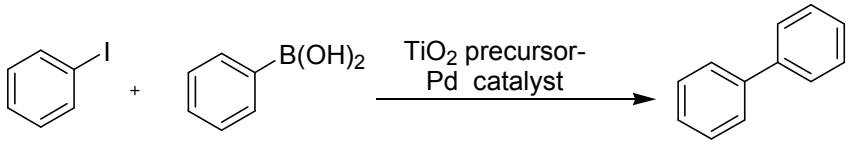

Scheme I.8. Suzuki reaction catalyzed by TiO_2 precursor-Pd catalyst.

I.2.3.5. ZrO_2

Cioffi and co-workers have been used Nanostructured zirconium oxide (ZrO_2) for supporting palladium NPs by an electrochemical technique.[22] The Pd/ZrO_2 nanocatalyst was very

efficient in C−C coupling reactions such as Heck, Ullmann and Suzuki cross–coupling (Scheme I.9).

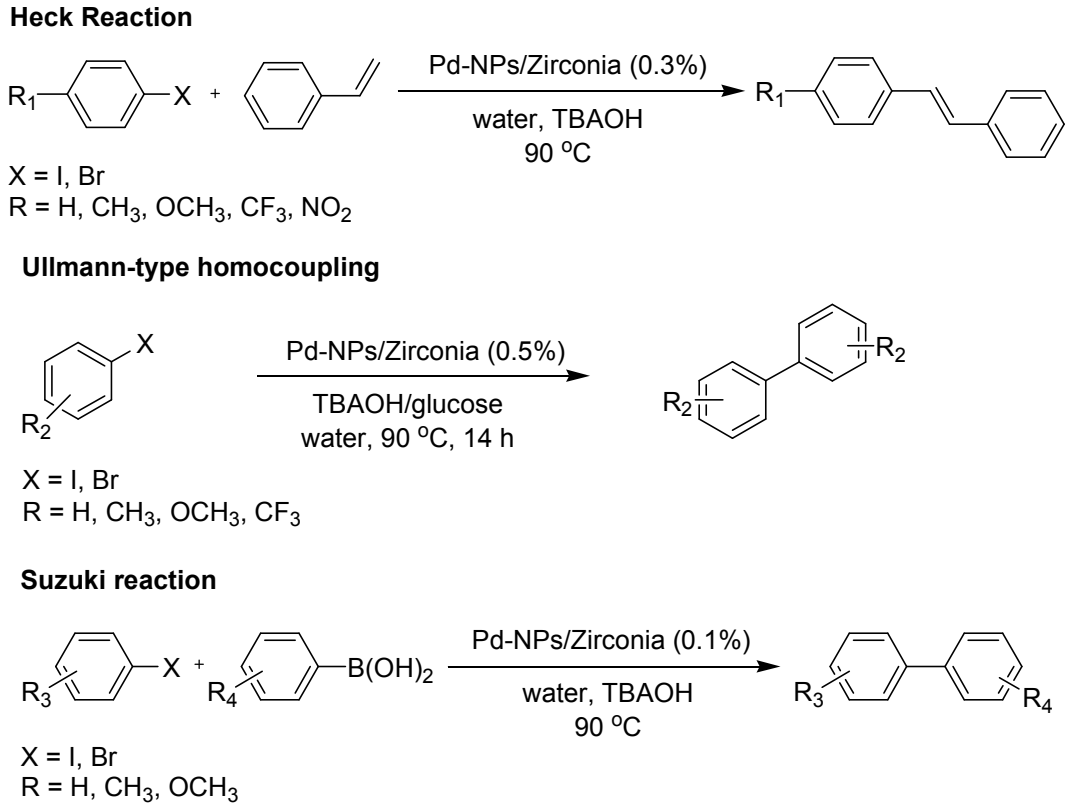

Scheme I.9. Pd/ZrO_2 nanocatalyst in Heck, Ullmann and Suzuki reaction.

Bhaumik and their group have synthesized self-assembled NiO-ZrO_2 nanocatalyst *via* evaporation induced self-assembly method.[23] The calcined material was highly crystalline with a cubic crystal structure. This nanocatalyst exhibits good catalytic activity in the C−S cross–coupling reaction in aqueous medium under aerobic conditions (Scheme I.10). Since this methodology was limited for certain diaryl sulphides.

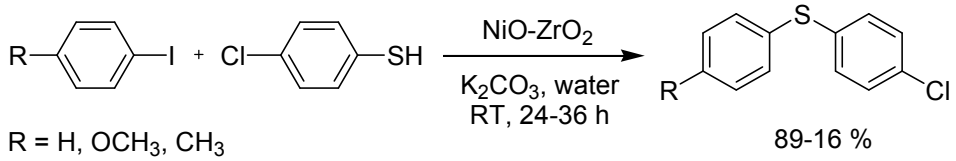

Scheme I.10. NiO-ZrO_2 catalyzed C−S cross–coupling reaction.

I.2.3.6. Al_2O_3

Alumina is probably the most common inorganic oxide that is used as the solid surface to catalyze or mediate a large variety of organic reactions. Alumina can act as a base, as an acid, or as a polar medium to cause molecular reorganizations in many types of organic compounds. Recently different composite materials were synthesized using alumina e.g. Cu/alumina,[24a] Ni-alumina,[24b] Pd/alumina[24c] and successively applied in C−S, C−N, C−O

and C–C cross–coupling reaction.

I.2.3.7. KF/Al_2O_3

Alumina doped with potassium fluoride (KF/alumina) has been extensively used as solid basic surface in vast range of organic transformation,[25] since it was introduced by Ando and Clark.[26]

Palladium-doped KF/Al_2O_3 was used in solvent–free Suzuki couplings under microwave irradiation (Scheme I.11).[27]

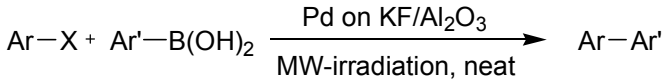

Ar—X	Ar'	condition	yield (%)
PhI	4-Me-Ph	2 min, 100 W	82
PhBr	4-Me-Ph	2 min, 100 W	52
PhCl	4-Me-Ph	2 min, 100 W	4

Scheme I.11. Palladium on KF/Al_2O_3, a heterogeneous catalyst for solvent-free Suzuki coupling.

I.2.4. Layered double hydroxide

In recent years layered double hydroxides of Mg and Al (LDHs) has been receiving considerable attention due to its cation exchange capacity of the brucite layer, anion exchange by inter layer, adjustable surface basicity and adsorption capacity.[28] In addition the ability to hold metal particles in the defect sites make LDHs good support in heterogeneous catalysis and by exploiting these properties of LDHs nanorhodium was incorporated and applies in Heck, Suzuki and Stille cross–coupling of haloarenes (Scheme I.12).[29]

I.2.5. Magnetic-materials

Catalyst recovery is a crucial feature of most of these processes. However, the use of magnetic nanoparticles as a support seems to be a promising option to overcome this separation problem. Because of the paramagnetic character of this support, the synthesised catalysts could also be recovered simply by using an external magnet without a filtration or centrifugation step. Recently, there has been an increasing trend towards the use of magnetically recoverable nanomaterials to develop more efficient and green chemical synthetic processes.[30]

Rana and co-workers have described a new methodology to immobilize metallic Pd on surface-functionalized ferrite nanoparticles leading to a magnetically separable catalyst,[31] wh-ich exhibits efficient catalytic activity in Suzuki–Miyaura coupling reactions (Scheme I.13).

Heck reaction

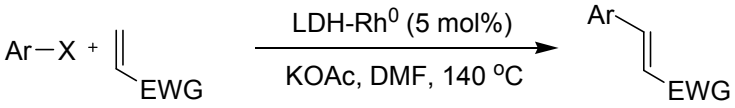

X = Br, I
Ar = Ph, 4-OMe-C_6H_4, 4-NO_2-C_6H_4
EWG = COOEt, COOBu, COOMe, Ph

Suzuki reaction

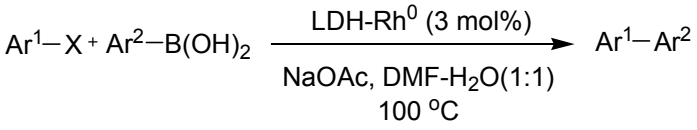

X = Br, I
Ar^1 = Ph, 4-OMe-C_6H_4,4-Me-C_6H_4, 4-NO_2-C_6H_4
Ar^2 = Ph, 4-OMe-C_6H_4,4-Me-C_6H_4

Stille reaction

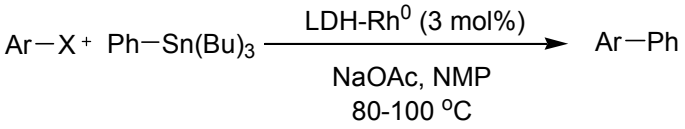

Scheme I.12. LDH-Rh^0 in Heck, Suzuki and Stille coupling.

The amine groups of branched polyethylenimine on the ferrite surface allow entrapping Pd nanoparticles and prevent metal leaching during the reaction. In addition, the environment provided by these groups leads to a structurally stable catalytic site, which makes them recyclable without any loss in activity.

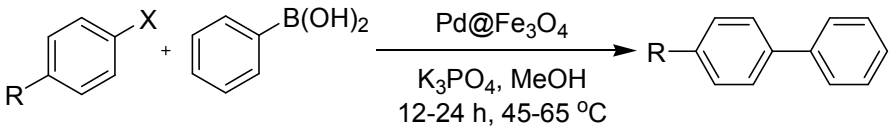

X = Cl, Br, I
R = CH_3, OCH_3, $COCH_3$, NO_2, H

Scheme I.13. Magnetically separable catalyst (Pd@Fe_3O_4), for Suzuki–Miyaura cross–coupling reaction.

I.2.6. Charcoal

Palladium on charcoal (activated carbon) (Pd/C) is the most frequently used catalyst in heterogeneous Pd-catalyzed cross-coupling reactions. It can be purchased from various laboratory suppliers, such as Acros, Aldrich, or from the manufacturers Degussa or Johnson Matthey in various qualities with a Pd content ranging from 1% to 20%. The materials can contain water up to 50%. Different procedures for the preparation of Pd/C were reported.[32]

The first example of Pd/C catalyzed Suzuki reaction was reported by Marck and co-workers in 1994.[33] After that several methodologies have been invented using Pd/C catalyst for aryl

bromide, chloride, iodide, or triflate. Pd/C was used with or without additional phosphine ligands, and often the application of aqueous solvents is advantageous.[34]

Lipshutz and their group synthesized Ni/C by different techniques and applying that catalyst for several cross-coupling reactions like Suzuki-, Kumada and aromatic aminations in presence suitable ligand (Scheme I.14).[35]

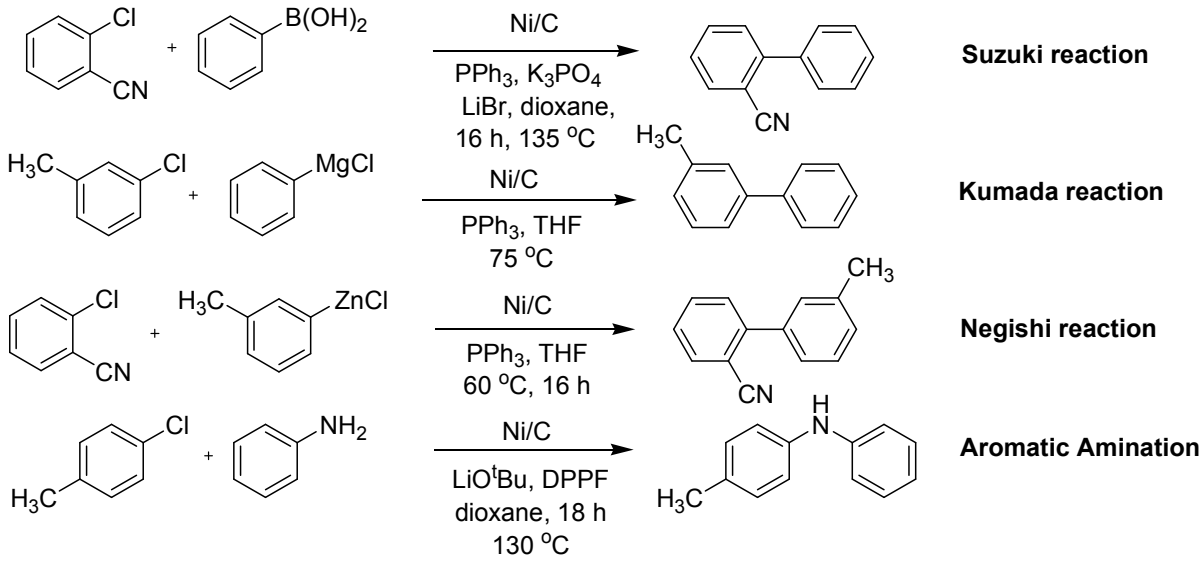

Scheme I.14. Ni/C catalyzed Suzuki, Kumada, Negishi and Aromatic amination reaction.

Impregnation of activated wood charcoal with $Cu(NO_3)_2$ in water using an ultrasonic bath leads to nanoparticle-sized Cu/C.[36] This heterogeneous material was an active catalyst for C−O cross coupling reaction (Scheme I.15).[37]

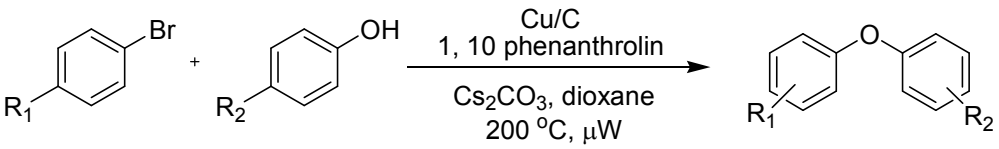

$R_1 = NO_2, CF_3, COCH_3, CHO$
$R_2 = H, CH_3, OCH_3, C(CH_3)_3$

Scheme I.15. C−O cross–coupling using Cu/C.

A new heterogeneous catalyst composed of copper and nickel oxide particles supported with charcoal has been developed. It catalyzes cross–couplings that traditionally use palladium, nickel, or copper, including Suzuki–Miyaura reactions, Buchwald-Hartwig aminations, vinylalane alkylations, etherifications of aryl halides (Scheme I.16).[38]

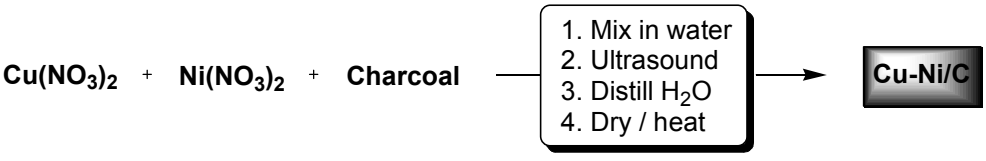

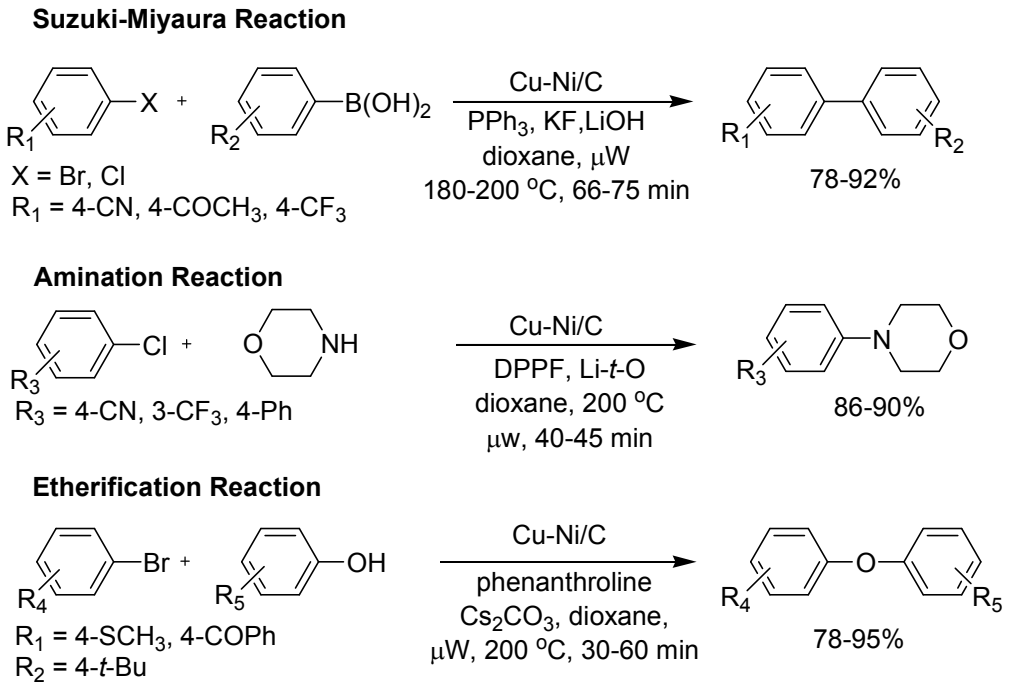

Scheme I.16. Use of Cu-Ni/C bimetallic catalyst in Suzuki–Miyaura, aromatic amination and etherification reaction.

I.2.7. Carbon nanotubes

Carbon nanotubes provide a new type of support for catalytic nanoparticles. Because of their small size, carbon nanotubes can be uniformly dispersed in solution, thus increasing contact between the reactants and the catalyst.[39]

Preparation of Pd and carbon nanotubes composites (Pd/CNTP) involves reduction of sodium tetrachloropalladate to Pd(0) on the surface of CNTs in presence SDS and ethylene glycol.[40] Ethylene glycol acts as a solvent as well as reducing agent. SDS self-assembled onto the surface of carbon nanotubes by the hydrophobic interaction between alkyl chains and graphitic surface. During the reduction process, the interaction between SDS and Pd nanoparticles resulted in the attachment of Pd nanoparticles onto the surface of carbon nanotubes. Thus, these well-dispersed spherical Pd nanoparticles were anchored tightly onto the external walls of MWNTs by the interaction between Pd nanoparitcles and SDS. The catalytic activities of these Pd/CNTP composites for Suzuki coupling reactions were investigated (Scheme I.17).

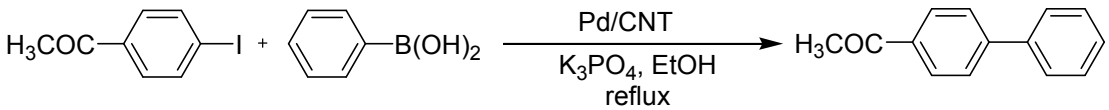

Scheme I.17. Pd/CNT catalyzed Suzuki reaction.

I.2.8. Graphene oxide

Graphene belongs to a new class of carbon nanomaterials – 2-D materials made up entirely of

conjugated sp^2 carbons arranged in a honeycomb structure. The main reason behind the fast paced enlargement of graphene research is due to the unique properties of graphene. Several experimentally measured properties have already surpassed those observed in other types of materials. With enhanced electrical conductivity, high mechanical strength, high thermal conductivity, high impermeability to gases and optical transparency, graphene holds great promise as the next wonder material.[41]

Graphene oxide was discovered much earlier than graphene. The most widely accepted structural model of GO is the Lerf–Klinowski model (Figure I.2) and is defined by two distinct regions in the GO structure: one of lightly functionalized, predominately sp^2-hybridized carbon (graphene-like) atoms and a second of highly oxygenated predominately sp^3-hybridized carbon atoms. In this model, hydroxyl and epoxide functional groups are proposed to decorate the basal plane which are segregated into islands among the lightly oxidized, graphene-like regions, while carboxylic acids or carboxylates, depending on the pH of the solution, are present on the edges of the sheets.[42]

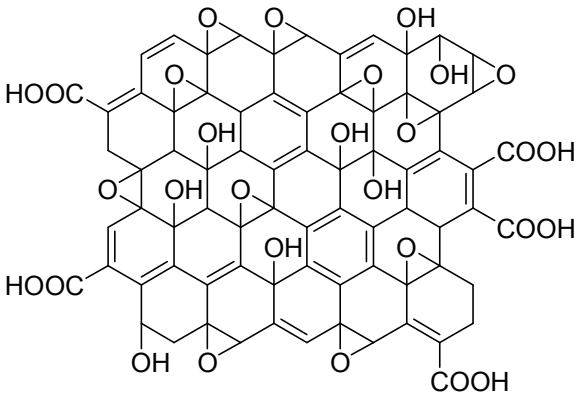

Figure I.2. Graphene oxide.

I.2.8.1. Chemical reactivity of GO

The catalytic efficiency of graphene oxide (GO) and other chemically modified graphenes (CMGs) as the carbocatalysts has raised enormous interest since the seminal papers from Bielawski and co-workers.[43] In current years GO was included in diverse organic reactions (Figure I.3).[44]

I.2.8.2. Metal on graphene

Graphene oxides (GO) and other chemically modified GOs have attracted much attention as potential carbonaceous materials to embed various metal/metal oxide resulting new nanocomposite materials.[45]

Immobilization of Pd^{2+} on graphite oxide (GO) via cation exchange and successive chemical reduction afforded Pd^0 nanoparticles and chemically derived graphenes (CDG).[46] The (GO)-

Pd and the (CDG)-Pd catalysts were effectively applied to the Suzuki–Miyaura coupling reaction (Scheme I.18). These novel heterogeneous catalysts were readily available and easy to handle as they are stable in air. Extraordinary high activities with turnover frequencies (TOF) of up to 39 000 h^{-1} and very low leaching make them an attractive alternative to commercially available Pd catalysts such as Pd on charcoal. However, recovery of the noble metal is possible because of very low leaching.

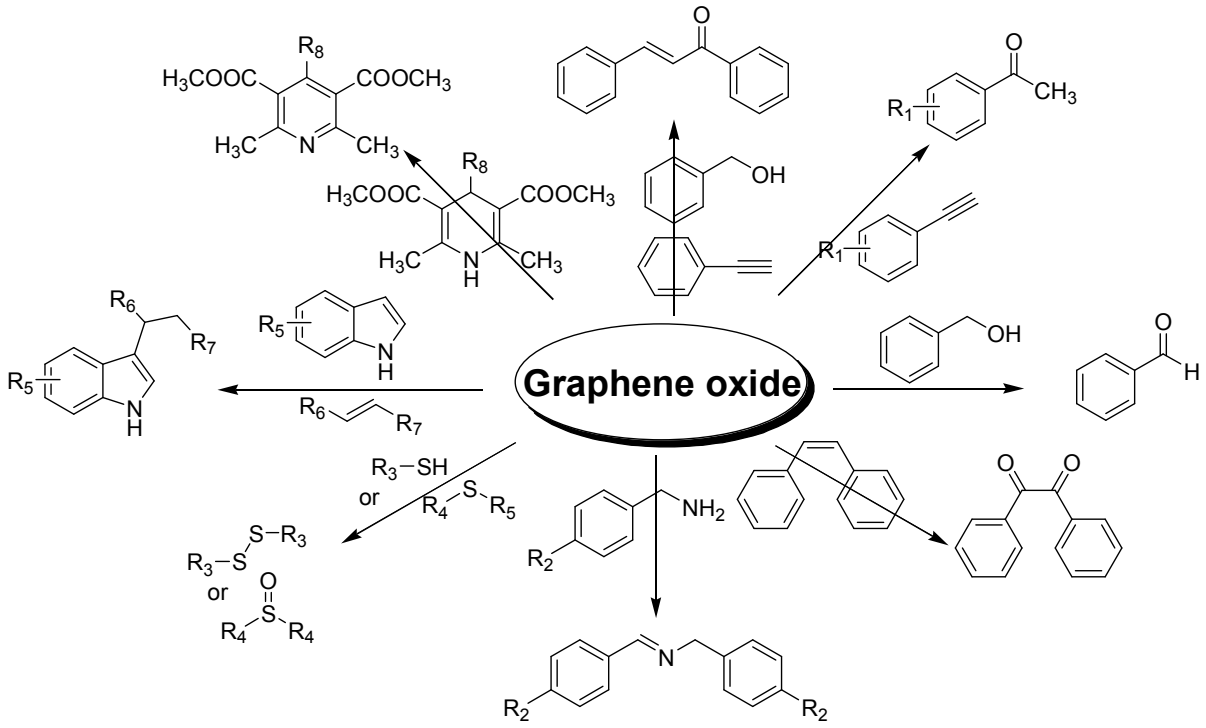

Figure I.3. Graphene oxide catalyzed organic transformations.

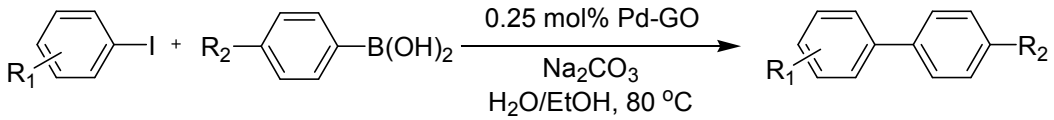

R_1 = OH, OCH_3, COOH, COOEt
R_2 = OCH_3, H

Scheme I.18. Pd-GO in Suzuki–Miyaura cross–coupling.

There are several routes available in literature for the synthesis of CuO NPs supported on graphene oxide but not for cross–coupling reactions.[47] One recent publication showed the preparation of copper oxide nanoparticles that are supported on graphene oxide be an active catalyst for ligand-free and solvent-free C–S cross-coupling reactions with weak bases such as triethylamine (Scheme I.19).[48] This nanocomposite was true heterogeneous and recycled up to six consecutive runs.

In 2013 Shaabani and their group designed a simple protocol to synthesized third generation

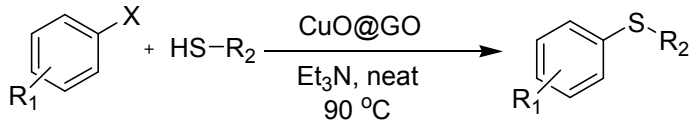

X = I, Br, Cl
R_1 = H, *p*-CF_3, *p*-Me, *p*-OMe, *t*-Bu, *p*-F
R_2 = aryl/alkyl, aryl, heterocyclic and aliphatic halides

Scheme I.19. CuO@GO catalyzed C−S cross–coupling reaction.

polypropylenimine (PPI) dendrimers were grown on the surface of functionalized graphene. The PPI-grafed graphene hybrid material was effectively employed as substrate for in situ generation of palladium cobalt alloy nanoparticles.[49] The as synthesized heterogeneous catalyst used for Sonogashira cross-coupling reactions under environmentally benign, aerobic and solvent free conditions at room temperature (Scheme I.20). The new hybrid material, under optimal reaction conditions, was used as an efficient heterogeneous catalyst for couplings between a wide range of terminal alkynes and aryl halides in high yield.

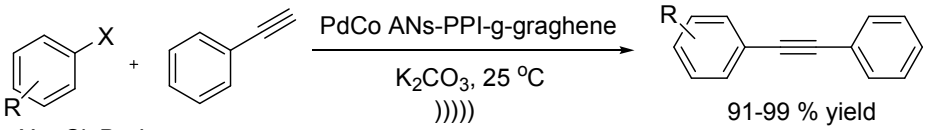

X = Cl, Br, I
R = Me, OMe, NO_2

Scheme I.20. Sonogashira cross–coupling with PdCo ANP–PPI-g-graphene hybrid material.

Graphene (G) supported Pd-Co bimetallic nanoparticles (NPs) as a highly active catalyst was prepared by a chemical reduction method and used for Sonogashira and Suzuki–Miyaura cross–coupling reactions (Scheme I.21).[50] With the characterization of X-ray diffraction, X-ray photoelectron spectroscopy, transmission electron microscopy, and Raman spectrum, the composition of resulting Pd-Co material was identified to be alloy structural. The recyclability also checked for Suzuki–Miyaura cross–coupling.

Sonogashira reaction

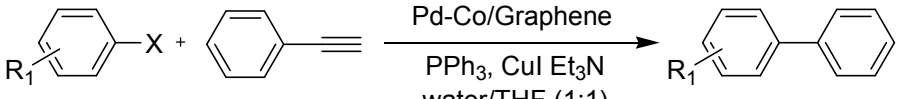

X = I, Br
R_1 = H, 2-NO_2, 4-NO_2, 4-CH_3

Suzuki-Miyaura reaction

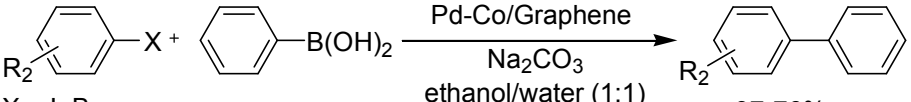

X = I, Br
R_2 = H, 4-NO_2, 4-CH_3, 4-OCH_3

Scheme I.21. Pd-Co/G catalyzed Sonogashira and Suzuki–Miyaura coupling reactions.

I.2.9. Organic polymers and related molecules

Over the last few decades, palladium nanoparticles have been mostly supported on inorganic materials, such as silica, other oxide-hydroxides and carbon nanotubes.[51] More recently, functionalised polymers have been used as supports in coupling reactions, and a variety of, polymers have proven to be versatile supports due to their potential to combine the easy reu se of heterogeneous catalysts and the high efficiency of homogeneous catalysts.[52]

I.2.9.1. PVP

A study by Sayed et al., detailing Suzuki cross-couplings using polymer supports, reported a series of PVP stabilised Pd nanoparticles with different Pd particle sizes, prepared using the stepwise growth technique reported by Teranishi et al.[53] Using this method, the authors succeeded in preparing different PVP-Pd composites with a narrow particle size distribution and average particle sizes of 3.0, 3.9, 5.2 and 6.6 nm. Most of the Pd nanoparticles prepared by this method showed a roughly spherical morphology. The turnover frequency (TOF) for the Suzuki reaction between phenylboronic acid and iodobenzene in aqueous solutions was found to depend on the Pd particle size and to exhibit a maximum size of ca. 3.9 nm.[54]

The immobilisation of Pd nanoparticles with functional ionic liquid grafted onto cross-linked polymer was also reported by Han and their group (Scheme I.22).[55] The nanocatalysts immobilized on the copolymers showed high catalytic activity in the Heck reaction for various substrates (Scheme I.23). The catalyst was very stable and could be easily separated from the products and reused because of the insoluble nature of the cross-linked copolymer and the coordination force between the amine group and the palladium nanoparticles.

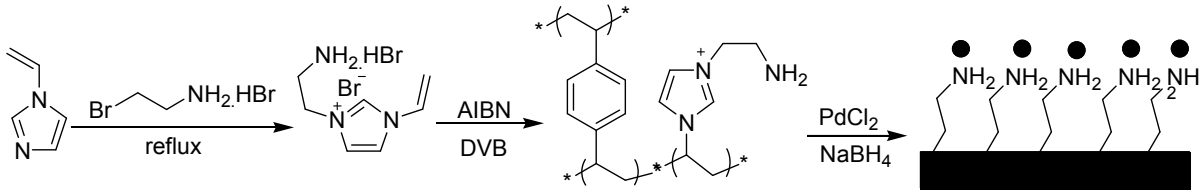

Scheme I.22. Immobilisation of Pd nanoparticles with functional ionic liquid grafted onto cross-linked polymer.

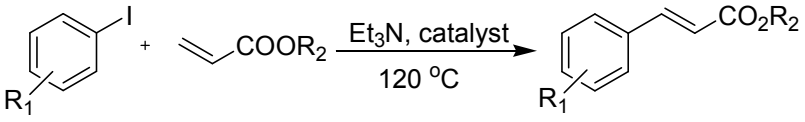

R_1 = H, 4-F, 4-Cl, 4-OH, 4-Me, 4-OMe
R_2 = Me, Et, Bu

Scheme I.23. Polymer supported Pd NPs in Heck reaction.

In recent years Kobayashi developed Copolymer-Incarcerated Nickel Nanoparticles with N-Heterocyclic Carbene Precursors.[56] These NHCs embedded in the polymer matrix were

characterized by FGSR-MAS NMR analysis. This heterogeneous catalyst was successfully applied to Corriu− Kumada−Tamao (CKT) reactions with quite wide substrate generality in high yields including functional group tolerance (Scheme I.24).

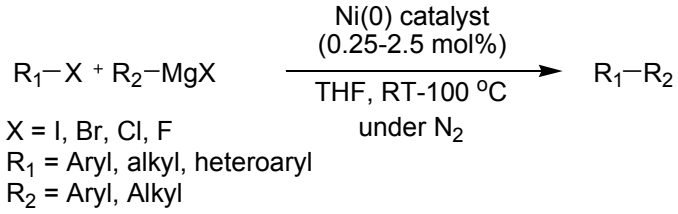

Scheme I.24. Nickel nanoparticles with N-heterocyclic carbene precursors as heterogeneous composite in CKT reaction.

I.2.9.2. Polystyrene Resin

The polymeric supports used by Merrifield for his early work in solid-phase peptide synthesis were based on 2% divinylbenzene (DVB) cross- linked polystyrenes (PS). Polytyrenes has been found to be one of the most accepted polymeric material used in various synthesis because it is inexpensive, readily available, mechanically robust, chemically inert, and smoothly functionalizable.[57] Cross-linking imparts mechanical stability, improved diffusion and swelling properties to the resin. Various percentages and types of cross- linking agents have been incorporated into the PS resins, the most common being DVB, but other examples include ethylene glycol dimethylacrylate (EGDMA) and tetraethylene glycol diacrylate (TEGDA) to give different solvation properties.[58] A schematic representation of polymerization of styrene with functionalized monomers is shown in Figure I.4.

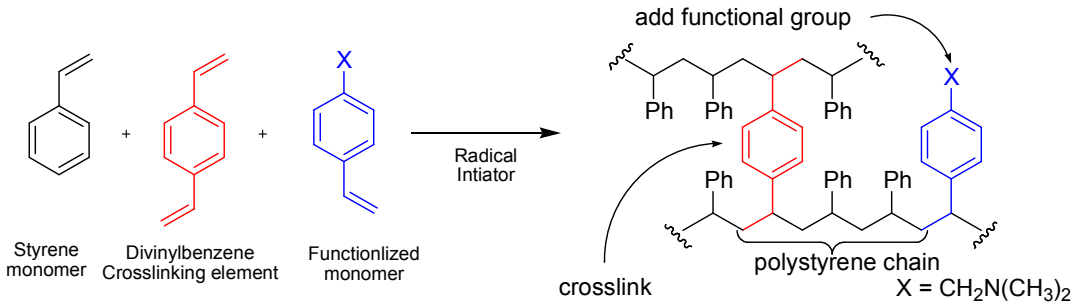

Figure I.4. Polystyrene resin formation.

TentaGel[59] and ArgoGel[60] are two commercially available examples, where the incorporation of the PEG chains dramatically increases resin compatibility with polar solvents.

Bradley and their group showed that soluble $Pd(OAc)_2$ can enter swollen resins and that amino groups on the resin can be "tied and tangled" by cross-linking, allowing permanent capture of the palladium on the resin without the assistance of any resin-bound ligand or stabilizer prior to conversion to stable palladium "nanoparticles".[61] The prepared catalyst designated as XL-RC Pd. Aminomethylated TentaGel resin was used for this immobilization

process. The as prepared catalyst has been used in Suzuki reaction (Scheme I.25). These supported catalysts are predominantly heterogeneous in nature and could be recycled without loss of activity.

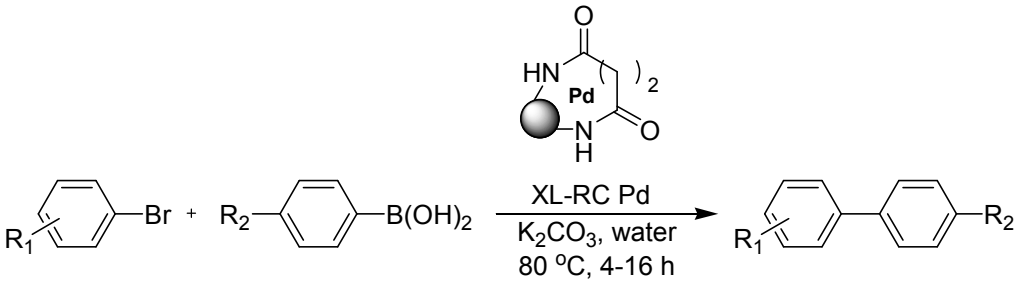

X = Br, Cl
R_1 = 4-CH_3CO, 4-CH_3, 2-NO_2, 2-CH_3, 4-OCH_3
R_2 = H, OCH_3

Scheme I.25. Aminomethylated TentaGel resin supported Pd NPs in Suzuki reaction.

I.2.9.3. Ion-Exchange resins

Ion-exchange materials are insoluble substances containing loosely held ions which are able to be exchanged with other ions in solutions which come in contact with them and normally obtained as beads of 1-2 mm diameter. These exchanges take place without any physical alteration to the ion exchange material. Ion exchangers are insoluble acids or bases which have salts which are also insoluble, and this enables them to exchange either positively charged ions (cation exchangers) or negatively charged ones (anion exchangers). Synthetic ion exchange materials based on coal and phenolic resins were first introduced for industrial use during the 1930s. A few years' later resins consisting of polystyrene with sulphonate groups to form cation exchangers or amine groups to form anion exchangers were developed. The most typical ion exchange resins are based on cross linked polystyrene and the required active groups can be introduced after polymerization, or substituted monomers can be used. For example, the cross linking is often achieved by adding 0.5-25% of divinylbenzene to polystyrene at the polymerization process. Non-cross linked polymers are used only rarely because they are less stable.

Types Ion-Exchange resin

There are four types of ion exchange resins:

- Strong cation-exchange resins, containing sulphonic acid group or the corresponding salts.
- Weak cation-exchange resins, containing carboxylic acid groups or the corresponding salts.
- Strong anion-exchange resins, containing quaternary ammonium groups.

- Weak anion-exchange resins, containing primary, secondary, and/or ternary amino groups, e.g. polyethyelene amine.

Ion exchange resins are widely used in different separation, purification and decontamination process examples are: Water softening, Water purification, Uranium recoveries from seawater, inversion of sucrose.

Catalytic activity of ion-exchange resin in organic reactions:

Amberlyst-15 is routinely used in organic synthesis as heterogeneous reusable acid catalysts for various selective transformations of simple and complex molecules (Figure I.5).[62]

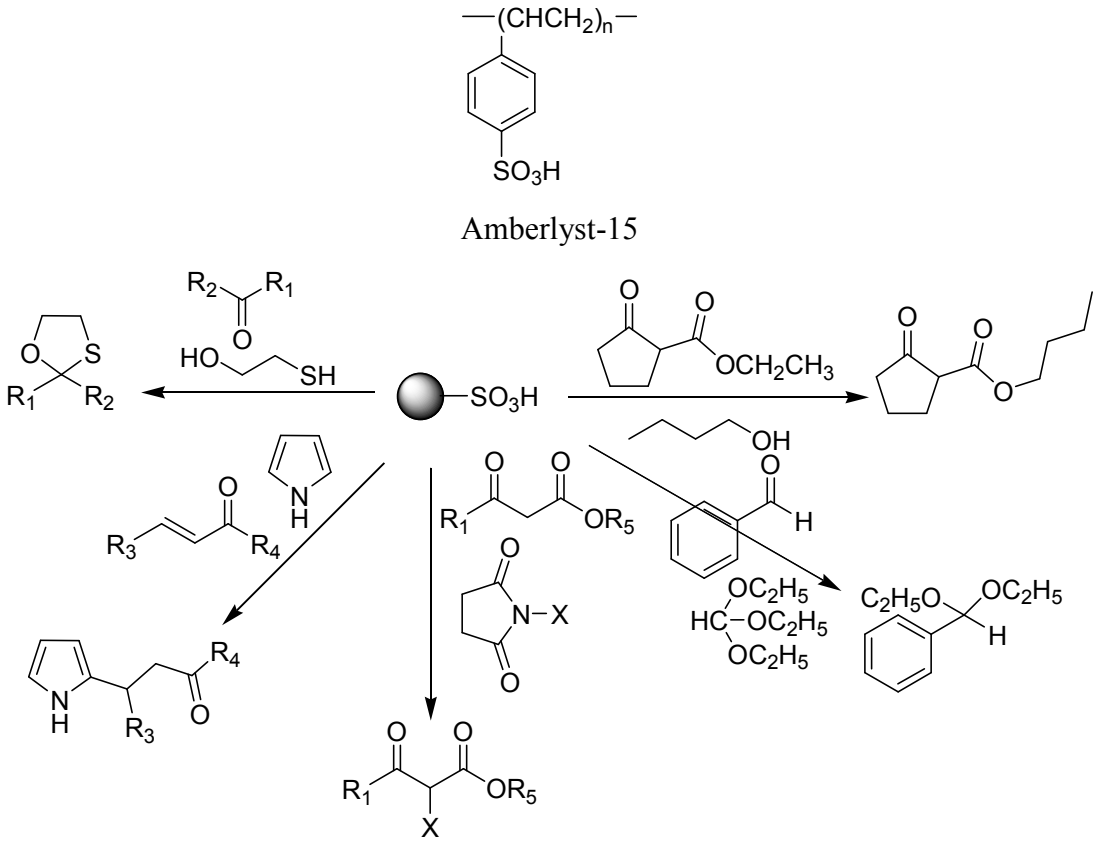

Figure I.5. Amberlyst-15 catalyzed organic transformation.

The selective reduction of functional groups is a common need in organic synthesis. Borohydride exchange resin,[63] (BER) was introduced in the 1970s and has since proven to be of considerable value in the reduction of organic compounds. This reagent reduces both ketones and aldehydes readily to corresponding alcohol (Scheme I.26)

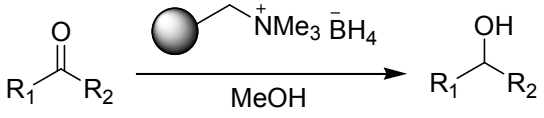

R_1 = H, alkyl group

Scheme I.26. Reduction of carbonyl compounds using Borohydride Borohydride exchange resin.

It was observed that Amberlite IRA-420 anion (chloride form) exchange resins, commercially available and inexpensive poly- ionic resin, could exchange the anion with formate anion ($HCOO^-$) easily and quantitatively. The resulting Amberlite Resin Formate (anion), designated as ARF, could be utilized as a solid-phase version of the H-donor in Pd-catalyzed catalytic transfer hydrogenation. The ARF was air stable, can be stored for several weeks and also can be recovered from a reaction and reused. Several alkenes, imine and nitroarenes were thus hydrogenated using the ARF and catalytic amount of palladium acetate under mild conditions (Scheme I.27).[64]

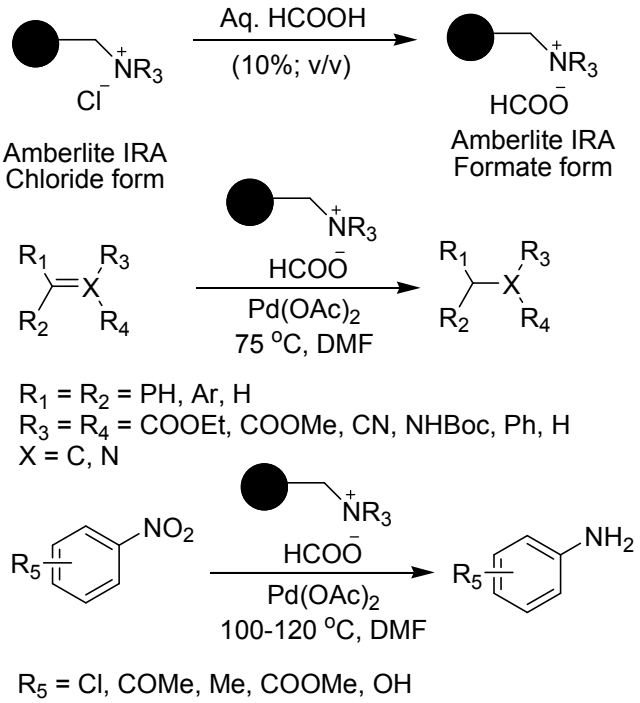

Scheme I.27. Amberlite resin formate in catalytic hydrogenation reactions.

The combination of formic acid and palladium acetate is known to undergo anionic ligand exchange to form a palladium diformate complex, eventually producing Pd(0) through decroxylation and loss of molecular hydrogen.[65] By applying this technique a new catalyst was invented from our laboratory. This heterogeneous catalyst was successfully applied in catalytic reduction and C–C cross–coupling reactions (Scheme I.28).[66]

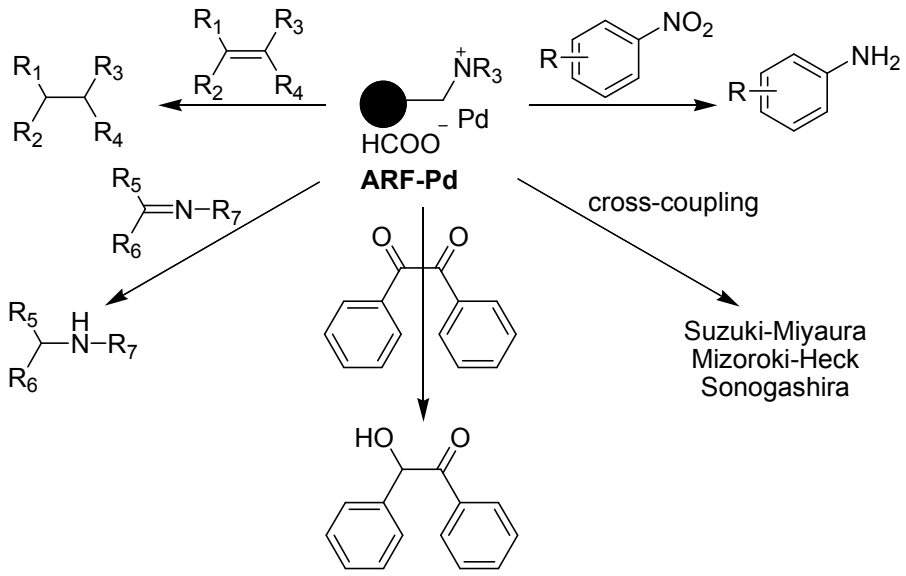

Scheme I.28. ARF supported Pd in catalytic reduction and C−C cross–coupling.

I.3. References

References are given in BIBLIOGRAPHY under Chapter I (pp. 141−145).

CHAPTER II

Synthesis of organic disulfides from thiocyanates promoted by poly-ionic resins hydroxide

II.1. Introduction

Organic disulfides bearing the −S−S− bond occur ubiquitously in proteins,[1] variety of natural products of pharmacological importance,[2] industrially find wide applications as vulcanizing agents for rubbers and elastomers,[3] and are useful intermediates in synthesis.[4] Over the last decades, alkyl disulfides are widely used for the preparation of highly ordered self-assembled monolayers (SAMs) on metal surface that find promising applications in the fields of biomaterials,[5] fluorochromogenic sensors[6] protective coatings,[7] etc.

Disulfide bonds constitute an important structural element in the folding of proteins and peptides. Many biologically active peptides and peptide mimetics possess unsymmetrical disulfide bonds. Figure II.1 represents three highly potent cyclic peptides such as somatostatin, octreotide and urotensin II.

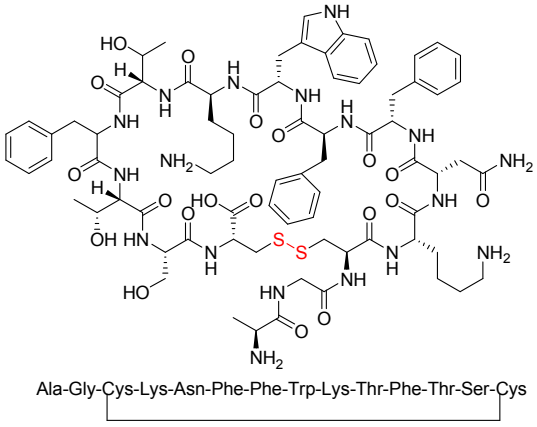

Somatostatin

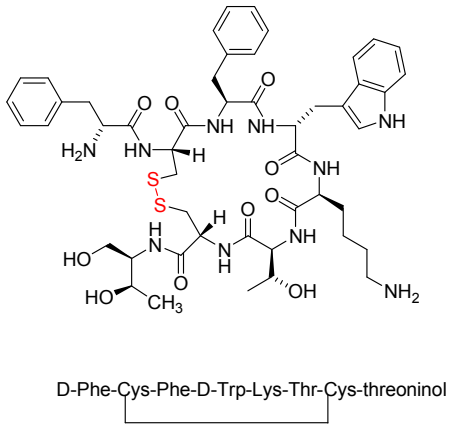

Octreotide

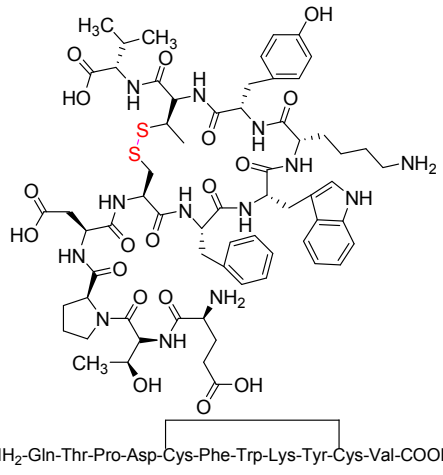

Urotensin II

Figure II.1. Disulfide bond in biologically active peptides.

To prepare organic disulfides, thiols are used as the starting materials in most cases. Numerous reagents and metal catalysts have been developed to oxidize thiols to disulfides under controlled conditions.[8] Disulfides can also be prepared by electrochemical approach via

a sulfenium cation under conditions of constant current.[9] Apart from thiols, organic thiocyantes are known to undergo reductive dimerization producing organic disulfides promoted by several catalysts leaving cyanide ion (Scheme II.1).

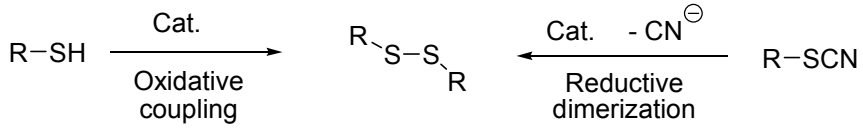

Scheme II.1. Disulfide formation from oxidative coupling and reductive dimerization.

II.2. Present Work: Background and Objective

The treatment of a base (e.g. NaOH, NH_3) with organyl thiocyanates is known to produce symmetrical disulfides in moderate to good yields.[10] The reaction is supposed to occur via a simple nucleophilic displacement of the cyanide anion and subsequent attack of the thiolate anion to another thiocyanate molecule resulting in the formation of S−S bond (Scheme II.2).

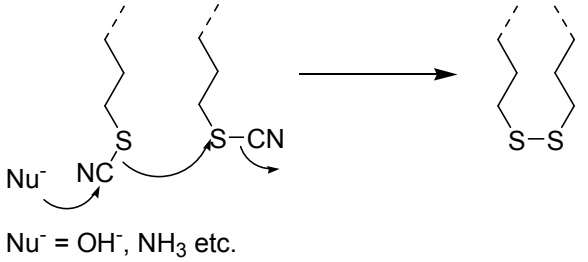

Scheme II.2. Formation of disulfides from thiocyanates.

Since the use of bases could be harmful to the thiocyanates bearing base-sensitive functionality (for example, ester or ketomethyl), Burns et al.[11] developed a method where organyl thiocyanates undergo disulfide formation in the presence of excess of tetrabutylammonium fluoride (TBAF) (Scheme II.3). The conditions do not however give good yields for cyclic disulfide formation, though intermolecular S–S bond formation is afforded in high yield.

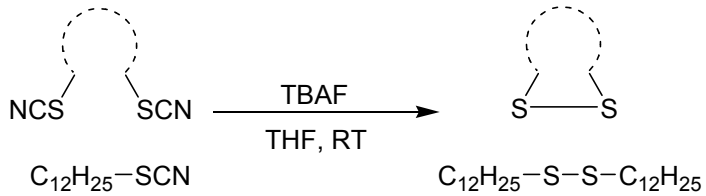

Scheme II.3. Preparation of disulfides from thiocyanates by treatment with TBAF.

Samarium diiodide (SmI_2) mediated reduction of thiocyanates was reported by Zhang et al.[12] The thiocyanates reacted with an equivalent amount of SmI_2 in THF for 10–15 min. The desired disulfides were obtained in 76–85% yields (Scheme II.4). It is observed that SmI_2 might convey one electron to thiocyanate to form the radical anion $(R\text{-}S\text{-}CN)^{\bullet-}$, which was dissociate into $RS^{\bullet}$ and CN^{-}. The coupling of the thiyl radical ($RS^{\bullet}$) gives the disulfide.

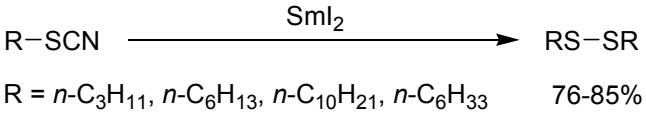

Scheme II.4. Disulfide synthesis from long-chain alkyl thiocyanates promoted by SmI_2.

In 1995 Chandrasekaran have described an interesting reductive dimerization of organic thiocyanates assisted by benzyltriethylammonium tetrathiomolybdate, $[(PhCH_2NEt_3)_2MoS_4]$,[13] leads to the formation of the corresponding disulfides in high yields (Scheme II.5). A large number of alkyl and aryl thiocyanates afford corresponding disulfides at room temperature. The tetrathiomolybdate anion is not involved in the S-transfer, instead it mediates the reductive dimerization of the thiocyanates.

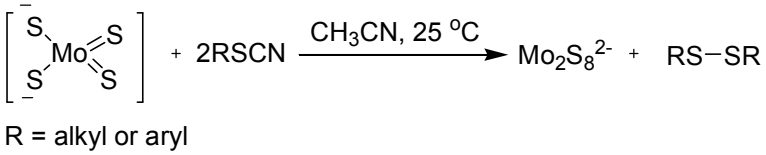

Scheme II.5. Synthesis of disulfide from thiocyanate using tetrathiomolybdate salt.

Zhang et al.[14] studied the oxidative dimerization of organyl thiocyanates using a combination of $TiCl_4$/Sm systems, the method is functional for both alkyl and aryl thiocyanates (Scheme II.6).

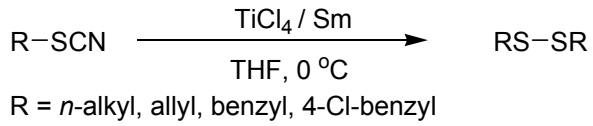

Scheme II.6. Disulfide from thiocyanate using a combination of $TiCl_4$ / Sm.

Use of polymeric reagents offers two-fold advantage: first, the reaction can be driven to completion using excess amounts of reagents and secondly, the reagent can be removed quantitatively after the reaction by simple filtration. In conjunction with our interest in solid-phase hetero bond-forming reactions,[15a-b] and use of poly-ionic resins in organic reactions and catalysis,[15c-d] we report herein a mild, efficient and metal-free aqueous protocol for the preparation of organic disulfides from alkyl (or acyl methyl) thiocyanates in the presence of ion-exchange resins, Amberlyst® A-26(OH).

II.3. Present Work: Result and Discussion

Initially, the organic thiocyanates were prepared from alkyl (or acyl methyl) halides by reaction of NH_4SCN in the presence polyethylene glycol (PEG 400) following a reported procedure with minor modifications.[16]

Optimization of the conversion of organic thiocyanate to symmetrical disulfide was performed using benzyl thiocyanate as the model compound (Table II.1). In a typical

experiment, benzyl thiocyanate (2 mmol) was stirred in water at room temperature in the presence of commercially available Amberlyst® A-26 (OH) (particle size: 0.35 mm, pH = 9.4, 300 mg) (entry 1). Since the conversion was not complete even after 10 h, we increased the temperature to 60 ^{o}C and now a complete conversion was achieved within 3h affording dibenzyl disulfide in 91% yield (entry 2). As the enzymatic (rhodanese) conversion of cyanide to thiocyanate is occurred in the presence of a sulfur donors,[17] we tested the same reaction in the presence of equimolar quantity of $Na_2S_2O_3$, cystine or cysteine (entries 3−5). It is observed that while the presence of $Na_2S_2O_3$ could have an effect in lowering the rate of the conversion, the amino acid bearing −SH group (cysteine) did show appreciable change in the rate of the conversion (rt / 2 h). However, there was no significant change by using cystine (–S–S– linkage) as the additive. The same reaction was also tested in the presence of other anion exchange amberlite resins, like commercially available Amberlite® IRA(Cl) or our laboratory derived Amberlite resin formate (ARF),[15c] with varying results (entries 6−7).

Table II.1. Optimization of disulfide formation from organic thiocyanates in water.[a]

Entry	Reagent[b]	Additive[c]	Temp (^{o}C)/ Time (h)	Yield (%)[d]
1	Amberlyst® A-26(OH)	Nil	RT / 12	52[e]
2	**Amberlyst® A-26(OH)**	**Nil**	**60 / 3**	**91**
3	Amberlyst® A-26(OH)	$Na_2S_2O_3.5H_2O$	60 / 20	76
4	Amberlyst® A-26(OH)	L-Cysteine	RT / 2	90
5	Amberlyst® A-26(OH)	L-Cystine	60 / 2.5	87
6	Amberlite® IRA-900(Cl)	Nil	60 / 12	Nil
7	Amberlite IRA-900(HCOO)	Nil	60 / 6	81

[a] Reactions were performed in 2 mmol scale in water (2 mL). [b] Different resins were used 150 mg mmol^{-1}. [c] Additives were used in stoichiometric quantities. [d] Yield refers to isolated product after column chromatography. [e] Starting thiocyanate still remains in the reaction mixture, as indicated on tlc.

We had chosen the optimized condition as in entry 2 for the easy formation of the dibenzyl disulfide from benzyl thiocyanate. We were interested to establish this mild, efficient and aqueous metal-free condition as a general protocol. Accordingly, several substituted benzyl thiocyanates were subjected to similar reaction. The results are presented in Table II.2. It is gratifying that different halo-substituted benzyl thiocyanates and naphthyl methyl thiocyanate underwent smooth conversion to the corresponding disulfides (entries 2–7). However, the nitro benzyl thiocyanate remained unchanged under the reaction conditions (entry 8). This could possibly be attributed to the strong electron-withdrawing nature of the nitro group that reduces nucleophilic character of the benzyl carbon and electron density on the sulfur atom.[18]

Purely aliphatic thiocyanates, *n*-octyl thiocyanate or other compounds such as 3-phenyl propyl thiocyanate or allyl thiocyantate derivative (3-phenyl-2-propenyl thiocyanate) also undergo disulfide formation in good to excellent yields (entries 9–11). In order to further generalize the reaction, acyl methyl thiocyanates were subjected to similar reaction. Organic disulfides flanked by two carbonyl groups at C-2 position would be the S-analogue of 1,6-diketones. Such bis(benzoylmethyl) disulfides could be easily prepared if benzoyl methyl thiocyanate undergoes similar dimerization. We had prepared different benzoyl methyl thiocyanates and carried out similar reactions using the resin hydroxide in water. As shown in Table II.2 (entries 12–16), the corresponding disulfides were formed efficiently and isolated in excellent yields except the nitro-bearing benzoyl methyl thiocyanate (entry 15), possibly due to the same reason as mentioned in the case of entry 8 of this Table.

Table II.2. Synthesis of various organic disulfides using Amberlyst® A-26(OH) in water.[a]

Entry	Substrate	Temp (°C) / Time (h)	Product[b]	Yield (%)[c]
1	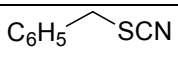	60 / 3	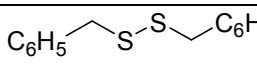	91
2	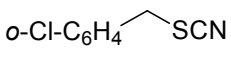	60 / 5	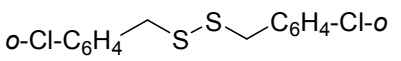	92
3	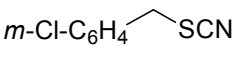	60 / 5	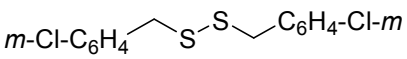	81
4	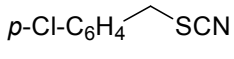	60 / 6	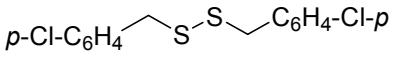	88
5	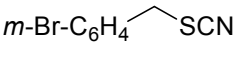	60 / 2	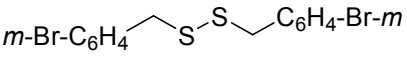	82
6	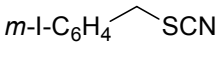	60 / 3	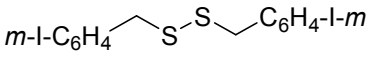	85
7	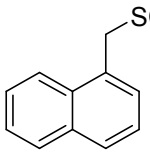	60 / 8	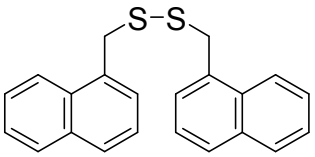	78
8	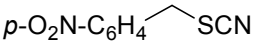	60 / 10	No reaction	
9	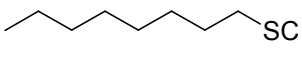	70 / 5	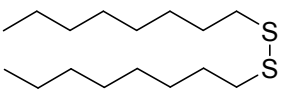	74

10	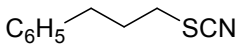	60 / 8	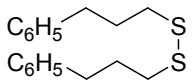	80
11	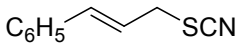	60 / 24	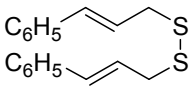	88
12	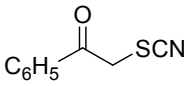	80 / 16	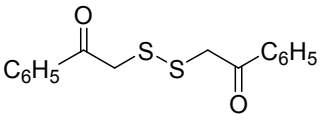	78
13	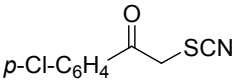	60 / 12	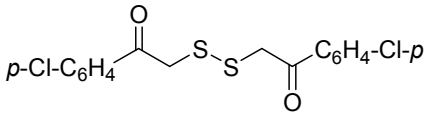	76
14	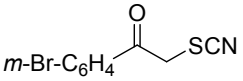	60 / 5	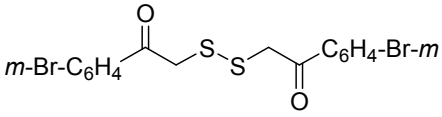	74
15	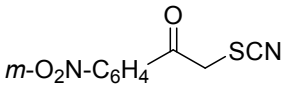	60 / 16	No reaction	
16	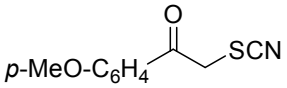	60 / 12	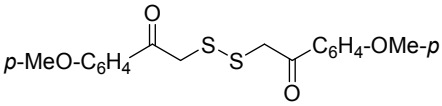	81

[a] All reactions were carried out in 2 mmol scale using 300 mg of Amberlyst® A-26(OH). [b] Products were characterized by NMR, HRMS and mp. [c] Yield refers to the pure product, isolated by column chromatography.

In order to verify any advantage of using poly-ionic resins hydroxide base, a comparison between the heterogeneous base Amberlyst® A-26(OH) and other homogeneous bases (NaOH, NH_3, K_2CO_3) was performed. Thus, the conversion of benzyl thiocyanate to dibenzyl disulfide was carried out using homogeneous bases NaOH, NH_3 and K_2CO_3 that respectively afford 83, 46 and 25% yield, while Amberlyst® A-26(OH) can give rise to 91% yield (Table II.3) under similar conditions. The variation of reactivity is even more prominent in the case of acyl methyl thiocyanates (Table II.4).

Comparative studies using *p*-methoxy benzoyl methyl thiocyanate as a model case revealed that the Amberlyst® A-26(OH) can lead to the formation of the corresponding disulfide in 81% yield with trace amount of *p*-methoxy acetophenone, while the base NaOH affords only *p*-methoxy acetophenone in 69% yield and no disulfide (Table II.4, entries 1-2). On the other hand, use of K_2CO_3 afforded a mixture of compounds as seen on tlc (no separation was att-

Table II.3. Comparative study of different bases for conversion of benzyl thiocyanate to dibenzyl disulfide in water.[a]

Entry	Base	Amount of base[b]	Time (h) / Temp (^oC)	Yield (%)[c]
1	Amberlyst® A 26(OH)	150 mg	3 / 60	91
2	NaOH	40 mg	3 / 60	83
3	K_2CO_3	138 mg	3 / 60	46
4	NH_3 solution	0.6 mL[d]	3 / 60	25

[a] Reactions were performed in 1 mmol scale in water (2 mL). [b] Quantity of bases used $mmol^{-1}$. [c] Yield refers to isolated product after column chromatography. [d] Ammonia solution (about 30%) (LR grade) obtained from Thomas Baker, India.

empted), while NH_3 solution gave a mixture of the corresponding disulfide and acetophenone in 21 and 18% yield respectively, the remaining was the starting material (60%), as analyzed by HPLC (Table II.4, entries 3 and 4). These results clearly establish the advantage of the heterogeneous base Amberlyst® A-26(OH) over the existing homogeneous bases.

Table II.4. Comparative study of different bases for conversion of *p*-methoxy benzoyl methyl thiocyanate to *p*-methoxy dibenzoyl disulfide and *p*-methoxy acetophenone in water.[a]

Entry	Base	Amount of base[b]	Time (h) / Temp (^oC)	Yield (%)	
				Disulfide	Ketone
1	Amberlyst® A 26(OH)	150 mg	12 / 60	81[c]	trace
2	NaOH	40 mg	12 / 60	Nil	69[c]
3	K_2CO_3	138 mg	12 / 60	Mixture of compounds[d]	
4	NH_3 solution	0.6 mL[e]	12 / 60	21[f]	18[f]

[a] Reactions were performed in 1 mmol scale in water (2 mL). [b] Quantity of bases used $mmol^{-1}$. [c]Yield refers to isolated product after column chromatography. [d] As seen on tlc. [e] Ammonia solution (about 30%) (LR grade) obtained from Thomas Baker, India. [f] Analyzed by HPLC [Column ZORBAX Rx-SIL (4.6 x 150 mm, 5μm); Mobile phase: hexane-ethyl acetate (9:1); flow rate = 0.5 mL/min].

We then focused our attention to explore whether this mild and eco-friendly protocol could be employed for the preparation of unsymmetrical disulfides. In order to get an unsymmetrical disulfide, it is required to perform the reaction taking a mixture of two different organyl thiocyanates. This might also help us to propose a possible pathway of the reaction. Firstly, we performed one reaction using two different benzyl thiocyanates. For example, carrying out the reaction using equimolar mixture of benzyl thiocyanate and *m*-

chlorobenzyl thiocyanate indeed afforded all three possible disulfides in varying amounts (two homo-coupled products and one cross-coupled product) (Table II.5, entry 1). After the reaction and work-up, HPLC analysis of the crude mixture showed three peaks of which two are from homo-coupled products (confirmed by co-injection), leaving the third peak assigned for the cross over product i.e. the unsymmetrical disulfide. Similar results are observed when a mixture of other alkyl thiocyanates is subjected to undergo the reaction (Table II.5, entries 2, 3). In all the three examples, the prominent similarity is in the formation of the unsymmetrical disulfide in larger quantity than homo-coupled disulfides. In the case of using acyl methyl thiocyanate as one of the partners, the cross product could not be distinctly analyzed by HPLC and appeared as two overlapping peaks of the total area about 26% only, which is in contrast to the observations in other cases (entry 4).

Table II.5. Synthesis of unsymmetrical disulfides and result analysis by HPLC.[a,b]

Entry	Substrate A	Substrate B	Product A-A (%) / RT (min) [c]	Product B-B (%) / RT (min)	Product A-B (%) / RT (min)
1	C_6H_5-CH_2-SCN	*m*-ClC_6H_4-CH_2-SCN	C_6H_5-CH_2-S-CH_2-C_6H_5 (38) / 4.37	*m*-ClC_6H_4-CH_2-S-CH_2-*m*-C_6H_4Cl (15) / 3.41	*m*-ClC_6H_4-CH_2-S-$CH_2C_6H_5$ (47) / 3.71
2	C_6H_5-CH_2-SCN	C_6H_5-$(CH_2)_3$-SCN	C_6H_5-CH_2-S-CH_2-C_6H_5 (37.4) / 3.36	C_6H_5-$(CH_2)_3$-S-$(CH_2)_3$-C_6H_5 (15.5) / 3.92	C_6H_5-$(CH_2)_3$-S-CH_2-C_6H_5 (47.1) / 3.55
3	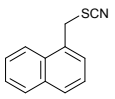	*p*-ClC_6H_4-CH_2-SCN	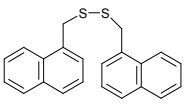 (22.0) / 9.54	*p*-ClC_6H_4-CH_2-S-CH_2-*p*-C_6H_4Cl (25.4) / 3.63	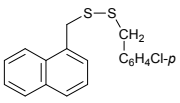 (52.6) / 5.29
4	C_6H_5-CH_2-SCN	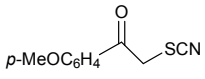	C_6H_5-CH_2-S-CH_2-C_6H_5 (27.8) / 1.79[d]	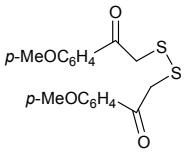 (45.7) / 8.35	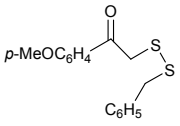 2.6 & 2.9 / 16.7 & 9.8[e]

[a] Column: ZORBAX Rx-SIL (4.6 x 150 mm, 5µm); Temperature: Ambient (25 ^oC); Mobile phase: hexane for entries (1-3), and 1% *i*-PrOH in hexane for entry 4; flow rate = 2 mL/min for all entries. [b] Peaks were confirmed by co-injection with homo-coupled disulfides. [c] t_R in minute for the peaks indicated by RI Detector, [d] t_R in minute for the peaks indicated by UV detector at λ = 380 nm. [e] Unsymmetrical disulfide showed overlapping of two peaks, as indicated with t_R (min) and area respectively.

As regard to the mechanism of the reaction, formation of the cross-over product suggests that the S–S linkage is made in a step-wise manner and not through a concerted process. In the presence of heterogeneous base, presumably the nucleophilic thiolate anion is formed initially, which could displace the cyanide ion of another organyl thiocyanate resulting in the

formation of the disulfide and the ion-exchange resins possibly could scavenge the cyanide ion (Scheme II.7).

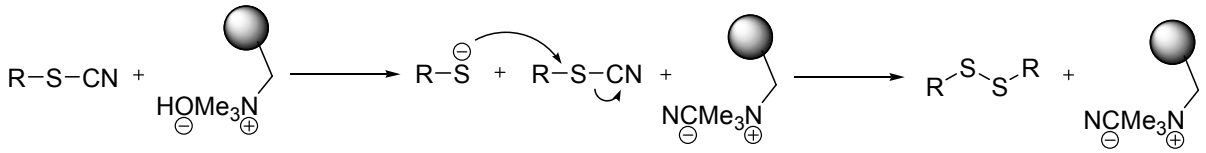

Scheme II.7. Probable mechanism of the reaction.

We also checked the reusability of the poly-ionic resins hydroxide taking the model reaction with benzyl thiocyanate. It is observed that the resins can be reused after filtration from the reaction mixture, washed with water followed by acetone and then dried under vacuum. Although, disulfide is obtained up to the fourth run requiring longer reaction time, the yield of the product showed a gradual decreasing trend (from 90 % to 75%) (Table II.6).

Table II.6. Recycling of Amberlyst® A-26(OH) in the dimerization of benzyl thiocyanates.[a]

Run	pH	Time (h)	Yield (%)
1	9.4	3	90
2	8.2	6	78
3	8.0	8	75
4	7.9	10	75

[a] Reactions were carried out using Amberlyst® A-26(OH) for 2 mmol of the substrate in water. [b] pH of the resin-suspended water was measured before each run.

II.4. Conclusion

We have developed an efficient and eco-friendly protocol to form disulfide bond (S−S linkage) from alkyl and acyl methyl thiocyanates producing corresponding disulfides in good to excellent yields by using Amberlyst® A-26(OH) in aqueous medium. The present protocol further establishes the advantage of using the heterogeneous base Amberlyst® A-26(OH) over some existing homogeneous bases (NaOH, NH_3, K_2CO_3). Other notable features are: (i) reaction can be carried out in water and simple filtration and removal of the water could afford the organic disulfide; (ii) the resins can be reused for three more runs tested with appreciable conversions; (iii) cross-over experiments revealed that the procedure is somewhat effective for the preparation of unsymmetrical disulfides.

II.5. Experimental section

II.5.1. General information

All the reactions were carried out in open vessel under aerobic conditions. Amberlyst® A-26 (

OH) was purchased from Sigma-Aldrich, India. For column chromatography: silica (60-120 mesh) (SRL, India), and for tlc, Merck plates coated with silica gel 60, F_{254} were used. NMR spectra of the disulfide were recorded in $CDCl_3$ on Bruker AV 300 spectrometer using TMS as the internal standard. HRMS data were obtained in Micromass Q-Tof micro Mass Spectrometer under ESI (positive mode). HPLC analyses were carried out in Agilent 1260 Series (Quaternary Pump) using ZORBAX Rx-SIL (4.6 x 150 mm, 5μm).

II.5.2. General procedure for the preparation of disulfide

To a mixture of alkyl/acyl methyl thiocyanate (2 mmol) in water (2 mL) was added Amberlyst® A-26(OH) (300 mg) (Source: Sigma-Aldrich) and the reaction mixture was stirred with a magnetic bar gently at 60-80 ^oC. The progress of the reaction was monitored by tlc. After the reaction continued for specific time, as mentioned in Table II.2, the resin beads were separated by filtration over a piece of cotton. The reaction mixture was washed repeatedly with diethyl ether and combined ethereal layer was dried over anhydrous Na_2SO_4 and concentrated. The crude product (almost pure) was further purified by column chromatography over silica gel. The products were identified on the basis of ^1H, ^{13}C NMR and HRMS data, and/or by comparison with the data reported in the literature.

II.5.3. Physical properties and spectral data of compounds

Table II.2, entry 1

1,2-Dibenzyldisulfane[8b]

White crystalline solid, mp 70-71 ^oC (Lit. mp 67 ^oC)

^1H NMR ($CDCl_3$, 300 MHz): δ/ppm 3.66 (s, 4H), 7.28-7.50 (m, 10H); ^{13}C NMR ($CDCl_3$, 75 MHz): δ/ppm 43.2, 127.4, 128.4, 129.4, 137.3; ESI-HRMS: m/z$[M+Na]^+$ for $C_{14}H_{14}S_2$, calculated 269.0434; observed 269.0412.

Table II.2, entry 2

1,2-Bis(2-chlorobenzyl)disulfane[18]

White crystalline solid, mp 89-90 ^oC (Lit. mp 89-90 ^oC)

^1H NMR ($CDCl_3$, 300 MHz): δ/ppm 3.79 (s, 4H), 7.20-7.28 (m, 6H), 7.35-7.39 (m, 2H); ^{13}C NMR ($CDCl_3$, 75 MHz): δ/ppm 41.1, 126.7, 128.9, 129.7, 131.6, 134.1, 135.0.

Table II.2, entry 3

1,2-Bis(3-chlorobenzyl)disulfane[19]

Colourless oil

^1H NMR ($CDCl_3$, 300 MHz): δ/ppm 3.49 (s, 4H), 7.02-7.06 (m, 2H), 7.15-7.20 (m, 6H); ^{13}C

NMR ($CDCl_3$, 75 MHz): δ/ppm 42.6, 127.5, 127.7, 129.5, 129.8, 134.3, 139.3.

Table II.2, entry 4

1,2-Bis(4-chlorobenzyl)disulfane[8b]

Crystalline solid, mp 58-60 °C (Lit. mp 62 °C)

^{1}H NMR ($CDCl_3$, 300 MHz): δ/ppm 3.57 (s, 4H), 7.14 (d, J = 6.3 Hz, 4H), 7.29 (d, J = 6.3 Hz, 4H); ^{13}C NMR ($CDCl_3$, 75 MHz): δ/ppm 42.5, 128.7, 130.7, 133.4, 135.8.

Table II.2, entry 5

1,2-Bis(3-bromobenzyl)disulfane

Colourless liquid

^{1}H NMR ($CDCl_3$, 300 MHz): δ/ppm 3.53 (s, 4H), 7.13-7.25 (m, 4H), 7.37-7.43 (m, 4H); ^{13}C NMR ($CDCl_3$, 75 MHz): δ/ppm 42.5, 122.4, 128.0, 130.1, 130.6, 132.3, 139.5; ESI-HRMS: m/z[M+Na]$^+$for $C_{14}H_{12}Br_2S_2Na$, calculated 424.8645; observed 424.8674.

Table II.2, entry 6

1,2-Bis(3-iodobenzyl)disulfane

Colourless liquid

^{1}H NMR ($CDCl_3$, 300 MHz): δ/ppm 3.51 (s, 4H), 7.05-7.10 (m, 2H), 7.19-7.21 (m, 2H), 7.58-7.63 (m, 4H); ^{13}C NMR ($CDCl_3$, 75 MHz): δ/ppm 42.4, 94.3, 128.7, 130.3, 136.5, 138.3, 139.6; ESI-HRMS: m/z[M+Na]$^+$for $C_{14}H_{12}I_2S_2Na$, calculated 520.8367; observed 520.8411.

Table II.2, entry 7

1-((Naphthalene-1-yl)methyl)-2-((naphthalene-5-yl)methyl)disulfane[20]

White crystalline solid, mp 106-108 °C (Lit. mp 108-109 °C)

^{1}H NMR ($CDCl_3$, 300 MHz): δ/ppm 3.95 (s, 4H), 7.10-7.12 (m, 2H), 7.32-7.37 (m, 2H), 7.48-7.53(m, 4H), 7.76-7.79 (m, 2H), 7.83-7.86 (m, 2H), 7.95-7.99 (m, 2H); ^{13}C NMR ($CDCl_3$, 75 MHz): δ/ppm 41.3, 124.1, 125.2, 125.9, 126.2, 128.2, 128.5, 128.8, 131.3, 132.7, 133.9; ESI-HRMS: m/z[M+Na]$^+$for $C_{22}H_{18}S_2Na$, calculated 369.0746; observed 369.0749.

Table II.2, entry 9

1,2-Dioctyldisulfane[21]

Colourless Oil

^{1}H NMR ($CDCl_3$, 300 MHz) δ/ppm 0.88 (t, J = 6.6 Hz, 6H), 1.26-1.41 (m, 20H), 1.58-1.72 (m, 4H), 2.68 (t, J = 7.2 Hz, 4H); ^{13}C NMR ($CDCl_3$, 75 MHz) δ/ppm 14.1, 22.7, 28.6, 29.20, 29.23, 29.7, 31.8, 39.2.

Table II.2, entry 10

1,2-Bis(3-phenylpropyl)disulfane[22]

Liquid

^{1}H NMR ($CDCl_3$, 300 MHz): δ/ppm 1.95-2.05 (m, 4H), 2.64-2.72 (m, 8H), 7.15-7.20 (m, 6H), 7.24-7.30 (m, 4H); ^{13}C NMR ($CDCl_3$, 75 MHz): δ/ppm 30.4, 33.9, 38.2, 125.6, 128.46, 128.5, 141.4.

Table II.2, entry 11

1,2-Dicinnamyldisulfane[23]

White crystalline solid, mp 89-90 ^{o}C (Lit. mp 90-91 ^{o}C)

^{1}H NMR ($CDCl_3$, 300 MHz): δ/ppm 3.47 (dd, *J* = 7.8 and 1.2 Hz, 4H), 6.11-6.21 (m, 2H), 6.45 (d, *J* = 15.6 Hz, 2H), 7.19-7.35 (m, 10H); ^{13}C NMR ($CDCl_3$, 75 MHz): δ/ppm 42.5, 124.5, 126.4, 127.7, 128.6, 133.6, 136.7.

Table II.2, entry 12

2,2'-Disulfanediylbis[1-(phenyl)ethanone][24]

White crystalline solid, mp 81-82 ^{o}C (Lit. mp 79-81 ^{o}C)

^{1}H NMR ($CDCl_3$, 300 MHz): δ/ppm 3.99 (s, 4H), 7.45-7.50 (m, 4H), 7.57-7.59 (m, 2H), 7.96-7.99 (m, 4H); ^{13}C NMR ($CDCl_3$, 75 MHz): δ/ppm 37.6, 128.6, 128.7, 133.6, 135.3, 194.2.

Table II.2, entry 13

2,2'-Disulfanediylbis[1-(4-chlorophenyl)ethanone][25]

White crystalline solid, mp 124 ^{o}C (Lit. mp 123-124 ^{0}C)

^{1}H NMR ($CDCl_3$, 300 MHz): δ/ppm 3.95 (s, 4H), 7.46 (d, *J* = 8.4 Hz 4H), 7.92 (d, *J* = 8.7 Hz 4H); ^{13}C NMR ($CDCl_3$, 75 MHz): δ/ppm 37.5, 129.1, 130.1, 133.6, 140.2, 192.9.

Table II.2, entry 14

2,2'-Disulfanediylbis[1-(3-bromophenyl)ethanone]

Yellow semi-solid, not crystalline

^{1}H NMR ($CDCl_3$, 300 MHz): δ/ppm 4.15 (s, 4H), 7.33-7.38 (m, 2H), 7.69-7.73 (m, 2H), 7.83-7.87 (m, 2H), 8.06-8.07 (m, 2H); ^{13}C NMR ($CDCl_3$): δ/ppm 37.5, 123.1, 127.2, 130.3, 131.6, 136.5, 136.9, 192.6; ESI-HRMS: m/z$[M+Na]^+$for $C_{16}H_{12}Br_2O_2S_2Na$, calculated 480.8543; observed 480.8732.

Table II.2, entry 16

2,2'-Disulfanediylbis[1-(4-methyoxyphenyl)ethanone][25b]

White solid, mp 92-93 ^{o}C

^{1}H NMR ($CDCl_3$, 300 MHz): δ/ppm 3.88 (s, 6H), 3.95 (s, 4H), 6.95 (d, *J* = 9 Hz, 4H), 7.97 (d, *J* = 9 Hz, 4H); ^{13}C NMR ($CDCl_3$, 75 MHz): δ/ppm 37.4, 55.5, 113.9, 128.3, 131.0, 163.8,

193.0; ESI-HRMS: m/z$[M+Na]^+$ for $C_{18}H_{18}S_2O_4Na$, calculated 385.0546; observed 385.0545.

II.6. References

References are given in BIBLIOGRAPHY under Chapter II (pp. 145−146).

CHAPTER III

Copper oxide nanoparticles embedded on macroporous poly–ionic resins (CuO@ARF): Applications to on–water C–S cross–coupling and synthesis of heterocyclic scaffold phenothiazine

III.1. Introduction

The carbon–sulfur bonds are present in numerous medicinally important natural products.[1] Indeed a number of drugs in various therapeutic uses such as HIV, cancer, diabetes, inflammatory, Alzheimer's and Parkinson's diseases contain the aryl sulphide functional group.[2] A few biologically active compounds possessing C−S bond are represented in Figure III.1. For example, phenothiazines are important class of organic compounds finding wide applications as drugs, insecticides, inhibitors of polymerization, antioxidants, paints, spectroscopic probes etc.[3]

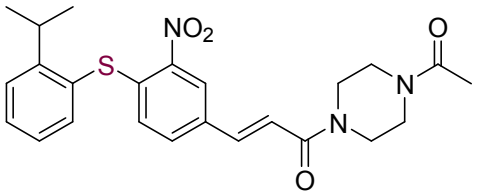

LFA-1/ICAM-1 Antagonists

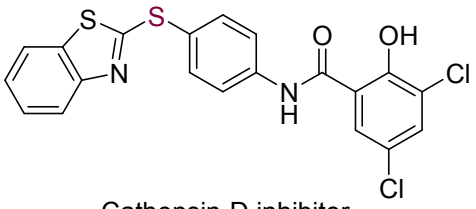

Cathepsin-D inhibitor

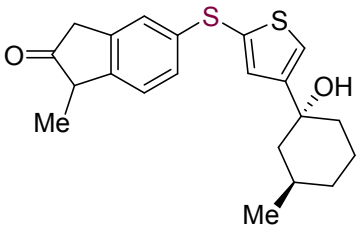

AZD4407
5-lipoxygenase inhibitor

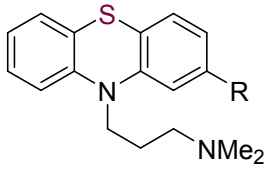

R = H, promazine
R = Cl, chloropromazine
R = CF_3, triflupromazine
Used for Psychotropic medication

Figure III.1. Some biologically active compounds bearing C−S bond.

The conventional methods for the C−S bond formation involve reduction of aryl sulfones or aryl sulfoxides using strong reducing agents like DIBAL-H or $LiAlH_4$.[4] In 1980, Migita et al. first showed the Pd-catalyzed thiation of aryl bromides using $Pd(PPh_3)_4$.[5] Subsequently, other metals like nickel,[6] copper,[6a,7] cobalt,[8] iron,[9] rhodium,[10] manganese[11] and indium[12] have also been employed, though in much less extent, as compared to other C−X (X = C, O, N, P) coupling reactions. Amongst various transition metals, copper has been considered as the most useful for the C−S coupling reactions due to its special redox properties and cost–effectiveness. Many strategies have been successful by using homogeneous copper salts in the presence of suitable electron–rich and precious ligands for the C−S coupling reactions.[13]

Two major aspects of green and sustainable processes includes: (i) catalytic transformations, more specifically through heterogeneous catalysis, and (ii) the eco-friendly reaction media, in particular reactions being performed in water. While heterogeneous catalysis offers easy separation of the product from the catalytic system and the possibility of further recycling of

the catalyst, on/in-water reactions are not only environmentally friendly but also economically more viable. Therefore, it is not surprising to see the significant growth for new catalytic transformations in aqueous medium.[14]

III.2. Present work: Background and Objectives

In previous years CuO nanoparticles are a good choice and indeed useful catalyst for C−S coupling reaction between aryl halide and thiols.[15] Since direct use of CuO in the C−S coupling reaction in water gave relatively poor yield as compared to other metal salts. Some literature reports for on water C−S coupling reactions have been discussed here.

Tellitu and co-workers have developed an environmentally friendly protocol to synthesized diaryl sulphides in water. The reactions were catalysed by a combination of a cuprous chloride and a 1,2-diamine derivative, (acting both as the ligand and as the base) at 120 ^{o}C (Scheme III.1).[16] The aqueous medium containing the active catalyst was recovered and reuse up to four catalytic cycles.

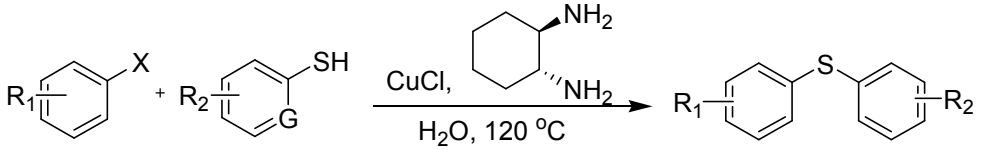

X = I, Br
R_1 = 4-NO_2, 4-OCH_3, 4-Cl, 2-$COCH_3$, 4-NH_2
R_2 = 4-OCH_3, 4-CH_3, 2-NH_2
G = C, N

Scheme III.1. S-arylation of thiophenol derivatives catalyzed by CuCl and 1,2-diamine in water.

Punniyamurthy et al. have described an efficient CuI- catalyzed C−S cross–coupling of thiols with aryl halides in the presence of tetrabutylammonium bromide in water (Scheme III.2).[17]

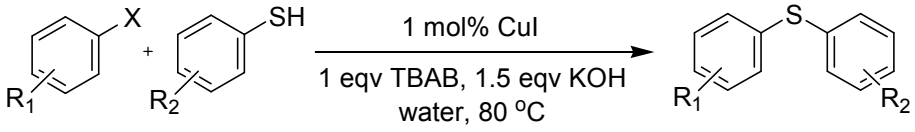

X = I, Br, Cl
R_1 = 4-NO_2, 4-OCH_3
R_2 = 2-CH_3, 4-CH_3, 4-NO_2, 4-OCH_3, 4-Cl

Scheme III.2. Cross–coupling of thiophenol with aryl halides using CuI, TBAB in water.

In 2009 Tsai and their group have reported, $FeCl_3 \cdot 6H_2O$/cationic 2,2'-bipyridyl system as a catalyst in the coupling of aryl iodides with thiols to form an aryl–sulfur bond in refluxed water under aerobic conditions (Scheme III.3).[18] This catalytic system was applicable for aryl iodide only. After extraction of product, remaining aqueous solution was recycled for six times.

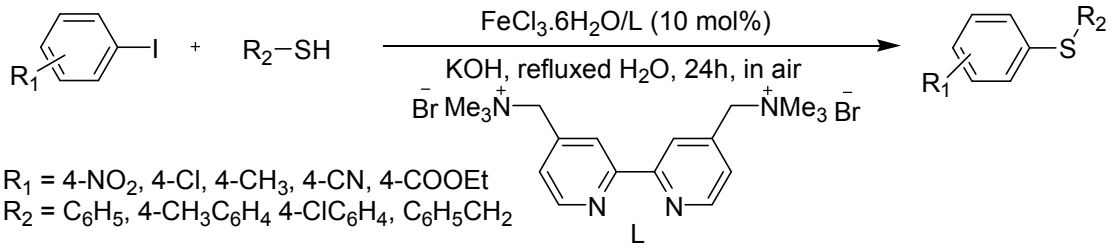

Scheme III.3. Iron-catalyzed S-arylation in water.

Tsai and their group reported another work where $CoCl_2.6H_2O$/cationic 2,2'-bipyridyl system was used for cross–coupling of aryl halides with thiols in water.[19] Aryl iodides and bromides could couple with a variety of thiols giving the analogous thioethers using 3 mol% catalyst loading in the presence of KOH and Zn at 100 ^oC (Scheme III.4). For aryl chlorides, reaction at 140 ^oC and prolongation of the reaction time was required.

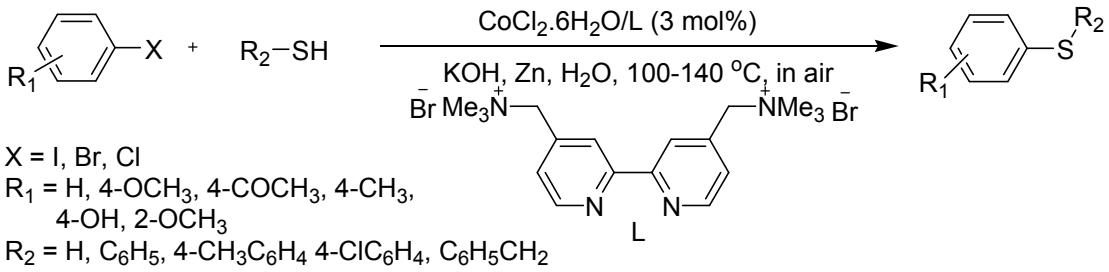

Scheme III.4. Cobalt-catalyzed S-arylation in water.

Chakraborty et al. showed a simple and efficient procedure for C−S cross–coupling of thiophenols with aryl bromides and iodides by using a combination of Bi_2O_3 and *N,N*-dimethylethane- 1,2-diamine in water (Scheme III.5).[20] Only aromatic thiols are used during reaction. They did not isolate the Bi_2O_3 from the aqueous suspension but the aqueous phase containing the catalyst could be recycled repeatedly without much loss in activity of the reaction or yield.

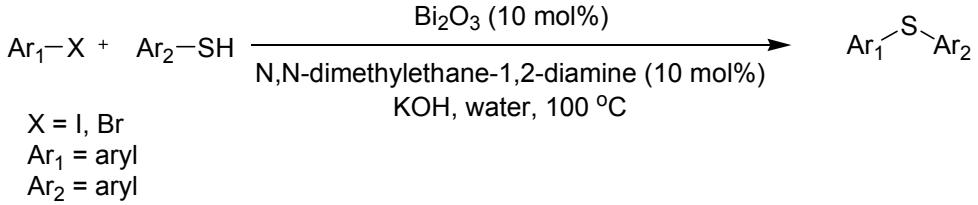

Scheme III.5. Bi_2O_3 catalyzed C−S cross–coupling reaction of thiophenols with aryl halides.

Based on the above observation and considering our experience in the field of developing polymer–supported metal NPs as the heterogeneous catalyst in various coupling reactions,[21] we were interested to develop Amberlite resin–supported CuO NPs and to use it as the catalyst in 'on–water' C−S coupling reaction between aryl halide and thiols.

III.3. Present work: Result and Discussion

III.3.1. Preparation of the heterogeneous CuO (CuO@ARF)

The Amberlite resin formate (ARF) was prepared from commercially available Amberlite IRA 900 (chloride form) by rising with 10% aqueous formic acid solution until free from chloride ion.[22] A mixture of ARF resin beads and $Cu(OAc)_2{\cdot}H_2O$ in DMF (50 mg g^{-1} of ARF) was heated at 110 ^oC in Teflon capped sealed tube for 30 min with occasional gentle shaking. White ARF beads turned brownish in colour during the process. Finally these resin beads were filtered off, washed with water and acetone, dried and characterized by FT–IR, XRD and TEM analysis and the copper content of the composite was estimated by AAS. Since XRD and TEM analyses suggest the presence of CuO nanoclusters distributed on the surface of ARF, we refer to the as–synthesised nanocomposite material as CuO@ARF.

III.3.2. Characterization of CuO@ARF

At first, the presence of copper in the resin composite was measured by the AAS study. For this purpose, the sample (100 mg) was digested with concentrated HNO_3 (1 mL) and Cu content was estimated to be 0.145 mmol g^{-1} of the resin–copper nanocomposite. The FT–IR spectra of CuO@ARF was recorded and compared with that of ARF (Figure III.2). In the case of similar heterogeneous Pd nanocomposite, as developed from this laboratory, significant increase in the stretching frequency of the carboxylate anion ($HCOO^-$) was observed.[21] Here, apparently no change of symmetric and anti–symmetric stretching vibrations (for the $HCOO^-$) was observed and appeared respectively at about 1345 and 1593 cm^{-1} for both ARF and CuO@ARF species (Figure III.2). However, it may be mentioned that CuO absorptions at 606, 525 cm^{-1} might be overlapped with similar absorptions by ARF.[23]

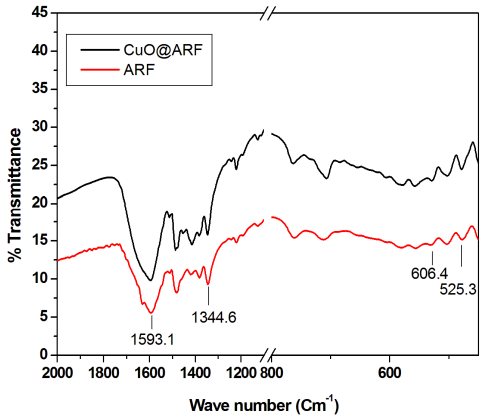

Figure III.2. FT–IR spectra of the ARF and CuO@ARF.

We therefore examined the powder XRD patterns of ARF and that of CuO@ARF, as shown in Figure III.3. The ARF resins are amorphous in nature and the Bragg diffraction patterns of

CuO@ARF indicate the presence of cupric oxide (CuO). The JCPDS peak positions of the CuO@ARF nanocomposite with relative intensities are in good agreement (Figure III.3b). The presence of XRD peaks at 2θ of 35.39, 38.29, 38.99, 57.91 and 61.64^{o} suggested the presence of CuO ($\bar{1}11$), (111), (200), (202) and ($\bar{1}13$) planes, respectively (JCPDS#01–089–2531). Further examination of high resolution TEM (HR–TEM) images of the CuO@ARF at different magnifications (Figure III.4a & III.4b) suggests that the CuO NPs are embedded on the resin polymeric matrices with average size around 2.6 nm (Figure III.4c).

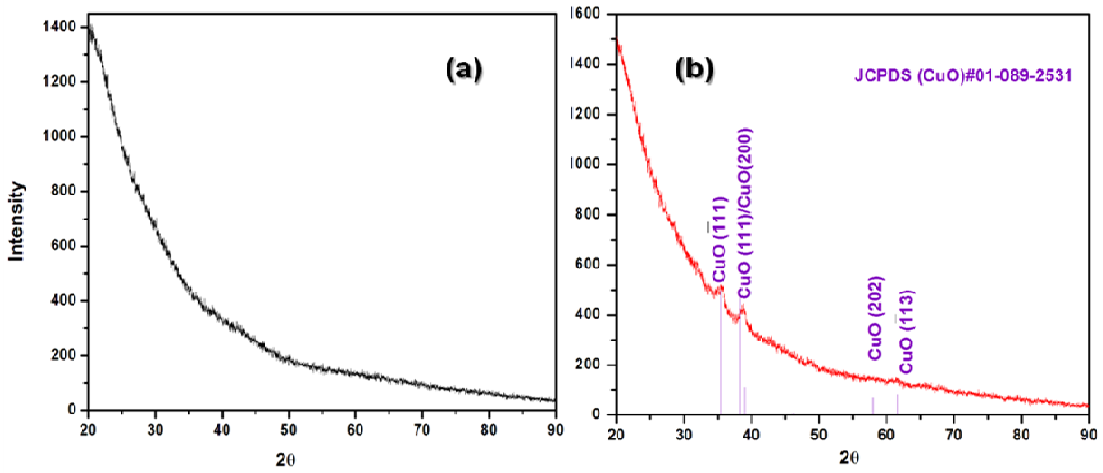

Figure III.3. XRD patterns of (a) ARF, (b) CuO embedded on the surface of Amberlite resin formate (CuO@ARF).

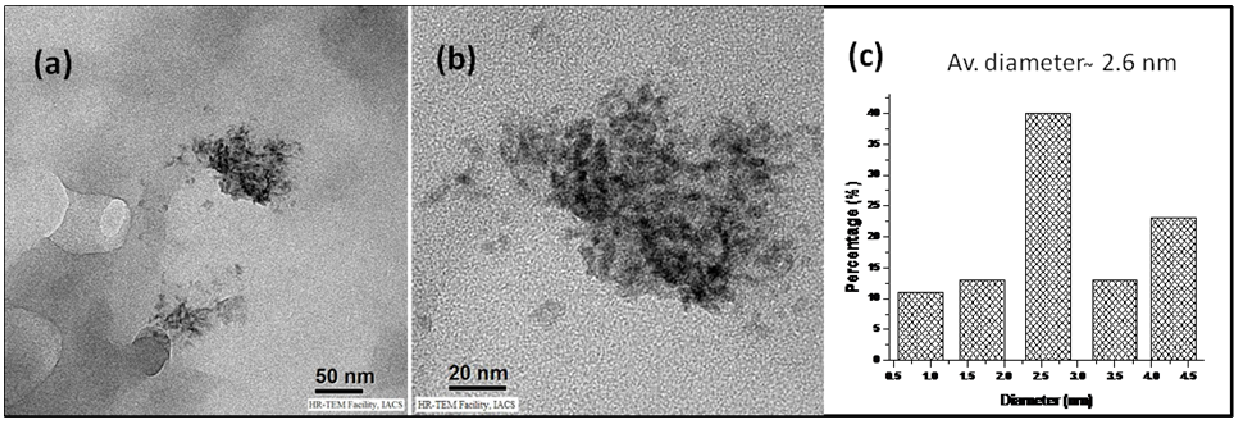

Figure III.4. TEM images of CuO@ARF: (a) scale bar 50 nm; (b) scale bar 20 nm; (c) average particle size distribution evaluated from (b).

III.3.3. Catalytic activity of CuO@ARF

In order to evaluate the catalytic activity of this newly developed nanocomposite (CuO@ARF) in C−S cross–coupling reaction between aryl halide and thiol, we performed a model study by taking a mixture of 4–iodoanisole and benzenethiol (in 1:1.2 ratios) and the catalyst (200 mg mmol^{-1} of aryl iodide) in water (Table III.1). First reaction in the presence

of a base (K_2CO_3) at 100 ^oC did afford the desired unsymmetrical sulfane but with a modest yield (62%) (Table III.1, entry 1). Considering that the modest conversion might be due to the poor solubility of aryl iodide in water, we used an additive – tetrabutylammonium bromide (TBAB), in equimolar quantity. This afforded the corresponding thioether in fairly good yield (83%; entry 2). Further improvement was achieved by using the catalytic amount of sodium dodecyl sulphate (SDS; 10 mol%),[24] which furnished the desired product in 90% isolated yield (entry 3). While there was no cross–coupling observed at room temperature, reaction carried out at 60 ^oC or in the absence of the base produced the sulfane in 56–68% isolated yields (entries 4–6). We also tried the reaction in DMF at 100 ^oC, which did not produce the desired sulfane in very good yield (entry 7). In each case, small quantity of the diphenylsulfide (≤ 5%) as the side product was also formed.

Table III.1. Optimization of reaction condition for the C−S cross–coupling using CuO@ARF.[a]

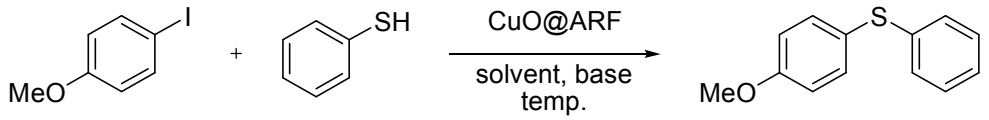

Entry	Solvent	Base	Additive	Temp./Time	Yield (%)[b,c]
1	Water	K_2CO_3	-	100 ^oC/24 h	62
2[d]	Water	K_2CO_3	TBAB	100 ^oC/8 h	83
3[e]	**Water**	**K_2CO_3**	**SDS**	**100 ^oC/8 h**	**90**
4[e]	Water	K_2CO_3	SDS	RT/24 h	00
5[e]	Water	K_2CO_3	SDS	60 ^oC/24 h	68
6[e]	Water	-	SDS	100 ^oC/24 h	56
7	DMF	K_2CO_3	-	100 ^oC/24 h	67

[a]4–Iodoanisole (1 mmol), benzenethiol (1.2 mmol), CuO@ARF (200 mg), K_2CO_3 (1.1 mmol), and solvent (3 mL). [b]Isolated yield. [c]Small quantity of diphenyl disulfide was formed (≤ 5%). [d]TBAB (1 eqv) was used. [e]SDS (10 mol%) was used.

After optimizing the reaction conditions, we examined the minimum amount of the catalyst loading that is required to obtain effective conversion to the sulfane. Experiments were performed with 4–iodoanisole (1 mmol) in the presence of varying quantities of CuO@ARF

(from 50 mg to 250 mg; i.e. 0.46 mg to 2.30 mg of copper $mmol^{-1}$ of iodoarene) and the results are shown in Figure III.5. Conversions to the thioether at different time intervals were measured by HPLC and the plot of %conversion (± 2%) versus time (h) revealed that minimum 200 mg of the catalyst (~1.8 mg of copper) $mmol^{-1}$ of iodoarene can give rise to the best result. In each case, reaction was continued up to 24 h and HPLC analysis showed no appreciable changes in the conversion (Figure III.5 was plotted up to 12h).

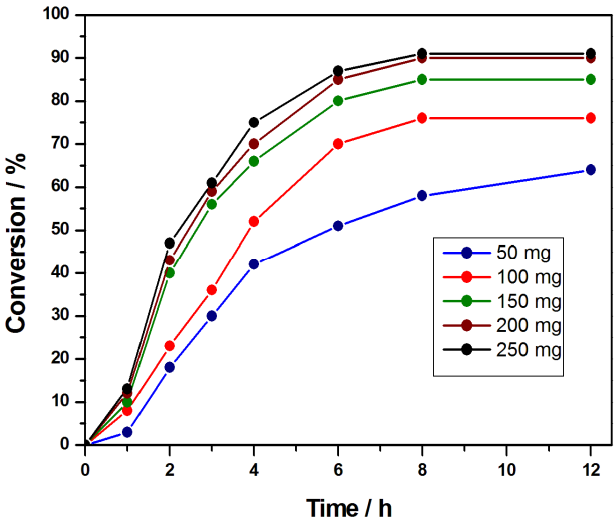

Figure III.5. Time conversion plots for the C−S cross–coupling between 4–iodoanisole and thiophenol under on–water condition at 100 °C in the presence of varied amounts of CuO@ARF. Conversions (± 2%) at different time intervals for each plot were measured by HPLC.

The optimized reaction conditions were then employed with different iodoarenes and other aromatic halides to couple with variety of aryl thiols to examine the scope and limitations of our catalyst for on–water C−S cross–coupling reaction. In general, it was observed that the cross-coupling reaction was successful producing corresponding diaryl sulphide in good to excellent yields. The results are presented in Table III.2. Iodoarenes with both activated (methoxy, methyl) and deactivated functional groups (nitro or acetyl) effectively underwent C−S cross–coupling with different aryl thiols (entries 1–5). On the other hand, similar coupling reactions with bromo– and chlorobenzenes, including *p*–chloroacetophenone were not successful (entries 6, 7). Increasing the catalyst loading and changing the base did not facilitate the C−S cross-coupling of *p*-bromotoluene (entry 8). The selectivity might be useful for substrates bearing different halides. Thus, iodobromoarenes and iodochloroarene were subjected to coupling with aryl thiols in the presence of this heterogeneous catalyst (CuO@ARF) affording highly chemoselective iodo–coupled product only (entries 9–11). Substituted thiophenol like 2,5–dimethylbenzenethiol also underwent smooth reactions (entry 12). Aliphatic thiols also gave cross–coupling products without any difficulty, but relatively

in lower yields as compared to aromatic thiols (entries 13–15). This finding might be attributable to the fact that aliphatic thiols are less reactive than aromatic thiols.[25] Bis–couplings were performed equally efficiently starting from 1,3–diiodobenzene and *p*–tolylthiol and affording the desired 1,3–bis(*p*–tolylthio)benzene as the only product in 79% isolated yield (entry 16). It may be mentioned that only benzenethiol and 4–tolylthiol gave a minor quantity of corresponding disulfides during the reaction (≤ 5%), while in other cases, no disulfide was detected on tlc or by HPLC analysis.

Table III.2. CuO@ARF–catalyzed C−S cross–coupling reactions between haloarenes and thiol.[a]

Entry	Aryl halide	Thiol	Time (h)	Product	Yield (%)[b]
1	(4-H_3CO)C_6H_4I	C_6H_5SH	8	(4-H_3CO)H_4C_6—S—C_6H_5	90
2	(3-H_3CO)C_6H_4I	(4-Cl)C_6H_4SH	12	(3-H_3CO)H_4C_6—S—C_6H_4(4-Cl)	85
3	(2-H_3CO)C_6H_4I	(4-CH_3)C_6H_4SH	18	(2-H_3CO)H_4C_6—S—C_6H_4(4-CH_3)	75
4	(3-NO_2)C_6H_4I	(4-CH_3)C_6H_4SH	11	(3-NO_2)H_4C_6—S—C_6H_4(4-CH_3)	78
5	(4-H_3CO)C_6H_4I	(4-CH_3)C_6H_4SH	10	(4-H_3CO)H_4C_6—S—C_6H_4(4'-CH_3)	75
6	(4-H_3C)C_6H_4Br	C_6H_5SH	24	No reaction	-
7	(4-CH_3CO)C_6H_4Cl	C_6H_5SH	24	No reaction	-
8[c]	(4-H_3C)C_6H_4Br	C_6H_5SH	24	No reaction	-
9	(5-Br)(2-H_3CO)C_6H_3I	C_6H_5SH	8	(5-Br)(2-H_3CO)H_3C_6—S—C_6H_5	90
10	(3-Br)C_6H_4I	(4-CH_3)C_6H_4SH	16	(3-Br)H_4C_6—S—C_6H_4(4-CH_3)	79
11	(3-Cl)C_6H_4I	(4-CH_3)C_6H_4SH	16	(3-Cl)H_4C_6—S—C_6H_4(4-CH_3)	79
12	(4-H_3CO)C_6H_4I	(2,5-CH_3)$_2C_6H_3SH$	7	(4-H_3CO)H_4C_6—S—C_6H_3(2,5-CH_3)$_2$	89
13	(4-H_3CO)C_6H_4I	CySH	16	(4-H_3CO)H_4C_6—S—Cy	70
14	(4-H_3CO)C_6H_4I	*n*-$C_5H_{11}SH$	16	(4-H_3CO)H_4C_6—S—C_5H_{11}-*n*	73
15	(3-H_3CO)C_6H_4I	*n*-$C_7H_{15}SH$	16	(3-H_3CO)H_4C_6—S—C_7H_{15}-*n*	76

16[d]	1,3-$C_6H_4I_2$	(4-CH_3)C_6H_4SH	14	1,3-((4-CH_3)$C_6H_4S)_2$—C_6H_4	79
17	(2-Br)C_6H_4I	(2-NH_2)C_6H_4SH	8	(2-Br)H_4C_6—S—C_6H_4(2-NH_2)	82

[a]Aryl halide: thiol: catalyst (1 mmol: 1.2 mmol: 200 mg), SDS (10 mol%) and K_2CO_3 (1.1 mmol) was taken in water (3 mL), heated at 100 ^oC. [b]Yield refers to pure isolated products characterized by spectroscopic (^1H and ^{13}C NMR) data. [c]Aryl bromide: thiol: catalyst (1 mmol: 1.2 mmol: 300 mg), SDS (10 mol%) and Cs_2CO_3 (1.1 mmol) was taken in water (3 mL), heated at 100 ^oC. [d]aryl halide: thiol: catalyst (0.5 mmol: 1.2 mmol: 200 mg), SDS (10 mol%) and K_2CO_3 (1.1 mmol) was taken in water (3 mL).

The mechanism of the resin embedded CuO–catalyzed C−S coupling reaction is believed to proceed through the oxidative addition followed by reaction with thiol and then reductive elimination steps ($Cu^{II} \rightarrow Cu^{III} \rightarrow Cu^{II}$).[15] The role of the additive SDS is presumably to solubilise the organic substrates in aqueous medium.[26]

III.3.4. Hot filtration test

Leaching of any metallic species from the amberlite resin polymeric matrices during or after the reaction was tested following the literature procedure.[27] Accordingly, the reaction mixture of the C−S cross–coupling between 4–iodoanisole and thiophenol is filtered off to separate out the solid catalysts after 2 h in hot condition, and the filtrate was analyzed by HPLC (~43% conversion). The AAS analysis of the filtrate solution did not show the presence of any copper species. Moreover, further continuing the reaction by heating the liquid phase at 100 ^oC for another 6 h in the absence of any added catalyst (CuO@ARF) did not afford any appreciable conversion (HPLC analysis). These observations signify that any copper species might not be leached out from the heterogeneous support during initial two hours of the reaction (Figure III.6).

III.3.5. Recycling experiments

One of the important factors for a heterogeneous catalyst lies in its efficiency for recycling. We investigated the reusability of CuO@ARF in the reaction between 4–iodoanisole and thiophenol again as the model case. After completion of the reaction, resin beads were filtered off from the reaction mixture, washed thoroughly with water followed by acetone (two times), and then dried under vacuum. The catalyst was reused in five consecutive runs including the first run. Gratifyingly, there was no considerable loss of the catalytic efficiency observed (Figure III.7).

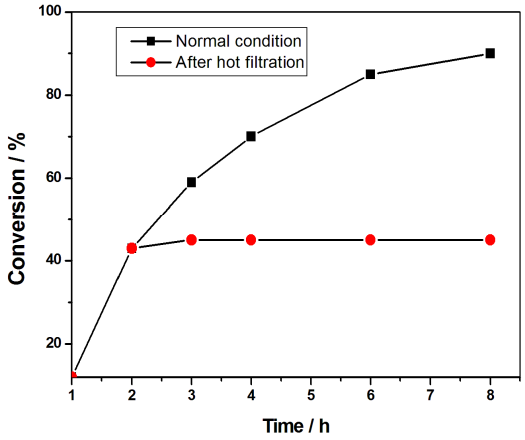

Figure III.6. Comparison of normal time profile with that of hot filtration test. Conversions (±2%) at different time intervals for each plot were measured by HPLC.

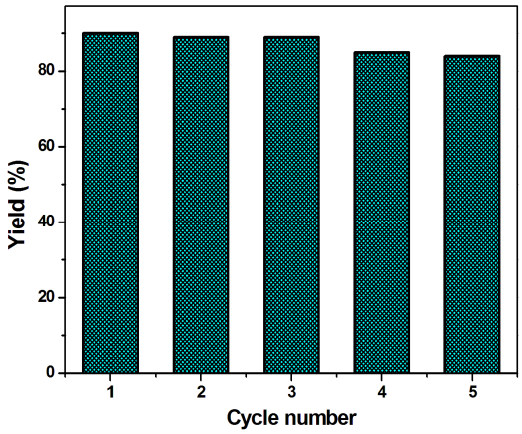

Figure III.7. Recycling experiments using CuO@ARF in the C−S cross–coupling reaction between 4–iodoanisole and thiophenol.

III.3.6. Further application

Since the present catalytic system is highly selective to aryl iodides only (i. e. the first oxidative addition to the sp^2 C−I bond), we decided to utilize this chemoselectivity between iodo– and bromo–substitutents attached to the aryl moiety. Thus, a reaction of 1,2–bromoiodobenzene with 2–aminothiophenol in the presence of the catalyst CuO@ARF under similar conditions in water was performed. The C−S coupling occurred selectively at sp^2 C−I bond and we obtained 2–(2–bromophenylthio)benzene in 82% yield (Scheme III.6). Further intramolecular Buchwald–Hartwig type coupling between amino– and bromo– substituents attached with two aromatic rings under Pd–BINAP catalyzed condition was carried out to afford phenothiazine in 84% isolated yield. The C−N coupling can also be accomplished by using the new catalyst (CuO@ARF) in the presence of L-proline as the ligand (Scheme III.6).[28] The ^{1}H–NMR spectra run in DMSO–D6 and DMSO–D6–D_2O confirmed formation of phenothiazine with the labile NH proton appeared at δ 8.5 ppm (Figure III.8). We also performed the intramolecular Buchwald coupling in water medium using both catalytic systems. Although the reactions works well with comparative yield of the phenothiazine in the case of using $Pd_2(dba)_3$, the use of CuO@ARF as the catalyst however does not give satisfactory yield of the desired cyclic product.

III.4. Conclusion

Our studies established that poly–ionic resin–supported CuO NPs (CuO@ARF) are efficient

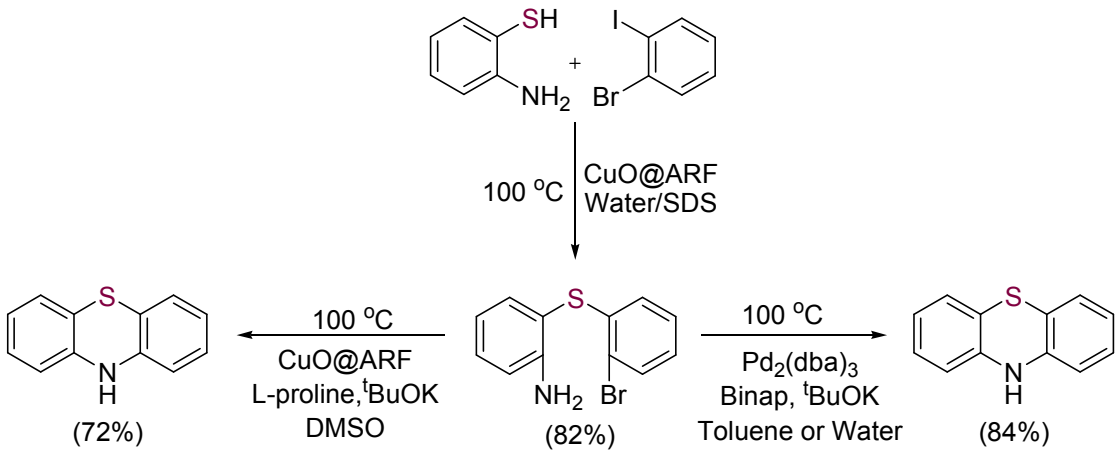

Scheme III.6. Synthesis of Phenothiazine.

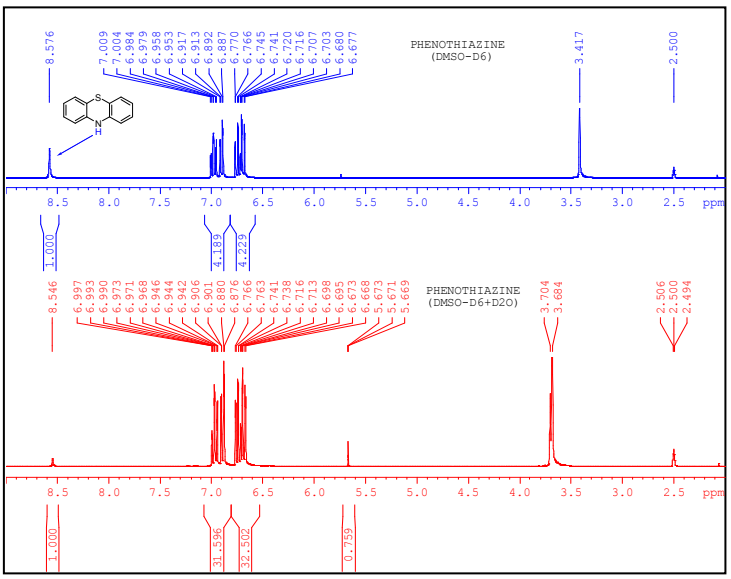

Figure III.8. ^{13}C–NMR spectra of phenothiazine in DMSO–D6 (blue) and DMSO–D6–D_2O (red).

catalyst in the C−S coupling reaction under ligand–free 'on–water' conditions. Low loading of the catalyst, recyclability without leaching and chemoselectivity amongst aromatic halides are notable features. Further application of the chemoselectivity has been demonstrated in the synthesis of bioactive heterocyclic scaffold phenothiazine. Considering the inexpensive catalytic system along with application to the synthesis of medicinally important structural scaffold, this heterogeneous catalyst and greener method can find wider applications in organic synthesis.

III.5. Experimental section

III.5.1. General information

Amberlite IRA 900 (chloride form) was purchased from Across Organics, Belgium and used

after washing with water and acetone followed by drying under vacuum. Cupric acetate was purchased from S.D. Fine Chem. Limited and other chemicals were purchased and used directly. For column chromatography: silica (60–120 mesh) (SRL, India), and for tlc, Merck plates coated with silica gel 60, F254 were used. FTIR spectra were recorded in FT–IR–8300 Shimadzu spectrophotometer. NMR spectra were taken in $CDCl_3$ using Bruker Avance AV–300 spectrometer operating for ^1H at 300 MHz and for ^{13}C at 75 MHz. The spectral data were measured using TMS as the internal standard (for ^1H) and $CDCl_3$ (for ^{13}C). AAS measurements were made using Varian SpectrAA 50B instrument. Progress of the reaction was monitored by HPLC (Agilent Technologies, 1260 Infinity), Column: ZORBAX Rx–SIL (4.6 x 150 mm, 5 μm), eluent: *n*–hexane (flow rate 2 mL min^{-1}). The X–ray diffraction (XRD) studies of the powder samples were done using the Rigaku SmartLab (9 kW) diffractometer using CuKα radiation. High Resolution Transmission Electron Microscopy (HRTEM) of the samples was recorded with JEOL JEM–2100F (FEG) operating at 200 kV.

The amberlite resin formate (ARF) was prepared from commercially available Amberlite IRA 900 (chloride form) (Source: Acros Organics, Belgium) by rinsing with 10% aqueous formic acid solution until free from chloride ions. The resin beads were then washed with water followed by acetone, dried under vacuum, and used for the preparation of CuO@ARF heterogeneous nanomaterial.

III.5.2. Preparation of CuO@ARF

To a solution of $Cu(OAc)_2{\cdot}H_2O$ (50 mg, 0.25 mmol) in DMF (5 mL) was added ARF (1 g) and the mixture taken in teflon capped sealed tube was heated at 110 ^oC for 30 min with occasional gentle shaking. The supernatant liquid became completely colourless by this time and the greyish beads of ARF visibly turned brownish. The mixture was cooled to room temperature and the resin beads were filtered off and washed repeatedly with water (3 x 5 mL) and acetone (2 x 5 mL). Resulting brown beads were dried under vacuum and used for analyses and evaluation of catalytic activity.

III.5.3. General procedure for C−S cross–coupling reaction

To a suspension of CuO@ARF (200 mg) in water (3 mL) were added aryl halide (1 mmol), thiol (1.2 mmol), K_2CO_3 (1.1 mmol) and SDS (10 mol%), and the reaction mixture was heated in a screw-capped sealed tube at 100 ^oC for several hours as mention in Table III.2. Proceeding of the reaction was monitored by tlc at time intervals. After completion, the mixture was cooled, diluted with water (5 mL) and then filtered through a cotton bed to

separate out the resin beads. The resin beads were washed with ethyl acetate (2 mL) and the filtrate was extracted with ethyl acetate (3 x 10 mL). The combined organic layer was dried over anhydrous Na_2SO_4 and concentrated under vacuum. The residue obtained was purified by column chromatography using light petroleum as the eluent. All products were identified on the basis of spectral data (^1H and ^{13}C NMR), and also compared with reported melting point (for solid compounds and as available).

The resin beads separated out from the reaction mixture were successively washed with water (3 x 5 mL), acetone (2 x 5 mL) and then dried under vacuum for use in the next batch of recycle run.

III.5.4. Preparation of phenothiazine from selective iodo-coupled product (Table III.2, entry 17) using Pd-BINAP catalyst

To a mixture of 2–(2–bromophenylthio)benzeneamine (1 mmol, 280 mg) in toluene were added ^{t}BuOK (1.5 mmol, 168 mg), $Pd_2(dba)_3$ (2 mol%) and BINAP (4 mol%). The reaction mixture taken in a screw-capped sealed tube was heated at 100 ^oC for 4 h. After cooling, the reaction mixture was diluted with water (5 mL) and extracted with ethyl acetate (3 x 10 mL). The combined extracts were washed with brine, dried (Na_2SO_4) and evaporated. The residue was purified over silica gel column to obtain white crystals of phenothiazine (167 mg, 84 %), characterized by ^1H and ^{13}C NMR and compared with literature data.

III.5.5. Preparation of phenothiazine from selective iodo-coupled product (Table III.2, entry 17) using CuO@ARF catalyst

To a mixture of 2–(2–bromophenylthio)benzeneamine (1 mmol, 280 mg) in dimethyl sulfoxide were added ^{t}BuOK (1.5 mmol, 168 mg), CuO@ARF (200 mg, 1.8 mg of copper, 2.83 mol% Cu) and L-proline (5.66 mol%). The reaction mixture taken in a screw-capped sealed tube was heated at 100 ^oC for 48 h. After cooling, the reaction mixture was diluted with water (5 mL) and extracted with ethyl acetate (3 x 10 mL). The combined extracts were washed with brine, dried (Na_2SO_4) and evaporated. The residue was purified over silica gel column to obtain white crystals of phenothiazine (143 mg, 72 %), characterized by ^1H and ^{13}C NMR and compared with literature data.

III.5.6. Physical properties and spectral data of compounds:

Table III.2, entry 1

(4–Methoxyphenyl)(phenyl)sulfane[29]

Colourless liquid

^{1}H NMR ($CDCl_3$, 300 MHz): δ/ppm 3.81 (s, 3H, OCH_3), 6.89 (dd, *J* = 2.1 and 6.9 Hz, 2H, ArH), 7.13–7.25 (m, 5H, ArH), 7.41 (dd, *J* = 2.1, 6.6 Hz, 2H, ArH); ^{13}C NMR ($CDCl_3$, 75 MHz): δ/ppm 55.3, 114.9, 124.1, 125.7, 128.1, 128.9, 135.3, 138.6, 159.7.

Table III.2, entry 2

(4–Chlorophenyl)(3–methoxylphenyl)sulfane[30]

Colourless liquid

^{1}H NMR ($CDCl_3$, 300 MHz): δ/ppm 3.75 (s, 3H, OCH_3), 6.80–6.81(m, 1H, ArH), 6.85–6.91(m, 2H, ArH), 7.20 (d, *J* = 8.1 Hz, 1H, ArH), 7.24–7.26 (m, 4H, ArH); ^{13}C NMR ($CDCl_3$, 75 MHz): δ/ppm 55.2, 113.1, 116.2, 123.2, 129.3, 130.1, 132.3, 133.1, 134.1, 136.4, 160.1.

Table III.2, entry 3

(2–Methoxyphenyl)(*p*–tolyl)sulfane[29]

Colourless liquid

^{1}H NMR ($CDCl_3$, 300 MHz): δ/ppm 2.35 (s, 3H, CH_3), 3.88 (s, 3H, OCH_3), 6.80–6.88 (m, 2H, ArH), 6.94 (dd, *J* = 1.5 and 7.8 Hz, 1H ArH), 7.13–7.20 (m, 3H, ArH), 7.31 (d, *J* = 8.1 Hz, 2H, ArH); ^{13}C NMR ($CDCl_3$, 75 MHz): δ/ppm 21.1, 55.8, 110.6, 121.2, 125.7, 127.4, 129.7, 129.8, 130.1, 132.9, 137.7, 156.5.

Table III.2, entry 4

(3–Nitrophenyl)(*p*–tolyl)sulfane[18]

Pale yellow solid, mp 57–58 ^{o}C (Lit. mp 60–61 ^{o}C)

^{1}H NMR ($CDCl_3$, 300 MHz): δ/ppm 2.39 (s, 3H, CH_3), 7.22 (d, *J* = 9.0 Hz, 2H, ArH), 7.37–7.45 (m, 4H, ArH), 7.94–7.96 (m, 2H, ArH); ^{13}C NMR ($CDCl_3$, 75 MHz): δ/ppm 21.2, 120.4, 122.2, 127.8, 129.5, 130.7, 133.3, 134.1, 139.5, 141.6, 148.6.

Table III.2, entry 5

(4–Methoxyphenyl)(*p*–tolyl)sulfane[31]

Colourless liquid

^{1}H NMR ($CDCl_3$, 300 MHz): δ/ppm 2.29 (s, 3H, CH_3), 3.79 (s, 3H, OCH_3), 6.86 (d, *J* = 9.0 Hz, 2H, ArH), 7.05 (d, *J* = 8.1 Hz, 2H, ArH), 7.13 (d, *J* = 8.1 Hz, 2H, ArH), 7.35 (d, *J* = 9.0 Hz, 2H, ArH); ^{13}C NMR ($CDCl_3$, 75 MHz): δ/ppm 20.9, 55.3, 114.8, 125.6, 129.3, 129.7, 134.3, 136.1, 159.4.

Table III.2, entry 9

(5–Bromo–2–methoxyphenyl)(phenyl)sulfane[29]

Colourless liquid

^{1}H NMR ($CDCl_3$, 300 MHz): δ/ppm 3.84 (s, 3H, OCH_3), 6.73 (d, *J* = 8.4 Hz, 1H, ArH), 7.03

(d, J = 2.4 Hz, 1H, ArH), 7.26 (dd, J = 2.4 and 8.7 Hz, 1H, ArH), 7.31–7.40 (m, 5H, ArH); ^{13}C NMR ($CDCl_3$, 75 MHz): δ/ppm 56.1, 112.1, 113.2, 127.7, 128.0, 129.4, 130.1, 132.1, 132.5, 132.7, 155.7.

Table III.2, entry 10

(3–Bromophenyl)(*p*–tolyl)sulfane[32]

Colourless liquid.

^{1}H NMR ($CDCl_3$, 300 MHz): δ/ppm 2.36 (s, 3H, CH_3), 7.10–7.18 (m, 4H, ArH), 7.24–7.28 (m, 1H, ArH), 7.32–7.35 (m, 3H, ArH); ^{13}C NMR ($CDCl_3$, 75 MHz): δ/ppm 21.2, 122.9, 127.2, 129.0, 129.4, 130.2, 130.3, 131.1, 133.2, 138.5, 140.3.

Table III.2, entry 11

(3–Chlorophenyl)(*p*–tolyl)sulfane

Colourless liquid

^{1}H NMR ($CDCl_3$, 300 MHz): δ/ppm 2.36 (s, 3H, CH_3), 7.07–7.19 (m, 6H, ArH), 7.34 (dd, J = 1.8 and 6.3 Hz, 2H, ArH); ^{13}C NMR ($CDCl_3$, 75 MHz): δ/ppm 21.2, 126.1, 126.7, 128.3, 129.4, 129.9, 130.3, 133.3, 134.8, 138.6, 140.0.

Table III.2, entry 12

(4–Methoxyphenyl)(2,5–dimethylphenyl)sulfane[33]

Colourless liquid

^{1}H NMR ($CDCl_3$, 300 MHz): δ/ppm 2.20 (s, 3H, CH_3), 2.32 (s, 3H, CH_3), 3.80 (s, 3H, OCH_3), 6.85–6.92 (m, 4H, ArH), 7.06 (d, J = 7.5 Hz, 1H, ArH), 7.29 (dd, J = 2.1 and 6.6 Hz, 2H, ArH); ^{13}C NMR ($CDCl_3$, 75 MHz): δ/ppm 19.8, 20.9, 55.3, 114.9, 124.9, 127.2, 130.1, 130.2, 133.9, 134.3, 136.0, 136.1, 159.2.

Table III.2, entry 13

Cyclohexyl(4–methoxyphenyl)sulfane[34]

Colourless liquid

^{1}H NMR ($CDCl_3$, 300 MHz): δ/ppm 1.21–1.94 (m, 10H, CH_2), 2.89 (m, 1H, S–CH), 3.80 (s, 3H, OCH_3), 6.83 (dd, J = 2.1 and 6.6 Hz, 2H, ArH), 7.36–7.40 (m, 2H, ArH); ^{13}C NMR ($CDCl_3$, 75 MHz): δ/ppm 25.8, 26.1, 33.4, 47.9, 55.3, 114.3, 125.1, 135.5, 159.3.

Table III.2, entry 14

(4–Methoxyphenyl)(pentyl)sulfane[35]

Colourless liquid

^{1}H NMR ($CDCl_3$, 300 MHz): δ/ppm 0.88 (t, J = 7.2 Hz, 3H), 1.26–1.40 (m, 4H, CH_2–CH_2), 1.56–1.61 (m, 2H, CH_2), 2.81 (m, 2H, S–CH_2), 3.79 (s, 3H, OCH_3), 6.83 (dd, J = 2.1 and 6.6

Hz, 2H, ArH), 7.33 (dd, J = 2.1 and 6.6 Hz, 2H, ArH); ^{13}C NMR ($CDCl_3$, 75 MHz): δ/ppm 13.9, 22.2, 29.0, 30.8, 35.7, 55.3, 114.4, 126.9, 132.9, 158.6.

Table III.2, entry 15

Heptyl(3–methoxyphenyl)sulfane

Colourless liquid

^{1}H NMR ($CDCl_3$, 300 MHz): δ/ppm 0.85–0.90 (m, 3H, CH_3 and CH_2), 1.26–1.68 (m, 10H, CH_2), 2.91 (t, J = 7.2 Hz, 2H, S–CH_2), 3.79 (s, 3H, OCH_3), 6.696 (ddd, J = 0.9, 2.4 and 8.1 Hz, 1H, ArH), 6.85–6.91(m, 2H, ArH), 7.16–7.25 (m, 1H, ArH); ^{13}C NMR ($CDCl_3$, 75 MHz): δ/ppm 14.0, 22.6, 28.8, 29.1, 31.3, 31.7, 33.3, 55.2, 111.2, 114.0, 120.8, 129.6, 138.5, 159.8.

Table III.2, entry 16

1,3–Bis(*p*–tolylthio)benzene[29]

White solid, mp 84–85 ^{o}C

^{1}H NMR ($CDCl_3$, 300 MHz): δ/ppm 2.34 (s, 6H, CH_3), 6.98–7.01 (m, 2H, ArH), 7.06–7.13 (m, 6H, ArH), 7.27 (dd, J = 1.5 and 6.3 Hz, 4H, ArH); ^{13}C NMR ($CDCl_3$, 75 MHz): δ/ppm 21.1, 126.6, 129.0, 129.3, 130.1, 132.9, 138.0, 138.7.

Table III.2, entry 17

2–(2–Bromophenylthio)benzenamine[28]

Brownish solid, mp 63–64 ^{o}C (Lit. mp 62–63 ^{o}C)

^{1}H NMR ($CDCl_3$, 300 MHz): δ/ppm 4.13 (s, 2H, NH_2), 6.60 (dd, J = 1.5 and 7.8 Hz, 1H, ArH), 6.75–6.83 (m, 2H, ArH), 6.92–6.98 (m, 1H, ArH), 7.05–7.10 (m, 1H, ArH), 7.23–7.30 (m, 1H, ArH), 7.43–7.52 (m, 2H, ArH); ^{13}C NMR ($CDCl_3$, 75 MHz): δ/ppm 113.0, 115.5, 119.0, 120.6, 126.1, 126.2, 127.7, 131.7, 132.7, 137.79, 137.8, 148.9.

NMR spectral data for Phenothiazine

10*H*–Phenothiazine[28]

White solid, mp 185–186 ^{o}C (Lit. mp 186–187 ^{o}C)

^{1}H NMR (DMSO–d6, 300 MHz): δ/ppm 6.72–6.77 (m, 4H, ArH), 6.89–7.01 (m, 4H, ArH), 8.58 (s, 1H, NH); ^{13}C NMR (DMSO–d6, 75 MHz): δ/ppm 114.4, 116.4, 121.8, 126.3, 127.5, 142.1.

III.6. References

References are given in BIBLIOGRAPHY under Chapter III (pp. 146−148).

CHAPTER IV

Pd/Cu bimetallic nanoparticles embedded in macroporous ion-exchange resins: An excellent heterogeneous catalyst for the Sonogashira reaction

IV.1. Introduction

Bronze is an alloy of copper and tin was the oldest record of a man-made bimetallic material, aimed to improving the performance of each of its two components. The bimetallic age of catalysis has taken a bit longer to come out, but it is now here pursuing the same purpose: better performance and new applications.

The field of heterogeneous catalysis, with particular emphasis on catalysis involving bimetallic nanomaterials (BNMs) that contain two different materials in the same nanoparticle, has seen many advances over the past few years. Significant progress has been made with regard to the preparation and characterization of a variety of different BNMs with well defined size, shape, and composition properties.[1]

Bimetallic nanoparticles (NPs), with two different metals, often show improved catalytic performances and find applications in several industrial processes, primarily in fuel industries or environmental catalytic processes, and more recently in C−C cross–coupling reactions.[2] Bimetallic catalysts represent an interesting class of catalysts because one metal can tune and/or modify the catalytic properties of the other due to the electronic and structural interactions.[3] They are also of importance because of the modification in their surface electrons relative to that of the individual metals.[4] There has been considerable interest in the formation, structure and further exploitation of the catalytic activity of bimetallic particles.[5] It has been often seen that metals interacting with either another metal or metal oxide at the nano level can form nanocomposites with superior activities not seen in bulk alloys.[6] From the standpoint of the reduction of environmental burdens and cost effectiveness, nanometal catalysts embedded in/on insoluble supports with ligand-free and minimal or no leaching are highly desirable. However, procedural simplicity, uniform dispersion, cheaper and robust polymeric surface, higher efficiency and life-cycle remain the major challenges for a heterogeneous catalyst.

Since several metal-catalyzed cross–coupling reactions require the presence of another metal either as a cocatalyst or to help control the overall process. Representative examples include: (i) Pd-catalyzed Heck coupling reaction in the presence of Ag salts, that is believed to occur via cationic mechanism and often has a profound effect in controlling the regio- and stereochemistry of the coupled product,[7] (ii) Sonogashira reaction between an aryl halide and terminal alkynes requires a combination of Pd and Cu as the catalysts, where Cu^{+} plays a catalytic role in transferring the alkynyl group to Pd,[8] (iii) in the Stille coupling reaction, the accelerating effect of CuI on the Pd-catalyzed coupling of aryl iodide and organostannane derivative has been quantitatively evaluated.[9]

Since in early 1990s, bimetallic Pd nanoparticles have received widespread attention because of their extensive use in hydrogenation reactions, C−H bond activation, C−C coupling reactions and environmental catalytic processes. In 1996 Reetz et al. observed that the presence of tetraalkylammonium salts can lead to nanostructured $R_4N^+X^-$-stabilized bimetallic cluster Pd/Ni, having better catalytic activity than corresponding Pd clusters. The excellent redox properties of the Pd/Cu system and the pronounced "Cu-effect" in the Pd-catalyzed cross–coupling reaction stimulate the development of several heterogeneous bimetallic composites.[10]

IV.2. Present work: Background and Objective

Palladium-copper bimetallic catalysts have excellent properties both for oxidation reaction reactions and for catalysis in reducing atmospheres. They in fact are of interest as catalyst for the oxidation of CO[11a] and for the oxygen-assisted water gas shift reaction,[11b] and the selective hydrogenation of dienes to olefins.[11c] Several previous studies have been devoted to the characterization of similar materials by different techniques.[12] Copper enrichment has been reported in the case of Pd-Cu/SiO_2 catalyst used for dehydrochlorination of 1,2-dichloroethane[12h] and in optical materials.[12i]

Recent report shows monodisperse bimetallic Pd–Cu nanoparticles with controlled size and composition were synthesized by a one-step multiphase ethylene glycol (EG) method.[13] The as prepared nanoparticles were loaded onto a Vulcan XC-72 carbon support. Supported Pd–Cu nanomaterials showed enhanced electrocatalytic activity towards methanol oxidation compared with supported Pd nanoparticles. The solid–solution alloy structures in the bimetallic catalyst played a key role in improving the electrochemical activity.

After that Chang and their group have demonstrated a facile approach for the preparation of PdCu bimetallic NPs with various morphologies through a surfactant-assisted growth at 95 ^oC.[14] This material was successfully applied in methanol oxidation reaction (MOR) in alkaline media. Upon increasing the copper content, the catalytic activity toward the MOR increases, mainly due to the advantages of the electroactive surface area.

Müslehiddinoglu et al.[15] developed a Pd-Cu/C catalyst as an alternative to Raney Ni for the highly diastereoselective hydrogenation of imines prepared from prochiral ketones and *α*-phenylethylamines (Scheme IV.1). These results revealed that chiral amines could be obtained with a diastereomeric excess (de) up to 94% using Pd-Cu/C, whereas conventional Pd/C catalysts only afforded a de of 72%. Further investigation revealed that a Pd:Cu ratio of 4:1 was required for a robust process.

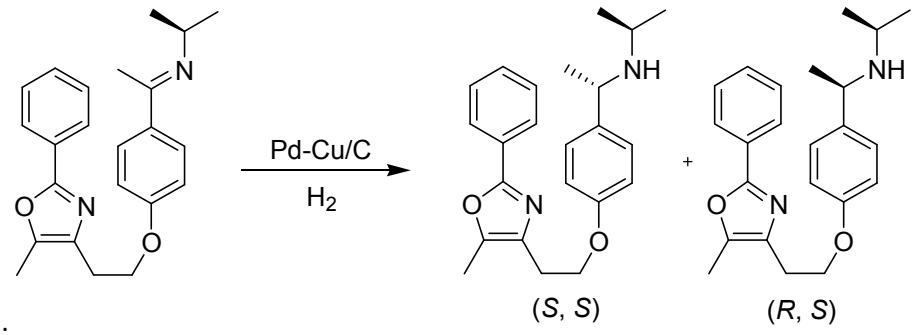

Scheme IV.1. Catalytic hydrogenation by Pd-Cu/C.

Palladium and copper exchanged montmorillonite K10 clay has been found to catalyse very efficiently the reaction between aryl halides (X = Br, I) and acrylates, and styrenes producing alkyl (*E*)-cinnamates and (*E*)-stilbenes respectively in high yields (Scheme IV.2).[16] The catalyst was recovered by simple filtration and reused up to three times without losing its activity.

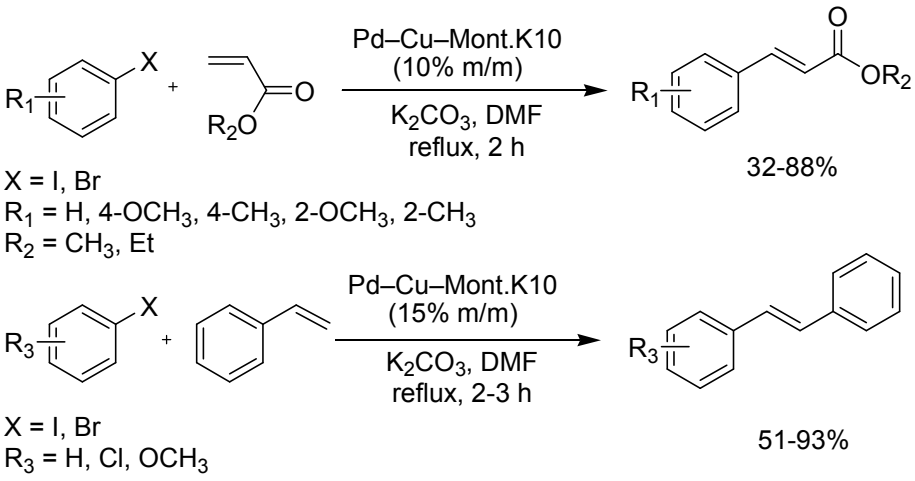

Scheme IV.2. Heck reaction using Pd–Cu–Mont.K10.

Another carbon-supported bimetallic Pd-M (M = Ag, Ni, and Cu) composites have been synthesized by Choi et al.[17] through γ-irradiation at room temperature, and the resulting Pd-Cu/C nanoparticles exhibited high catalytic efficiency in the Suzuki- and Heck-type coupling reactions.

Heshmatpour and their group have synthesized spherical metal NPs (Pd, Ag, Pd/Ag, Pd/Ni, and Pd/Cu) using a water-in-oil microemulsion system of water/dioctyl sulfosuccinate sodium salt (aerosol-OT, AOT)/isooctane at 25 ^oC based on the reverse micelle technique.[18] Among different combinations Pd/Cu (4:1) exhibits highest activity in the Heck reaction compare to other (Scheme IV.3). This catalyst was separated by centrifugation and used for recycling experiments. The activity of Pd catalyst was gradually decreased but the catalytic activity of Pd/Cu remains constant up to six consecutive runs.

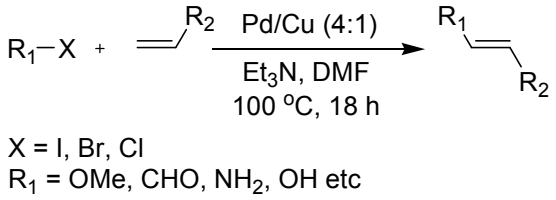

Scheme IV.3. Heck reaction of aryl halides with olefins catalyzed by Pd/Cu (4:1).

Very recently Gao et al.[19] have synthesized montmorillonite supported Pd-Cu nanoparticles (MMT@Pd/Cu), exhibits catalytic activity towards the Sonogashira coupling reaction using triphenylphosphine (PPh_3) as a ligand (Scheme IV.4). These catalysts were prepared on the basis of the unique metal ion adsorption capacity of montmorillonite and sequential reductive carbonylation via the thermolysis of *N*,*N*-dimethylformide. Kinetic studies revealed that the water-promoted swelling of the montmorillonite as well as the Pd-Cu bimetallic synergistic effect played a critical role in the high activity of the catalyst.

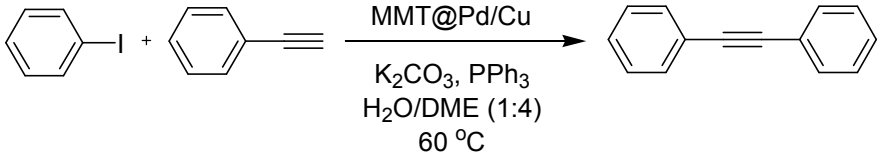

Scheme IV.4. MMT@Pd/Cu catalyzed Sonogashira coupling reaction.

Our previous lab report depicts the successful immobilization of Pd NPs on macroporous polystyrene-trimethylammonium anion-exchange resins and finds its application in various catalytic reduction and C−C coupling–coupling reactions.[20] However, to the best of our knowledge, there is no report available in the literature for the synthesis of bimetallic NPs impregnated on insoluble poly-ionic resins and to explore its heterogeneous catalytic activity in cross–coupling reactions. Here we report the synthesis and characterization of new class of heterogeneous Pd/Cu bimetallic composite NPs embedded on poly-ionic amberlite resins, which have shown efficient catalytic activity in the Sonogashira cross–coupling reaction under phosphine-ligand-free conditions with high recyclability.

IV.3. Present work: Results and Discussion

IV.3.1. Preparation of Heterogeneous Pd/Cu composite

Amberlite resin formate (ARF) was prepared from commercially available inexpensive Amberlite resin chloride by ion–exchange process as reported from this laboratory.[20,21] The resin beads were then washed with water followed by acetone, dried under vacuum and used for the preparation of heterogeneous bimetallic nanocomposites. Impregnation of bimetallic Pd/Cu on the ARF was performed by heating an equimolar mixture of solutions of palladium

acetate and cupric acetate in dimethylformamide (DMF) at different concentrations. Initial experiment using low concentration of each salt (0.033 mmol) afforded the composite material, which was denoted as Pd/Cu−ARF(I) and similar experiment using higher concentration of salts (0.25 mmol each) that furnished a new entity, denoted as Pd/Cu−ARF(II).

IV.3.2. Characterizations of Pd/Cu−ARF

The morphology and microstructure of the samples were examined by FTIR spectroscopy, TEM equipped with EDS, powder XRD and AAS.

Initially we have focused on Pd/Cu−ARF(I). The AAS analysis shows nearly 90% of the added copper was present in it. The surface topopraphy and dispersion of active components over the ARF were examined by scanning electron microscopy (SEM) (Figure IV.1).

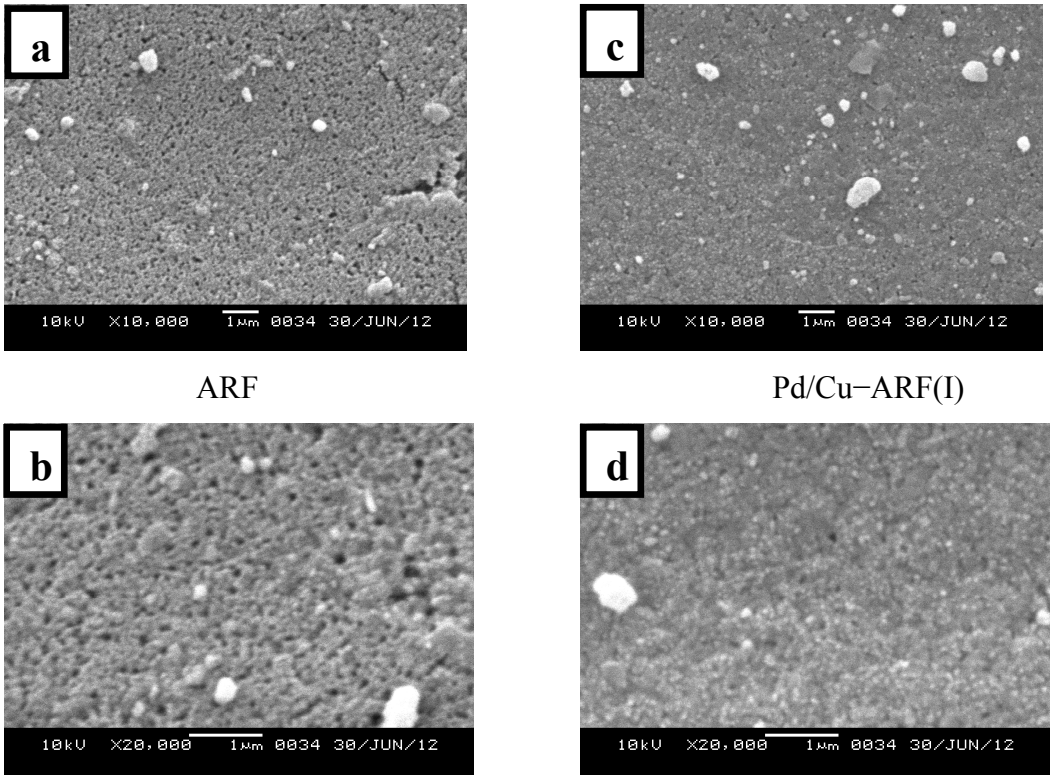

Figure IV.1. Scanning electron micrographs of ARF (a, b), Pd/Cu−ARF(I) (c, d) at different magnifications.

The powder XRD patterns of ARF and Pd/Cu−ARF(I) are presented in Figure IV.2. It is evident that the support (ARF) and supported bimetal at low concentration [Pd/Cu−ARF(I)] appeared almost identical and however showed no signature of NPs.

To understand the actual structural morphology of the composite material, Pd/Cu−ARF(II) was prepared and characterized in details.

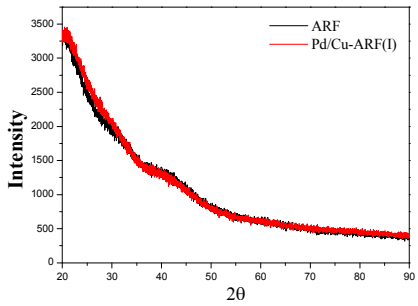

Figure IV.2. Powder XRD of ARF and the corresponding Pd-Cu incorporated resin (Pd/Cu−ARF(I)).

The FTIR spectra of bimetallic species were recorded in the range 4000–400 cm^{-1} and compared with that of ARF. Figure IV.3 show the FTIR spectra in the range of 2000–400 cm^{-1}. While the carboxylate anion ($HCOO^{-}$) of the ARF exhibits both symmetric and anti-symmetric stretching vibrations respectively at 1346 and 1593 cm^{-1}, the composites Pd/Cu−ARF(I) and Pd/Cu−ARF(II) absorb at 1412 and 1655 cm^{-1} for these vibrations. A clear shifting of the bands in the range of 60-65 cm^{-1} was observed conforming to our previous studies with the monometallic Pd−ARF (Figure IV.3),[20] and suggesting possible electrostatic binding of the metallic species with the poly-ionic resins. It can also be noted from Figure IV.3 that an intense FTIR peak around 1575 cm^{-1} is appeared in the case of Pd/Cu−ARF(II), which is almost absent in Pd/Cu−ARF(I). This may be assigned as a peak of COO^{-}, bonded with the metal in amberlite resin,[22] and appeared sharply in Pd/Cu−ARF(II) possibly due to the larger amount of metal doping.

The XRD patterns of amberlite resins formate, (ARF) and that of the corresponding Pd/Cu incorporated resins (Pd/Cu−ARF(II)) are shown in Figure IV.4. Here, we did not observe any signals related to the Pd- and Cu-acetate, indicating complete decomposition of the salts in the case of Pd/Cu−ARF(II). The impregnated resins Pd/Cu−ARF(II) (dried at 60 °C) exhibited Bragg diffractions corresponding to the cupric oxide (CuO), palladium oxide (PdO) and palladium (Pd), while the pure ARF showed amorphous characteristics. The peak positions are labelled in Figure IV.4. The corresponding JCPDS peak positions with relative intensities are also shown as green (PdO), blue (CuO) and pink (Pd) lines. The broad XRD pattern of Pd/Cu−ARF(II) suggested poor crystalline nature of the embedded materials. Nevertheless the existence of XRD peaks at 34.48, 46.16, 55.89 and 61.75° 2θ clearly suggested the PdO (002), (102), (112) and (103) planes, respectively (JCPDS#01-075-0200). The appearance of peaks at 40, ~46.5 and 67.91° 2θ indicated the presence of (111), (200) and (220) planes, respectively of fcc Pd (JCPDS#01-088-2335). Further, we found peaks near 35.39, 46.25, 57.91, 61.64° 2θ, which could be indexed as ($\bar{1}$11), ($\bar{1}$12), (202) and ($\bar{1}$13) of CuO, respectively (JCPDS#01-089-2531).

The TEM analysis of Pd/Cu−ARF(II) is presented in Figure IV.5. Low resolution TEM images showing nanoparticles embedded in resin matrix are shown in Figure IV.5a,b. The

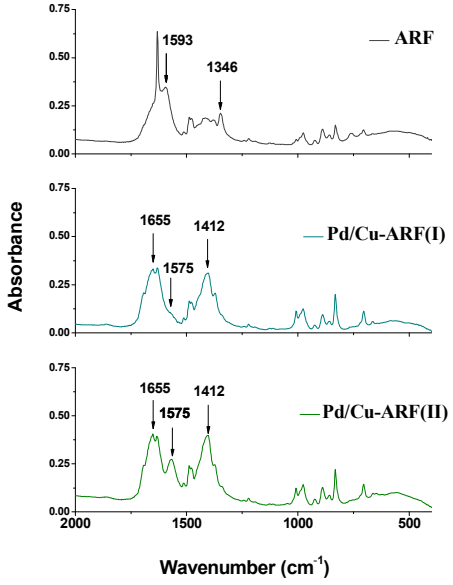

Figure IV.3. FTIR spectra of the ARF and bimetallic composites [Pd/Cu−ARF(I) and Pd/Cu−ARF(II)].

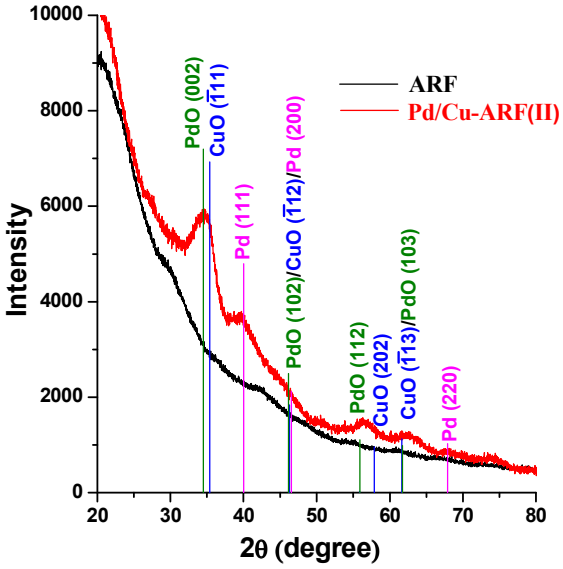

Figure IV.4. High angle XRD patterens of ARF and bimetallic composite Pd/Cu−ARF(II).

presence of diffused ring as well as spots corresponding to the Pd(111), PdO (002) and CuO ($\bar{1}$11) in the SAED (inset of Figure IV.5a) indicate existence of crystalline NPs, which is also supported by the XRD pattern (Figure IV.4). We magnified a small portion of Figure IV.5a for clarification and presented it as Figure IV.5b. It shows homogeneous distribution of NPs throughout the matrix. Figure IV.5c shows the particle size distribution, estimated from Figure IV.5b, and the mean diameter of the particle was found to be ~4.9 nm. Energy dispersive X-ray scattering (EDX) analysis of Pd/Cu-ARF(II) (Figure IV.5d) confirmed the presence of Pd, Cu and O and C in the sample. To understand the structure of the NPs, high resolution TEM (HRTEM) studies were undertaken using field emission gun (FEG) transmission electron microscope and results are presented in Figure IV.5e-f. Figure IV.5e shows NPs with clear crystalline fringe patterns. Magnified view of a representative NP (marked by 'A' in Figure IV.5e) is shown in Figure IV.5f with labelling of characteristic fringes. The Fourier diffractogram (FFT) obtained from (IV.5e) is shown in Figure IV.5g. The co-existence of Pd (111) and PdO/CuO lattice spacings are clearly observed in the NPs (Figure IV.5f,g). Thus, HRTEM studies as well as SAED revealed the composite nature of NPs.

From XRD and TEM analysis, we can thus say that composite NPs, made of Pd/PdO/CuO, have been embedded in the poly-ionic amberlite resins. The CuO might be formed by the ox-

idation of initially formed Cu(0) NPs, as also observed previously in the preparation of other

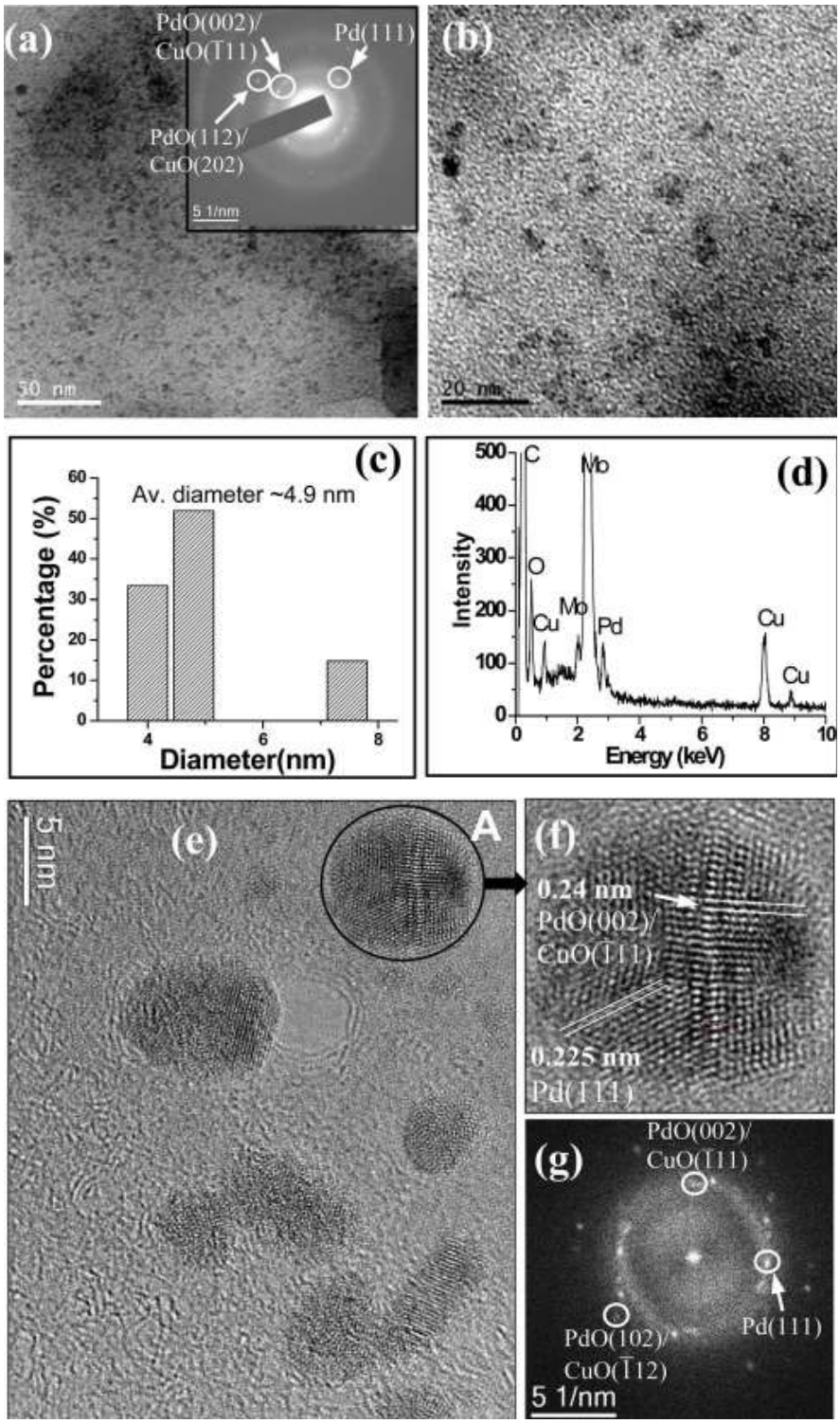

Figure IV.5. (a) Bright field low resolution TEM images of Pd/Cu−ARF(II); the inset shows the selected area electron diffraction (SAED) pattern; (b) representation of the magnified view of a small portion of (a); (c) particle size distribution evaluated from (b); (d) EDX pattern of the sample showing the existence of elemental C (very strong), O, Pd and Cu; a part of C and very strong Mo signals are from the carbon coated Mo grid used for the TEM study; (e) high resolution TEM image showing crystalline NPs; (f) magnified view of the NP marked by 'A' in (e); (g) Fourier diffractogram taken from (e).

heterogeneous bimetallic Cu-M nanocomposites.[23] Total copper present in the heterogeneous nanocomposite material, Pd/Cu−ARF(II) has been estimated by the AAS. For this purpose 50 mg of the sample was digested with concentrated HNO_3 (1 mL) and analysed. From such analysis Cu content has been estimated to be 0.205 mmol g^{-1} of the Pd/Cu−ARF(II).

IV.3.3. Catalytic Activity of Pd/Cu−ARF(II)

The metal-catalyzed sp^2–sp coupling reaction between aryl or alkenyl halides and terminal alkynes, known as the Sonogashira reaction,[24] is one of the most important reactions for the formation of C−C bonds in organic synthesis.[25] Combination of Pd and Cu salts along with suitable phosphine ligands as the catalytic system for such cross–coupling reactions of sp^2-C halides with terminal acetylenes requires careful choice of substrates and skilful tailoring of the reaction conditions.[26] Competing homo-coupling of terminal alkynes in the presence of Pd/Cu catalysts remain one of the major side reactions, which is often avoided or minimized by conducting the Sonogashira reaction under a blanket of N_2 or a mixture of N_2 and H_2.[27] On the other hand, few successful examples of copper-free Sonogashira coupling require expensive aminophosphine ligands.[28] We optimized the reaction conditions with 4-iodotoluene and propargyl acetate using the newly developed heterogeneous combination of Pd/CuO nanocomposites, and the best conversion was achieved in the presence of K_2CO_3 as the base in CH_3CN solvent at 80 °C under N_2 for 12h. As regard to the amount of the catalysts, it was observed that 100 mg $mmol^{-1}$ was sufficed to catalyze the process. To explore the scope and limitations of the catalyst, a range of substituted iodoarenes was tested and found to undergo Sonogashira coupling with different aliphatic and aromatic alkynes (Scheme IV.5). The results are presented in Table IV.1. The cross–coupling with electron-rich aryl bromides was not successful, though hetero-aromatic bromide such as 3-bromoquinoline or electron-deficient bromoarenes gave the corresponding coupled product in excellent yield.

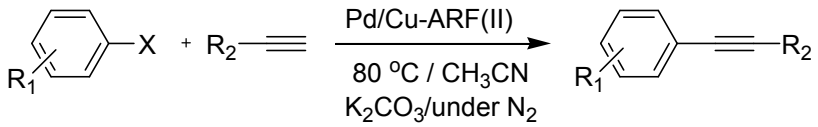

Scheme IV.5. Sonogashira cross–coupling in the presence of Pd/Cu−ARF(II).

Poor catalytic activity with deactivated aryl bromide in Sonogashira coupling has been exploited with a suitable example. 1-Bromo-3-iodobenzene showed excellent chemoselectivity when the Sonogashira coupling with 4-tolyl acetylene was carried out in the presence of Pd/Cu−ARF(II) to obtain selectively 1-(2-(3-bromophenyl) ethynyl)-4

methylbenzene in 92% yield (Table IV.1, entry 12A). Subsequently, the same catalytic system was used for Suzuki–Miyaura coupling with phenylboronic acid to obtain 1-(2-(3 biphenyl)ethynyl)-4-methylbenzene in 81% yield (Table IV.1, entry 12B). This reaction established that the catalytic system, Pd/Cu−ARF(II), is effective for the Suzuki–Miyaura cross–coupling reaction as well.

Table IV.1. Sonogashira coupling reactions of haloarenes with terminal alkynes in the presence of catalytic Pd/Cu−ARF(II).[a]

Sl. No.	Ar-X	Alkyne	Time (h)	Product	Yield[b] (%)
1	4- $H_3COC_6H_4I$	$\equiv C_6H_5$	6	4- $H_3COH_4C_6-\equiv-C_6H_5$	85
2	4- $H_3CC_6H_4I$	$\equiv CH_2OCOCH_3$	12	4- $H_3CH_4C_6-\equiv-CH_2OCOCH_3$	90
3	2- $H_3CC_6H_4I$	$\equiv CH_2OCOCH_2CH_3$	10	2- $H_3CH_4C_6-\equiv-CH_2OCOCH_2CH_3$	87
4	3- $H_3COC_6H_4I$	$\equiv CH_2CH_2C_6H_5$	6	3- $H_3COH_4C_6-\equiv-CH_2CH_2C_6H_5$	84
5	3- $NO_2C_6H_4I$	$\equiv C_6H_5$	3	3- $NO_2H_4C_6-\equiv-C_6H_5$	95
6	3- BrC_6H_4I	$\equiv CH_2OCOCH_2CH_3$	12	3- $BrH_4C_6-\equiv-CH_2OCOCH_2CH_3$	77
7	3- ClC_6H_4I	$\equiv CH_2OCOCH_2CH_3$	12	3- $ClH_4C_6-\equiv-CH_2OCOCH_2CH_3$	78
8[c]	3- $H_3CC_6H_4Br$	$\equiv C_6H_5$	16	No Reaction	-
9	4- $H_3CCOC_6H_4Cl$	$\equiv CH_2CH_2C_6H_5$	16	No Reaction	-
10	3- C_9H_6NBr	$\equiv C_6H_5$	12	3- $C_9H_6N-\equiv-C_6H_5$	77
11	3- $NO_2C_6H_4Br$	$\equiv C_6H_5$	10	3- $NO_2H_4C_6-\equiv-C_6H_5$	93
12A	1-Br-3-IC_6H_4	$\equiv C_6H_4(4\text{-}CH_3)$	6	1-Br-3-$C_6H_4-\equiv-C_6H_5(4\text{-}CH_3)$	92
12B[d]	1-Br-3-$C_6H_4-\equiv-C_6H_5(4\text{-}CH_3)$	$C_6H_5B(OH)_2$	6	1-C_6H_5-3-$C_6H_4-\equiv-C_6H_5(4\text{-}CH_3)$	81

[a]Pd/Cu−ARF(II) (100 mg), ArX (1 mmol), alkyl acetylene (1.1 mmol)/aryl acetylene (1.5 mmol), K_2CO_3 (1.5 mmol), MeCN (3 mL), heating the reaction at 80 ^oC under N_2. [b]Yields are for isolated pure compounds, characterized by mp, IR and NMR spectral data. [c]Homo-coupled diyne was isolated in 62% yield. [d]Suzuki–Miyaura cross–coupling reaction using same catalytic system, [Pd/Cu−ARF(II)], (see experimental).

Although the exact mechanism for the Sonogashira cross–coupling reaction is not known,[26a] the catalytic process may be considered to involve two parts: (i) Pd^0 undergoes oxidative addition to aryl halide, and (ii) Cu^{+2} is *in situ* reduced to Cu^{+1}, which forms transient copper acetylide species. The process is then completed via transmetalation followed by reductive elimination to finally afford the cross–coupled product. We also examined Sonogashira coupling reaction in the presence of Pd/Cu−ARF(I), which is much less efficient as compared to Pd/Cu−ARF(II), producing the Sonogashira coupled product in 25-40% isolated yield.

IV.3.4. Heterogeneity Test

IV.3.4.1. Hg(0) and CS_2 poisoning tests

The heterogeneity of the catalyst is often checked by catalyst-poisoning experiments, and addition of Hg(0) in the reaction medium to see any poisoning of the catalytic activity has been suggested by Whitesides,[29] and Crabtree,[30] followed by other groups.[31] Similar experiment was performed in Sonogashira coupling between 3-iodonitrobenzene and phenyl acetylene (1:1.5 mmol) in acetonitrile in the presence of Pd/Cu−ARF(II) (100 mg) and Hg(0) (250 mg) with gentle magnetic stirring at 80 °C. After heating the reaction mixture for 1h, it was analyzed by HPLC that showed the ratio of iodoarene and the coupled product in 67:33. The reaction was then continued for another 2h and now HPLC analysis showed complete conversion to the coupled product. Further experiment using excess Hg(0) (1.5 g, 340 equivalents per palladium) and stirring the reaction vigorously did not show suppression of catalytic activity, and complete conversion was observed after 3h. Although poisoning by elemental mercury is often used as a test for heterogeneous catalysis, this is not definitive probably in the context of metal-catalyzed coupling chemistries.[32] Poisoning experiment using ligand like CS_2 can also be powerful if performed quantitatively.[33] We therefore conducted catalyst poisoning tests in Sonogashira coupling between 3-iodonitrobenzene and phenyl acetylene by adding varying quantities of CS_2 to the reaction mixture. After about 15% conversion of the product (by HPLC), CS_2 was added and the reaction was continued for 3h to check the amount of conversion. Figure IV.6 shows the results of five independent experiments as a plot of % conversion (± 2−3%) to the cross coupled product as a function of amounts of CS_2 added. Near complete cessation of the Sonogashira coupling was observed with 1 mg of CS_2 (0.013 mmol) as against 0.022 mmol of the palladium (<1.0 eq), suggesting that the Pd/Cu−ARF(II) nanocomposites are indeed heterogeneous catalyst.

IV.3.4.2. Hot filtration test

Leaching of any metal from the resin-soaked heterogeneous surface was tested following the literature procedure.[30,34] Accordingly, the Sonogashira reaction mixture is filtered off to separate the solid catalysts after 1h in hot condition, and the filtrate was analyzed by HPLC (~33% conversion). The AAS analysis of the filtrate showed absence of any copper. The liquid phase was heated under reflux for another 3h in the absence of any added catalyst and subsequent HPLC analysis did not show further conversion, signifying that the metals are not leached out from the polymeric support during the first hour of the reaction.

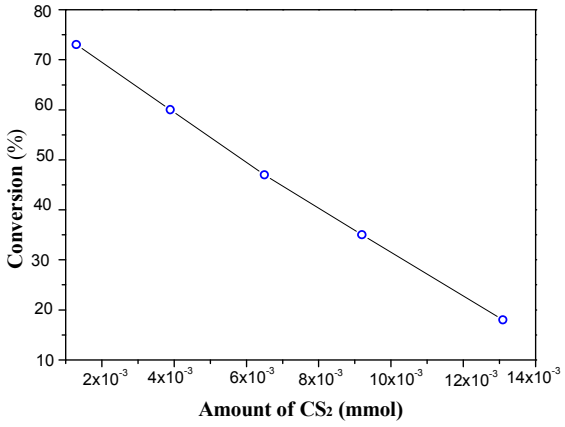

Figure IV.6. Plot of % conversions (± 2−3%) to the cross coupled product versus quantities of CS_2 (in mmol) used as the catalyst poisoning in Sonogashira reaction.

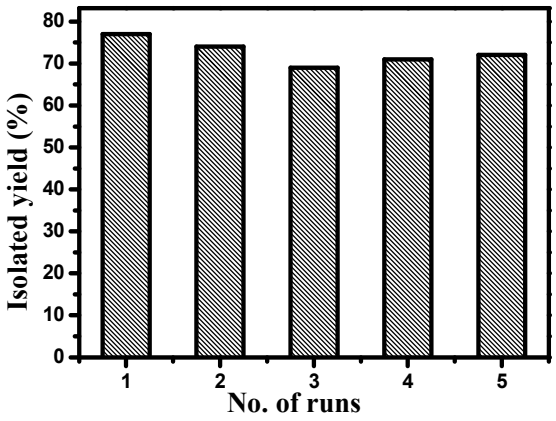

Figure IV.7. Recycling experiments using Pd/Cu−ARF(II) in the cross–coupling reaction between 4-iodotoluene and propargyl acetate.

IV.3.5: Test for Recyclability

We also checked the reusability of Pd/Cu−ARF(II) in the reaction between 4-iodotoluene and propargyl acetate. After the reaction, resin beads were recovered from the reaction mixture by simple filtration, washed thoroughly with water followed by acetone, and then dried under vacuum. The recovered catalyst was reused four times without losing its activity (Figure IV.7).

IV.4. Conclusion

In conclusion, a new class of poly-ionic resin-supported Pd/Cu based bimetallic nanocomposite has been synthesized, characterized and applied as the catalyst in Sonogashira cross–coupling reaction. The bimetallic nanoparticles composed of metallic Pd/PdO/CuO has found to be distributed very homogeneously throughout the polymeric matrix. The heterogeneous catalytic activity was examined by hot-filtration and metal-scavenger experiments and found to be highly efficient and recyclable at least for five consecutive runs. This Pd/Cu based nanocomposite catalytic system has been applied for the first time in Sonogashira cross–coupling reactions under ligand free conditions.

IV.5. Experimental section

IV.5.1. General information

Amberlite IRA 900 (chloride form) was purchased from Acros Organics, Belgium and used after washing with water and acetone followed by drying under vacuum. Other chemicals were purchased and used directly. FTIR spectra were recorded with a Nicolet 380 FTIR

spectrometer using KBr pellet method. NMR spectra were taken in $CDCl_3$ using Bruker Avance AV-300 spectrometer operating for ^1H at 300 MHz and for ^{13}C at 75 MHz. The spectral data were measured using TMS as the internal standard. AAS measurements were made using Varian SpectrAA 50B instrument. The X-ray diffraction (XRD) studies of the powder samples were done using the Rigaku SmartLab (9 kW) diffractometer using CuKα radiation. Transmission electron microscopy (TEM) of the samples were recorded with Tecnai G2 30ST (FEI Company) operating at 300 kV and JEOL JEM–2100F (FEG) operating at 200 kV. To prepare the TEM sample, a small amount of ground sample was first dispersed in acetone. Then one small drop of this dispersion was applied on a carbon-coated molybdenum grid.

The amberlite resin formate (ARF) was prepared from commercially available Amberlite IRA 900 (chloride form) (Source: Acros Organics, Belgium) by rinsing with 10% aqueous formic acid solution until free from chloride ions. The resin beads were then washed with water followed by acetone, dried under vacuum, and used for the preparation of heterogeneous bimetallic nanocomposites.

IV.5.2. Preparation of Pd/Cu−AFR(I) & Pd/Cu−AFR(II)

Pd/Cu−AFR(I)

To a solution of $Pd(OAc)_2$ (7.5 mg, 0.033 mmol) and $Cu(OAc)_2$ (6.6 mg, 0.033 mmol) in DMF (3 mL) was added ARF (1 g) and the mixture taken in screw-capped sealed tube was heated at 60 ^oC for 1 h with occasional shaking. The supernatant liquid appeared completely colourless by this time and the greyish beads of ARF turned black. The mixture was cooled to room temperature and the resin beads were filtered off and washed with water (3 x 5 mL) and acetone (2 x 5 mL). Resulting black resin beads were dried under vacuum and used for analyses and reactions.

Pd/Cu−AFR(II)

Similar procedure was followed using a solution of $Pd(OAc)_2$ (56 mg, 0.25 mmol) and $Cu(OAc)_2$ (50 mg, 0.25 mmol) in DMF (10 mL) for the ARF (1 g).

IV.5.3. Sonogashira cross–coupling reaction using Pd/Cu−ARF(II)

To a suspension of Pd/Cu−ARF(II) (100 mg) in acetonitrile (3 mL) were added aryl halide (1 mmol), acetylene (1.1 mmol for aliphatic alkynes and 1.5 mmol for aromatic alkynes) and K_2CO_3 (1.5 mmol). The reaction mixture was then heated under N_2 with gentle magnetic stirring for hours, as mentioned in the Table IV.1 and monitored by tlc. After cooling, the mixture was diluted with water (5 mL), and filtered through a cotton bed. The filtrate was

extracted with diethyl ether (3 x 10 mL) and the combined organic extracts were washed with brine (5 mL), dried over sodium sulphate and concentrated under vacuum. The residue was purified by passing through a short silica gel column and elution with light petroleum or 2% ethyl acetate-light petroleum. All products were characterized by ^{1}H, ^{13}C NMR and FTIR spectral data, and also compared with reported melting point (for known solid compounds).

IV.5.4. Suzuki–Miyaura cross–coupling reaction using Pd/Cu−ARF(II) (Table IV.1, entry 12B)

A mixture of 1-(2-(3-bromophenyl)ethyl)-4-methylbenzene (271 mg, 1 mmol), phenylboronic acid (134 mg, 1.1 mmol), K_2CO_3 (152 mg, 1.1 mmol) and the Pd/Cu−ARF(II) (150 mg) in DMF (3 mL) was heated at 90 ^{o}C with occasional magnetic stirring. The reaction was monitored by tlc and after 6h, the mixture was cooled, diluted with water (5 mL) and extracted with diethyl ether (3 x 10 mL). The combined ethereal extracts was dried (Na_2SO_4) and evaporated to afford an oily residue. Column chromatography over silica gel and elution with light petroleum furnished the desired product, 1-(2-(3-biphenyl)ethynyl)-4-methylbenzene (217 mg, 81%). The product was characterized by NMR spectral data.

IV.5.5. Physical properties and spectral data of compounds

Table IV.1, entry 1

1-Methoxy-4-(2-phenylethynyl)benzene[35]

White crystalline solid, mp 56-58 ^{o}C (Lit. mp 58-60 ^{o}C)

IR (in KBr): ν_{max} 2216 cm^{-1}

^{1}H NMR ($CDCl_3$, 300 MHz): δ/ppm 3.82 (s, 3H, OCH_3), 6.86-6.89 (m, 2H, ArH), 7.31-7.33 (m, 3H, ArH), 7.45-7.53 (m, 4H, ArH); ^{13}C NMR ($CDCl_3$, 75 MHz): δ/ppm 55.3, 88.0, 89.3, 114.0, 115.4, 123.6, 127.9, 128.3, 131.4, 133.0, 159.6.

Table IV.2, entry 2

3-*p*-Tolylprop-2-ynyl acetate

Colourless liquid

IR (neat) ν_{max} 2237, 1747 cm^{-1}

^{1}H NMR ($CDCl_3$, 300 MHz): δ/ppm 2.13 (s, 3H, C$\underline{H}_3$CO), 2.35 (s, 3H, ArC$\underline{H}_3$), 4.90 (s, 2H, CH_2), 7.12 (d, *J* = 8.1 Hz, 2H, ArH), 7.34 (d, *J* = 8.1 Hz, 2H, ArH); ^{13}C NMR ($CDCl_3$, 75 MHz): δ/ppm 20.8, 21.5, 52.9, 82.1, 86.6, 119.0, 129.0,131.8, 139.0, 170.4.

Table IV.1, entry 3

3-*o*-Tolylprop-2-ynyl propionate

Colourless liquid

IR (neat): ν_{max} 2229, 1743 cm^{-1}

^1H NMR ($CDCl_3$, 300 MHz): δ/ppm 1.19 (t, *J* = 7.5 Hz, 3H, C<u>H</u>$_3$), 2.38-2.45 (m, 5H, ArC<u>H</u>$_3$, C<u>H</u>$_2$), 4.95 (s, 2H, O-CH_2), 7.10-7.26 (m, 3H, ArH), 7.41 (d, *J* = 7.5 Hz, 1H, ArH); ^{13}C NMR ($CDCl_3$, 75 MHz): δ/ppm 9.0, 20.6, 27.4, 52.8, 85.3, 86.8, 121.9, 125.5, 128.7, 129.4, 132.2, 140.5, 173.8.

Table IV.1, entry 4

1-Methoxy-3-(4-phenylbut-1-ynyl)benzene[20]

Colourless liquid

IR (neat): ν_{max} 2227 cm^{-1}

^1H NMR ($CDCl_3$, 300 MHz): δ/ppm 2.69 (t, *J* = 7.5 Hz, 2H, CH_2), 2.92 (t, *J* = 7.5 Hz, 2H, CH_2-Ar), 3.78 (s, 3H, O-CH_3), 6.82-6.85 (m, 1H, ArH), 6.90-6.91 (m, 1H, ArH), 6.95-6.98 (m, 1H, ArH), 7.16-7.32 (m, 6H, ArH); ^{13}C NMR ($CDCl_3$, 75 MHz): 21.7, 35.1, 55.2, 81.2, 89.4, 114.2, 116.4, 124.0, 124.8, 126.3, 128.4, 128.5, 129.2, 140.7, 159.2.

Table IV.1, entry 5

1-(2-(3-nitrophenyl)ethynyl)benzene[33]

Yellow solid, 69-71 ^oC (Lit. mp 67-69 ^oC)

IR (in KBr): ν_{max} 2207 cm^{-1}

^1H NMR ($CDCl_3$, 300 MHz): δ/ppm 7.38-7.39 (m, 3H, ArH), 7.50-7.57 (m, 3H, ArH), 7.80-7.84 (m, 1H, ArH), 8.15-8.19 (m, 1H, ArH), 8.37-8.38 (m, 1H, ArH); ^{13}C NMR ($CDCl_3$, 75 MHz): δ/ppm 86.7, 91.9, 122.2, 122.9, 125.2, 126.4, 128.5, 129.0, 129.3, 131.8, 137.2, 148.2.

Table IV.1, entry 6

3-(3-Bromophenyl)prop-2-ynyl propionate

Colourless liquid

IR (neat): ν_{max} 2229, 1743 cm^{-1}

^1H NMR ($CDCl_3$, 300 MHz): δ/ppm 1.18 (t, *J* = 7.5 Hz, 3H, CH_3), 2.41 (q, *J* = 7.5 Hz, 2H, C<u>H</u>$_2$-CH_3), 4.90 (s, 2H, O-C<u>H</u>$_2$), 7.15-7.21 (m, 1H, ArH), 7.36-7.39 (m, 1H, ArH), 7.45-7.48 (m, 1H, ArH), 7.60-7.61 (m, 1H, ArH); ^{13}C NMR ($CDCl_3$, 75 MHz): 8.9, 27.3, 52.4, 84.4, 84.7, 122.1, 124.1, 129.7, 130.4, 131.9, 134.6, 173.7.

Table IV.1, entry 7

3-(3-Chlorophenyl)prop-2-ynyl propionate

Colourless liquid

IR (neat): ν_{max} 2229, 1743 cm^{-1}

^1H NMR ($CDCl_3$, 300 MHz): δ/ppm 1.18 (t, *J* = 7.2 Hz, 3H, CH_3), 2.40 (q, *J* = 7.5 Hz, 2H,

C$\underline{H_2}$-CH_3), 4.90 (s, 2H, O-C$\underline{H_2}$), 7.21-7.34 (m, 3H, ArH), 7.44 (s, 1H, ArH); ^{13}C NMR ($CDCl_3$, 75 MHz): 8.9, 27.3, 52.4, 84.3, 84.8, 123.8, 128.9, 129.5, 129.9, 131.7, 134.1, 173.6.

Table IV.1, entry 10

3-(2-Phenylethynyl)quinoline[36]

Yellow solid, 65-68 ^{o}C (Lit. mp 67-70 ^{o}C)

IR (in KBr): ν_{max} 2218 cm^{-1}

^{1}H NMR ($CDCl_3$, 300 MHz): 7.38-7.41 (m, 3H, ArH), 7.55-7.61 (m, 3H, ArH), 7.70-7.76 (m, 1H, ArH), 7.79-7.82 (m, 1H, ArH), 8.12 (d, *J* = 8.4 Hz, 1H, ArH), 8.32 (d, *J* = 1.8 Hz, 1H, ArH), 9.00 (d, *J* = 1.8 Hz, 1H, ArH); ^{13}C NMR ($CDCl_3$, 75 MHz): 86.4, 92.7, 117.5, 122.5, 127.3, 127.4, 127.6, 128.5, 128.8, 129.1, 130.2, 131.7, 138.5, 146.4, 151.9.

Table IV.1, entry 12A

1-(2-(3-Bromophenyl)ethynyl)-4-methylbenzene[37]

White crystalline solid, mp 91-93 ^{o}C (Lit. mp 89-91 ^{o}C)

IR (in KBr): ν_{max} 2222 cm^{-1}

^{1}H NMR ($CDCl_3$, 300 MHz): δ/ppm 2.37 (s, 3H, OCH_3), 7.14-7.25 (m, 3H, ArH), 7.40-7.46 (m, 4H, ArH), 7.67 (t, *J* = 1.8 Hz, 1H, ArH); ^{13}C NMR ($CDCl_3$, 75 MHz): δ/ppm 21.5, 87.1, 90.9, 119.6, 122.1, 125.5, 129.1, 129.7, 130.0, 131.1, 131.5, 134.2, 138.8.

Table IV.1, entry 12B

1-(2-(3-Biphenyl)ethynyl)-4-methylbenzene

White Solid, mp 69-71 ^{o}C

^{1}H NMR ($CDCl_3$, 300 MHz): δ/ppm 2.37 (s, 3H, OCH_3), 7.16 (d, *J* = 8.1 Hz, 2H, ArH), 7.36-7.53 (m, 8H, ArH), 7.59-7.62 (m, 2H, ArH), 7.76-7.77 (m, 1H, ArH); ^{13}C NMR ($CDCl_3$, 75 MHz): δ/ppm 21.5, 88.7, 89.7, 120.2, 124.0, 126.9, 127.1, 127.6, 128.7, 128.8, 129.1, 130.3, 131.5, 138.4, 140.4, 141.4.

IV.6. References

References are given in BIBLIOGRAPHY under Chapter IV (pp. 148−151).

CHAPTER V

Pd/Cu bimetallic nanoparticles embedded in macroporous ion-exchange resins: Further application to Suzuki–Miyaura and Mizoroki–Heck reactions

V.1. Introduction

Palladium catalysed C−C bond formations, such as the Mizoroki–Heck reaction and the Suzuki–Miyaura reaction, had its origin in the seventies of the previous century (Scheme V.1).[1] Since carbon–carbon bonds have huge applicability in the field of liquid crystals, pharmaceuticals, conducting polymers and also in multiple organic transformations,[2] academic and industrial significance of these reactions have improved and researchers develops newer cross–coupling methodologies over the years. In 1990s pioneering studies by Bonneman and Reetz have revealed that PdNPs generated by the reduction of different palladium salts, be actual catalysts for Suzuki–Miyaura and Mizoroki–Heck reactions.[3]

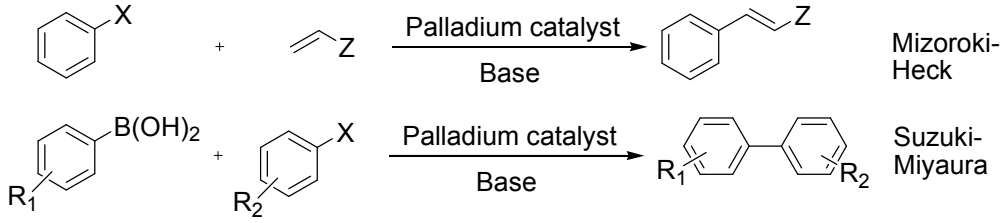

Scheme V.1. Palladium catalyzed C−C bond formation.

In recent years different carbene complexes of palladium or palladium with different bulky tertiary phosphine ligands, are well known for such C−C coupling reactions,[4] but these soluble palladium reagents are so expensive and difficult to recover. To overpower these limitations, researchers have made active palladium catalyst, where palladium was encapsulated or embedded some solid supports.[5] These heterogeneous Pd-catalysts are more promising because they can be easily separated from the reaction mixture and reused for a number of cycles.

Other transition metals like nickel, copper, gold have been effectively used in Suzuki and/or Heck reaction.[6] So ongoing research put forwards to reduce the cost of Pd species and increases their effectiveness by inducing a second metal.[7]

V.2. Present Work: Background and Objective

In 1996 Reetz et al. have been used tetraalkylammonium salts ($R_4N^+X^-$)-stabilized Pd and Pd/Ni bimetallic clusters as an effective catalyst for Suzuki and Heck reaction.[8] They found that Pd/Ni bimetallic clusters appear to be somewhat more efficient than the pure Pd clusters in Suzuki reaction.

After that different bimetallic combinations like Pd/Rh,[9a] Pd/Cu,[9b-d] Cu/Ni,[9e] Pd/Ni,[9b,c,f] Pd/Ag,[9b,c] Pd/Au[9g] and Pd/Co[9h] have been made in liquid phase or in solid support, and successively employed in Suzuki–Miyaura and/or Mizoroki–Heck reactions.

Since recently we have synthesized Pd/Cu bimetallic composite nanoparticles embedded in

macroporous ion-exchange resins and find its application in Sonogashira reaction. Herein we report the potential of our heterogeneous bimetallic composite Pd/Cu−ARE(II) in other coupling reactions, Suzuki–Miyaura and Mizoroki–Heck.

V.3. Present Work: Result and Discussion

To begin our study, we prepared Pd/Cu−ARF(II) according to our standard procedure, stated in previous chapter.[10] Then Pd/Cu−ARF(II) heterogeneous composite was applied in the following reactions separately.

V.3.1. Pd/Cu−ARF(II) catalyzed Suzuki–Miyaura reaction

In Suzuki–Miyaura cross–coupling reaction 4-iodoanisole and phenylboronic acid was consider as a model substrate and 100 mg of catalyst was used. In order to optimize solvent, various solvents, including water, water-ethanol mixture, toluene and DMF were tried as indicated in Table V.1, DMF to be the best solvent in terms of yield. The influence of base also studied, K_2CO_3 was the best and 65 ^oC was the optimized reaction temperature (Table V.1, entry 3).

Table V.1. Optimization of Suzuki–Miyaura reaction using Pd/Cu-ARF(II).[a]

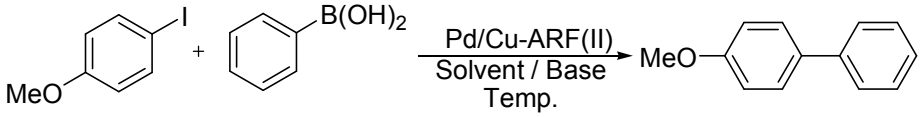

Entry	Solvent	Base	Temperature (^oC)	Time (h)	Yield[b] (%)
1	DMF	K_2CO_3	RT	12	52
2	DMF	K_2CO_3	50	10	88
3	**DMF**	**K_2CO_3**	**65**	**4**	**91**
4	DMF	KF	65	12	71
5	Water	K_2CO_3	65	12	55
6	Water:Ethanol (1:1)	K_2CO_3	65	12	66
7	Toluene	K_2CO_3	65	12	80
8	Methanol	K_2CO_3	65	12	58

[a] 4-Iodoanisole (1 mmol), phenylboronic acid (1.2 mmol), base (1.1 mmol) Pd/Cu−ARF(II), (100 mg) and solvent (3 mL). [b]Isolated yield.

To find out the limitation of our methodology, variety of aryl halides and boronic acids were tested and the results are shown in Table V.2. Different substituted iodo arenes undergo smooth reactions (entries 1−4). Aryl bromide efficiently reacts with boronic acid and produced corresponding cross–coupling product in extremely high yield (entry 5). On the other hand aryl chloride remains unaltered under this reaction condition. Heterocyclic aryl

bromide (3-bromoquinoline) reacts nicely and yielded 89% of cross–coupled product (entry 6). Different poly aromatic compounds easily be synthesized using this methodology. Phenylboronic acid reacts with different di iodo, bromo iodo and di bromo compounds and produces corresponding terphenyl compounds with excellent yield (entries 8−10).

Table V.2. Suzuki–Miyaura cross–coupling using Pd/Cu−ARF(II).[a]

Entry	Aryl halide	Boronic acid	Time (h)	Product	Yield (%)[b]
1	$(4\text{-}H_3CO)C_6H_4I$	$C_6H_5B(OH)_2$	4	$(4\text{-}H_3CO)H_4C_6{-}C_6H_5$	91
2	$(3\text{-}H_3CO)C_6H_4I$	$(3\text{-}H_3CO)C_6H_4B(OH)_2$	3.5	$(3\text{-}H_3C)H_4C_6{-}C_6H_4(3'\text{-}OCH_3)$	92
3	$(2\text{-}H_3CO)C_6H_4I$	$C_6H_5B(OH)_2$	5	$(2\text{-}H_3CO)H_4C_6{-}C_6H_5$	90
4	$(2\text{-}F_3C)C_6H_4I$	$(4\text{-}H_3CO)C_6H_4B(OH)_2$	2	$(2\text{-}F_3C)H_4C_6{-}C_6H_4(4'\text{-}OCH_3)$	93
5	$(4\text{-}H_3C)C_6H_4Br$	$(4\text{-}H_3CO)C_6H_4B(OH)_2$	2	$(4\text{-}H_3C)H_4C_6{-}C_6H_4(4'\text{-}OCH_3)$	94
6	C_9H_6NBr	$C_6H_5B(OH)_2$	3	$C_9H_6N{-}C_6H_5$	89
7	$(4\text{-}H_3CO)C_6H_4Cl$	$C_6H_5B(OH)_2$	24	No reaction	-
8[c]	$1,2\text{-}C_6H_4I_2$	$C_6H_5B(OH)_2$	4	$1,2\text{-}(C_6H_5)_2{-}C_6H_4$	90
9[c]	$(3\text{-}Br)C_6H_4I$	$C_6H_5B(OH)_2$	4	$1,3\text{-}(C_6H_5)_2{-}C_6H_4$	91
10[c]	$1,4\text{-}C_6H_4Br_2$	$C_6H_5B(OH)_2$	4	$1,4\text{-}(C_6H_5)_2{-}C_6H_4$	89

[a]Reaction condition: ArX (1 mmol), boronic acid (1.2 mmol), K_2CO_3 (1.1 mmol), Pd/Cu−ARF(II) (100 mg), DMF (3 mL), heating the reaction mixture at 65 ^oC. [b]Isolated yield. [c]ArX_2 (1.0 mmol), boronic acid (2.4 mmol), K_2CO_3 (2.2 mmol), Pd/Cu−ARF(II) (100 mg), DMF (3 mL), heating the reaction mixture at 65 ^oC.

V.3.2. Pd/Cu−ARE(II) catalyzed Mizoroki–Heck reaction

After successfull completion of Suzuki–Miyaura cross–coupling, the catalytic efficiency of bimetallic Pd/Cu−ARF(II) catalyst was explored in Mizoroki–Heck reaction. Considering the coupling partner 4-iodoanisole and *n*-butyl acrylate, best result was achieved using triethylamine as base and DMF as a solvent at 70 ^oC within 2h, (Table V.3). Triethylamine was suitable over other inorganic bases like K_2CO_3 and NaOAc.

Initial entries of Table V.4, exhibite the results for Heck reaction between aryl iodides and acrylates (Table V.4, entries 1−4). Aryl bromides and chlorides are reluctant towards the reaction under this condition. Bis coupled products are obtained in good yield when diiodo compounds react with ethyl acrylate. We have synthesized different substituted trans stilbenes following the optimized condition (entries 8−10). It may be noted that trans selectivity in the coupled product was observed in each case.

We have extended this Mizoroki–Heck cross–coupling methodology for the preparation of

Table V.3. Optimization of Mizoroki–Heck reaction using Pd/Cu−ARF(II).[a]

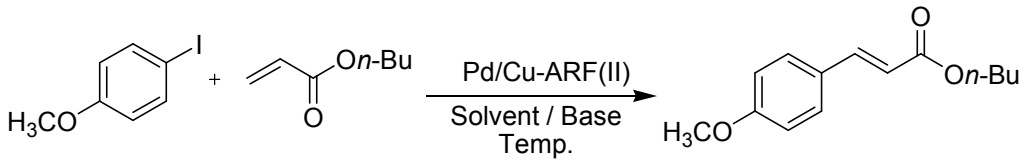

Entry	Solvent	Base	Temperature (^oC)	Time (h)	Yield[b] (%)
1	DMF	Et_3N	RT	10	12
2	DMF	Et_3N	55	10	69
3	**DMF**	**Et_3N**	**70**	**2**	**94**
4	DMF	NaOAc	70	6	88
5	DMF	K_2CO_3	70	6	76
6	DMF	KF	70	10	82

[a] 4-Iodoanisole (1 mmol), *n*-butyl acrylate (1.2 mmol), base (1.1 mmol), Pd/Cu−ARF(II) (100 mg) and solvent (3 mL).[b] Isolated yield.

Table V.4. Mizoroki–Heck cross–coupling using Pd/Cu−ARF(II).[a]

Entry	Aryl halide	Olefine	Time (h)	Product	Yield (%)[b]
1	$(4\text{-}H_3CO)C_6H_4I$		1.5	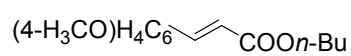	95
2	$(4\text{-}H_3C)C_6H_4I$	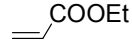	2	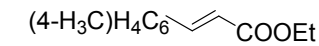	91
3	$(3\text{-Br})C_6H_4I$	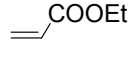	4	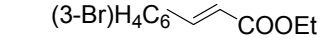	78
4	$(2\text{-}NH_2)C_6H_4I$	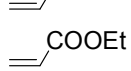	4	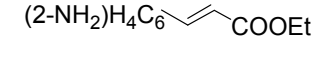	89
5	$(4\text{-}H_3C)C_6H_4Br$		12	No reaction	-
6	$(4\text{-}H_3C)C_6H_4Cl$	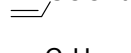	12	No reaction	-
7[c]	$1,3\text{-}C_6H_4I_2$	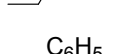	3.5	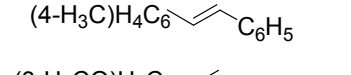	79
8	$(4\text{-}H_3C)C_6H_4I$	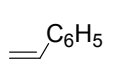	3	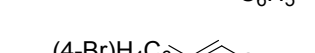	86
9	$(3\text{-}H_3CO)C_6H_4I$	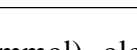	3	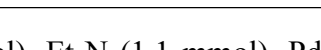	82
10	$(4\text{-Br})C_6H_4I$	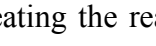	2.5	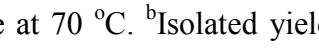	83

[a]Reaction condition: ArX (1 mmol), olefine (1.2 mmol), Et_3N (1.1 mmol), Pd/Cu−ARF(II) (100 mg), DMF (3 mL), heating the reaction mixture at 70 ^oC. [b]Isolated yield. [c] ArI_2 (1.0 mmol), ethylacrylate (2.4 mmol), Et_3N (2.2 mmol), Pd/Cu−ARF(II) (100 mg), DMF (3 mL), heating the reaction mixture at 70 ^oC.

substituted heteocyclic compound like indole. Reaction of 2-iodoaniline with allyl bromide over silica surface generates a mono *N*-allylatd product,[11] when this material was used as a

starting substance for Heck reaction we get 3-methylindole (Scheme V.2) as the sole product.

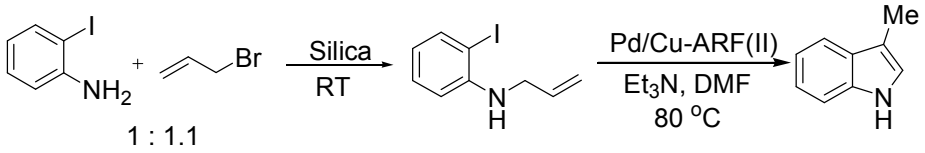

Scheme V.2. Synthesis of 3-methylindole via Mizoroki–Heack coupling with Pd/Cu−ARF(II) catalyst.

V.3.3. Comparative study

The catalytic efficiecy of the bimetallic Pd/Cu−ARF(II) composite was then compared with that of monometallic Pd−ARF catalyst. We immobilized Pd on ARF surface according to our reported procedure and maintain the molar proportion of palladium same as that of bimetallic catalyst Pd/Cu−ARF(II).[12] Considering Suzuki–Miyaura coupling, both Pd–ARF and Pd/Cu-ARF(II) shows almost similar activity for entry 1, listed in Table V.2 (see Figure V.1a) but when we concerned about Mizoroki–Heck reaction (entry 1, Table V.4), bimetallic catalyst (Pd/Cu−ARF(II)) shows much higher activity compared to mono metallic catalyst (Figure V.1b). For Mizoroki–Heck coupling Pd/Cu−ARF(II) serve 97% conversion within 2h while using Pd–ARF only 83% conversion was achieved within this period and reaches maximum up to 94% after 3.5h.

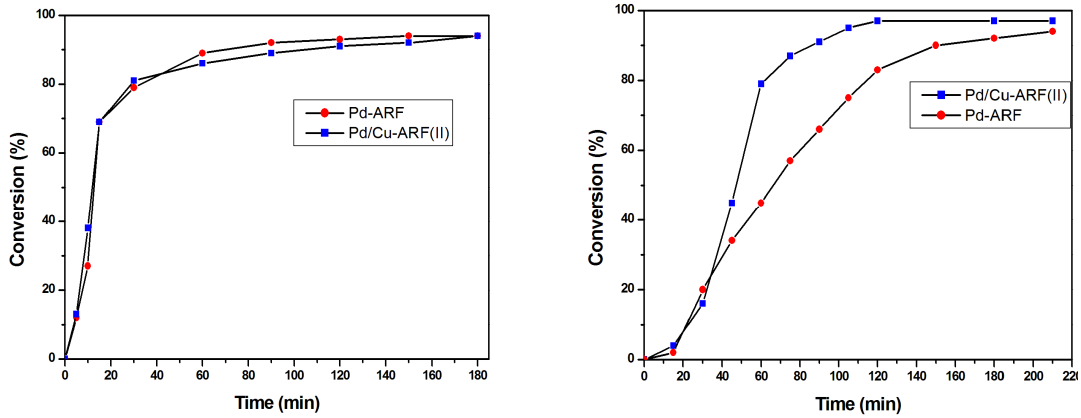

(a) **(b)**

Figure V.1. Time conversion plot for (a) Suzuki–Miyaura and (b) Mizoroki–Heck coupling reaction using Pd/Cu−ARF(II) and ARF Pd.

V.3.4. Recycling experiments

The recyclability of the catalyst Pd/Cu−ARF(II) was also checked for both Suzuki–Miyaura and Mizoroki–Heck reactions. After completion of reaction, catalysts were collected through simple filtration, properly washed with water followed by acetone, dried under vacuumed for 30 min and used for next cycle. The results are summarised in Figure V.2. The catalyst can be

reused at least seven times for both Suzuki–Miyaura and Mizoroki–Heck reactions separately without decrease in catalytic activity.

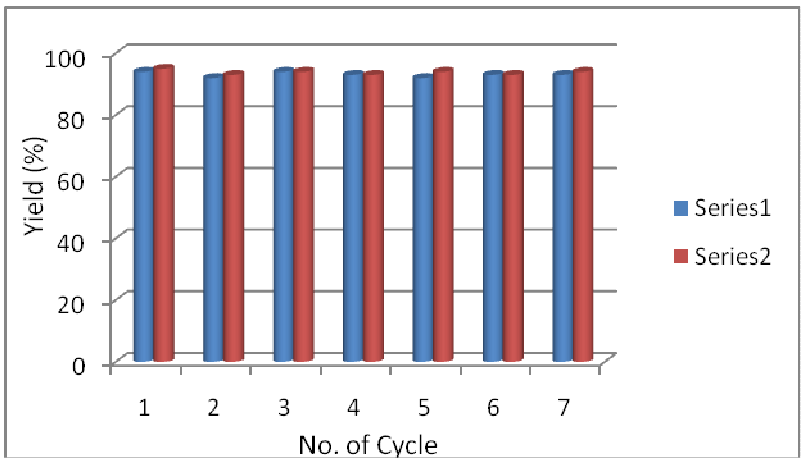

Figure V.2. Recycling experiments using Pd/Cu−ARF(II); **series1:** Suzuki–Miyaura cross–coupling between 4-bromotoluene and 4-methoxyphenylboronic acid; **series2:** Mizoroki–Heck cross–coupling between 4-iodotoluene and ethyl acrylate.

V.3.5. Characterization of recovered catalyst

After 7th catalytic cycles the bimetallic Pd/Cu−ARF(II) composite material was characterized by XRD (Figure V.3). Peaks related to PdO was disappeared but surprisingly peak corresponds to Pd(0) becomes more sharper compare to initial catalyst i.e. during catalysis (Mizoroki–Heck) Pd NPs become more crystalline in nature. However, CuO was found to be unaltered.

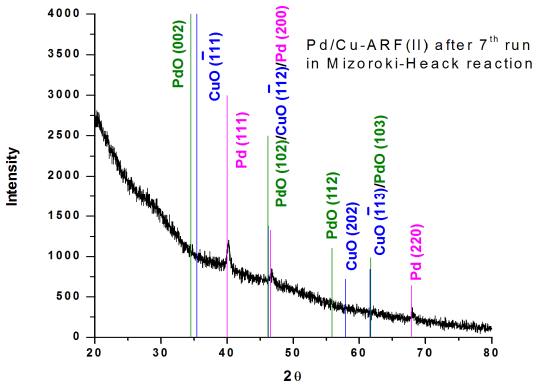

Figure V.3. XRD analysis of Pd/Cu−ARF(II) catalyst after 7th consecutive runs in Mizoroki–Heck reaction.

V.4. Conclusion

In summary, we have demonstrated Pd/Cu−ARF(II) bi-metallic composite nanoparticles as an efficient heterogeneous catalyst for Suzuki–Miyaura and Mizoroki–Heck coupling reactions under ligand-free and mild conditions. The bi-metallic nanocomposite material

Pd/Cu−ARF(II) was much effective as compare to monometallic Pd–ARF catalyst in Mizoroki–Heck coupling. Further studies included a sequential *N*-allylation and Mizoroki–Heck cross–coupling of 2-iodoaniline provides a heterocyclic moiety, 3-methylindole. The catalyst can be recycled up to seven runs without significant loss of catalytic activity.

V.5. Experimental section

V.5.1. General information

Amberlite IRA 900 (chloride form) was purchased from Acros Organics, Belgium and used after washing with water and acetone followed by drying under vacuum. Other chemicals were purchased and used directly. The X-ray diffraction (XRD) studies of the powder samples were done using the Rigaku SmartLab (9 kW) diffractometer using CuKα radiation. NMR spectra were taken in $CDCl_3$ using Bruker Avance AV-300 spectrometer operating for ^1H at 300 MHz and for ^{13}C at 75 MHz. The spectral data were measured using TMS as the internal standard.

V.5.2. Preparation of Pd/Cu−ARF(II)

To a solution of $Pd(OAc)_2$ (56 mg, 0.25 mmol) and $Cu(OAc)_2$ (50 mg, 0.25 mmol) in DMF (10 mL) was added ARF (1 g) and the mixture taken in screw-capped sealed tube was heated at 60 ^oC for 1h with occasional shaking. The supernatant liquid appeared completely colourless by this time and the greyish beads of ARF turned black. The mixture was cooled to room temperature and the resin beads were filtered off and washed with water (3 x 5 mL) and acetone (2 x 5 mL). Resulting black resin beads were dried under vacuum and used for analyses and reactions.

V.5.3. Preparation of Pd–ARF

$Pd(OAc)_2$ (56 mg, 0.25 mmol) in DMF (10 mL) was added ARF (1 g) and the mixture taken in screw-capped sealed tube was heated at 60 ^oC for 1h with occasional shaking. The supernatant liquid appeared completely colourless by this time and the greyish beads of ARF turned black. The mixture was cooled to room temperature and the resin beads were filtered off and washed with water (3 x 5 mL) and acetone (2 x 5 mL). Resulting black resin beads were dried under vacuum and used for analyses and reactions.

V.5.4. General procedure for Suzuki–Miyaura cross–coupling using Pd/Cu−ARF(II)

Aryl halide (1 mmol), arylboronic acid (1.2 mmol), potassium carbonate (1.1 mmol), Pd/Cu−ARF(II) (100 mg) and DMF (3 mL) were charged in a 15 mL sealed tube and heated

the reaction mixture at 65 ^{o}C under gentle magnetic starring. The reaction progress was monitored by TLC. After completion of reaction the mixture was allowed to cool to room temperature and diluted with water (5 mL). The mixture was passes through a cotton bed and the filtrate part was extracted with diethyl ether. The organic part was dried over sodium sulphate and concentrated under vacuumed. The residue was purified by passing through a short silica gel column and elution with light petroleum. All products were characterized by ^{1}H, ^{13}C NMR spectral data, and also compared with reported melting point (for known solid compounds).

V.5.5. General procedure for Mizoroki–Heck coupling using Pd/Cu−ARF(II)

Aryl halide (1 mmol), activated alkene (1.2 mmol), triethylamine (1.1 mmol), Pd/Cu−ARF(II) (100 mg) and DMF (3 mL) were charged in a 15 mL sealed tube and heated the reaction mixture at 70 ^{o}C under gentle magnetic starring. The reaction progress was monitored by TLC. After completion of reaction the mixture was allowed to cool to room temperature and diluted with water (5 mL). The mixture was passes through a cotton bed and the filtrate part was extracted with diethyl ether. The organic part was dried over sodium sulphate and concentrated under vacuumed. The residue was purified by passing through a short silica gel column and elution with light petroleum or 2% ethyl acetate-light petroleum. All products were characterized by ^{1}H, ^{13}C NMR spectral data, and also compared with reported melting point (for known solid compounds).

V.5.6. Preparation of 3-Methylindole

Step I: An equimolar mixture of 2-iodoaniline and allyl bromide was mixed with pre-activated silica (Grade: TLC; HF254) in a mortar pestle and the solid mixture was transferred into a flask. Gentle agitation was then provided by a magnetic spin bar at room temperature for 2h. After completion, the reaction mixture was washed repeatedly with diethyl ether and combined ethereal layer was dried over anhydrous Na_2SO_4 and concentrated. The crude product was then purified by column chromatography over silica gel and isolating the desired product *N*-allyl-2-iodobenzenamine (216 mg, 82%).

Step II: A mixture of *N*-allyl-2-iodobenzenamine (1 mmol, 164 mg), triethyl amine (1.1 mmol) and Pd/Cu-ARF(II) in DMF was taken in a sealed tube and heated at 80 ^{o}C for 3h. After completion of reaction the mixture was cool at room temperature and diluted with water (5 mL). The mixture was extracted with diethyl ether, dried over Na_2SO_4 and concentrated under vacuumed. The crude product was than purified by passing through a silica gel column

and elution with light 5% ethyl acetate-light petroleum. The product was characterized by NMR.

V.5.7. Physical properties and spectral data of compounds

Table V.2, entry 1

4-Methoxybiphenyl[13]

White solid, mp 91-92 ^{o}C (Lit. mp 90-91 ^{o}C)

^{1}H NMR ($CDCl_3$, 300 MHz): δ/ppm 3.84 (s, 3H,), 6.97 (dd, J = 2.1 and 6.9 Hz, 2H), 7.29-7.32 (m, 1H), 7.38-7.43 (m, 2H), 7.51-7.56 (m, 4H); ^{13}C NMR ($CDCl_3$, 75 MHz): δ/ppm 55.3, 114.2, 126.6, 126.7, 128.1, 128.7, 133.8, 140.8, 159.2.

Table V.2, entry 2

3-Methoxy-3'-methylbiphenyl[13]

Colourless liquid

^{1}H NMR ($CDCl_3$, 300 MHz): δ/ppm 2.41 (s, 3H), 3.84 (s, 3H), 6.87-6.89 (m, 1H), 7.11-8.18 (m, 3H), 7.28-7.39 (m, 4H); ^{13}C NMR ($CDCl_3$, 75 MHz): δ/ppm 21.5, 55.2, 112.6, 112.8, 119.6, 124.3, 127.9, 128.1, 128.6, 129.6, 138.3, 141.0, 142.8, 159.8.

Table V.2, entry 3

2-Methoxybiphenyl[13]

Colourless liquid

^{1}H NMR ($CDCl_3$, 300 MHz): δ/ppm 3.81 (s, 3H), 6.97-7.06 (m, 2H), 7.29-7.43 (m, 5H), 7.51-7.54 (m, 2H); ^{13}C NMR ($CDCl_3$, 75 MHz): δ/ppm 55.5, 111.2, 120.8, 126.9, 127.9, 128.6, 129.5, 130.7, 130.9, 138.5, 156.4.

Table V.2, entry 4

4-Methoxy-2'-trifluoromethylbiphenyl[14]

Colourless liquid

^{1}H NMR ($CDCl_3$, 300 MHz): δ/ppm 3.81 (s, 3H), 6.90-6.94 (m, 2H), 7.22-7.31 (m, 3H), 7.37-7.42 (m, 1H), 7.48-7.53 (m, 1H), 7.71 (d, J = 7.8 Hz, 1H); ^{13}C NMR ($CDCl_3$, 75 MHz): δ/ppm 55.1, 113.2, 122.4, 126.0 (q, J = 5.4 Hz), 127.0, 128.5 (q, J = 29.4 Hz), 130.1 (d, J = 1.3 Hz), 131.2, 132.2, 132.3, 141.2 (d, J = 1.9 Hz), 159.1.

Table V.2, entry 5

4-Methoxy-4'-methylbiphenyl[13]

White solid, mp 111-112 ^{o}C (Lit. mp 112-113 ^{o}C)

^{1}H NMR ($CDCl_3$, 300 MHz): δ/ppm 2.38 (s, 3H), 3.84 (s, 3H), 6.96 (d, J = 8.7 Hz, 2H), 7.22 (d, J = 8.4 Hz, 2H), 7.45 (d, J = 8.1 Hz, 2H), 7.51 (d, J = 8.7 Hz, 2H); ^{13}C NMR ($CDCl_3$, 75

MHz): δ/ppm 21.0, 55.3, 114.1, 126.5, 127.9, 129.4, 133.7, 136.3, 137.9, 158.9.

Table V.2, entry 6

3-Phenylquinoline[15]

Colourless liquid

^{1}H NMR ($CDCl_3$, 300 MHz): δ/ppm 7.38-7.56 (m, 4H), 7.65-7.72 (m, 3H), 7.83 (dd, *J* = 1.2 and 7.8 Hz, 1H), 8.14 (d, *J* = 8.4 Hz, 1H), 8.25 (d, *J* = 2.4 Hz, 1H), 9.17 (d, *J* = 2.4 Hz, 1H); ^{13}C NMR ($CDCl_3$, 75 MHz): δ/ppm 126.9, 127.3, 127.9, 128.0, 129.0, 129.3, 133.1, 133.7, 137.7, 147.1, 149.7.

Table V.2, entry 8

***o*-Terphenyl**[13]

Solid, mp 54-55 ^{o}C (Lit. mp 54-55 ^{o}C)

^{1}H NMR ($CDCl_3$, 300 MHz): δ/ppm 7.13-7.26 (m, 10H), 7.40-7.44 (m, 4H); ^{13}C NMR ($CDCl_3$, 75 MHz): δ/ppm 126.4, 127.4, 127.8, 129.9, 130.6, 140.6, 141.5.

Table V.2, entry 9

***m*-Terphenyl**[13]

White solid, m.p. 84-85 ^{o}C (Lit. mp 83-85 ^{o}C)

^{1}H NMR ($CDCl_3$, 300 MHz): δ/ppm 7.33-7.38 (m, 2H), 7.43-7.59 (m, 7H), 7.63-7.66 (m, 4H), 7.79-7.80 (m, 1H); ^{13}C NMR ($CDCl_3$, 75 MHz): δ/ppm 126.1, 126.2, 127.3, 127.4, 128.8, 129.2, 141.2, 141.8.

Table V.2, entry 10

***p*-Terphenyl**[12]

White solid, mp 211-212 ^{o}C (Lit. mp 212-214 ^{o}C)

^{1}H NMR ($CDCl_3$, 300 MHz): δ/ppm 7.35-7.38 (m, 2H), 7.43-7.48 (m, 4H), 7.63-7.67 (m, 8H); ^{13}C NMR ($CDCl_3$, 75 MHz): δ/ppm 127.0, 127.3, 127.5, 128.8, 140.1, 140.7.

Table V.4, entry 1

(*E*)-Butyl 3-(4-methoxyphenyl)acrylate[16]

Colourless liquid

^{1}H NMR ($CDCl_3$, 300 MHz): δ/ppm 0.96 (t, *J* = 7.5 Hz, 3H), 1.42-1.71 (m, 4H,), 3.83 (s, 3H), 4.20 (t, *J* = 6.6 Hz, 2H), 6.31 (d, *J* = 15.9 Hz, 1H), 6.90 (dd, *J* = 2.1 and 6.9 Hz, 2H), 7.48 (dd, *J* = 2.1 and 6.9 Hz, 2H), 7.64 (d, *J* = 15.9 Hz, 1H); ^{13}C NMR ($CDCl_3$, 300 MHz): δ/ppm 13.7, 19.2, 30.7, 55.3, 64.2, 114.2, 115.7, 127.1, 129.6, 144.2, 161.2, 167.4.

Table V.4, entry 2

(*E*)-Ethyl 3-*p*-tolylacrylate[17]

Colourless liquid

^{1}H NMR ($CDCl_3$, 300 MHz): δ/ppm 1.32 (t, *J* = 7.2 Hz, 3H), 2.35 (s, 3H), 4.25 (q, *J* = 7.2 Hz, 2H), 6.38 (d, *J* = 15.9 Hz, 1H), 7.17 (d, *J* = 7.8 Hz, 2H), 7.41 (d, *J* = 6.6 Hz, 2H), 7.66 (d, *J* = 15.9 Hz, 1H); ^{13}C NMR ($CDCl_3$, 300 MHz): δ/ppm 14.2, 21.3, 60.3, 117.0, 127.9, 129.5, 131.6, 140.5, 144.5, 167.1.

Table V.4, entry 3

(*E*)-Ethyl 3-(3-bromophenyl)acrylate[12]

Colourless liquid

^{1}H NMR ($CDCl_3$, 300 MHz): δ/ppm 1.33 (t, *J* = 7.2 Hz, 3H), 4.26 (q, *J* = 7.2 Hz, 2H), 6.42 (d, *J* = 15.9 Hz, 1H), 7.21-7.26 (m, 1H), 7.41-7.50 (m, 2H), 7.58 (d, *J* = 15.9 Hz, 1H), 7.64-7.66 (m, 2H); ^{13}C NMR ($CDCl_3$, 300 MHz): δ/ppm 14.2, 60.6, 119.6, 122.9, 126.5, 130.2, 130.6, 132.8, 136.4, 142.7, 166.4.

Table V.4, entry 4

(*E*)-Ethyl 3-(2-aminophenyl)acrylate[12]

Yellow solid, mp 75-76 ^{o}C (Lit. mp 76-78 ^{o}C)

^{1}H NMR ($CDCl_3$, 300 MHz): δ/ppm 1.33 (t, *J* = 7.2 Hz, 3H), 3.89 (br s, 2H), 4.25 (q, *J* = 7.2 Hz, 2H), 6.35 (d, *J* = 15.9 Hz, 1H), 6.68-6.78 (m, 2H), 7.13-7.19 (m, 1H), 7,37 (dd, *J* = 1.5 and 7.5 Hz, 1H), 7.83 (d, *J* = 15.9 Hz, 1H); ^{13}C NMR ($CDCl_3$, 300 MHz): δ/ppm 14.2, 60.4, 116.7, 118.0, 118.9, 119.8, 127.9, 131.2, 140.0, 145.4, 167.3.

Table V.4, entry 7

Ethyl (*E*)-3-{3-[(*E*)-2-(Ethoxycarbonyl)vinyl]phenyl}acrylate[12]

White solid, mp 50-51 ^{o}C (Lit. mp 50-52 ^{o}C)

^{1}H NMR ($CDCl_3$, 300 MHz): δ/ppm 1.34 (t, *J* = 7.2 Hz, 3H), 4.23 (q, *J* = 7.2 Hz, 2H), 6.47 (d, *J* = 15.9 Hz, 1H), 7.40-7.54 (m, 4H), 7.67 (d, *J* = 16.2 Hz, 1H); ^{13}C NMR ($CDCl_3$, 300 MHz): δ/ppm 14.2, 60.5, 119.1, 127.5, 129.3, 135.0, 143.5, 166.6.

Table V.4, entry 8

(*E*)-4-Methylstilbene[18a-c]

White solid, 120-121 ^{o}C (Lit mp 121.7-122.3 ^{o}C)

^{1}H NMR ($CDCl_3$, 300 MHz): δ/ppm 2.35 (s, 3H), 7.06 (d, *J* = 1.5 Hz, 2H), 7.16 (d, *J* = 8.4 Hz, 2H), 7.23-7.26 (m, 1H), 7.31-7.42 (m, 4H), 7.48-7.51 (m, 1H); ^{13}C NMR ($CDCl_3$, 300 MHz): δ/ppm 21.2, 126.4, 126.41, 127.4, 127.7, 128.6, 129.4, 134.5, 137.5.

Table V.4, entry 9

(*E*)-3-Methoxylstilbene[19]

^{1}H NMR ($CDCl_3$, 300 MHz): δ/ppm 3.86 (s, 3H), 6.82 (ddd, J = 0.9, 2.7 and 8.1 Hz, 1H), 7.05-7.13 (m, 4H), 7.24-7.38 (m, 4H), 7.50-7.53 (m, 2H); ^{13}C NMR ($CDCl_3$, 300 MHz): δ/ppm 55.2, 111.7, 113.3, 119.2, 126.5, 127.7, 128.6, 128.7, 129.0, 129.6, 137.2, 138.8, 159.9.

Table V.4, entry 10

(*E*)-4-Bromostilbene[18c,d]

White Solid, mp 139-140 ^{o}C (Lit mp 136.5-139 ^{o}C)

^{1}H NMR ($CDCl_3$, 300 MHz): 7.06 (d, J = 7.5 Hz, 2H), 7.26-7.52 (m, 9H); ^{13}C NMR ($CDCl_3$, 300 MHz): δ/ppm 121.3, 126.5, 127.4, 127.9, 128.0, 128.7, 129.4, 131.8, 136.3, 137.0.

Scheme 1, step II

3-Methyl-1*H*-indole[20]

Off white solid, mp 92-93 ^{o}C (Lit. mp 91-92 ^{o}C)

^{1}H NMR ($CDCl_3$, 300 MHz): 2.34 (d, J = 0.9 Hz, 3H), 6.96 (d, J = 0.9 Hz, 1H), 7.09-7.21 (m, 2H), 7.32-7.36 (m, 1H), 7.86 (br s, 1H); ^{13}C NMR ($CDCl_3$, 300 MHz): δ/ppm 9.6, 110.9, 111.7, 118.8, 119.1, 121.5, 121.8, 128.3, 136.3.

V.6. References

References are given in BIBLIOGRAPHY under Chapter V (pp. 151−152).

CHAPTER VI

Graphene oxide as "carbocatalyst" for one-pot sequential dehydration–hydrothiolation of secondary aryl alcohols and chemoselective thioacetalization of aldehydes

VI.1. Introduction

The efficiency of graphene oxide (GO) and other chemically modified graphenes (CMGs) as the carbocatalysts has raised enormous interest since the seminal papers from Bielawski and co-workers.[1] GO possesses rich chemical functionality, is slightly acidic (pH 4.5 at 0.1 mg mL^{-1})[2], and has long been recognized as having strong oxidizing properties.[3] Accordingly, GO has been mostly employed in oxidation of different functional groups.[4] For example, oxidation of benzyl alcohol to benzaldehyde,[4a,b] oxidation of thiol to disulfide,[4c] or amine to imine etc.[4d]

Additional advantages of graphene-based materials as catalysts are sustainability and absence of transition metals in their composition. Because graphene oxide (GO) is prepared by the oxidation of graphite[5] and contains only carbon, it can be considered as renewable and can be obtained from natural carbon sources. Thus, carbon and oxygen are the main elements present in GO, and because of the absence of extra transition metals in GO, the contamination of the products can be avoided easily.

Sulfated graphene ($G-SO_3H$) obtained by hydrothermal sulfation of reduced graphene oxide with fuming sulfuric acid at 180 ^oC was tested as catalyst for different acid catalyzed reactions like esterification of acetic acid, the Pechmann condensation and hydration of propylene oxide.[6] Some recent literature reports have revealed that GO obtained from conventional Hummers method acts as solid heterogeneous acid catalyst without any subsequent post treatment.[7]

VI.2. Persent work: Background and Objective

In 2011 Chauhan co-workers have been execute Graphite oxide as solid acid catalysts for the room temperature preparation of dipyrromethanes and calix[4]pyrroles under ambient conditions in both organic and aqueous solutions (Scheme VI.1).[8]

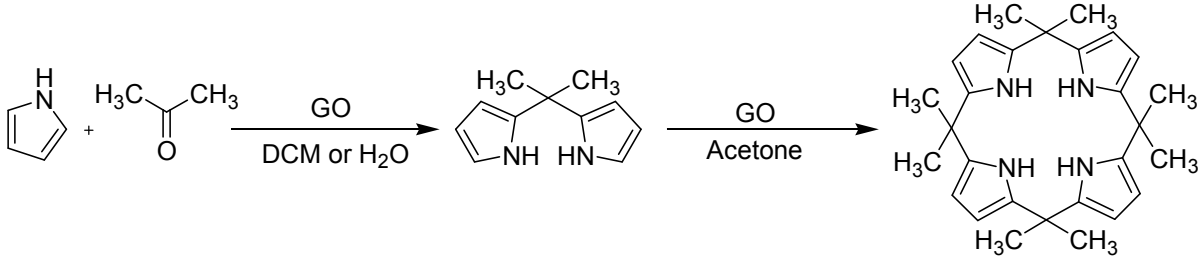

Scheme VI.1. GO catalyzed condensation of pyrrole and ketones into dipyrromethanes and calix[4]pyrroles.

Jain et al. showed graphene oxide as a simple and efficient catalyst for the synthesis of various amino-substituted compounds via aza-Michael addition of amines and electron

deficient olefins (Scheme VI.2).[9] These reactions were found to proceed under relatively mild conditions and afforded excellent product yields within shorter reaction times. Moreover, the catalyst was found to be easily recoverable and recyclable with the consistent catalytic activity. However, the exact mechanism of the reaction was not clear.

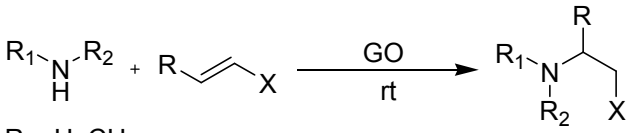

R = H, CH_3
R_1 = Et, *n*-Bu, *n*-Pr, Bz
R_2 = Et, *n*-Bu, *n*-Pr, Bz
X = CN, $CONH_2$, $COOCH_3$

Scheme VI.2. GO catalyzed Aza-Michael addition of amines.

In the similar direction Garcia co-workers used GO as an acid catalyst for the ring opening of styrene oxide in methanol under ambient conditions. In the presence of GO, almost >99% conversion with 93% selectivity toward 2-methoxy-2-phenylethanol was achieved within 1h (Scheme VI.3).[10] Nevertheless, the yield of secondary product, increased significantly with increasing reaction time. The protocol was successfully extended for a variety of epoxide substrates with different nucleophiles. In most of the cases, the regioselectivity was high and expected from an acid-catalyzed S_N1 ring opening mechanism.

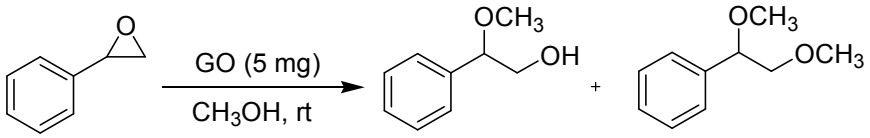

Scheme VI.3. GO catalyzed RO of styrene oxide.

In their next work Gracia group showed GO obtained through the standard Hummers oxidation of graphite is a highly efficient reusable heterogeneous catalyst for the acetalization of aldehydes (Scheme VI.4).[11] Analytical and spectroscopic evidence suggests that sulfate groups introduced spontaneously during Hummers oxidation are the sites responsible for catalysis.

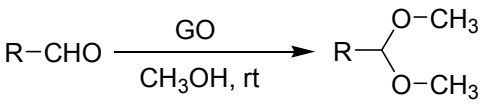

R = aryl, alkyi, heteroaryl

Scheme VI.4. Acetalization of various aldehydes with methanol catalyzed by GO.

GO was found to be an active catalyst for etherification of benzyl alcohol to dibenzyl ether in the absence of added solvent (Scheme VI.5).[12] The dehydrative etherification of alcohols is a reaction that typically is performed by strong Brönsted acids, and the catalytic results suggest

that adsorption of benzyl alcohol on the GO sheet can increase the reaction rate in a comparable way as alternative use of strong acids.

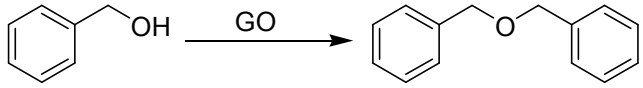

Scheme VI.5. Dehydrative etherification of benzyl alcohol over graphene oxide.

GO was found to be an efficient and a recyclable acid catalyst for conversion of fructose-based biopolymers into 5-ethoxymethylfurfural (Scheme VI.6).[13] Under optimal catalyst loading (20 mg), a 92% yield of 5-ethoxymethylfurfural was achieved with 96% conversion of 5-hydroxymethylfurfural. On the other hand, natural flake graphite or the rGO showed no reaction under the same reaction conditions.

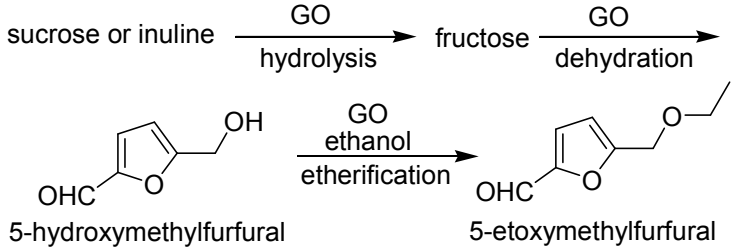

Scheme VI.6. GO-Catalyzed Conversion of Carbohydrates to 5-Ethoxymethylfurfural and Ethyl Levulinate.

In other works, synthesis of xanthenes and benzoxanthenes have been reported using GO or sulfated rGO microsheets as Bronsted acid catalysts (Scheme VI.7).[14] GO was obtained through a modified Hummers method, and rGO-Ar-SO_3H was obtained using an arylsulfonate diazonium salt as intermediate to anchor covalently aryl sulfonic groups on the GO sheet. Importantly, only 20 mg of rGO-Ar-SO_3H or 30 mg of GO is needed to condense 1 mmol of reactant. Both rGO-Ar-SO_3H and GO can be reused for at least five cycles with a slight decrease of the yield from 94% to 81% and from 91% to 74%, respectively.

In 2013, Eigler and co-worker shows, GO obtained from Hummers method possess sulphur functionality (scheme VI.8), which influences the structural, bonding, and physicochemical properties of GO.[15] These sulfate groups (estimated to be present at approximately one sulfate per twenty carbon atoms[15]) are believed to be the source of GO's acidity (pKa 3–4 in water), which is appreciably lower than what would be expected for carboxylates or other simple carbon–oxygen acidic species.[16]

So there is a scope to explore this particular property of GO i.e. the acidic property in other organic transformations. Herein we report GO as carbocatalyst in two separate reactions. In our initial studies we describe a new sequential dehydration–hydrothiolation reaction of mixtures of secondary aryl alcohols and thiols catalyzed by graphene oxide for the preparati-

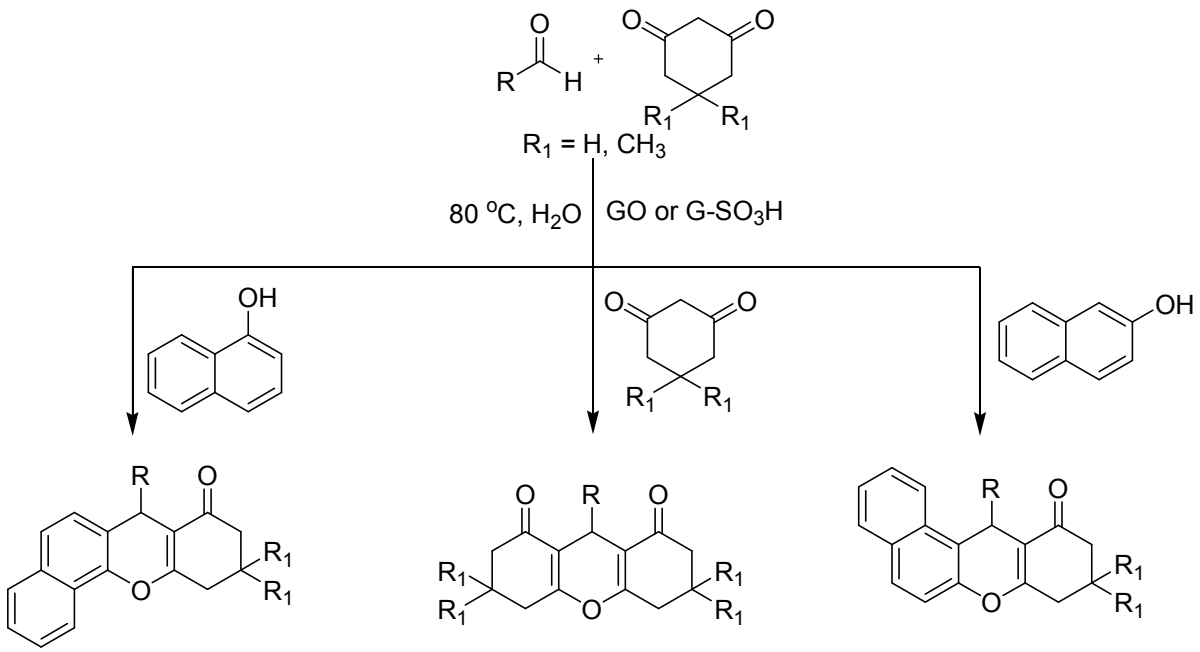

Scheme VI.7. Preparation of xanthene and benzoxanthene derivatives using GO or G-SO_3H.

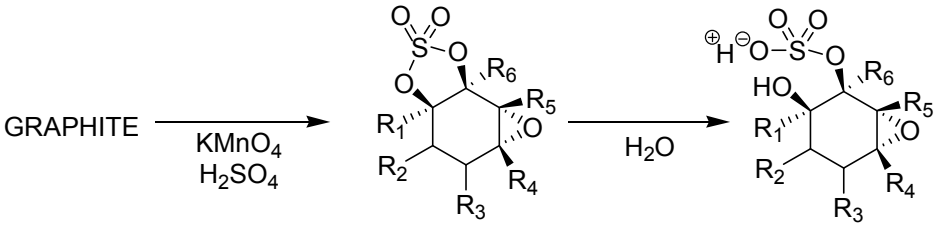

Scheme VI.8. Organosulfates present in GO prepared via the Hummers method.

on of unsymmetrical thioethers (Scheme VI.9).

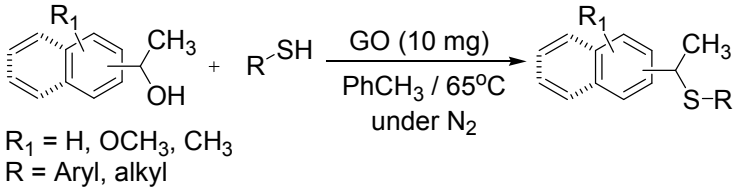

Scheme VI.9. Graphene oxide (GO)-catalyzed one-pot sequential dehydration-hydrothiolation.

In our second experement we report an efficient method for the preparation of dithioacetal (symmetrical, unsymmetrical and cyclic) from aryl/alkyl aldehydes with the aid of catalytic amount of graphene oxide (Scheme VI.10).

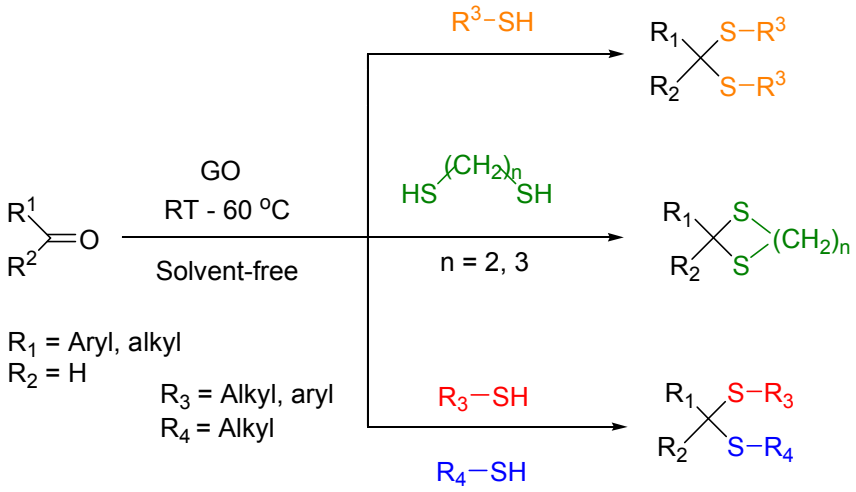

Scheme VI.10. General scheme illustrating GO-catalyzed diverse dithioacetals formation.

VI.3. Present work: Result and Discussion

VI.3.1. Graphene oxide preparation and characterization

To begin our study, we prepared GO from graphite powder according to the modified Hummers method.[17] The FT-IR spectrum of the resulting GO was compared with that of the reported absorption bands,[10,11,18] and found fairly similar absorption bands for the functional groups.

Figure VI.1 shows the FT-IR spectra of prepared GO. GO exhibits a broad peak around 3360 cm^{-1}, which was assigned to O−H stretching vibrations. The other stretching vibration bands at 1719, 1618, 1412 and 1218 cm^{-1} are assigned respectively for COOH, C=C, O−H, and C−O (epoxy) groups, respectively.[18] The SO_3−H stretching vibration bands appear at 1052 cm^{-1}.[10,11]

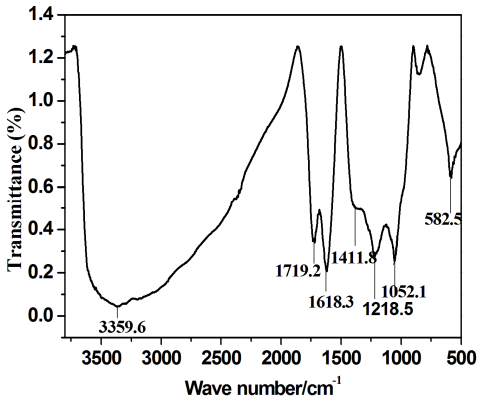

Figure VI.1. FT-IR spectra of graphene oxide.

VI.3.2. Sequential dehydration–hydrothiolation reaction

Bielawski and co-workers have reported the GO-facilitated oxidation of benzylic alcohols to the corresponding aldehydes or ketones with varying yields.[4a] From their observations, it was

noted that diphenylmethanol afforded a >98% conversion to the corresponding ketone, while 1-phenylethanol gave only 26% acetophenone. They also observed minimal oxidation of benzyl alcohol to benzaldehyde with low catalyst loadings or reaction temperatures. Interestingly, the oxidation reactions of alcohols did not proceed under a N_2 atmosphere.

Considering that *sec*. aryl alcohols are also prone towards dehydration, we envisaged that the course of the reaction might be altered and driven towards dehydration depending upon some variations such as, lower loading of GO (w%) and carrying out the reaction under milder conditions and N_2-atmosphere. Preliminary studies with 1-(2-naphthyl)ethanol revealed that the dehydration is indeed possible by heating its solution of toluene (N_2- bubbled) at 80−100 ^oC in the presence of GO (5−20 w%), but not to the extent that is well acceptable (40−45%). We reasoned that the dehydration may perhaps be driven, if the resulting alkene is reacted immediately with some other reactant. While a combination of alkene and thiol represents an atom-economic 'click' reaction,[19] Bielawski and coworkers,[4c,20] reported the GO-catalyzed thiol oxidation to disulfide and also the polymerization of styrene under solvent-free conditions. Based on this background, we designed the experiments starting from a mixture of a secondary aryl alcohol and a thiol.

To optimize the reaction condition, an equimolar mixture of 1-(2-naphthyl)ethanol and 4-chlorobenzenethiol in toluene was heated at different temperatures in the presence of varying amounts of GO (summarized in Table VI.1). Initial stirring at up to 50 ^oC yielded no desired product except a certain amount of disulfide, formed by the oxidative dimerization of the thiol (entries 1 and 2). Increasing the reaction temperature and quantity of thiol however, gave the expected thiol-addition product (67–79%), characterized as [(4-chlorophenyl)(1-phenylethyl)sulfane], obtained through the sequential dehydration–hydrothiolation reaction in an entirely Markovnikov fashion (entries 3 and 4), with minimal amounts of diphenyldisulfide (8%). Further heating (80 ^oC) did not show significant improvement except slightly more disulfide formation (entry 5). Increasing or decreasing the amount of GO (wt%), or changing the solvent was not effective either (entries 6–10). The reactions carried out in DMF or without GO did not produce traces of the desired thioether (entries 11 and 12). Since these findings are new and thioethers are important building blocks for the synthesis of biologically active compounds,[21] we became interested in extending the reaction protocol, as in entry 4, with a variety of secondary aryl alcohols and thiols to finally create a general and practical method for the preparation of unsymmetrical thioethers via a one-pot GO-facilitated metal-free sequential dehydration–hydrothiolation reaction. The preparation of thioethers from secondary aryl alcohols has been previously reported via Pd-catalyzed S_N1 reactions.[22]

Table VI.1. Optimization of sequential dehydration-hydrothiolation reaction conditions.[a]

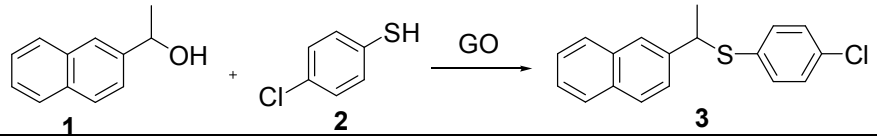

1 **2** **3**

Entry	GO (mg / w%)	Solvent	Temp (^oC)	Time (h)	Product yield (%)[b] 3	Disulfide	2-Vinylnaphthalene
1	10 / 6	Toluene	rt	24	Nil	14	Nil
2	10 / 6	Toluene	50	24	Nil	22	Nil
3	10 / 6	Toluene	65	2	67	8	12
4	**10 / 6**	**Toluene**	**65**	**2**	**79**	**8**	**Nil**
5	10 / 6	Toluene	80	1.5	65	16	Nil
6	20 / 12	Toluene	65	1.5	47	23	Nil
7	5 / 3	Toluene	65	6	49	17	Nil
8	10 / 6	1,4-dioxane	65	3.5	51	20	Nil
9	10 / 6	THF	65	3	48	22	Nil
10	10 / 6	MeCN	65	2	58	15	Nil
11	10 / 6	DMF	65	24	Nil	31	Nil
12	Nil	Toluene	65	24	Nil	10	Nil

[a] Reactions were performed in 1 (1 mmol), 2 (1 mmol) for entries 1-3 and 1 (1 mmol), 2 (1.2 mmol) for entries 4−11 in solvents (2 mL). [b] Isolated yield.

The first few examples in Table VI.2 represent the reaction of a mixture of 1-(2-naphthyl)ethanol and different aromatic thiols bearing Cl, Me, F and NH_2 groups (Table VI.2, entries 1–5). The reaction protocol was found to be successful, except in entry 5 with the NH_2 group, yielding the corresponding thioether in 67–79% yield along with 8–10% diaryldisulfide. A similar reaction sequence was also observed with 1-(1-naphthyl) ethanol and different arylthiols (entries 6 and 7). In the series of 1-phenylethanol, the variation of the functional groups in either the aryl moiety was also successful and the corresponding unsymmetrical thioethers were obtained in good yields (entries 8–10 and 12). However, the reaction with the aryl alcohol bearing a NO_2 group was unsuccessful, even after leaving the reaction for 24h (entry 11). The disulfide was isolated along with the starting alcohol, 1-(3-nitrophenyl)ethanol. To broaden the scope of the reaction, we attempted a similar reaction sequence with aliphatic thiols. The reactions with both long chain and alicyclic thiols worked without any difficulty. Entries 13–17 demonstrate that the reactions did occured quite well giving the desired unsymmetrical thioethers in fairly good yields (68–81%), along with a minimal formation of the thiol corresponding disulfides. It was observed that the presence of

electron-donating groups in the aryl ring of the alcohol favoured the dehydration–hydrothiolation sequence.

Table VI.2. Graphene oxide (GO) - catalyzed reaction of sec. aryl alcohols with different aromatic thiols.[a]

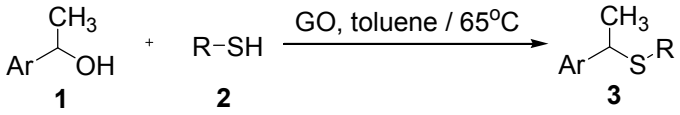

Entry	Ar	R	Time (h)	Yield (%) **3**[b]
1	2-$C_{10}H_7$	4-ClC_6H_4	2	79
2	2-$C_{10}H_7$	4-$CH_3C_6H_4$	1.5	67
3	2-$C_{10}H_7$	2,6-$(CH_3)_2C_6H_3$	2	70
4	2-$C_{10}H_7$	4-FC_6H_4	2	77
5	2-$C_{10}H_7$	4-$NH_2C_6H_4$	3	nil
6	1-$C_{10}H_7$	4-ClC_6H_4	2.5	72
7	1-$C_{10}H_7$	4-FC_6H_4	2.5	74
8	C_6H_5	4-$CH_3C_6H_4$	1.5	69
9	C_6H_5	C_6H_5	1.5	73
10	3,4-$(OCH_3)_2C_6H_3$	C_6H_5	2	78
11	3-$NO_2C_6H_4$	4-FC_6H_4	24	nil
12	3,4-$(OCH_3)_2C_6H_3$	4-ClC_6H_4	2	78
13	2-$C_{10}H_7$	$CH_3(CH_2)_4$	2.5	68
14	2-$C_{10}H_7$	Cy	1	71
15	1-$C_{10}H_7$	$CH_3(CH_2)_6$	2	81
16	4-$CH_3C_6H_4$	$CH_3(CH_2)_4$	3	69
17	3,4-$(OCH_3)_2C_6H_3$	$CH_3(CH_2)_4$	3	80
18[c]	C_6H_5	4-$CH_3C_6H_4$	2	Phenethyl(p-tolyl)sulfane 82
19[d]	C_6H_5	4-$CH_3C_6H_4$	4	74
20[e]	C_6H_5	4-$CH_3C_6H_4$	4	77

[a] Reaction conditions: 1 (1 mmol), 2 (1.2 mmol), GO (10 mg) in toluene (2 mL), was heated at 65 °C under gentle magnetic stirring in a screw-capped vial under N_2. [b] Isolated yield. [c] In the absence of GO. [d] In the presence of GO. [e] In the presence of graphite.

In order to suggest a plausible mechanism and to test whether GO also catalyzes the hydrothiolation providing entirely the Markovnikov addition product, we performed experiments taking a solution of styrene and 4-tolylthiol in toluene under similar reaction conditions, both in the absence and presence of GO. It was interesting to observe that the resulting thioether was then obtained completely in an anti-Markovnikov fashion (Table VI.2,

entries 18 and 19). Further reaction using graphite also gave by the anti-Markovnikov addition (entry 20). We initially observed the partial conversion of the aryl alcohol to styrene, when stirred with GO in the absence of any thiol, and stirring the mixture of styrene and GO in toluene showed a partial decomposition after 12h. Carrying out the experiments under an atmosphere of N_2 might suppress the possibility of polymerization,[20] as well as the further oxidation of the disulfide to thione. Since we obtained the reverse addition product in other cases (i.e. the Markovnikov addition product), we presume that GO participates in the overall process, i.e. the one-pot dehydration–hydrothiolation reaction, via an acid-catalyzed Markovnikov addition.[21e]

The reusability of the GO as an heterogeneous carbocatalyst was also investigated with the same combination of reactants used for the optimization of the reaction conditions. The recovered GO from the first batch was washed with diethyl ether, dried and reused subsequently in four batches with appreciable conversions and without any loss of catalytic activity. In each run, a minimal formation of disulfide (8–10%) was noticed (Table VI.3). The FT-IR spectrum of the recovered GO (after the first run) was measured and displayed essentially the same absorptions, indicating no apparent changes in the functional groups of GO (Figure VI.2).

Table VI.3. Recyclability test of GO in carbocatalysis of one-pot sequential dehydration-hydrothiolation of 1-(2- naphthyl)ethnol and 4-chlorobenzenethiol.[a]

Entry	Yield (%)[b]	Yield(%)[c]
1st run	79	8
2nd run	79	8
3rd run	78	10
4th run	76	8
5th run	76	10

[a] Reaction conditions: alcohol (1 mmol) and thiol (1.2 mmol) in toluene (2 mL) at 65 °C. [b] Isolated yield of thioether (3a). [c] Isolated yield of disulfide.

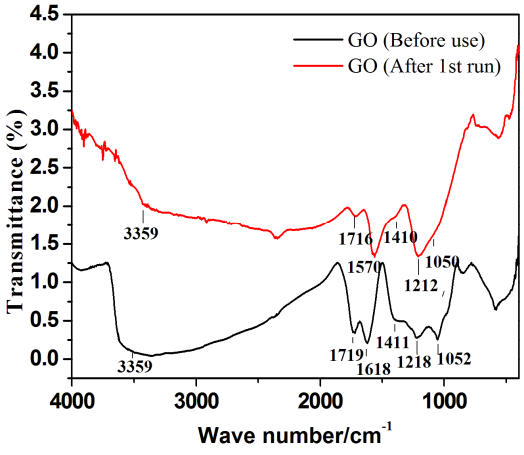

Figure VI.2. Comparative FT-IR spectra of GO before and after 1st use in the reaction 1-(2-naphthyl)ethnol and 4-chlorobenzenethiol in toluene at 65 ^{o}C.

VI.3.3.Thioacetalization of Aldehydes

Thioacetals are the result of Brønsted and Lewis acid catalyzed condensation reaction of aldehydes and ketones with thiols or dithiols and a vast number of methods are available in the literature.[23] Over the past decade, several heterogeneous acid catalysts such as *p*-TsOH/silicagel,[24a] $H_3PW_{12}O_{40}/SiO_2$,[24b] Montmorillonite K-10 Clay,[24c] Amberlyst- 15,[24d] PPA/SiO_2,[24e] Melamine trisulfonic acid (MTSA),[24f] silicasulfuric acid (SSA),[24g] solid-supported dithiolanylium or dithianylium tetrafluoroborate salts,[24h] and also ionic liquids,[24i,j] have been employed for the preparation of thioacetals.

Moreover, while in most cases the catalyst is not recoverable, heterogeneous acid catalysts often do not find wide applicability to various substrates. We were interested to explore the feasibility and catalytic efficiency of GO in thioacetalization of aldehydes and ketones and report an efficient and practical method for the preparation of dithioacetal from aryl/alkyl aldehydes with the aid of catalytic amount graphene oxide (GO).

Optimization of the GO-catalyzed thioacetalization was examined with *p*-anisaldehyde and *n*-pentanethiol (1: 2.2 ratios) as the model case and the results are shown in Table VI.4. Initially, a mixture of the aldehyde and mercaptan (in 1:2.2 ratios) was gently stirred in neat at room temperature in the presence of GO (10 mg $mmol^{-1}$ of the aldehyde) under aerobic condition. Monitoring the reaction by tlc at intervals showed the presence of the starting aldehyde along with the desired dithioacetal even after 24h. The reaction was stopped and the desired dithioacetal obtained in 51% yield (entry 1). Increasing the quantity of GO (50 mg $mmol^{-1}$ of the aldehyde) revealed that nearly complete conversion of the aldehyde to dithioacetal could be achieved at room temperature within 3h under aerobic condition (entry 3). Significantly, there was no detectable amount of disulfide formed under the aerobic condition. A control experiment was performed in the absence of the GO under similar reaction condition, which did not produce any dithioacetal even after 24h (entry 4). In order to see any faster conversion, the reaction was also carried out at 60 ^{o}C. This however resulted in partial conversion of the mercaptan into the corresponding disulfide along with the desired dithioacetal in relatively lower yield (entry 5). Moreover, the same reaction at 60 ^{o}C and under a blanket of N_2 did not stop the formation of disulfide (entry 6). Conducting the experiments in a solvent (THF, toluene or water) showed rather a negative effect affording the desired dithioacetal in relatively lower yields (entries 7−9). To scale up the reaction, one

set of reaction was performed (in 5 mmol) using the same quantity of catalyst (GO = 50 mg). Excellent yield of the dithioacetal was realized in this case as well signifying that the minimum quantity of the catalyst can promote the reaction in a longer time (entry 10).

Table VI.4. Optimization of dithioacetal formation from *p*-anisaldehyde and *n*-pentane thiol.[a]

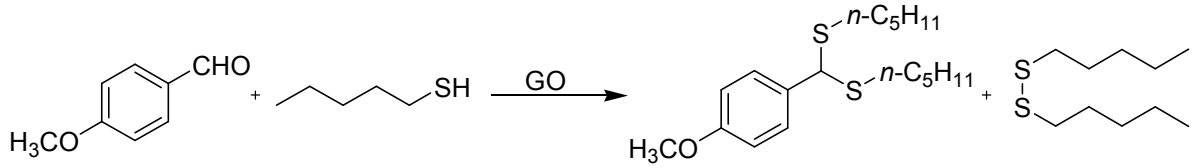

Entry	GO (in mg $mmol^{-1}$)	Reaction medium	Time (h) / Temp(^{o}C)	Dithioacetal (%)[b]	Disulfide (%)[b]
1	10	Neat	24 / RT	51	Not observed
2	25	Neat	24 / RT	65	Not observed
3	**50**	Neat	**3 / RT**	**95**	**Not observed**
4	Nil	Neat	24 / RT	Not observed	Not observed
5	50	Neat	3 / 60	61	10
6[c]	50	Neat	3 / 60	57	8
7	50	THF	20 / RT	35	trace[d]
8	50	PhMe	12 / RT	68	Not observed
9	50	H_2O	12 / RT	55	trace[d]
10[e]	50	Neat	16 / RT	91	trace[d]

[a]*p*-Anisaldehyde (1 mmol), *n*-pentanethiol (2.2 mmol), [b]Isolated yield. [c]Reaction carried out under N_2. [d]Detected only on tlc, not isolated.[e]*p*-Anisaldehyde (5 mmol), pentanethiol (11 mmol).

With this mild and solvent-free optimized condition at our hand, we became interested to explore the general applicability of the reaction. A variety of aryl aldehydes were subjected to the reaction in the presence of thiols, are presented in Table VI.5. It can be seen that aryl aldehydes bearing different functional groups react easily with aliphatic thiols in the presence of catalytic amount of GO under solvent-free aerobic condition. The reactions were completed in 3-8 h and the products were realized in excellent yields (Table VI.5, entries 1-5). Higher temperature was required for α-naphthaldehyde and *p*-chlorobenzaldehyde, which caused partial formation of disulfide (~5-8%) (entries 6, 7). However, the reaction with *p*-nitrobenzaldehyde needed much longer time and higher temperature, and gave the dithioacetal in relatively lower yield along with disulfide (Table VI.5, entry 8). Trying the reaction with aromatic thiols afforded the desired dithioacetal in 80-85% yields but achieved only at higher temperature (60^{o}C) and was associated with the formation of diaryl disulfides in 5-12% isolated yields (entries 9–11). In the case of using 1,2- and 1,3-dithiol, corresponding cyclic thioacetals were obtained in excellent yields (95-98%) and the reaction was also successful with aliphatic cyclohexyl aldehyde (entries 12–15). However, there was no such formation of dithioketals from a ketone under the GO-catalyzed reaction condition

(entry 16). So, there is excellent chemoselectivity observed between the aldehyde and keto-carbonyl groups.

Heteroaryl compounds often exhibit promising pharmacological activities and open chain dithioacetals of heteroaryl aldehydes such as thiophene-based dithioacetals are important scaffolds for design and discovery of new medicines.[25] Since the reaction conditions are mild and solvent-free, we were interested to extend the GO-catalyzed dithioacetalization to thiophene aldehydes and also of other heteroaryl aldehydes. Indeed, 5-bromothiophene-2-carbaldehyde and furfural result in the formation of corresponding dithioacetals with variety of aliphatic and benzenethiol without any difficulty (Table VI.6, entries 1–5). Other heteroaryl aldehyde indole-3-carbaldehyde also produces corresponding dithioacetals with long chain aliphatic thiols without any difficulty and in excellent yields (Table VI.6, entry 6). Cyclic dithioacetals of furfural and indole-3-carbaldehyde were obtained in excellent yields under mild conditions (entries 7, 8).

In order to further broaden the scope of the reaction, we attempted synthesis of unsymmetrical dithioacetal using two different thiols. Gratifyingly, the reactions of *p*-anisaldehyde or vanillin with two different aliphatic thiols (*n*-pentyl- and *n*-heptyl thiols) resulted in the formation of unsymmetrical dithioacetals as the only product in 85-88% isolated yields (Table VI.7, entries 1, 2). HPLC analysis of the crude product (before column chromatographic purification) showed the unsymmetrical thioether as the sole product. On the other hand, use of one aliphatic and one aromatic thiol gave rise to a mixture of all three possible products in varying proportions, as seen from the analysis of the crude product mixture by HPLC (Table VI.7, entry 3). This might be attributable to the difference in reactivity between aliphatic or aromatic thiols as the thioacetal from benzenethiol was formed in highest quantity amongst the three products.

Table VI.5. GO-catalyzed thioacetalization of aldehydes with different thiols.[a]

Entry	Aldehyde	Thiol	Time (h)	Temp	Product	Yield[b] (%)
1	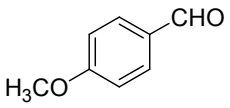	n-C_5H_{11}−SH	3	RT	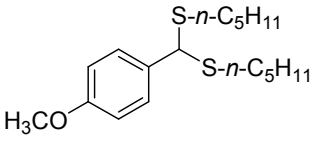	95
2	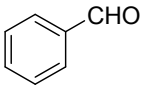	n-C_5H_{11}−SH	5	RT	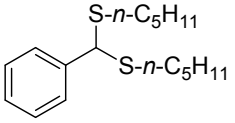	91

3	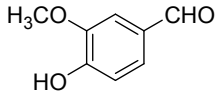	*n*-C_7H_{15}−SH	5	RT	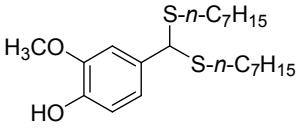	95
4	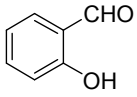	*n*-C_5H_{11}−SH	8	RT	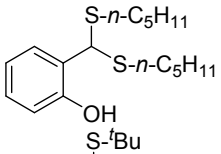	89
5	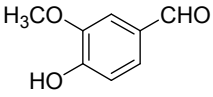	Bu^t−SH	5	RT	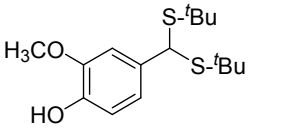	93
6[c]	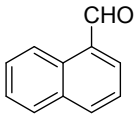	*n*-C_7H_{15}−SH	3	60°C	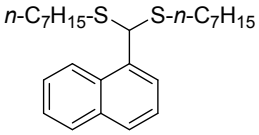	87
7[c]	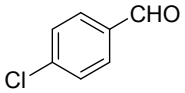	CySH	5	60°C	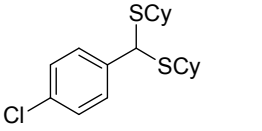	90
8[c]	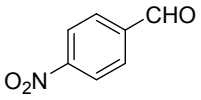	*n*-C_5H_{11}−SH	14	60°C	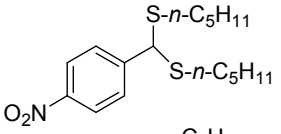	68
9[c]	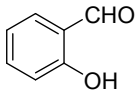	C_6H_5−SH	10	60°C	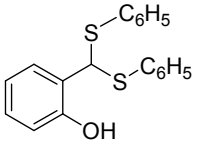	80
10[c]	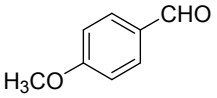	C_6H_5−SH	10	60°C	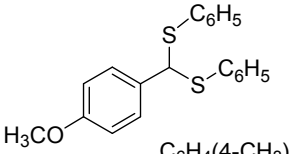	85
11[c]	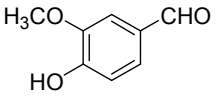	(H$_3$C-4)C_6H_4−SH	10	60°C	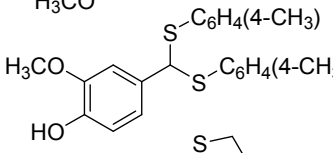	82
12[d]	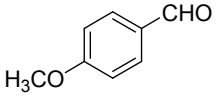	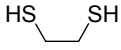	5	RT	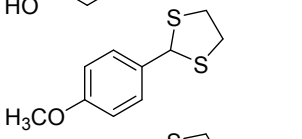	98
13[d]	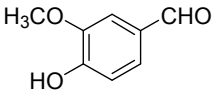	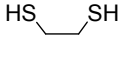	5	RT	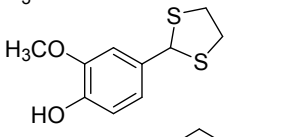	98
14[d]	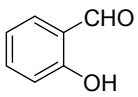		5	RT	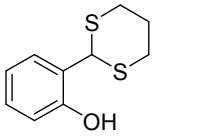	98
15[d]	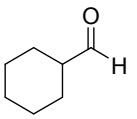		5	RT	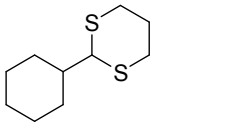	95
16	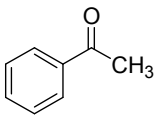	*n*-C_5H_{11}−SH	24	RT/ 60°C	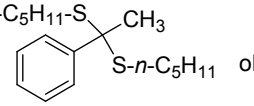	Not observed

[a]Aldehyde : thiol : GO (1 mmol : 2.2 mmol : 50 mg) and reactions were performed at room temperature. [b]Isolated yield. [c]Corresponding disulfides (5-12%) were formed. [d]Aldehyde : thiol : GO (1 mmol : 1.1 mmol : 50 mg).

Table VI.6. GO-catalyzed thioacetalization of heteroaryl aldehydes.[a]

Entry	Aldehyde	Thiol	Time(h)	Product	Yield (%)[b]
1	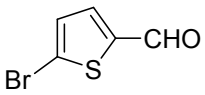	Bu^t-SH	8	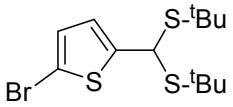	89
2[c]	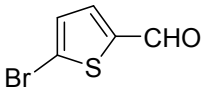	C_6H_5-SH	10	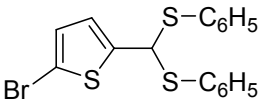	81
3	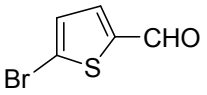	$n\text{-}C_7H_{15}-SH$	8	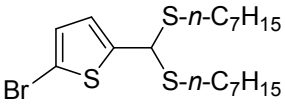	89
4	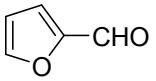	$n\text{-}C_5H_{11}-SH$	3	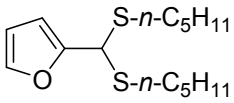	92
5	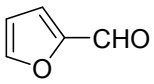	CySH	3	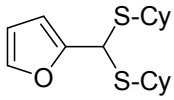	88
6	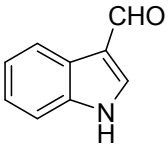	$n\text{-}C_7H_{15}-SH$	8	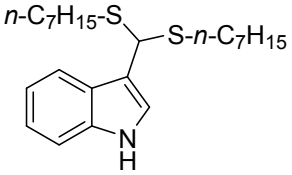	85
7[d]	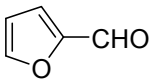	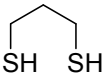	3	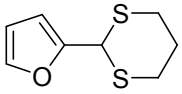	90
8[d]	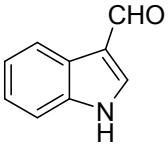	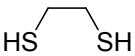	5	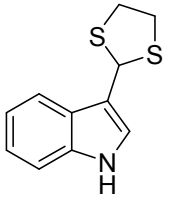	93

[a]Aldehyde : thiol : GO (1 mmol : 2.2 mmol : 50 mg) and reactions were performed at room temperature. [b]Isolated yield. [c]Isolated yield of disulfide was ~ 5%. [d]Aldehyde : thiol : GO (1 mmol : 1.1mmol : 50 mg).

Table VI.7. Unsymmetrical thioacetals from aryl aldehydes using two different thiols.[a]

Entry	Aldehyde	Thiol (A)	Thiol (B)	Time	Product	Yield (%)
1	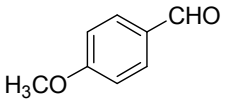	*n*-C_5H_{11}-SH	*n*-C_7H_{15}-SH	5	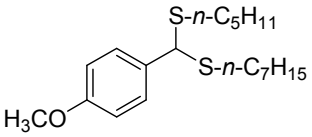	88[b]
2	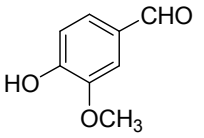	*n*-C_5H_{11}-SH	*n*-C_7H_{15}-SH	5	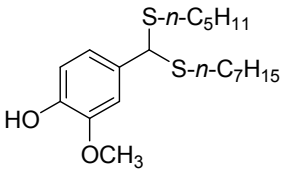	85[b]
3[c]	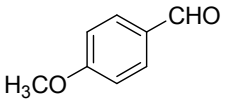	*n*-C_5H_{11}-SH	C_6H_5−SH	10	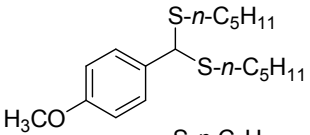	13[d]
					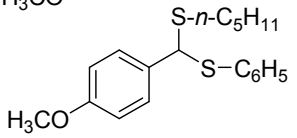	39[d]
					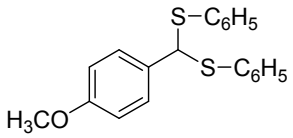	48[d]

[a]Thiol (A):thiol (B):GO (1.1 mmol:1.1 mmol:50 mg) for 1 mmol of aldehyde and the reaction was done at RT for entries 1 and 2; [b]Isolated yield; [c]Reaction performed at 60 ^oC; [d]Product ratios are from HPLC analysis.

As regard to the plausible mechanism for the reaction, we wanted to probe the nature of active sites present in GO. In the recent years, the acidic nature of GO has been attributed mostly to the organosulfate group being originated during the oxidation of graphite using Hummers method in the presence of sulphuric acid,[11,26] though previous measurements of acidic pH were attributable to the presence of surface attached carboxylic functions.[2] The FT-IR spectrum of GO showed the presence of carboxyl (1719 cm^{-1}; COOH stretching) and sulphate functional groups (1052 cm^{-1}; SO_3–H stretching), which are comparable with that reported in the literature.[10,11,18] In this case we measured the pH of the GO in aqueous suspension (pH = 3.9; 50 mg in 50 ml 0.5M aqueous NaCl solution), and found it in fair agreement with previous observations.[2] The pH of GO remains fairly similar when measured after the reaction and also of a mixture of *n*-pentane thiol and GO in water. On the other hand, thioacetal formation is greatly retarded when the reaction is carried out in water or in other organic solvents (Table VI.4, entries 7, 8 and 9). GO also gave positive Carius test and Lassaigne's test signifying qualitatively the presence of S-containing functional groups.

The above results suggest that GO is an acid catalyst and we tend to believe that the acidity of GO might be originating from a combination of both carboxyl and organosulfate groups, which is more pronounced in neat. Mechanistically, surface active acidic functional groups of GO facilitate activation of the aldehyde carbonyl group, more effectively in neat condition, and subsequent nucleophilic attack by the thiol results in the eventual formation of thioacetal. The reusability of the GO as heterogeneous acid catalyst was examined with the combination of reactants: *p*-anisaldehyde and *n*-pentanethiol in 1:2.2 ratios at room temperature. The GO was recovered from the first batch of reaction by centrifugation and washed with diethyl ether, dried and reused for subsequent four batches of reactions. In all recycling experiments carried out at room temperature, appreciable conversions were achieved (Figure VI.3). A comparison of the FT-IR spectra of the GO before and after use does not indicate any changes of the absorption bands, signifying that the catalyst remain same after the reaction (Figure VI.4).

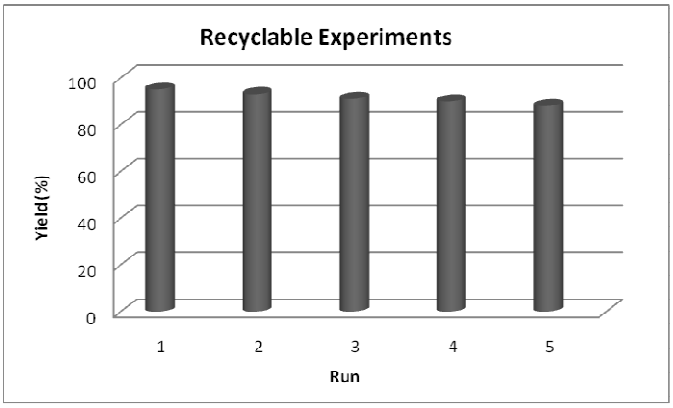

Figure VI.3. Recyclability of GO in the thioacetalization of *p*-anisaldehyde and *n*-pentanethiol.[a]

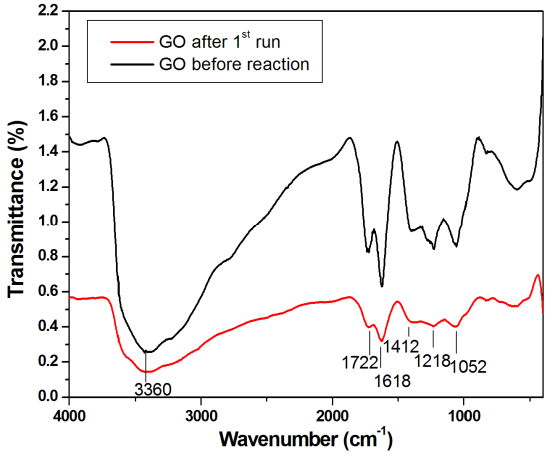

Figure VI.4. Comparative FT-IR spectra of GO before and after 1st use in the reaction between *p*- anisaldehyde and *n*-pentanethiol under neat condition.

VI.4. Conclusion

Herein, we have demonstrated that the GO, obtained by oxidation of graphite powder following Hummers method, is a highly efficient heterogeneous catalyst for (i) sequential dehydration–hydrothiolation reaction of mixtures of secondary aryl alcohols and thiols in toluene and (ii) chemoselective thioacetalization of aldehyde under mild, solvent-free and aerobic conditions. Both the reactions are useful for a large variety of substrates molecules showing tolerance with diverse functional groups. The reaction conditions are mild, easy separation and isolation of the product with high yields. Finally, the GO can be recovered and reused without having any changes of the surface morphology and catalytic performance.

VI.5. Experimental Section

VI.5.1. General Information

All chemicals were purchased and used directly. For the column chromatography, silica (60–120 mesh) (SRL, India) was used, and for tlc, Merck plates coated with silica gel 60, F254 were used. FT-IR spectra were recorded in a FT-IR-8300 SHIMADZU spectrophotometer. The NMR spectral data (^{1}H and ^{13}C NMR) were recorded in $CDCl_3$ on a Bruker AV 300, operating respectively at 300 MHz and 75 MHz. ^{1}H chemical shifs are reported in ppm relative to tetramethylsilane serving as the internal standard (δ = 0 ppm). ^{13}C NMR spectra were recorded with complete proton decoupling. Chemical shifts are reported in ppm with the solvent resonance as the internal standard ($CDCl_3$: δ 77.0 ppm). HPLC analyses were carried out using HPLC (Agilent Technologies, 1260 Infinity), Column: ZORBAX Rx–SIL (4.6 x 150 mm, 5 μm), eluent: *n*–hexane (flow rate 3 mL min^{-1}). High resolution Mass Spectra (HRMS) were performed in Micromass Q-TOF Spectrometer under ESI (positive mode), by the services at the Indian Association for the Cultivation of Science, Kolkata.

VI.5.2. Preparation of Graphene Oxide

GO was prepared according to the modified Hummers method.[17]

To an ice-cold concentrated sulfuric acid (46 mL) was slowly added sodium nitrate (0.1 g) and then graphite powder (2 g) with vigorous magnetic stirring. After the complete addition of graphite powder, potassium permanganate (6 g) was added to the reaction mixture very slowly, keeping the temperature within 0–5 ^{o}C to avoid any possible explosion. The mixture was allowed to stir at room temperature for 6 h forming a thick paste. It was diluted with distilled water (92 mL) under stirred condition. The temperature of the solution was raised to about 90 ^{o}C and the mixture was allowed to stir for 30 min. Finally, 280 mL water was added followed by slow addition of 3 mL H_2O_2 (30%). The colour of the solution changes from

dark brown to yellowish brown. The overall solution was exfoliated under sonication followed by centrifuged at 15000 rpm to collect the solid mass at the bottom. This process was continued for several times until the pH of the supernatant aqueous part becomes neutral (using pH paper). Finally, the brown mass was collected and dried at 60 ^{o}C under vacuum to obtain solid graphene oxide.

VI.5.3. General procedure for one-pot sequential dehydration-hydrothiolation

To a solution of alcohol (**1**) (1 mmol) and thiol (**2**) (1.2 mmol) in toluene (2 mL) was added graphene oxide (10 mg), and the mixture was bubbled with N_2 gas for 2-3 min and immediately screw-capped to ensure the reaction mixture under nitrogen atmosphere. The sealed tube was stirred with a magnetic spin bar at 65 ^{o}C for hours as mentioned in Table VI.2. After the reaction, the catalyst was filtered off, washed with diethyl ether (3 x 5 mL) and the combined filtrate was concentrated to afford a mixture of thioether and disulfide. The crude mixture was separated by column chromatography over silica gel and elution with pet ether afforded the desired thioether in pure form.

VI.5.4. Physical properties and spectral data of compounds

Table VI.2, entry 1

(4-Chlorophenyl)(1-(naphthalene-6-yl)ethyl)Sulfane

White crystalline solid, mp 72-74 ^{o}C

^{1}H NMR (300 MHz, $CDCl_3$) δ 1.69 (d, *J* = 7.2 Hz, 3H, CH_3), 4.43 (q, *J* = 6.9 Hz, 1H, CH), 7.10-7.19 (m, 4H, ArH), 7.40-7.51 (m, 3H ArH), 7.58 (s, 1H ArH), 7.71-7.79 (m, 3H ArH); ^{13}C NMR ($CDCl_3$, 75 MHz): δ 22.1, 48.4, 125.4, 125.7, 125.8, 126.1, 127.6, 127.7, 128.3, 128.8, 132.6, 133.1, 133.3, 133.9, 140.2.

Table VI.2, entry 2

(1-(Naphtyalen-6-yl)ethyl)(*p*-tolyl)sulfane

White solid, mp 69-71 ^{o}C

^{1}H NMR ($CDCl_3$, 300 MHz): δ 1.69 (d, *J* = 6.9 Hz, 3H, CH_3), 2.27 (s, 3H, $ArCH_3$), 4.42 (q, *J* = 6.9 Hz, 1H, CH), 6.99 (d, *J* = 8.1 Hz, 2H, ArH), 7.16-7.21 (m, 2H, ArH), 7.40-7.46 (m, 2H, ArH), 7.52 (dd, *J* = 8.4 and 1.8 Hz, 1H, ArH), 7.59 (s, 1H, ArH), 7.71-7.81 (m, 3H, ArH); ^{13}C NMR ($CDCl_3$, 75 MHz): δ 21.1, 22.2, 48.6, 125.6, 125.69, 125.7, 126.0, 127.6, 127.8, 128.1, 129.4, 131.1, 132.6, 133.2, 137.4, 140.7.

Table VI.2, entry 3

(2,6-Dimethylphenyl)(1-(naphthalene-6-yl)sulfane

Pale yellow liquid

^{1}H NMR ($CDCl_3$, 300 MHz): δ 1.69 (d, *J* = 7.2 Hz, 3H, CH_3), 2.14 (s, 3H, $ArCH_3$), 2.27 (s, 3H, $ArCH_3$), 4.41 (q, *J* = 6.9 Hz, 1H, CH), 6.86 (dd, *J* = 7.5 and 1.2 Hz, 1H, ArH), 6.98 (d, *J* = 7.8 Hz, 1H, ArH), 7.09 (s, 1H, ArH), 7.37-7.42 (m, 2H, ArH), 7.48-7.51 (dd, *J* = 8.4 and 1.8 Hz, 1H, ArH), 7.58 (s, 1H, ArH), 7.67- 7.76 (m, 3H, ArH); ^{13}C NMR ($CDCl_3$, 75 MHz): δ 20.2, 20.7, 22.1, 47.6, 125.5, 125.61, 125.64, 125.9, 127.5, 127.7, 128.0, 128.1, 129.9, 132.6, 133.2, 133.6, 133.9, 135.6, 136.9, 140.6.

Table VI.2, entry 4

(4-Fluorophenyl)(1-(naphthalene-6-yl)ethyl)sulfane

White solid, mp 73-75 ^{o}C

^{1}H NMR ($CDCl_3$, 300 MHz): δ 1.69 (d, *J* = 6.9 Hz, 3H, CH_3), 4.38 (q, *J* = 6.9 Hz, 1H, CH), 6.82-6.90 (m, 2H, ArH), 7.19-7.25 (m, 2H, ArH), 7.39-7.47 (m, 3H, ArH), 7.50-7.51 (m, 1H, ArH), 7.69-7.74 (m, 1H, ArH), 7.77-7.81 (m, 2H, ArH); ^{13}C NMR ($CDCl_3$, 75 MHz): δ 21.9, 49.1, 115.6, 115.8, 125.5, 125.8, 126.1, 127.6, 127.7, 128.2, 132.6, 133.1, 135.6, 135.8, 140.3, 160.9, 164.2.

Table VI.2, entry 6

(4-Chlorophenyl)(1-(naphthalene-8-yl)ethyl)sulfane,[27]

White crystalline solid, mp 96-98 ^{o}C

^{1}H NMR ($CDCl_3$, 300 MHz): δ 1.73 (d, *J* = 6.9 Hz, 3H, CH_3), 5.10 (q, *J* = 6.9 Hz, 1H, CH), 7.10-7.18 (m, 4H, ArH), 7.36 (t, *J* = 7.5 Hz 1H, ArH), 7.44-7.55 (m, 3H, ArH), 7.72 (d, *J* = 8.1 Hz, 1H, ArH), 7.82-7.85 (m, 1H, ArH), 8.16 (d, *J* = 8.4 Hz, 1H, ArH); ^{13}C NMR ($CDCl_3$, 75 MHz): δ 21.9, 43.0, 122.9, 124.2, 125.3, 125.6, 126.1, 128.0, 128.8, 129.0, 130.7, 133.2, 133.4, 133.6, 133.9, 137.7.

Table VI.2, entry 7

(4-Fluorophenyl)(1-(naphthalene-8-yl)ethyl)sulfane

White solid, mp 83-85 ^{o}C

^{1}H NMR ($CDCl_3$, 300 MHz): δ 1.70 (d, *J* = 6.9 Hz, 3H, CH_3), 5.02 (q, *J* = 6.9 Hz, 1H, CH), 6.80-6.86 (m, 2H, ArH), 7.15-7.21 (m, 2H, ArH), 7.31-7.52 (m, 4H, ArH), 7.69 (d, *J* = 8.1 Hz, 1H, ArH), 7.79-7.82 (m, 1H, ArH), 8.16 (d, *J* = 8.4 Hz, 1H, ArH); ^{13}C NMR ($CDCl_3$, 75 MHz): δ 21.7, 43.4, 115.5, 115.8, 123.0, 124.2, 125.2, 125.5, 126.0, 127.8, 128.9, 129.49, 129.5, 130.7, 133.8, 135.5, 135.6, 137.9, 160.8, 164.1.

Table VI.2, entry 8

(1-Phenylethyl)(*p*-tolyl)sulfane, [27]

Colourless liquid

^{1}H NMR ($CDCl_3$, 300 MHz) δ 1.60 (d, *J* = 7.2 Hz, 3H, CH_3), 2.29 (s, 3H, $ArCH_3$), 4.26 (q, *J* = 6.9 Hz, 1H, CH), 7.02 (d, *J* = 8.1 Hz 2H, ArH), 7.17-7.27 (m, 7H, ArH); ^{13}C NMR ($CDCl_3$, 75 MHz): δ 21.1, 22.1, 48.3, 127.0, 127.3, 128.3, 129.4, 131.2, 133.2, 137.3, 143.3.

Table VI.2, entry 9

Phenyl(1-phenylethyl)sulfane, [27]

Pale yellow liquid

^{1}H NMR ($CDCl_3$, 300 MHz): δ 1.63 (d, *J* = 6.9 Hz, 3H, CH_3), 4.34 (q, *J* = 6.9 Hz, 1H, CH), 7.19-7.31 (m, 10H, ArH); ^{13}C NMR ($CDCl_3$, 75 MHz): δ 22.3, 48.0, 127.1, 127.2, 128.4, 128.6, 132.5, 135.1, 143.2.

Table VI.2, entry 10

(1-(3,4-Dimethoxyphenyl)ethyl)(phenyl)sulfane

Pale yellow solid, mp 53-55 ^{o}C

^{1}H NMR ($CDCl_3$, 300 MHz): δ 1.61 (d, *J* = 6.9 Hz, 3H, CH_3), 3.81 (s, 3H, OCH_3), 3.83 (s, 3H, OCH_3), 4.30 (q, *J* = 6.9 Hz, 1H, CH), 6.72-6.75 (m, 1H, ArH), 6.79-6.82 (m, 2H, ArH), 7.17-7.31 (m, 5H, ArH); ^{13}C NMR ($CDCl_3$, 75 MHz): δ 22.2, 47.7, 55.6, 55.7, 110.3, 110.7, 119.1, 127.0, 128.5, 132.5, 135.0, 135.6, 147.9, 148.6.

Table VI.2, entry 12

(4-Chloro phenyl)(1-(3,4-dimethoxyphenyl)ethyl)sulfane

Colourless liquid

^{1}H NMR ($CDCl_3$, 300 MHz): δ 1.60 (d, *J* = 6.9 Hz, 3H, CH_3), 3.84 (s, 3H, OCH_3), 3.85 (s, 3H, OCH_3), 4.26 (q, J = 6.9 Hz, 1H, CH), 6.73-6.80 (m, 3H, ArH), 7.18 (s, 4H, ArH); ^{13}C NMR ($CDCl_3$, 75 MHz): δ 22.2, 48.1, 55.7, 55.8, 110.3, 110.7, 119.3, 128.7, 133.3, 133.5, 134.0, 135.3, 148.1, 148.7.

Table VI.2, entry 13

(1-(Naphthalen-6-yl)ethyl)(pentyl)sulfane

Colourless liquid

^{1}H NMR ($CDCl_3$, 300 MHz): δ 0.82 (t, *J* = 6.9 Hz, 3H, CH_3), 1.19-1.28 (m, 4H, -CH_2-CH_2-), 1.45-1.52 (m, 2H, CH_2), 1.64 (d, *J* = 7.2 Hz, 3H, CH_3), 2.23-2.33 (m, 2H, S-CH_2), 4.11 (q, *J* = 6.9 Hz, 1H, S-CH-Ar), 7.42-7.49 (m, 2H, ArH), 7.53-7.57 (dd, *J* = 8.4 and 1.8 Hz, 1H, ArH), 7.68 (s, 1H, ArH), 7.78-7.83 (m, 3H, ArH); ^{13}C NMR ($CDCl_3$, 75 MHz): δ 13.9, 22.2, 22.5, 29.0, 31.1, 31.2, 44.3, 125.4, 125.6, 125.7, 126.1, 127.6, 127.7, 128.4, 132.6, 133.2, 141.5.

Table VI.2, entry 14

Cyclohexyl(1-(naphthalene-6-yl)ethyl)sulfane

Colourless liquid

^{1}H NMR ($CDCl_3$, 300 MHz): δ 1.43-1.73 (m, 9H, Cy-H), 1.61 (d, *J* = 6.9 Hz, 3H, CH_3), 1.99 (m, 1H, CyH), 2.35-2.39 (m, 1H, S-CyH), 4.21 (q, *J* = 7.2 Hz, 1H, S-CH-Ar), 7.42-7.49 (m, 2H, ArH), 7.56 (dd, *J* = 8.7 and 1.8 Hz ,1H, ArH), 7.70 (s, 1H, ArH), 7.79-7.83 (m, 3H, ArH); ^{13}C NMR ($CDCl_3$, 75 MHz): δ 23.1, 25.7, 25.8, 25.9, 33.3, 33.9, 42.7, 42.75, 125.4, 125.6, 126.0, 127.6, 127.7, 128.3, 132.6, 133.3, 142.1.

Table VI.2, entry 15

Heptyl(1-(naphthalene-5-yl)ethyl)sulfane

Colourless liquid

^{1}H NMR ($CDCl_3$, 300 MHz): δ 0.84 (t, *J* = 6.6 Hz, 3H, CH_3), 1.17-1.27 (m, 8H, C_4H_8), 1.43-1.52 (m, 2H, CH_2), 1.72 (d, *J* = 7.2 Hz, 3H, CH_3), 2.35-2.41 (m, 2H, S-CH_2), 4.80 (q, *J* = 6.9 Hz, 1H, S-CH-Ar), 7.41-7.53 (m, 3H, ArH), 7.67-7.73 (m, 2H, ArH), 7.81-7.85 (m, 1H, ArH), 8.19 (d, *J* = 8.4 Hz, 1H, ArH); ^{13}C NMR ($CDCl_3$, 75 MHz): δ 14.0, 22.5, 28.76, 28.8, 29.4, 31.3, 31.6, 39.4, 123.0, 124.3, 125.4, 125.8, 127.4, 128.9, 131.0, 133.9, 139.3.

Table VI.2, entry 16

Pentyl(1-*p*-tolyiethyl)sulfane

Colourless liquid

^{1}H NMR ($CDCl_3$, 300 MHz): δ 0.85 (t, *J* = 6.9 Hz, 3H, CH_3), 1.21-1.29 (m, 4H, CH_2-CH_2), 1.45-150 (m, 2H, CH_2), 1.54 (d, *J* = 6.9 Hz, 3H, CH-C<u>H</u>$_3$), 2.24-2.34 (m, 5H, CH_2 & $ArCH_3$), 3.91 (q, *J* = 7.2 Hz, 1H, CH), 7.11 (d, *J* = 7.8 Hz, 2H, ArH), 7.21-7.24 (m, 2H, ArH); ^{13}C NMR ($CDCl_3$, 75 MHz): δ 13.9, 21.0, 22.2, 22.6, 29.0, 31.1, 31.2, 43.7, 127.1, 129.0, 136.5, 141.1.

Table VI.2, entry 17

(1-(3,4-dimethoxyphenyl)ethyl)(pentyl)sulfane

Colourless liquid

^{1}H NMR ($CDCl_3$, 300 MHz): δ 0.83-0.88 (m, 3H, CH_3), 1.25-1.30 (m, 4H, CH_2-CH_2), 1.47-1.52 (m, 2H, CH_2), 1.54 (d, *J* = 7.2 Hz, 3H, CH_3), 2.26-2.34 (m, 2H, S-CH_2), 3.86 (s, 3H, OCH_3), 3.89 (s, 3H, OCH_3), 3.92 (q, *J* = 7.2 Hz, 1H, C<u>H</u>-CH_3), 6.77-6.92 (m, 2H, ArH), 6.93 (d, *J* = 1.8 Hz, 1H, ArH); ^{13}C NMR ($CDCl_3$, 75 MHz): δ 13.8, 22.1, 22.7, 28.9, 31.0, 31.1, 43.8, 55.69, 55.7, 110.0, 110.6, 119.2, 136.6, 147.8, 148.9.

Table VI.2, entry 18

Phenethyl(*p*-toyl)sulfane

Colourless liquid

^{1}H NMR ($CDCl_3$, 300 MHz): δ 2.31 (s, 3H, CH_3), 2.88 (t, *J* = 7.2 Hz, 2H, CH2-Ar), 3.08-3.13 (m, 2H, S-CH2), 7.08-7.28 (m, 9H, ArH); ^{13}C NMR ($CDCl_3$, 75 MHz): δ 20.9, 35.67, 35.7, 126.3, 128.4, 128.44, 129.6, 130.0, 132.4, 136.1, 140.2.

VI.5.5. General procedure for the preparation of dithioacetal

To a mixture of aldehyde (1 mmol) and thiol (2.2 mmol), 50 mg of graphene oxide was added and stirred the reaction mixture at room temperature for hours as mentioned in the Tables (VI.5-VI.7). After completion of reaction, diethyl ether (5 mL) was added, stirred gently and then allowed to stand. The supernatant liquid was carefully collected in another flask and this process was repeated three times more. The liquid part was concentrated and the residue was purified through column chromatography over silica gel. Elution with light petroleum or ethyl acetate-light petroleum (2:98) affords the pure dithioacetal (% Yield as mentioned in the Tables). All products were characterized by ^{1}H, ^{13}C NMR data and compared with the reported melting points for known solid compounds.

VI.5.6. Physical properties and spectral data of dithioacetals

Table VI.5, entry 1

1-(bis(pentylthio)methyl)-4-methoxy benzene

Colourless oil

^{1}H NMR ($CDCl_3$): δ 0.86 (t, *J* = 6.9 Hz, 6H, CH_3), 1.36-1.23 (m, 8H, CH_2), 1.58-1.49 (m, 4H, CH_2), 2.58-2.43 (m, 4H, CH_2), 3.74 (s, 3H, OCH_3), 4.86 (s, 1H, CH), 6.84-6.80 (m, 2H, ArH), 7.37-7.33 (m, 2H, ArH); ^{13}C NMR ($CDCl_3$): δ 14.0, 22.3, 28.9, 31.1, 32.2, 52.6, 55.1, 113.7, 128.8, 132.6, 159.0.

Table VI.5, entry 2

1-(bis(pentylthio)methyl)benzene

Colourless oil

^{1}H NMR ($CDCl_3$): δ 0.86 (t, *J* = 6.9 Hz, 6H, CH_3), 1.34-1.23 (m, 8H, CH_2), 1.57-1.49 (m, 4H, CH_2), 2.59-2.44 (m, 4H, CH_2), 4.88 (s, 1H, CH), 7.32-7.22 (m, 3H, ArH), 7.45-7.32 (m , 2H, ArH); ^{13}C NMR ($CDCl_3$): δ 14.0, 22.3, 28.9, 31.1, 32.2, 53.2, 127.7, 128.4, 140.7.

Table VI.5, entry 3

4-(bis(heptylthio)methyl)-2-methoxyphenol

Colourless oil

^{1}H NMR ($CDCl_3$): δ 0.89-0.84 (m, 6H, CH_3), 1.36-1.21 (m, 16H, CH_2), 1.57-1.49 (m, 4H, CH_2), 2.56-2.47 (m, 4H, CH_2), 3.94 (s, 3H, OCH_3), 4.82 (s, 1H, CH), 6.83 (dd, *J* = 2.1 and

12.9 Hz, 2H, ArH), 7.04 (d, *J* = 1.8 Hz, 1H, ArH); ^{13}C NMR ($CDCl_3$): δ 13.9, 22.5, 28.7, 29.1, 31.6, 32.3, 53.0, 55.8, 109.8, 113.6, 120.7, 132.4, 145.2, 146.6.

Table VI.5, entry 4

2-(bis(pentylthio)methyl)phenol

Colourless oil

^{1}H NMR ($CDCl_3$): δ 0.88-0.84 (m, 6H, CH_3), 1.34-1.24 (m, 8H, CH_2), 1.58-1.51 (m, 4H, CH_2), 2.57-2.51 (m, 4H, CH_2), 5.08 (s, 1H, CH), 6.90-6.83 (m, 2H, ArH), 7.03 (s, 1H, OH), 7.22-7.17 (m, 2H, ArH); ^{13}C NMR ($CDCl_3$): δ 13.8, 22.1, 28.7, 30.8, 32.4, 50.0, 117.6, 120.2, 123.5, 129.4, 129.6, 154.9.

Table VI.5, entry 5

4-(bis(tert-butylthio)methyl)-2-methoxyphenol

White solid, mp-78-80 ^{o}C

^{1}H NMR ($CDCl_3$): δ 1.31 (s, 18H, CH_3), 3.90 (s, 3H, OCH_3), 5.00 (s, 1H, CH), 5.60 (s, 1H, OH), 6.80 (d, *J* = 8.1 Hz, 1H, ArH), 6.86 (dd, *J* = 2.1 and 8.1 Hz, 1H, ArH), 7.08 (d, *J* = 1.8 Hz, 1H, ArH); ^{13}C NMR ($CDCl_3$): δ 31.2, 45.6, 48.8, 56.0, 110.4, 113.8, 120.0, 135.7, 145.0, 146.8.

Table VI.5, entry 6

1-(bis(heptylthio)methyl)naphthalene

Colourless oil

^{1}H NMR ($CDCl_3$): δ 0.87-0.83 (m, 6H, CH_3), 1.60-1.21 (m, 20H, CH_2), 2.69-2.47 (m, 4H, CH_2), 5.66 (s, 1H, CH), 7.57-7.48 (m, 3H, ArH), 7.87-7.75 (m, 3H, ArH), 8.24 (d, *J* = 7.8 Hz, 1H, ArH); ^{13}C NMR ($CDCl_3$): δ 14.0, 22.5, 28.8, 28.8, 29.1 31.6, 32.3, 32.5, 123.3, 125.0, 125.6, 125.8, 126.0, 126.2, 128.5, 128.9, 130.4, 134.0, 135.2.

Table VI.5, entry 7

1-(bis(cyclohexylthio)methyl)-4-chlorobenzene

Colourless oil

^{1}H NMR ($CDCl_3$): δ 1.35-1.17 (m, 10H, CyH), 1.55 (d, *J* = 4.5 Hz, 2H, CyH), 1.74-1.70 (m, 4H, CyH), 1.92-1.85 (m, 4H, CyH), 2.74-2.67 (m, 2H, CyH), 4.96 (s, 1H, CH), 7.30-7.26 (m, 2H, ArH), 7.42-7.38 (m, 2H, ArH); ^{13}C NMR ($CDCl_3$): δ 25.6, 25.7,33.2, 33.2 44.2, 48.9, 128.5, 129.0, 133.0, 139.9.

Table VI.5, entry 8

1-(bis(pentylthio)methyl)-4-nitrobenzene

Pale yellow oil

^{1}H NMR ($CDCl_3$): δ 0.89 (m, 6H, CH_3), 1.36-1.25 (m, 8H, CH_2), 1.59-1.51 (m, 4H, CH_2), 2.62-2.49 (m, 4H, CH_2), 4.93 (s, 1H, CH), 7.64-7.61 (m, 2H, ArH), 8.20-8.17 (m, 2H, ArH); ^{13}C NMR ($CDCl_3$): δ 13.8, 22.2, 28.7, 30.9, 32.3, 52.5, 123.7, 128.6, 147.2, 148.4.

Table VI.5, entry 9

2-(bis(phenylthio)methyl)phenol

Colourless oil

^{1}H NMR ($CDCl_3$): δ 5.73 (s, 1H, CH), 6.39 (s, 1H, OH), 6.83-6.73 (m, 2H, ArH), 7.25-7.09 (m, 8H, ArH), 7.39-7.35 (m, 4H, ArH); ^{13}C NMR ($CDCl_3$): δ 56.4, 117.0, 120.7, 128.0, 128.8, 129.5, 129.6, 132.5, 133.6.

Table VI.5, entry 10

1-((4-methoxyphenyl)(phenylthio)methylthio)benzene,[28]

White solid, mp 71-73 ^{o}C

^{1}H NMR ($CDCl_3$): δ 3.73 (s, 3H, OCH_3), 5.42 (s, 1H, CH), 6.77 (d, *J* =8.7 Hz, 2H, ArH), 7.34-7.20 (m, 12H, ArH); ^{13}C NMR ($CDCl_3$): δ 55.1, 59.6, 113.7, 127.5, 128.7, 129.0, 131.5, 132.2, 134.6, 159.1.

Table VI.5, entry 11

4-(bis(p-tolylthio)methyl)-2-methoxyphenol

White solid, mp 70-72 ^{o}C

^{1}H NMR ($CDCl_3$): δ 2.29 (s, 3H, CH_3), 3.79 (s, 3H, OCH_3), 5.28 (s, 1H, CH), 5.60 (s, 1H, OH), 6.76 (d, *J* = 0.9 Hz, 2H, ArH), 6.86 (s, 1H, ArH), 7.04 (d, *J* = 8.1 Hz, 4H, ArH), 7.24-7.22 (m, 4H, ArH); ^{13}C NMR ($CDCl_3$): δ 21.1, 55.8, 60.9, 110.2, 113.9, 121.0, 129.5, 130.9, 131.7, 133.0, 137.9, 145.2, 146.3.

Table VI.5, entry 12

2-(4-methoxyphenyl)-1, 3-dithiolane,[29]

White solid, mp 58-60 ^{o}C

^{1}H NMR ($CDCl_3$): δ 3.37-3.29 (m, 2H, CH_2), 3.52-3.44 (m, 2H, CH_2), 3.78 (s, 3H, OCH_3), 5.63 (s, 1H, CH), 6.83 (dd, *J* = 2.1 and 6.6 Hz, 2H, ArH), 7.44 (dd, *J* = 2.1 and 6.6 Hz, 2H, ArH); ^{13}C NMR ($CDCl_3$): δ 40.1, 55.2, 55.9, 113.7, 129.0, 131.7, 159.3.

Table VI.5, entry 13

4-(1, 3-dithiolan-2-yl)-2-methoxyphenol

White solid, mp 81-83 ^{o}C

^{1}H NMR ($CDCl_3$): δ 3.35-3.27 (m, 2H, CH_2), 3.50-3.41 (m, 2H, CH_2), 3.85 (s, 1H, OCH_3), 5.61 (s, 1H, CH), 6.81 (d, *J* = 8.1 Hz, 1H, ArH), 6.98 (dd, *J* = 2.1 and 8.1 Hz, 1H, ArH), 7.08

(d, J = 2.1 Hz, 1H, ArH); ^{13}C NMR ($CDCl_3$): δ 39.9, 55.8, 56.5, 110.2, 113.9, 120.9, 131.1, 145.4, 146.3.

Table VI.5, entry 14

2-(1,3-dithian-2-yl)phenol,[30]

White crystalline solid, mp 131-133 ^{o}C

^{1}H NMR ($CDCl_3$) : δ 1.96-1.92 (m, 1H, CH_2), 2.18-2.11 (m, 1H, CH_2), 2.92-2.84 (m, 2H, CH_2), 3.09-2.99 (m, 2H, CH_2), 5.44 (s, 1H, CH), 6.55 (s, 1H, OH), 6.90-6.84 (m, 2H, ArH), 7.33-7.15 (m, 2H, ArH) ; ^{13}C NMR ($CDCl_3$) : δ 24.9, 31.7, 47.0, 117.1, 120.8, 123.9, 129.1, 130.0, 154.2.

Table VI.5, entry 15

2-cyclohexyl-1, 3-dithiane,[31]

White solid, mp 49-51 ^{o}C

^{1}H NMR ($CDCl_3$): δ 2.12-1.21 (m, 13H, CyH), 2.88-2.82 (m, 4H, CH_2), 4.04-3.99 (m, 1H, CH); ^{13}C NMR ($CDCl_3$): δ 26.1, 26.1, 26.3, 30.3, 30.8, 43.0, 55.2.

Table VI.6, entry 1

2-(bis(tert-butylthio)methyl)-5-bromothiophene

White crystalline solid, mp 68-70 ^{o}C

^{1}H NMR ($CDCl_3$): δ 1.33 (m, 18H, CH_3), 5.17 (s, 1H, CH), 6.82 (s, 2H, ArH); ^{13}C NMR ($CDCl_3$): δ 31.0, 43.4,

46.2, 111.8, 124.5, 129.0, 151.1.

Table VI.6, entry 2

2-(bis(phenylthio)methyl)-5-bromothiophene

Pale yellow oil

^{1}H NMR ($CDCl_3$): δ 5.55 (s, 1H, CH), 6.66 (d, J = 3.6 Hz, 1H, ArH), 6.76 (d, J = 3.9 Hz, 1H, ArH), 7.29-7.21 (m, 6H, ArH), 7.41-7.35 (m, 4H, ArH); ^{13}C NMR ($CDCl_3$): δ 55.7, 112.8, 126.8, 128.3, 129.0, 129.3, 129.4, 132.8, 133.7, 145.5.

Table VI.6, entry 3

2-(bis(heptylthio)methyl)-5-bromothiophene

Colourless oil

^{1}H NMR ($CDCl_3$): δ 0.89-0.84 (m, 6H, CH_3), 1.37-1.24 (m, 16H, CH_2), 1.59-1.51 (m, 4H, CH_2), 2.67-2.54 (m, 4H, CH_2), 5.04 (s, 1H, CH), 6.85-6.81 (m, 2H, ArH); ^{13}C NMR ($CDCl_3$): δ 14.0, 22.5, 28.8, 28.8, 29.0, 31.6, 32.1, 48.6, 112.3, 125.9, 129.1, 147.1.

Table VI.6, entry 4

2-(bis(pentylthio)methyl)furan

Pale yellow liquid

^{1}H NMR ($CDCl_3$): δ 0.90-0.85 (m, 6H, CH_3), 1.37-1.26 (m, 8H. CH_2), 1.60-1.50 (m, 4H, CH_2), 2.70-2.50 (m, 4H, CH_2), 4.99 (s, 1H, CH), 6.31 (d, *J* = 1.5 Hz, 2H, ArH), 7.36 (t, *J* = 1.5 Hz, 1H, ArH); ^{13}C NMR ($CDCl_3$): δ 13.8, 22.1, 28.7, 31.0, 31.4, 45.8, 107.5, 110.3, 142.0, 152.3.

Table VI.6, entry 5

2-(1, 3-dicyclohexylpropan-2-yl) furan

Colourless oil

^{1}H NMR ($CDCl_3$): δ 1.37-1.22 (m, 10H, CyH), 1.93-1.55 (m, 10H, CyH), 2.82-2.80 (m, 2H, CyH), 5.09 (m, 1H, CH), 6.34-6.29 (m, 2H, ArH), 7.35-7.34 (m, 1H, ArH); ^{13}C NMR ($CDCl_3$): δ 25.6, 25.7, 25.7, 33.2, 33.3, 42.7, 43.9, 107.1, 110.2, 141.7, 153.1.

Table VI.6, entry 6

3-(bis(heptylthio)methyl)-1H-indole

Colourless oil

^{1}H NMR ($CDCl_3$): δ 0.88-0.83 (m, 6H, CH_3), 1.35-1.22 (m, 16H, CH_2), 1.65-1.51 (m, 4H, CH_2), 2.69-2.48 (m, 4H, CH_2), 5.28 (s, 1H, CH), 7.26-7.11 (m, 4H, ArH), 7.84-7.80 (m, 1H, ArH), 8.00 (s, 1H, NH); ^{13}C NMR ($CDCl_3$): δ 13.9, 22.5, 28.7, 28.8, 29.1, 31.6, 31.9, 45.7, 111.2, 114.9, 119.5, 119.6, 122.3, 123.0, 125.5, 136.4.

Table VI.6, entry 7

2-(1, 3-dithian-2-yl)furan,[32]

Colourless oil

^{1}H NMR ($CDCl_3$): δ 2.02 -1.96 (m, 1H, CH_2), 2.16-2.10 (m, 1H, CH_2), 3.00-2.93 (m, 4H, $2CH_2$), 5.22 (s, 1H, CH), 6.40-6.33 (m, 2H, ArH), 7.37-7.26 (m, 1H, ArH); ^{13}C NMR ($CDCl_3$): δ 25.2, 30.2, 42.0, 107.8, 110.5, 142.2, 151.7.

Table VI.6, entry 8

3-(1, 3-dithiolan-2-yl)-1H-indole

Pale yellow solid, mp 121-123 ^{o}C

^{1}H NMR ($CDCl_3$): δ 3.50-3.31 (m, 4H, CH_2), 6.03 (s, 1H, CH), 7.32 - 7.11 (m, 4H, ArH), 7.81 (d, *J* = 7.2 Hz, 1H, ArH), 8.00 (s, 1H, NH); ^{13}C NMR ($CDCl_3$): δ 39.4, 48.9, 111.4, 114.9, 119.7, 122.5, 123.1, 125.8, 136.8.

Table VI.7, entry 1

1-(bis(pentylthio)methyl)-4-methoxybenzene

Colourless oil

^{1}H NMR ($CDCl_3$): δ 0.89-0.84 (m, 6H, CH_3), 1.35-1.24 (m, 12H, CH_2), 1.56-1.51 (m, 4H, CH_2), 2.58-2.46 (m, 4H, CH_2), 3.78 (s, 3H, OCH_3), 4.85 (s, 1H, CH), 6.84 (dd, *J* = 2.1 and 6.6 Hz, 2H, ArH), 7.36 (dd, *J* = 2.1 and 6.6 Hz, 2H, ArH); ^{13}C NMR ($CDCl_3$): δ 13.8, 13.9, 22.1, 22.5, 28.7, 28.7, 29.0, 30.9, 31.6, 32.1, 52.5, 55.1, 113.6, 128.7, 132.5, 158.9; ESI-HRMS: for $C_{20}H_{34}KOS_2$, calculated 393.1688; observed 393.1676.

Table VI.7, entry 2

4-(bis(pentylthio)methyl)-2-methoxyphenol

Pale yellow oil

^{1}H NMR ($CDCl_3$): δ 0.89 - 0.84 (m, 6H, CH_3), 1.35 -1.24 (m, 12H, CH_2), 1.57-1.50 (m, 4H, CH_2), 2.58-2.48 (m, 4H, CH_2), 3.89 (s, 3H, OCH_3), 4.82 (s, 1H, CH), 5.70 (s, 1H, OH), 7.04 (d, *J* = 2.1 Hz, 1H, ArH); ^{13}C NMR ($CDCl_3$): δ 13.8, 13.9, 22.1, 22.5, 28.7, 28.8, 29.1, 30.9, 31.6, 32.3, 32.3, 53.0, 55.8, 109.8, 113.7, 120.7, 132.4, 145.2, 146.6; ESI-HRMS: for $C_{20}H_{34}O_2S_2Na$, calculated 393.1898; observed 393.1898.

VI.6. References

References are given in BIBLIOGRAPHY under Chapter VI (pp. 152–155).

CHAPTER VII

Ni(0) supported with reduced graphene oxide (RGO): Efficient heterogeneous catalyst for Kumada–Corriu cross–coupling reaction

VII.1. Introduction

During the last few years, graphene oxide (GO)[1] and reduced graphene oxide (RGO) based carbon nanomaterials have attracted immense research interest in the field of catalysis.[2] The electronic properties[3] and high surface area [4] of RGO opens up new opportunities for its use as a next-generation catalyst or catalyst support.[5] The reduced graphene oxide has the more potential to behave as catalyst supports.[6] Because, they can form stable dispersions in aqueous or organic media, and can be blended with other nanomaterials to form nanocomposites.[7] Various metal nanoparticles (NP) have been incorporated in 2D catalyst support RGO to synthesize potential catalyst in different reactions. In recent literatures RGO supported Pd, Au and Pt have been used in organic reactions as catalyst.[8] It was observed that in most of the papers RGO supported noble metals have been used as catalyst. Surprisingly there are very few reports on RGO supported low cost first row transition metals as potential catalyst in different organic reactions.[9]

In the recent years, RGO as the catalyst support has shown some significant advantages in the area of cross–coupling chemistry. Usually organic ligand-stabilized zero valent homogeneous complexes are used as catalysts in cross–coupling reactions.[10] The drawbacks regarding the recovery and reusability of a homogeneous catalyst was overcome by using RGO supported ligand-free heterogeneous catalysts. The C–C cross–coupling reactions, such as Mizoroki–Heck, Sonogashira and Suzuki–Miyaura, have been successfully catalysed by heterogeneous Pd/RGO composite materials.

The Kumada–Corriu cross–coupling reaction is frequently used to synthesize functionalized biaryls.[11] This reaction has the major advantage over Suzuki–Miyaura and Mizoroki–Heck reactions because all aromatic halides including sp^2 C–F can undergo cross–coupling with Grignard reagent.[12] In this reaction, the catalyst undergoes a fundamental catalytic cycle involving oxidative addition to a reactive substrate, transmetalation with a Grignard reagent, and reductive elimination to form a carbon–carbon bond. The Ni-catalyzed cross–coupling between aryl halide and Grignard reagent is notable for being among the first cross–coupling reaction reported concurrently by Kumada and Corriu in 1972. Several modifications including Pd-catalyzed conditions and variations in the use of ligands have been developed over the years,[13] and the Kumada–Corriu cross–coupling continues to enjoy many synthetic applications both in the laboratory as well as in industries. The reaction can be carried out over a wide range of temperatures from -20 ^{o}C to refluxing solvents; however, for industrial competence a room temperature reaction is preferable.

VII.2. Present work: Background and Objective

The majority of nickel catalyzed Kumada–Corriu reactions of aryl halides with Grignard reagents have been performed with homogeneous catalysts. Despite the high activities that can sometimes be achieved with homogeneous catalysts, the difficulties and high costs associated with recovery and reuse of homogeneous catalysts can hinder their commercial utilization. Thus, heterogeneous catalysts are often preferred in practical applications. An approach to develop such catalysts is to anchor coordination complexes to supports in the hope that they not only retain the desired catalytic properties of their homogeneous counterparts, but are also recoverable due to their attachment to an easily recovered solid.

A nickel(II) co-ordination complex, covalently immobilised on a Merrifield resin, is an effective recyclable heterogeneous catalyst in a room temperature coupling reaction between a Grignard reagent and an organobromide (Scheme VII.1).[14] Both aromatic and aliphatic Grignard reagents were successfully employed in the reaction. This catalyst was easily collected through filtration and recycles up to 10 consecutive runs.

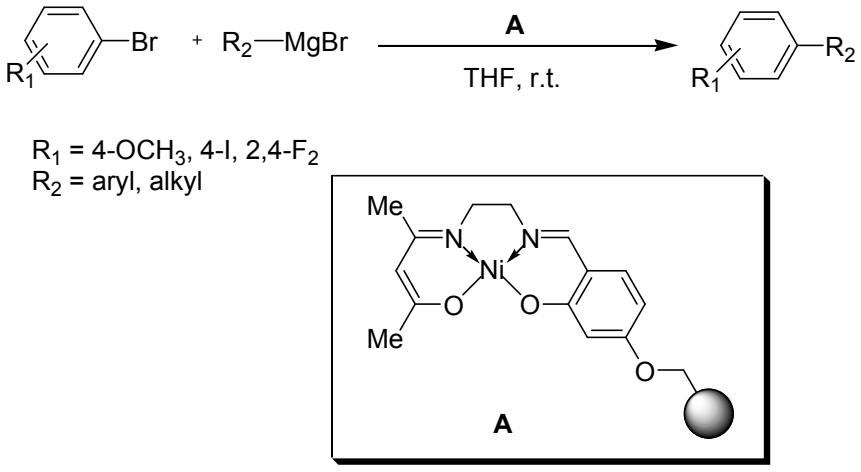

Scheme VII.1. Polymer-supported nickel(II) catalyst for room temperature Tamao–Kumada–Corriu coupling reactions.

Styring and their group have reported another similar type of work where unsymmetrical salen-type nickel(II) complex was readily immobilised onto functionalised silica.[15] The supported complex was an effective recyclable heterogeneous catalyst in a room temperature cross–coupling reaction between 4-bromoanisole and phenylmagnesium chloride (Scheme VII.2). Several bi product was formed during this process, 4,4'- dimethoxybiphenyl, anisole and biphenyl.

Tsai et al. observed that NS-MCM-41-Pd can catalyze the coupling of various aryl halides with arylmagnesium bromides to generate corresponding biaryls in good to excellent yields (Scheme VII.3).[16] The loading of Pd in a single batch reaction can be reduced to as low as

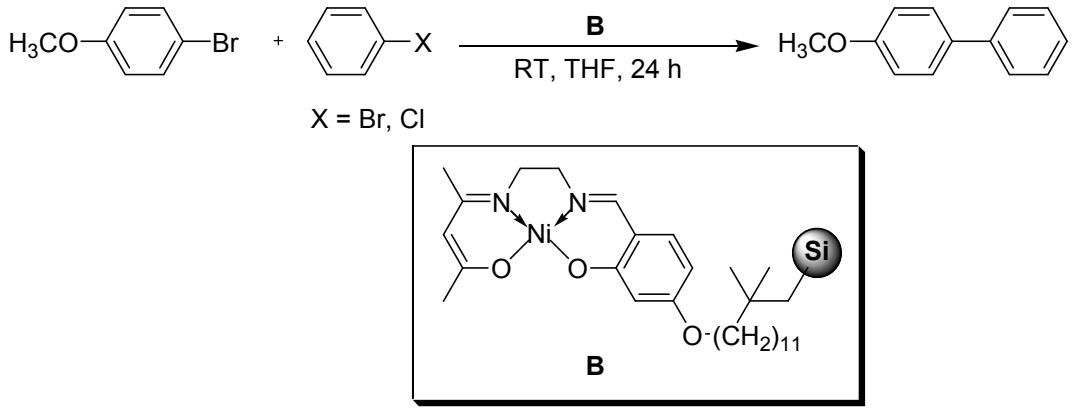

Scheme VII.2. The Kumada reaction of 4-bromoanisole and a phenylmagnesium halide catalyzed by silica supported Ni (II) complex.

0.02 mol %. The nanosized MCM-41 provides easy transport of the reactants and products such that no loss of activity was observed after prolonged use. The catalyst can be easily recovered and re-used several times without loss of activity.

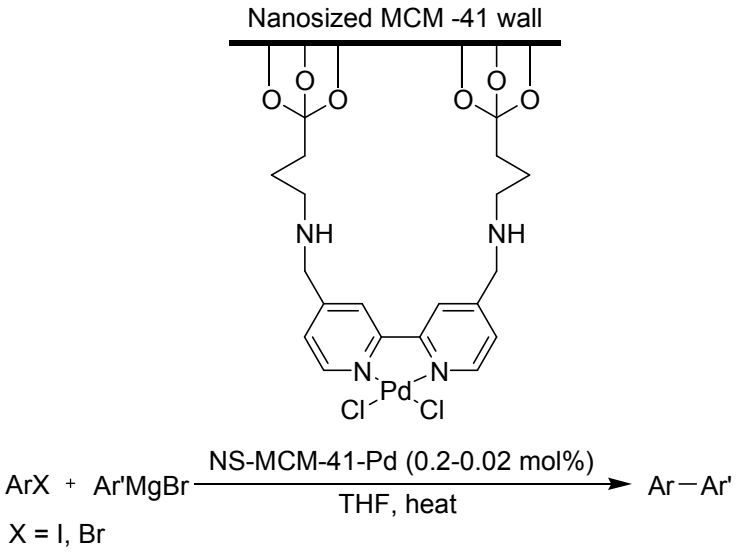

Scheme VII.3. Kumada–Corriu reaction Using NS-MCM-41Pd.

Ni(II) acetate was immobilized onto diamine ligands anchored to (i) a cross-linked poly(styrene) support and (ii) a mesoporous silica support, are successfully used to promote Kumada–Corriu reactions of 4-bromoanisole with phenylmagnesium chloride (Scheme VII.4).[17] Activity from leached metal was demonstrated by both room temperature filtration tests during and after the reaction. It is not the presence of aryl halide that promotes leaching, but rather the presence of Grignard that pulls nickel into solution either by degradation of the ligand or reduction to Ni(0). Anchored nickel could be reused three times without significant loss in final yield and 46% loss of nickel after the third run was detected.

Among the many contributions on Ni systems dedicated to C−C cross–coupling reactions, only a few have focused on the development of surface chemistry by using Ni NPs. One of

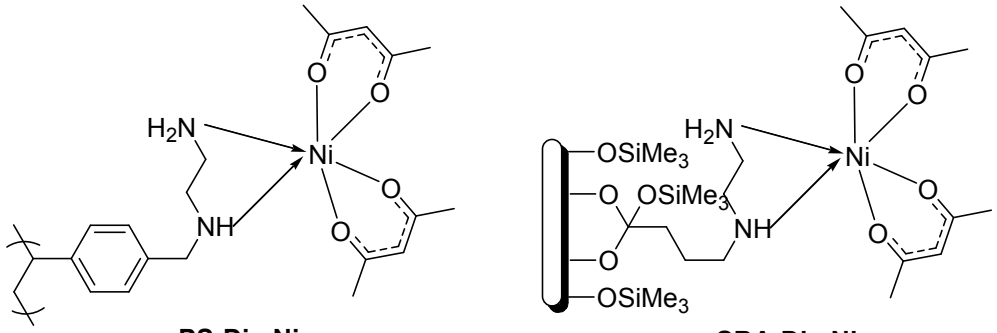

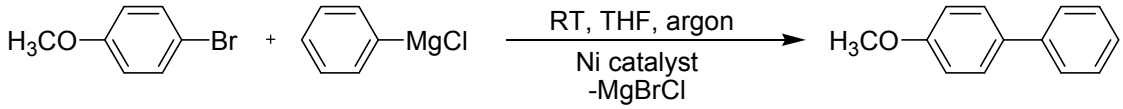

Scheme VII.4. Kumada–Corriu reaction Using nickel precatalysts PS-Dia-Ni and SBA-Dia-Ni.

the first such studies was developed by Lipshutz's group to immobilized nickel on carbon, Ni/C, was rigorously examined for Kumada–Corriu reactions.[18]

In 2013 Kobayashi et al. have synthesized heterogeneous polymer- incarcerated Ni-NPs. The matrix structure of these catalysts incorporates both *N*-heterocyclic carbenes (NHCs) as ligands and Ni-NPs. These NHCs embedded polymer matrix were characterized by FGSR-MAS NMR analysis. The catalyst was successfully applied to Corriu–Kumada–Tamao reactions with a broad substrate scope including functional group tolerance, and the catalyst could be recovered and reused several times without loss of activity.[19]

Recently, De group have developed[20] an approach to stabilize high amount of metallic Ni NP in ambient condition by using RGO support (Ni/RGO), the composite material was characterized and used as a potential redox material to convert Cr(VI) to Cr(III) in a short period of time at room temperature. Considering our experience in the field of developing heterogeneous catalyst in various cross–coupling reactions, we were interested to utilise this well characterized Ni/RGO heterogeneous material in Kumada–Corriu cross–coupling reaction.

VII.3. Present work: Result and Discussion

VII.3.1. Ni/RGO catalyst in Kumada–Corriu cross–coupling reaction

We have synthesized Ni/RGO catalyst following the same literature procedure.[20] Detailed characterization revealed high surface area of the composite (125 m^2 g^{-1}) and existence of highly concentrated but separated Ni NP (40 wt%) of average size ~11 nm on the RGO surface (designated as Ni/RGO-40). In general, bare Ni NP is very unstable and prone to

oxidation in air, but in the Ni/RGO-40 composite, Ni NP can be stabilized by RGO. The RGO surface contains many free electrons [21] and these free electrons help to stabilize the Ni in its zero-valent state. Because of this kind of electronic environment, the metallic Ni NP resides on the RGO surface in tightly bound condition and do not get oxidized. Also, the high surface area and planer structure of RGO prevent the Ni NP from agglomeration into larger particles. As a result, very high Ni loading (40 wt%) was possible without any agglomeration. It can be noted here that we also prepared Ni/RGO-60 and Ni/RGO-20 to compare the catalytic performance with Ni/RGO-40.

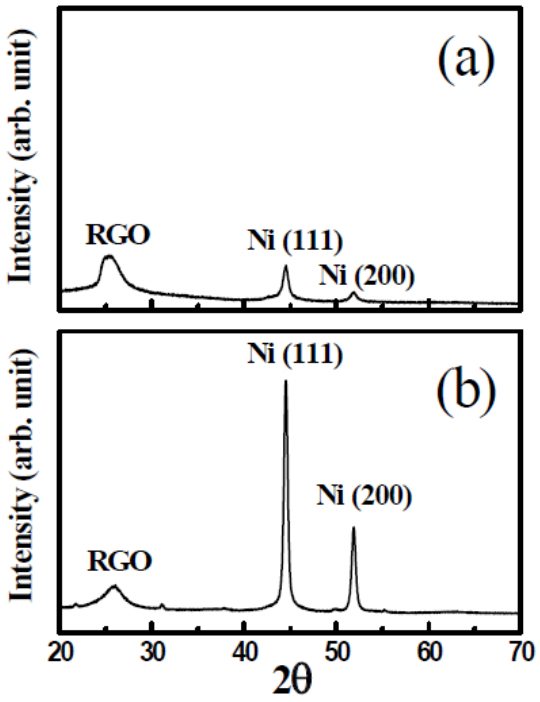

Figure VII.1. XRD patterns: (a) Ni/RGO-20 and (b) Ni/RGO-60

Both the materials were characterized by XRD and the results are shown in Figure VII.1. Both samples show characteristic peaks of Ni(111), Ni(200) and RGO similar to those of Ni/RGO-40. However, as expected, the relative XRD peak intensities of metallic Ni and RGO are different due to the variation of compositions. The crystallite size of Ni in the three Ni/RGO samples was evaluated using the X-ray line broadening method (scherre's equation) from Figure VII.1 and VII.3a. In case of Ni, the crystallite size was evaluated from both the (111) and (200) peaks. Following this method we found the average crystallite size of Ni as 10, 12 and 17 nm in Ni/RGO-20, Ni/RGO-40 and Ni/RGO-60 samples, respectively. TEM of Ni/RGO-40 confirms existence of Ni NPs of average size ~11 nm.[20]

Initially, we tested the cross–coupling between 4-iodoanisole and PhMgCl in the presence of catalytic amounts (0.05 and 0.1 mmol with respect to 1 mmol of 4-iodoanisole) of Ni/RGO-40. The reaction was indeed successful as we obtained the desired biphenyl in 81–89% isolated yields (Table VII.1, entries 1–2). Further variations in temperature and changing solvent however did not produce any appreciable changes in terms of the isolated yield of the biphenyl. The optimization of reaction conditions has been presented in Table VII.1.

To achieve the better performance from Ni/RGO, we are applying three different composites Ni/RGO-40, Ni/RGO-60 and Ni/RGO-20. The results are summarized in Table VII.2. It was

Table VII.1. Optimization of Kumada–Corriu cross–coupling reaction conditions using Ni/RGO-40 as the catalyst.[a]

Entry	Solvent	Catalyst [Ni content (with respect to 4-iodo-anisole)(mmol)]	Temperature (°C)	Time (h)	Yield (%)[b]
1	THF	0.05	25	6	81
2	**THF**	**0.1**	**25**	**4**	**89**
3	THF	0.1	40	4	88
4	THF	0.1	60	4	91
5	Dioxane	0.1	25	6	84

[a]4─Iodoanisole (1 mmol), PhMgCl (1 mL, 25 wt% in THF, 1.84 mmol), solvent (2 mL), under N_2, [b]Isolated yield.

Table VII.2. Control reactions to compare the catalytic activity of Ni/RGO-40.[a]

Entry	Solvent	Catalyst	Ni content [with respect to 4-iodo-anisole)(mmol)]	Temperature (^oC)	Time (h)	Yield[b] (%)
1	**THF**	**Ni/RGO-40**	**0.1**	**25**	**4**	**89**
2	THF	Ni/RGO-60	0.1	25	4	67
3	THF	Ni/RGO-20	0.1	25	4	77
4	THF	Ni NPs	0.1	25	4	63
5	THF	Nil	00	25	4	08
6	THF	Nil	00	25	24	14

[a] 4─Iodoanisole (1 mmol), PhMgCl (1 mL, 25 wt% in THF, 1.84 mmol), solvent (2 mL), under N_2, [b] Isolated yield.

found that Ni/RGO-40 showed the highest catalytic activity compair to others.

The deterioration of catalytic activity of Ni/RGO-60 (Table VII.2; entry 2) can be understood because of larger size of Ni NPs (17 nm) with lower active surfaces. This is expected because chances of agglomeration of Ni would be higher due to high amount of Ni loading. Although we found little lowering of Ni NPs' size (10 nm) in case of Ni/RGO-20, the yield of the reaction was found to be dropped in this case also (Table VII.2; entry 3) when compared with Ni/RGO-40 (Table VII.2; entry 1). In case of Ni/RGO-20, we believe that the exposed Ni surface got reduced due to the presence of more RGO.

The bare Ni NPs[22] of size around 10 nm was also tested as catalyst (Table VII.2 entry 4) under similar reaction conditions which produces only 63% yield. The control reaction without any catalyst showed 8% yield (Table VII.2; entry 5) and the yield can be increased to 14% if the reaction continued up to 24h (Table VII.2; entry 6). Therefore from the above

results, it can be concluded that Ni/RGO-40 is an optimized composition for the Kumada–Corriu cross–coupling reactions.

Following the optimized reaction condition we carried out similar cross–coupling reactions on varying the combination of aryl halide (ArX) and Grignard reagent. The results are presented in Table VII.3. The 3-iodoanisole (entry 2) and 2- iodoanisole (entry 3) successfully react with PhMgCl and produced the corresponding biphenyl derivatives in 85 and 77% yields, respectively. The feasibility of the reaction between other iodoarenes and Grignard reagents (ArMgX) were also undertaken to obtain the corresponding biaryls. We observed that the *p*-methyliodobenzene (entry 4) and iodobenzene (entry 5) were successfully reacted with para and meta isomer of methoxyphenylmagnesium bromide, respectively to produce the corresponding biaryls with a high yield. Similar cross–coupling were performed on different bromo- and chloro- arenes and resulting biaryls were isolated in 80−88% yields (entries 6−9).

Multiple cross–couplings were experienced with diiodo-, bromoiodo-, chloroiodo- and fluoroiodo-benzenes using excess PhMgCl as the coupling partner in the presence of Ni/RGO-40 (amount of catalyst equivalent to 0.1 mmol Ni was used for 1 mmol haloarene). In each case, we obtained corresponding biscoupled products (terphenylenes) in good to excellent yields (entries 10–14). Thus the present catalytic system was found to be equally active for the oxidative addition to the sp^2 C–F bond (entry 13). Further, application of the catalyst in Kumada–Corriu crossc–oupling was examined with aliphatic Grignard reagent like isopropylmagnesium chloride (*i*-PrMgCl). Interestingly, the 4- iodoanisole did not couple with the isopropyl group, rather a homo-coupled biphenyl, 4,4'-dimethoxybiphenyl was obtained in appreciable yield (entry 15). On the other hand, 2-methyl-4-bromoanisole remained unreacted when treated with *i*-PrMgCl in THF in the presence of the catalyst (entry 16). We presume that there is an exchange reaction between 4-iodoanisole and using *i*-PrMgCl to generate 4-anisylmagnesium chloride, which then undergoes homo-coupling to produce the 4,4'-dimethoxybiphenyl in 76% yield. Such homo-coupling is however previously known with Fe-catalyzed reactions between aryl halide and Grignard reagent.[23] The scope of the catalytic application has been further broaden with successful cross−coupling with hetero-aryl bromide such as 2-bromopyridine resulting in the formation of 2-phenylpyridine in brilliant yield (entry 17).

VII.3.2. Recovery and Reusability of the catalyst

After the reaction of aryl halide (1 mmol) and Grignard reagent (1.8 mmol) in the presence of

Table VII.3. Kumada–Corriu cross–coupling reaction of halo-arenes with Grignard reagents in the presence of catalyst (Ni/RGO-40).[a]

Entry	Aryl halide	Grignard reagent	Time (h)	Product	Yield (%)[b]
1	$(4\text{-}H_3CO)C_6H_4I$	C_6H_5MgCl	4	$(4\text{-}H_3CO)H_4C_6\text{—}C_6H_5$	89
2	$(3\text{-}H_3CO)C_6H_4I$	C_6H_5MgCl	4	$(3\text{-}H_3CO)H_4C_6\text{—}C_6H_5$	85
3	$(2\text{-}H_3CO)C_6H_4I$	C_6H_5MgCl	12	$(2\text{-}H_3CO)H_4C_6\text{—}C_6H_5$	77
4	$(4\text{-}H_3C)C_6H_4I$	$(4\text{-}H_3CO)C_6H_4MgBr$	6	$(4\text{-}H_3C)H_4C_6\text{—}C_6H_4(4'\text{-}OCH_3)$	84
5	C_6H_5I	$(3\text{-}H_3CO)C_6H_4MgBr$	6	$H_5C_6\text{—}C_6H_4(3\text{-}OCH_3)$	80
6	$(3\text{-}H_3C)C_6H_4Br$	$(3\text{-}H_3CO)C_6H_4MgBr$	9	$(3\text{-}H_3C)H_4C_6\text{—}C_6H_4(3'\text{-}OCH_3)$	86
7	$(4\text{-}H_3CO\text{-}3\text{-}H_3C)C_6H_3Br$	C_6H_5MgCl	7	$(4\text{-}H_3CO\text{-}3\text{-}H_3C)H_3C_6\text{—}C_6H_5$	80
8	C_6H_5Br	$(4\text{-}H_3CO)C_6H_4MgBr$	10	$H_5C_6\text{—}C_6H_4(4\text{-}OCH_3)$	88
9	$(4\text{-}H_3CO)C_6H_4Cl$	C_6H_5MgCl	12	$(4\text{-}H_3CO)H_4C_6\text{—}C_6H_5$	82
10[c]	$1,3\text{-}C_6H_4I_2$	C_6H_5MgCl	12	$1,3\text{-}(C_6H_5)_2\text{—}C_6H_4$	78
11[c]	$(3\text{-}Br)C_6H_4I$	C_6H_5MgCl	12	$1,3\text{-}(C_6H_5)_2\text{—}C_6H_4$	72
12[c]	$(3\text{-}Cl)C_6H_4I$	C_6H_5MgCl	12	$1,3\text{-}(C_6H_5)_2\text{—}C_6H_4$	73
13[c]	$(2\text{-}F)C_6H_4I$	C_6H_5MgCl	12	$1,2\text{-}(C_6H_5)_2\text{—}C_6H_4$	76
14[c]	$(2\text{-}Br)C_6H_4I$	C_6H_5MgCl	12	$1,2\text{-}(C_6H_5)_2\text{—}C_6H_4$	73
15	$(4\text{-}H_3CO)C_6H_4I$	$(CH_3)_2CHMgCl$	24	$((4\text{-}H_3CO)H_4C\text{-})_2$	76
16	$(4\text{-}H_3CO\text{-}3\text{-}CH_3)C_6H_3Br$	$(CH_3)_2CHMgCl$	24	No Reaction	-
17	C_5H_4NBr	C_6H_5MgCl	10	$C_5H_4N\text{-}C_6H_5$	91

[a] ArX (1 mmol), PhMgCl (1 mL, 1.84 mmol)/ArMgBr (1.5 mmol), Ni/RGO-40 (0.1 mmol), THF (2 mL) stirring at room temperature (25 ^oC) under N_2. [b] Isolated yield. [c] PhMgCl (2 mL, 3.68 mmol per mmol of bis-aryl halides).

catalytic Ni/RGO-40 for the time period as mentioned in Table VII.3, dry and distilled ethyl acetate (3 mL) was added to the reaction mixture and stirred at room temperature for 5 min. The reaction mixture was allowed to settle down and the supernatant liquid was decanted. The process was repeated three times and then water (1 mL) was added to the catalyst containing reaction mixture. The mixture was extracted with ethyl acetate (5 mL) and the aqueous part was separated out, evaporated to dryness using rotary evaporator and dried under vacuum to get free flowing powder.

Reusability of a catalyst is an important aspect from the commercial point of view. Reusability increases the potentiality of the catalyst. In order to check the reusability, Ni/RGO-40 was recovered from the reaction mixture, as described above. It was used for the

next batch of reactions. The recycling experiments were carried out with 4-iodoanisole and PhMgCl and consecutive six runs were performed with appreciable conversion to the coupled

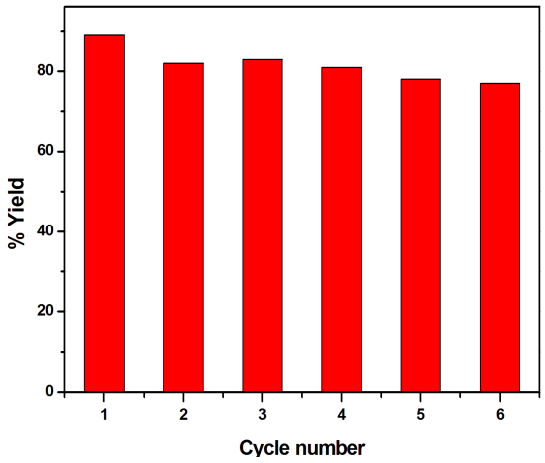

Figure VII.2. Reusability of Ni/RGO-40 in consecutive six cycles of Kumada–Corriu cross–coupling reaction.

product (Figure VII.2). In the first cycle, the yield was 89% whereas after six cycles the yield of the product was 77%. The results confirm that the heterogeneous catalyst Ni/RGO-40 is potentially recyclable.

VII.3.3. Characterization of recovered catalyst

XRD analysis

After recovery from the reaction mixture the catalyst was characterized by XRD and Raman to confirm that after reaction the oxidation state of Ni remains unchanged. It is noteworthy here that although we tried to eliminate the bi-products (Mg salts formed during the decomposition of Grignard reagent and mixed with the catalyst) by washing, the weight of recovered catalyst after the first cycle was found to be higher (22 mg) than the initial weight (14.7 mg). The weight of the recovered catalyst is gradually increasing as the cycles are progressing. The XRD of the recovered Ni/RGO-40 after the first cycle shows clear peaks corresponding to the metallic Ni NPs at 44.49^{o} (111), 51.8^{o} (200) and RGO layers at 25.4^{o} 2θ (Figure VII.3). It clearly indicates that the catalyst remains unchanged even after the reaction. However, as mentioned above the recovered catalyst also shows presence of other peaks originated from MgO/$Mg(OH)_2$ species. The different peaks of $Mg(OH)_2$ and MgO are marked by different symbols in the Figure VII.3b. The XRD pattern of recovered catalyst after sixth cycle showed that the intensity of the peaks related to Mg species got increased significantly, however, Ni remains in the metallic state (Figure VII.3c). It is to be noted here

that the presence of $MgO/Mg(OH)_2$ in the recovered catalyst did not deteriorate the performance of the catalyst in the subsequent cycles.

Raman analysis

The Raman spectrum of the original Ni/RGO-40 catalyst shows the characteristic D (A_{1g} vibrations of the six-membered sp^2 carbon rings)[24] and G (first-order scattering of the E_{2g} mode of sp^2 domains)[25] bands at 1344 and 1580 cm^{-1}, respectively (Figure VII.4a).[20] The Raman spectrum of recovered Ni/RGO-40 after the first (Figure VII.4b) and sixth cycles (Figure VII.4c) did not show any peak related to the oxidized Ni (NiO), and the intensity ratio of D over G band remained same. Therefore it can be concluded that the characteristics of the Ni/RGO-40 in the recovered catalysts remained similar after recycling.

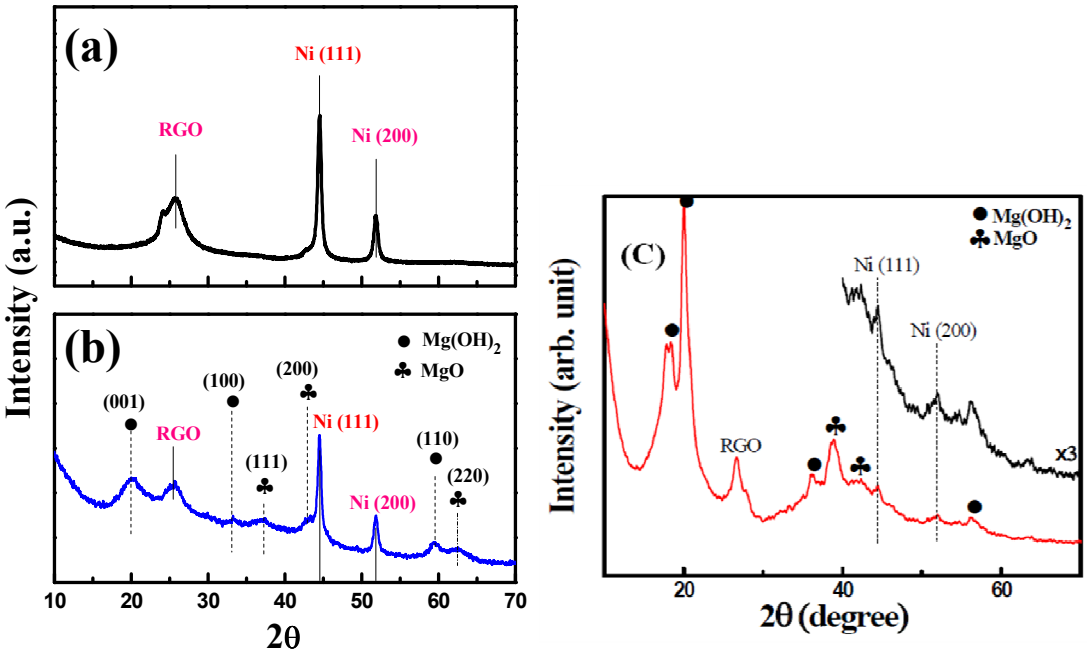

Figure VII.3. XRD analysis of Ni/RGO-40: (a) before use as catalyst, (b) recovered catalyst after the first cycle of reaction and (c) recovered catalyst after sixth cycle.

VII.4. Conclusion

An excellent catalytic activity of Ni/RGO-40 in Kumada–Corriu cross–coupling reaction has been established. The reactions on varying the haloarene and Grignard reagent produced the expected coupled product with good to excellent yields. Interestingly, this catalyst was found to be equally active for the oxidative addition to the sp^2 C−F bond. Our results confirmed that Ni/RGO-40 is a promising catalyst as a replacement of Pd based and other ligand-stabilized homogeneous catalysts. Ni/RGO-40 has enough potential as an economic high performance reusable catalyst and can be of technological viability.

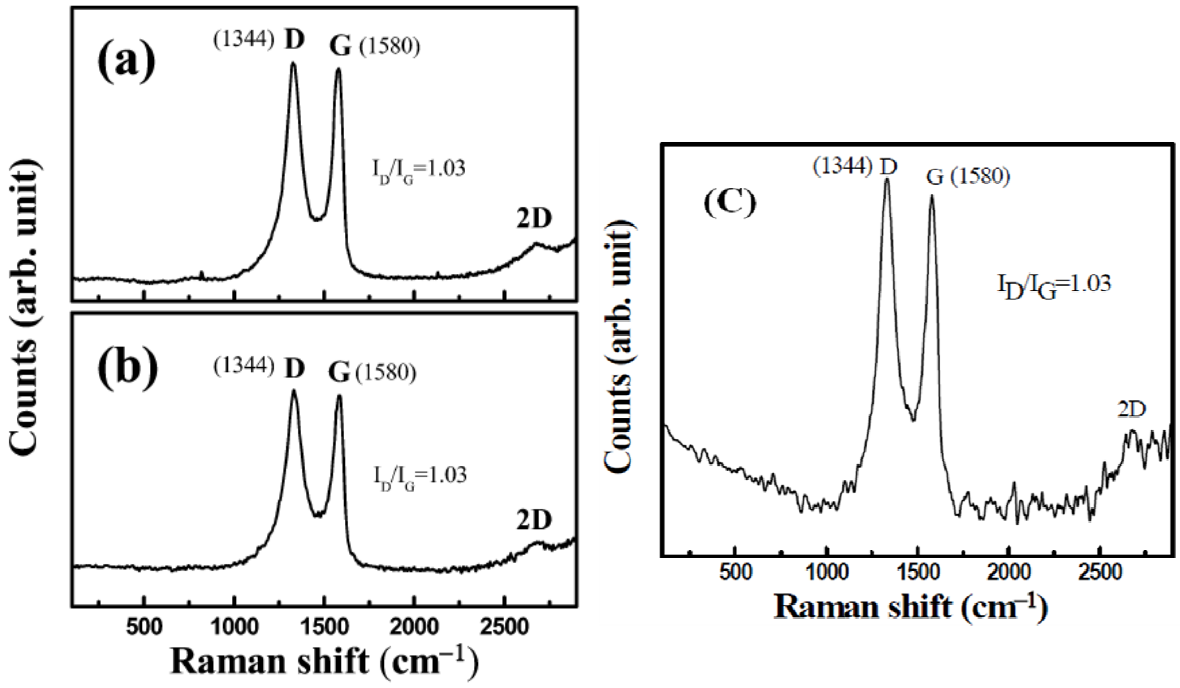

Figure VII.4. Raman analysis of Ni/RGO-40: (a) before use as catalyst, (b) recovered catalyst after the first cycle of reaction and (c) recovered catalyst after 6th cycle.

VII.5. Experimental section

VII.5.1. General information

Chemicals were used as received. ^{1}H and ^{13}C NMR spectra were taken in $CDCl_3$ using Bruker Avance AV-300 spectrometer operating at 300 MHz and 75 MHz respectively. Chemical shifts are reported relative to tetramethylsilane served as internal standard (δ 0 ppm). ^{13}C NMR spectra were recorded with complete proton decoupling and chemical shifts are reported in ppm with the solvent resonance as the internal standard ($CDCl_3$: δ 77.00 ppm). X-ray diffraction (XRD) and Raman studies of the powder samples were performed with Rigaku SmartLab X-ray diffractometer operating at 9 kW (200 mA; 45 kV) using Cu-Ka radiation and Renishaw In Via micro Raman spectrometer, respectively.

VII.5.2. Synthesis of Ni/RGO composite materials

Ni/RGO composites were synthesized and characterized by De et al[20]. A brief procedure is given below, though it was prepared in the research group of G. De.

1.5 g of GO was ultrasonically dispersed in 350 mL of water. $NiCl_2 \cdot 6H_2O$ (3.5 mmol) and Hexamethylenetetramine (7.0 mmol) were dissolved in 250 and 100 mL of water, respectively, in two separate flasks. The molar ratio of HMT to $NiCl_2$ was maintained at 2:1. All three solutions were mixed together in a round-bottomed flask, stirred for 10 min, and

finally sealed in a 2 L Teflon-lined stainless steel autoclave for hydrothermal reaction at 120 °C for 4h to obtain a $Ni(OH)_2$-embedded GO composite [$Ni(OH)_2$-GO]. The black powder was washed several times with water to remove excess Ni salt and HMT and dried. The powder was then heated in air to 380 °C for 1h to obtain NiO NP-embedded RGO sheets. *In situ* reduction of NiO NP in the presence of RGO at 350 °C with a continuous flow of H_2 gas (10% H_2-balance N_2) yielded Ni/RGO composite containing 40 wt% Ni NPs.

For control experiments Ni/RGO-60 (60 wt% Ni) and Ni/RGO-20 (20 wt% Ni) were also prepared following the above method. Bare Ni NP was prepared following the method available in the literature.[22]

VII.5.3. Representative procedure of Kumada–Corriu cross–coupling reaction using Ni/RGO-40

A mixture of 4-iodoanisole (234 mg, 1 mmol) and Ni/RGO-40 catalyst (14.7 mg, Ni content: 0.1 mmol) in freshly distilled THF (2 mL) under N_2 atmosphere was prepared. Then a solution of PhMgCl (1 mL, 25 wt% in THF, 1.84 mmol) was added dropwise at room temperature (25 ^oC) with gentle magnetic stirring. The progress of the reaction was monitored by TLC. After completion of the reaction, dry and distilled ethyl acetate (3 mL) was added, stirred gently and then allowed to stand. The supernatant liquid was carefully decanted in another flask and this process was repeated three times more. The combined washings (organic part) were washed with water, dried over anhydrous Na_2SO_4, concentrated and the residue was purified by column chromatography over silica gel. Elution with light petroleum afforded 4-methoxybiphenyl (164 mg, 89%) as white crystalline solid. The product was characterized by ^1H and ^{13}C NMR spectral data, and also compared with reported melting point.

VII.5.4. Physical properties and spectral data of compounds

Table 2, entry 1, 8, 9

4-Methoxybiphenyl[26]

White solid, m.p. 90-91 ^oC (Lit. 91-92 ^oC)

^1H NMR ($CDCl_3$, 300 MHz): δ/ppm 3.84 (s, 3H, OCH_3), 6.97 (dd, J = 6.9 and 2.1 Hz, 2H, ArH), 7.29-7.32 (m, 1H, ArH), 7.38-7.43 (m, 2H, ArH), 7.51-7.56 (m, 4H, ArH); ^{13}C NMR ($CDCl_3$, 75 MHz): δ/ppm 55.3, 114.2, 126.6, 126.7, 128.1, 128.7, 133.8, 140.8, 159.2.

Table VII.2, entry 2, 5

3-Methoxybiphenyl[27]

Colorless liquid

^{1}H NMR ($CDCl_3$, 300 MHz): δ/ppm 3.86 (s, 3H, OCH_3), 6.90 (ddd, J = 8.1 Hz, 2.4 Hz and 0.9 Hz, 1H, ArH), 7.12-7.13 (m, 1H, ArH), 7.16-7.20 (m, 1H, ArH), 7.33-7.38 (m, 2H, ArH), 7.41-7.46 (m, 2H, ArH), 7.57-7.60 (m, 2H, ArH); ^{13}C NMR ($CDCl_3$, 75 MHz): δ/ppm 55.3, 112.7, 112.9, 119.7, 127.2, 127.4, 128.7, 129.7, 141.1, 142.8, 159.9.

Table VII.2, entry 3

2-Methoxybiphenyl[27]

Colorless liquid

^{1}H NMR ($CDCl_3$, 300 MHz): δ/ppm 3.81 (s, 3H, OCH_3), 6.97-7.06 (m, 2H, ArH), 7.29-7.43 (m, 5H, ArH), 7.51-7.54 (m, 2H, ArH); ^{13}C NMR ($CDCl_3$, 75 MHz): δ/ppm 55.5, 111.2, 120.8, 126.9, 127.9, 128.6, 129.5, 130.7, 130.9, 138.5, 156.4.

Table VII.2, entry 4

4-Methoxy-4'-methylbiphenyl[28]

White solid, m.p. 112-113 ^{o}C (Lit. 111-112 ^{o}C)

^{1}H NMR ($CDCl_3$, 300 MHz): δ/ppm 2.38 (s, 3H, CH_3), 3.84 (s, 3H, OCH_3), 6.96 (d, J = 8.7 Hz, 2H, ArH), 7.22 (d, J = 8.4 Hz, 2H, ArH), 7.45 (d, J = 8.1 Hz, 2H, ArH), 7.51 (d, J = 8.7 Hz, 2H, ArH); ^{13}C NMR ($CDCl_3$, 75 MHz): δ/ppm 21.0, 55.3, 114.1, 126.5, 127.9, 129.4, 133.7, 136.3, 137.9, 158.9.

Table VII.2 entry 6

3-Methoxy-3'-methylbiphenyl[27]

Colourless liquid

^{1}H NMR ($CDCl_3$, 300 MHz): δ/ppm 2.41 (s, 3H, CH_3), 3.84 (s, 3H, OCH_3), 6.87-6.89 (m, 1H, ArH), 7.11-8.18 (m, 3H, ArH), 7.28-7.39 (m, 4H, ArH); ^{13}C NMR ($CDCl_3$, 75 MHz): δ/ppm 21.5, 55.2, 112.6, 112.8, 119.6, 124.3, 127.9, 128.1, 128.6, 129.6, 138.3, 141.0, 142.8, 159.8.

Table VII.2, entry 7

4-Methoxy-3'-methylbiphenyl[29]

White solid, m.p. 75-76 ^{o}C (Lit. 74-75 ^{o}C)

^{1}H NMR ($CDCl_3$, 300 MHz): δ/ppm 2.28 (s, 3H, CH_3), 3.87 (s, 3H, OCH_3), 6.89 (d, J = 9.3 Hz, 1H, ArH), 7.25-7.31 (m, 1H, ArH), 7.38-7.43 (m, 4H, ArH), 7.53-7.56 (m, 2H, ArH); ^{13}C NMR ($CDCl_3$, 75 MHz): δ/ppm 16.4, 55.4, 110.1, 125.3, 126.5, 126.7, 126.9, 128.6, 129.5, 133.3, 141.0, 157.3.

Table VII.2, entry 10, 11, 12

***m*-Terphenyl**[30]

White solid, m.p. 83-85 ^{o}C (Lit. 84-85 ^{o}C)

^{1}H NMR ($CDCl_3$, 300 MHz): δ/ppm 7.33-7.38 (m, 2H, ArH), 7.43-7.59 (m, 7H, ArH), 7.63-7.66 (m, 4H, ArH), 7.79-7.80 (m, 1H, ArH); ^{13}C NMR ($CDCl_3$, 75 MHz): δ/ppm 126.1, 126.2, 127.3, 127.4, 128.8, 129.2, 141.2, 141.8.

Table VII.2, entry 13, 14

***o*-Terphenyl**[29]

White Solid, m.p. 54-55 ^{o}C (Lit. 54-56 ^{o}C)

^{1}H NMR ($CDCl_3$, 300 MHz): δ/ppm 7.13-7.26 (m, 10H, ArH), 7.40-7.44 (m, 4H, ArH); ^{13}C NMR ($CDCl_3$, 75 MHz): δ/ppm 126.4, 127.4, 127.8, 129.9, 130.6, 140.6, 141.5.

Table VII.2, entry 15

4,4′-Dimethoxybiphenyl[23]

White crystalline solid, m.p. 179-180 ^{o}C (Lit. 178-179 ^{o}C)

^{1}H NMR ($CDCl_3$, 300 MHz): δ/ppm 3.84 (s, 6H, OCH_3), 6.96 (d, J = 9 Hz, 4H, ArH), 7.48 (d, J = 8.7 Hz, 4H, ArH); ^{13}C NMR ($CDCl_3$, 75 MHz): δ/ppm 55.3, 114.1, 127.7, 133.4, 158.6.

Table VII.2, entry 17

2-Phenylpyridine[31]

Colorless liquid

^{1}H NMR ($CDCl_3$, 300 MHz): δ/ppm 7.18-7.26 (m, 1H, ArH), 7.39-7.51 (m, 3H, ArH), 7.72-7.80 (m, 2H, ArH), 7.96-8.00 (m, 2H, ArH), 8.70 (d, J = 4.5 Hz, 1H, ArH); ^{13}C NMR ($CDCl_3$, 75 MHz): δ/ppm 115.4, 120.7, 122.1, 127.0, 128.7, 129.0, 129.6, 136.8, 139.3, 149.6, 157.5.

VII.6. References

References are given in BIBLIOGRAPHY under Chapter VII (pp. 155−157).

CHAPTER VIII

Ni(0) supported with reduced graphene oxide (RGO): Efficient heterogeneous catalyst for C–S cross–coupling reaction

VIII.1. Introduction

In recent years graphene and composite material has becomes much popular among researcher because of its unique physical, mechanical and chemical properties.[1] Graphene, consists of a single atomic layer of conjugated sp^2 carbon atoms with large contact area can adopt several guest particles.[2] Reduced graphene oxide (RGO) with high surface area form stable dispersion in aqueous or non aqueous medium, can easily blended with nanomaterials to produce stable nanocamposites.[3] To date various metal, metal oxide, magnetic and semiconducting NPs have been hosted on the surface of GO and studied their photocatalytic and electrochemical properties.[4] However, few papers which execute the utilization of the graphene metal nanocomposite towards organic cross–coupling reaction.[5]

The transition metal catalyzed C–S cross–coupling is an essential step for the synthesis of various biologically active entities, which have been used in several therapeutic areas such as HIV, cancer, diabetes, inflammatory, Alzheimer's and Parkinson's diseases etc.[6] In 1980 the first palladium-catalyzed arylation of thiols has been reported by Migita and co-workers.[7] Soon after Cristau and co-workers have reported a nickel-catalyzed route to synthesize the same.[8] Increasing interest in this field people have continuing their studies with different metal like Cu, Co, Fe, Bi and In with a variety of ligands either in homogeneous or heterogeneous condition.[9]

VIII.2. Present work: Background and Objective

Ni catalyzed C−S cross–coupling reactions are generally studied by using Ni-salts, Ni(II) phosphine complexes or by generating the Ni–NHCs.

Takeda co-woeker reported nickel(0) triethyl phosphite complex as an effective catalyst for stereoselective transformation of (*E*)-alkenyl halides into sulphides. Aryl halides were also transformed into aryl sulphides using the same reagent system (Scheme VIII.1).[10] But (Z)-alkenyl halides gave alkynes under the same reaction conditions.

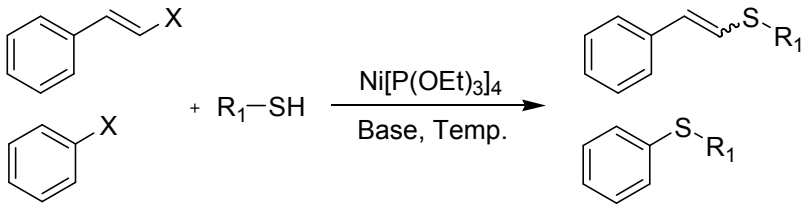

X = Br, I
R_1 = Aryl, Alkyl, benzyl

Scheme VIII.1. Stereoselective transformation of (*E*)-alkenyl and aryl halides into sulphides using nickel(0) triethyl phosphite complex.

Zhang and their group have developed Ni-NHC catalysts, showed good to excellent activities

toward various aryl halides in C−S coupling reactions (Scheme VIII.2). The new catalysts were inexpensive, easy to synthesize, and environmentally friendly. It was also found that the electronic and steric characteristics of NHC ligand greatly affected the catalytic activities.[11]

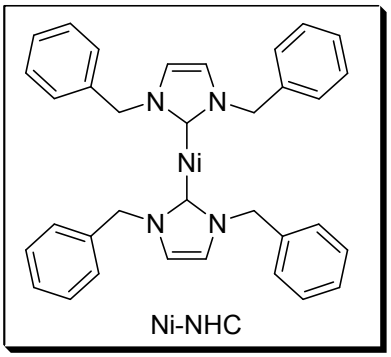

Ni-NHC

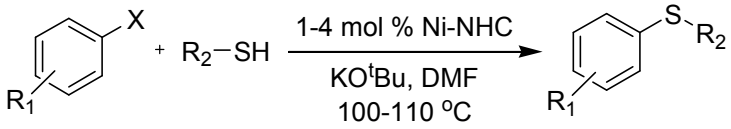

X = I, Br, Cl
R_1 = H, 4-OMe, 4-Me, 2-Me, 4-NMe_2, 4-F, 3-CF_3
R2 = C_6H_5

Scheme VIII.2. Ni-NHC catalyze arylation of thiol.

Cao and their group have developed a convenient and efficient method for preparing aryl sulfides by the reaction of aryl bromides with thiols catalyzed by PEG400, nickel bromide, and zinc without solvent (Scheme VIII.3). However, zinc was added as the reductive reagent, converted Ni(II) to Ni(0) which actually catalyzed the ultimate reaction. Both aromatic and aliphatic thiols are undergo smooth reaction and produces corresponding thioethers.[12]

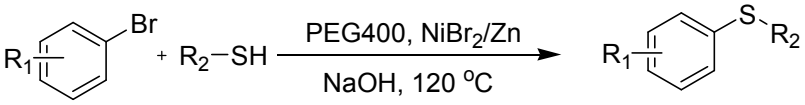

R_1 = 4-Me, 4-OMe, 2-OMe, 2-Me, 4-Br
R_2 = Aryl, Alkyl

Scheme VIII.3. Preparation of aryl sulphide using nickel bromide and zinc catalyst.

Punniyamurthy et al. have described a simple and efficient procedure for the C−S cross–coupling of aromatic and benzyl thiols with aryl iodides using $NiCl_2 \cdot 6H_2O$ in TBAB under air (Scheme VIII.4). It is ligand-free and the NiL_n/TBAB can be recovered and recycled without the loss of activity.[13]

Guan et al. have developed an efficient nickel pincer system for the catalytic cross–coupling of aryl iodides and thiols in the presence of KOH (Scheme VIII.5). The cross–coupling reactions are more likely to be catalyzed by secondary phosphine oxide ligated Ni(0) species, which can be available from catalyst degradation. During catalysis the nickel pincer

complexes are converted to less reactive catalytic mixtures, preventing the catalysts from being reused.[14]

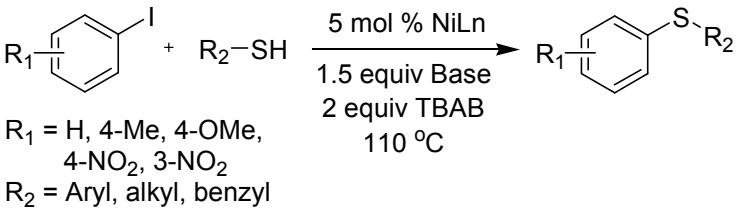

Scheme VIII.4. C−S cross–coupling using $NiCl_2.6H_2O$ in TBAB under ligand-free condition.

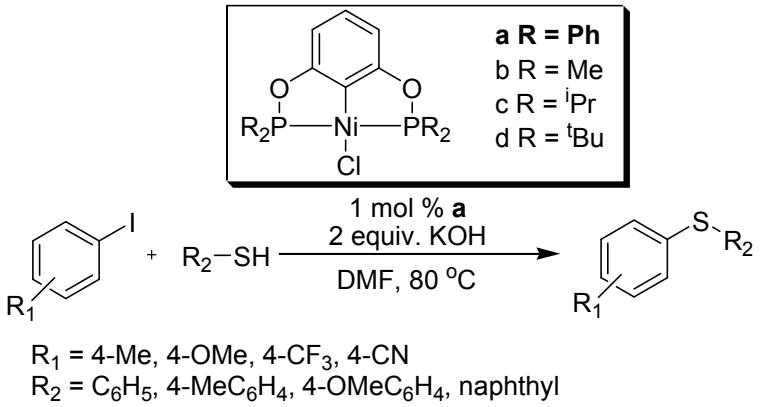

Scheme VIII.5. Reaction of aryl iodide with thiophenol using nickel pincer complex.

Cao et al. have demonstrated a simple and efficient protocol for the C−S coupling reaction of aromatic and aliphatic thiols with aryl halides (iodides, bromides and chlorides) using anhydrous $Ni(OAc)_2$ with NHC under argon (Scheme VIII.6). This catalytic system showed good activities toward various aryl halides in C−S coupling reactions.[15]

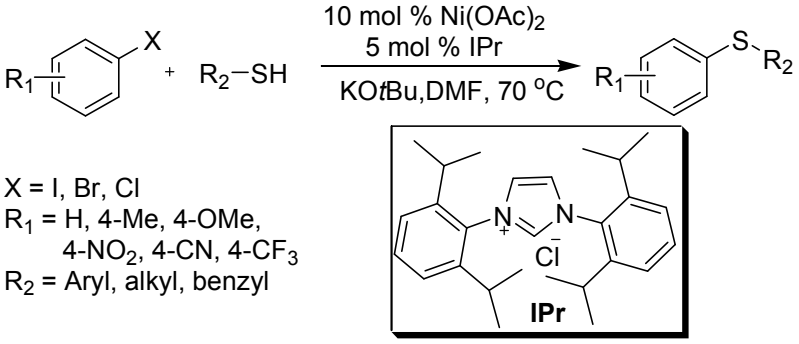

Scheme VIII.6. Reaction of aryl halide with thiol using $Ni(OAc)_2$ with NHC.

$NiO–ZrO_2$ nanocrystal is a heterogeneous solid supported Ni catalyst that has been applied for C–S cross–coupling reaction. This methodology was limited to certain substrate with poor yield.[16]

In general, bare Ni NPs are very unstable and readily oxidized in air. Surprisingly there are very few reports on solid supported Ni-NPs as potential catalyst in organic cros–coupling re-

actions.[17] Since the RGO surface contains many free electrons,[18] the unstable bare Ni NPs get stabilized when embedded in the RGO sheets and form a stable composite.[19] This composite material reduce Cr(VI) to Cr(III) in presence of formic acid at room temperature. Recently, we have utilized this material in organic catalysis and represents Ni/RGO as heterogeneous reusable catalyst for Kumada–Corriu cross–coupling reaction.[20] Herein, we use this heterogeneous composite material as a potential recyclable catalyst for C−S cross–coupling reaction under ligand-free condition with high yield

VIII.3. Present work: Result and Discussion

VIII.3.1. Ni/RGO catalyst in C−S cross–coupling reaction

Initially we have synthesized Ni/RGO having three different compositions such as Ni/RGO-20 (20 wt% Ni), Ni/RGO-40 (40 wt% Ni) and Ni/RGO-60 (60 wt% Ni) following the standard method.[19,20] These materials were well characterized by XRD. The crystallite size of Ni in the three Ni/RGO samples was calculated using the X-ray line broadening method based on (111) and (200) peaks.[20] Following this method we found the average crystallite size of Ni as 10, 12 and 17 nm in Ni/RGO-20, Ni/RGO-40 and Ni/RGO-60 samples, respectively.

In our preliminary studies Ni/RGO-40 was applied in the cross–coupling of 3-iodoanisole and thiophenol using K_2CO_3 as base at 100 ^{o}C, under nitrogen. In this process various parameters such as temperature, base, solvent were varied and corresponding results were presented in Table VIII.1.

Solvent optimization was started with water (entry 1) followed by toluene (entry 2) and isolating diaryl sulphide only 6-8% after 10h while in DMSO it raises up to 86% within 3h (entry 3). Further enhancement was achieved when DMSO was replaced by DMF and isolating 92% of diaryl sulphide (entry 4). However, drop in catalyst loading or temperature, suppresses the overall process and yield also goes down (entries 5, 6). Without base we got only 74% product and using KOH we have 83% of diaryl sulphide (entries 7, 8). At last we setup another reaction similar to that of entry 4 but excluding the nitrogen atmosphere (entry 9). This gives only 61% of thioether along with 15% of diphenyl disulfide. Therefore entry 4, would be the ultimate optimized condition.

After optimizing the reaction conditions, some control experiments were performed with three different composites i.e. Ni/RGO-20, Ni/RGO-40 and Ni/RGO-60. Table VIII.2 show the entire result. The NPs size of first two composites was lies in between 10−11 and they showed nearly same activities and produce the corresponding thioether in 91−92% yield

Table VIII.1. Optimization of CS cross–coupling reaction conditions using Ni/RGO-40.[a]

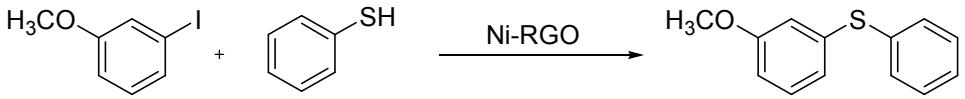

Entry	Catalyst Ni content (mol%)	Solvent	Base	Temperature (^oC)	Time (h)	Yield (%)[b]
1	15	Water	K_2CO_3	100	10	8
2	15	Toluene	K_2CO_3	100	10	6
3	15	DMSO	K_2CO_3	100	3	86
4	**15**	**DMF**	**K_2CO_3**	**100**	**3**	**92**
5	10	DMF	K_2CO_3	100	3	81
6	15	DMF	K_2CO_3	80	10	61
7	15	DMF	Nil	100	10	74
8	15	DMF	KOH	100	3	83
9[c]	15	DMF	K_2CO_3	100	3	63

[a]3-Iodoanisole (1 mmol), thiophenol (1.2 mmol), K_2CO_3 (1.2 mmol) and solvent (3 mL) heated at 100 ^oC under N_2. [b] Isolated yield. [c] Reaction was performed without nitrogen, 15 % diphenyl disulfide was isolated.

(entries 1 and 2). Whereas a drop of catalytic activity was observed with Ni/RGO-60 (entry 3), may be due to larger size of Ni NPs (17 nm) with lower active surfaces. On the other hand bare Ni NPs of size around 10 nm yielded only 79% of corresponding cross–couple product (entry 4), this may be due to agglomeration of NPs or may be oxidation of Ni NPs.

Table VIII.2. Effect of particle size on catalysis.[a]

Entry	Catalyst	Ni content (mol%)	Temperature (^oC)	Time (h)	Yield[b] (%)
1	Ni/RGO-20	15	100	3	91
2	Ni/RGO-40	15	100	3	92
3	Ni/RGO-60	15	100	3	84
4	Ni NPs	15	100	3	79

[a] 3-Iodoanisole (1 mmol), thiophenol (1.2 mmol), K_2CO_3 (1.2 mmol), Ni-RGO (15 mol%) and DMF (3 mL) heated at 100 ^oC under N_2. [b] Isolated yield.

To borden the scope of catalysis, a range of aryl halides/thiols combinations were tested and results are summarised in Table VIII.3. In general it was observed that activated iodoarenes with methoxy and methyl group underwent smooth reaction with different thiols to produces corresponding thioether in excellent yield (entries 1−6) within few hour. But thioethers obtained from iodoarenes containing electron withdrawing group (nitro and acetyl group) in relatively smaller amount (entries 7−9). On the other hand, reactions of iodobromoarenes or

iodochloroarenes with thiols produce only iodo coupled products (entries 10 and 11). Since bromoarenes remains unchanged under this condition but when we added an equivalent amount of another reducing metal like Zn in addition to Ni/RGO-40, cross–coupling was happened and obtaining corresponding thioethers in relatively good amount (entries 12, 13).[12] 1,2-diiodobenzene and 1,3-diiodobenzene react smoothly with *p*-tolylthiol affords the bis-coupled product exclusively (entries 14 and 15). Since the reactivity of aliphatic thiols are somewhat low compare to that of aromatic thiol.[13] Here, also moderate amount of thioethers were obtained when *n*-pentanethiol and *n*-heptanethiol reacts with corresponding aryl iodides (entries 16,17).

Table VIII.3. Ni/RGO-40 catalyzed C−S cross coupling between aryl halide and thiol.[a]

Entry	Aryl halide	Thiol	Time (h)	Product	Yield[b] (%)
1	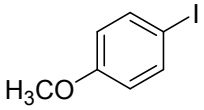	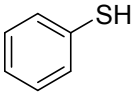	2	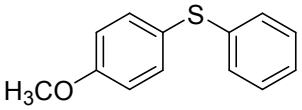	93
2	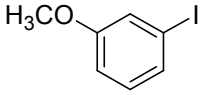	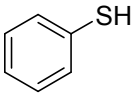	3	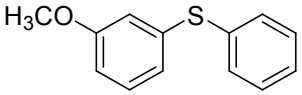	92
3	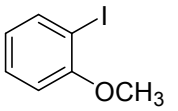	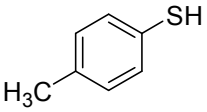	5	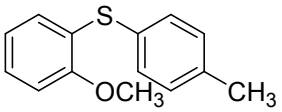	90
4	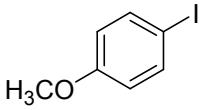	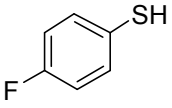	4	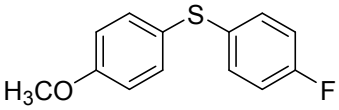	91
5	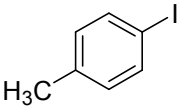	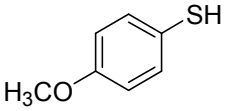	3	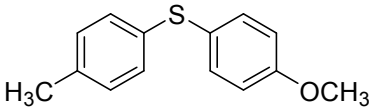	93
6	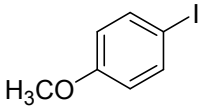	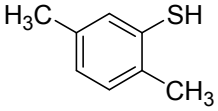	4	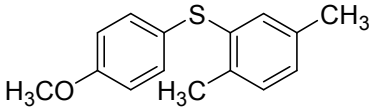	90
7	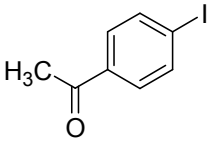	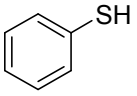	8	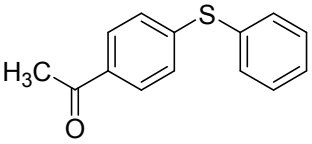	85
8	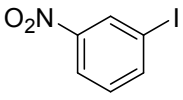	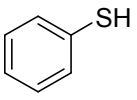	8	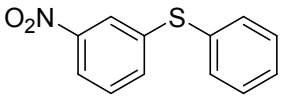	86

9	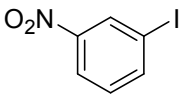	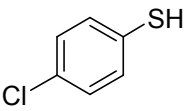	8	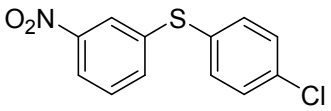	88
10	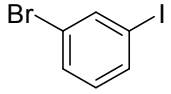	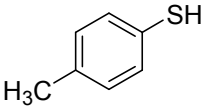	6	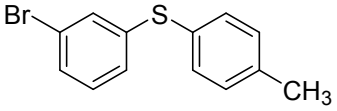	86
11	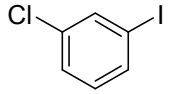	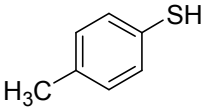	6	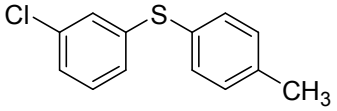	85
12[c]	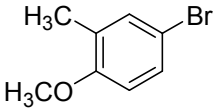	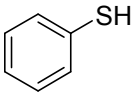	10	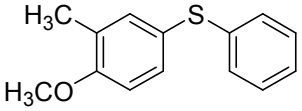	81
13[c]	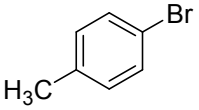	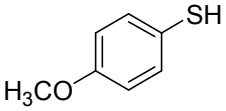	10	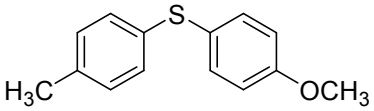	87
14[d]	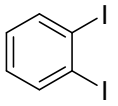	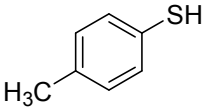	8	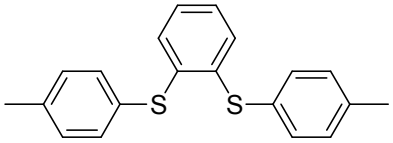	87
15[d]	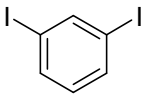	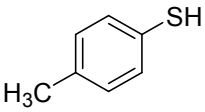	8	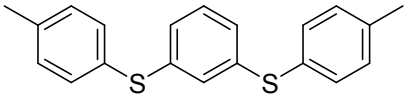	84
16	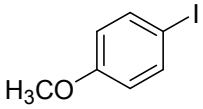	n-C_5H_{11}−SH	10	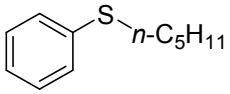	79
17	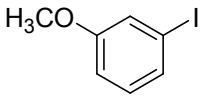	n-C_7H_{15}−SH	10	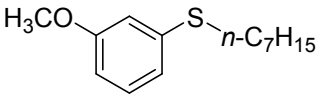	72

[a] ArX (1 mmol), thiol (1.2 mmol), K_2CO_3 (1.2 mmol), Ni/RGO-40 (40 wt%, 22 mg) and DMF (3 mL) heated at 100 ^oC under nitrogen. [b] Isolated yield. [c] Equivalent amount of Zn dust (1 mmol) was added. [d] ArX_2, (1 mmol), thiol (2.4 mmol), K_2CO_3 (4.4 mmol), Ni/RGO-40 (40 wt%, 22 mg) and DMF (3 mL) heated at 100 ^oC under nitrogen.

Hot Filtration test

Leaching of metallic NPs from RGO support during the reaction was tested following the literature procedure.[21] The reaction mixture of the C−S cross–coupling between 4–iodoanisole and thiophenol is filtered off to separate out the solid catalysts after 30 min in hot condition, and the filtrate was analyzed by HPLC (~54% conversion). Further continuing the reaction by heating the liquid phase at 100 ^oC for another 5h in the absence of any added catalyst (Ni/RGO-40) did not afford any appreciable conversion (HPLC analysis). These

observations signify that Ni NPs might not be leached out from the heterogeneous support during initial course of the reaction (Figure VIII.1).

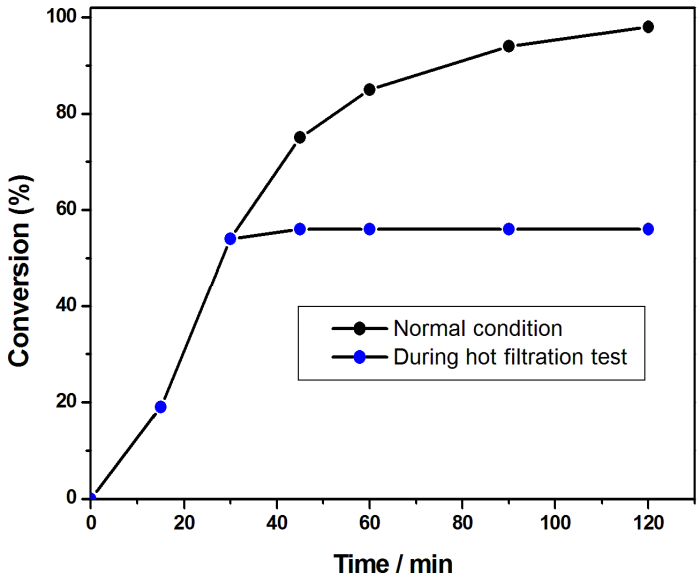

Figure VIII.1. Comparison of normal time profile with that of hot filtration test. Conversions (±2%) at different time intervals for each plot were measured by HPLC.

VIII.3.2. Recovery and reusability of the catalyst

We also checked the reusability of the Ni/RGO-40. After completion of reaction ethyl acetate was added into the reaction vessel, stirred for a few min and allowed to stand for 15 min. The supernatant liquid was carefully transferred into another vessel and this process was repeated three times more. Similarly remaining catalyst was properly washed with water (3 mL/3 times) followed by acetone (3 mL/3 times) and dried under vacuume to obtain the free-flowing black powder. This material was used for next catalytic cycle. The catalyst can be reused at least six times for C−S cross–coupling reaction separately without decrease in catalytic activity. The results are summarised in Figure VIII.2.

VIII.3.3. Characterization of recovered catalyst

The recovered catalyst was analyzed by Raman spectroscopy. It was observed that the catalyst Ni/RGO-40 shows characteristic D (A_{1g} vibrations of the six-membered sp^2 carbon rings) and G (first-order scattering of the E_{2g} mode of sp^2 domains) bands at 1344 and 1580 cm^{-1} in Raman spectra respectively (Figure VIII.3). Due to significant electronic interaction between RGO and Ni the D and G band has been red shifted compared to bare RGO.[19] The Raman spectrum of recovered Ni/RGO-40 after sixth cycles (Figure VIII.3) did not show any peak related to the oxidized Ni (NiO) and the intensity ratio of D over G band was found 1.03 which is similar with the intensity ratio of catalyst before using in C–S coupling. To reconfir-

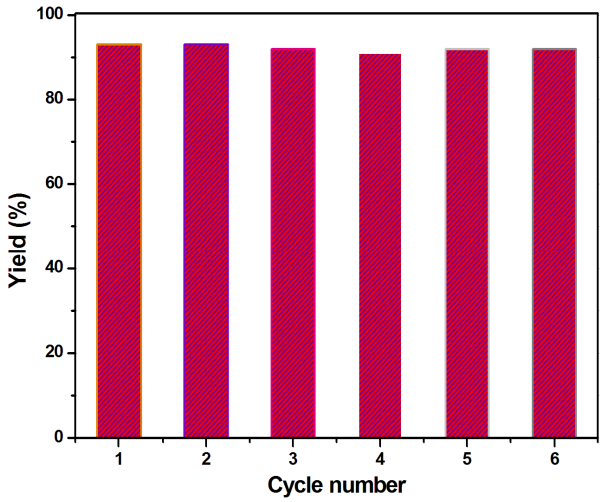

Figure VIII.2. Recycling experiment of Ni-RGO catalyst in C−S cross–coupling reaction.[a]

m the oxidation state of Ni, XRD of Ni/RGO-40 recovered after sixth cycle was performed. The XRD (Figure VIII.4) clearly shows the peak of Ni(111) and Ni(200). Therefore it can be concluded that the characteristics of the Ni/RGO-40 in the recovered catalysts remained similar after 6th cycles.

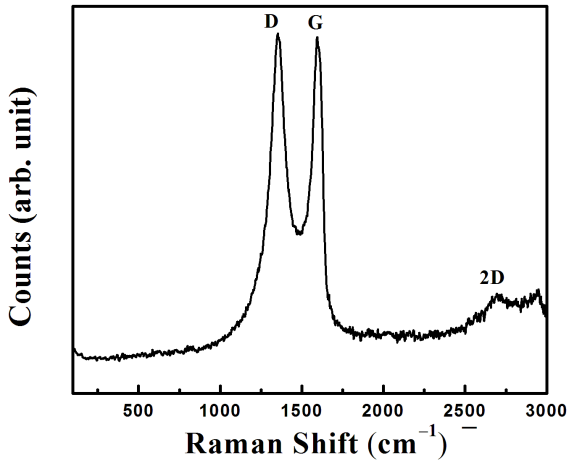

Figure VIII.3. Raman spectrum of Ni/RGO-40 recovered after sixth cycle of C−S coupling.

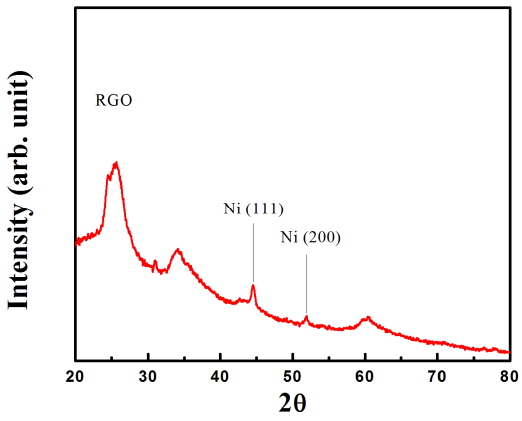

Figure VIII.4. XRD of Ni/RGO-40 recovered after sixth cycle of C−S coupling. The peaks other than Ni and RGO are due to presence of potassium carbonate as an impurity originated from reaction mixture.

VIII.4. Conclusion

An excellent catalytic activity of Ni/RGO-40 in C−S cross–coupling reaction has been established. Several aryl iodides are efficiently react with thiols to give the desired products in high yields. Aryl bromides have been reacting with thiols in presence of Zn. The Ni/RGO-40 catalyst can be reused for six times and no leaching was observed in a hot filtration test. The recovered Ni/RGO-40 was characterized by X-ray diffraction (XRD) and Raman spectroscopy and found to be unaffected.

VIII.5. Experimental section

VIII.5.1. General information

Chemicals were used as received. ^{1}H and ^{13}C NMR spectra were taken in $CDCl_3$ using Bruker Avance AV-300 spectrometer operating at 300 MHz and 75 MHz respectively. Chemical shifts are reported relative to tetramethylsilane served as internal standard (δ 0 ppm). ^{13}C NMR spectra were recorded with complete proton decoupling and chemical shifts are reported in ppm with the solvent resonance as the internal standard ($CDCl_3$: δ 77.00 ppm). X-ray diffraction (XRD) and Raman studies of the powder samples were performed with Rigaku SmartLab X-ray diffractometer operating at 9 kW (200 mA; 45 kV) using Cu-Ka radiation and Renishaw In Via micro Raman spectrometer, respectively.

VIII.5.2. General procedure for C−S cross−coupling using Ni/RGO-40

Aryl halide (1 mmol), thiol (1.2 mmol), potassium carbonate (1.2 mmol), Ni−RGO catalyst (22 mg, Ni content (8.8 mg, 0.15 mmol, 15 mol %)) and DMF (3 mL) were taken in a 15 mL sealed tube and heated the reaction mixture at 100 ^{o}C under nitrogen atmosphere with gentle magnetic starring for several hours. The progress of the reaction was monitored by TLC. After completion of reaction the mixture was allowed to cool at room temperature and diluted with ethyl acetate (3 mL), stirred gently and then allowed to stand for 15 min. The supernatant liquid was carefully collected in another flask and this process was repeated three times more. The organic part was washed with water, dried over anhydrous Na_2SO_4, concentrated and the residue was purified by column chromatography over silica gel, elution with light petroleum. All products were characterized by spectroscopic data (^{1}H, ^{13}C NMR) and also compared with reported melting point (for known solid compounds).

VIII.5.3. Physical properties and spectral data of compounds

Table VIII.3, entry 1

(4–Methoxyphenyl)(phenyl)sulfane[22]

Colourless liquid

^{1}H NMR ($CDCl_3$, 300 MHz): δ/ppm 3.81 (s, 3H, OCH_3), 6.89 (dd, J = 2.1 and 6.9 Hz, 2H, ArH), 7.13–7.25 (m, 5H, ArH), 7.41 (dd, J = 2.1, 6.6 Hz, 2H, ArH); ^{13}C NMR ($CDCl_3$, 75 MHz): δ/ppm 55.3, 114.9, 124.1, 125.7, 128.1, 128.9, 135.3, 138.6, 159.7.

Table VIII.3, entry 2

(3-Methoxyphenyl)(phenyl)sulfane[23]

Colourless liquid

^{1}H NMR ($CDCl_3$, 300 MHz): δ/ppm 3.71 (s, 3H, ArH), 6.75 (ddd, *J* = 0.9, 2.7 and 8.4 Hz), 6.85-6.91 (m, 2H, ArH), 7.15-7.37 (m, 6H, ArH); ^{13}C NMR ($CDCl_3$, 75 MHz): δ/ppm 55.1, 112.7, 115.8, 122.9, 127.2, 129.1, 129.9, 131.3, 135.2, 137.1, 160.0.

Table VIII.3, entry 3

(2–Methoxyphenyl)(*p*–tolyl)sulfane[22]

Colourless liquid

^{1}H NMR ($CDCl_3$, 300 MHz): δ/ppm 2.35 (s, 3H, CH_3), 3.88 (s, 3H, OCH_3), 6.80–6.88 (m, 2H, ArH), 6.94 (dd, *J* = 1.5 and 7.8 Hz, 1H ArH), 7.13–7.20 (m, 3H, ArH), 7.31 (d, *J* = 8.1 Hz, 2H, ArH); ^{13}C NMR ($CDCl_3$, 75 MHz): δ/ppm 21.1, 55.8, 110.6, 121.2, 125.7, 127.4, 129.7, 129.8, 130.1, 132.9, 137.7, 156.5.

Table VIII.3, entry 4

(4-Fluorophenyl)(4-methoxyphenyl)sulfane[24]

Colourless liquid

^{1}H NMR ($CDCl_3$, 300 MHz): δ/ppm 3.83 (s, 3H, ArH), 6.89-7.01 (m, 4H, ArH), 7.21-7.26 (m, 2H, ArH), 7.38-7.41 (m, 2H, ArH); ^{13}C NMR ($CDCl_3$, 75 MHz): δ/ppm 55.2, 115.0, 115.8, 116.1, 125.2, 131.0, 131.1, 133.06, 133.1, 134.4, 159.6, 159.9, 163.2.

Table VIII.3, entry 5

(4–Methoxyphenyl)(*p*–tolyl)sulfane[25]

Colourless liquid

^{1}H NMR ($CDCl_3$, 300 MHz): δ/ppm 2.29 (s, 3H, CH_3), 3.79 (s, 3H, OCH_3), 6.86 (d, *J* = 9.0 Hz, 2H, ArH), 7.05 (d, *J* = 8.1 Hz, 2H, ArH), 7.13 (d, *J* = 8.1 Hz, 2H, ArH), 7.35 (d, *J* = 9.0 Hz, 2H, ArH); ^{13}C NMR ($CDCl_3$, 75 MHz): δ/ppm 20.9, 55.3, 114.8, 125.6, 129.3, 129.7, 134.3, 136.1, 159.4.

Table VIII.3, entry 6

(4–Methoxyphenyl)(2,5–dimethylphenyl)sulfane[26]

Colourless liquid

^{1}H NMR ($CDCl_3$, 300 MHz): δ/ppm 2.20 (s, 3H, CH_3), 2.32 (s, 3H, CH_3), 3.80 (s, 3H, OCH_3), 6.85–6.92 (m, 4H, ArH), 7.06 (d, *J* = 7.5 Hz, 1H, ArH), 7.29 (dd, *J* = 2.1 and 6.6 Hz, 2H, ArH); ^{13}C NMR ($CDCl_3$, 75 MHz): δ/ppm 19.8, 20.9, 55.3, 114.9, 124.9, 127.2, 130.1, 130.2, 133.9, 134.3, 136.0, 136.1, 159.2.

Table VIII.3, entry 7

1-(4-(Phenylthio)phenyl)ethanone[23]

White solid, mp 62-63 (Lit. mp 63-64 ^{o}C)

^{1}H NMR ($CDCl_3$, 300 MHz): δ/ppm 2.52 (s, 3H, CH_3), 7.20 (d, *J* = 8.7 Hz, 2H, ArH), 7.36-7.49 (m, 5H, ArH), 7.78-7.81 (m, 2H, ArH); ^{13}C NMR ($CDCl_3$, 75 MHz): δ/ppm 26.3, 127.3, 128.6, 128.7, 129.5, 131.9, 133.7, 134.3, 144.7, 196.9.

Table VIII.3, entry 8

(3-Nitrophenyl)(phenyl)sulfane[27]

Yellowish liquid

^{1}H NMR ($CDCl_3$, 300 MHz): δ/ppm 7.40-7.53 (m, 7H, ArH), 8.00-8.05 (m, 2H, ArH); ^{13}C NMR ($CDCl_3$, 75 MHz): δ/ppm 120.9, 123.1, 128.9, 129.6, 129.8, 132.1, 133.4, 134.2, 140.6, 148.7.

Table VIII.3, entry 9

(4-Chlorophenyl)(3-nitrophenyl)sulfane[27]

Yellow solid, mp 72-73 (Lit. mp 70-71 ^{o}C)

^{1}H NMR ($CDCl_3$, 300 MHz): δ/ppm 7.36-7.54 (m, 6H, ArH), 8.03-8.06 (m, 2H, ArH); ^{13}C NMR ($CDCl_3$, 75 MHz): δ/ppm 121.3, 123.4, 129.8, 130.0, 130.8, 134.4, 134.5, 135.1, 139.7, 148.6.

Table VIII.3, entry 10

(3–Bromophenyl)(*p*–tolyl)sulfane[28]

Colourless liquid

^{1}H NMR ($CDCl_3$, 300 MHz): δ/ppm 2.36 (s, 3H, CH_3), 7.10–7.18 (m, 4H, ArH), 7.24–7.28 (m, 1H, ArH), 7.32–7.35 (m, 3H, ArH); ^{13}C NMR ($CDCl_3$, 75 MHz): δ/ppm 21.2, 122.9, 127.2, 129.0, 129.4, 130.2, 130.3, 131.1, 133.2, 138.5, 140.3.

Table VIII.3, entry 11

(3–Chlorophenyl)(*p*–tolyl)sulfane

Colourless liquid

^{1}H NMR ($CDCl_3$, 300 MHz): δ/ppm 2.36 (s, 3H, CH_3), 7.07–7.19 (m, 6H, ArH), 7.34 (dd, *J* = 1.8 and 6.3 Hz, 2H, ArH); ^{13}C NMR ($CDCl_3$, 75 MHz): δ/ppm 21.2, 126.1, 126.7, 128.3, 129.4, 129.9, 130.3, 133.3, 134.8, 138.6, 140.0.

Table VIII.3, entry 12

(4-Methoxy-3-methylphenyl)(phenyl)sulfane

Colourless liquid

^{1}H NMR ($CDCl_3$, 300 MHz): δ/ppm 2.22 (s, 3H, ArH), 3.87 (s, 3H, ArH), 6.83 (d, *J* = 8.4 Hz, 1H, ArH), 7.14-7.35 (m, 7H, ArH); ^{13}C NMR ($CDCl_3$, 75 MHz): δ/ppm 16.1, 55.4, 110.8, 123.6, 125.6, 128.1, 128.9, 132.9, 136.3, 138.9, 158.1.

Table VIII.3, entry 14

1,2-Bis(*p*-tolylthio)benzene[29]

White solid, mp 76-77 ^{o}C (Lit mp. 75.5 ^{o}C)

^{1}H NMR ($CDCl_3$, 300 MHz): δ/ppm 2.34 (s, 6H, CH_3), 7.04-7.05 (m, 4H, ArH), 7.13-7.17 (m, 4H, ArH), 7.28-7.31 (m, 4H, ArH); ^{13}C NMR ($CDCl_3$, 75 MHz): δ/ppm 21.1, 127.0, 130.1, 130.5, 132.5, 137.5, 137.8.

Table VIII.3, entry 15

1,3–Bis(*p*–tolylthio)benzene[22]

White solid, mp 84–85 ^{o}C

^{1}H NMR ($CDCl_3$, 300 MHz): δ/ppm 2.34 (s, 6H, CH_3), 6.98–7.01 (m, 2H, ArH), 7.06–7.13 (m, 6H, ArH), 7.27 (dd, *J* = 1.5 and 6.3 Hz, 4H, ArH); ^{13}C NMR ($CDCl_3$, 75 MHz): δ/ppm 21.1, 126.6, 129.0, 129.3, 130.1, 132.9, 138.0, 138.7.

Table VIII.3, entry 16

(4–Methoxyphenyl)(pentyl)sulfane[30]

Colourless liquid

^{1}H NMR ($CDCl_3$, 300 MHz): δ/ppm 0.88 (t, *J* = 7.2 Hz, 3H), 1.26–1.40 (m, 4H, CH_2–CH_2), 1.56–1.61 (m, 2H, CH_2), 2.81 (m, 2H, S–CH_2), 3.79 (s, 3H, OCH_3), 6.83 (dd, *J* = 2.1 and 6.6 Hz, 2H, ArH), 7.33 (dd, *J* = 2.1 and 6.6 Hz, 2H, ArH); ^{13}C NMR ($CDCl_3$, 75 MHz): δ/ppm 13.9, 22.2, 29.0, 30.8, 35.7, 55.3, 114.4, 126.9, 132.9, 158.6.

Table VIII.3, entry 17

Heptyl(3–methoxyphenyl)sulfane

Colourless liquid

^{1}H NMR ($CDCl_3$, 300 MHz): δ/ppm 0.85–0.90 (m, 3H, CH_3 and CH_2), 1.26–1.68 (m, 10H, CH_2), 2.91 (t, *J* = 7.2 Hz, 2H, S–CH_2), 3.79 (s, 3H, OCH_3), 6.696 (ddd, *J* = 0.9, 2.4 and 8.1 Hz, 1H, ArH), 6.85–6.91(m, 2H, ArH), 7.16–7.25 (m, 1H, ArH); ^{13}C NMR ($CDCl_3$, 75 MHz): δ/ppm 14.0, 22.6, 28.8, 29.1, 31.3, 31.7, 33.3, 55.2, 111.2, 114.0, 120.8, 129.6, 138.5, 159.8.

VIII.6. References

References are given in BIBLIOGRAPHY under Chapter VIII (pp. 157−159).

BIBLIOGRAPHY

CHAPTER I

1. (a) D. J. Cole-Hamilton, *Science*, 2003, **299**, 1702; (b) R. T. Baker and W. Tumas, *Science*, 1999, **284**, 1477.
2. (a) C. Coperet, M. Chabanas, R. P. Saint-Arroman and J. M. Basset, *Angew. Chem., Int. Ed.*, 2003, **42**, 156; (b) J. M. Basset and A. Choplin, *J. Mol. Catal.*, 1993, **21**, 95; (c) N. Mizuno and M. Misono, *Chem. Rev.*, 1998, **98**, 199; (d) F. Lefebvre and J. M. Basset, *J. Mol. Catal. A: Chem.*, 1999, **146**, 3.
3. (a) J. M. Thomas, *ChemCatChem*., 2010, **2**, 127; (b) Astruc, D. (2008) Nanoparticles and Catalysis (ed. D. Astruc), Wiley-VCH Verlag GmbH, Weinheim, Germany, p. 1.
4. (a) G. Schmid, M. Baumle, M. Geerkens, I. Heim, C. Osemann and T. Sawitowski, *Chem. Soc. Rev*., 1999, **28**, 179; (b) C.N.R. Rao, A.K. Cheetham, *J. Mater. Chem*., 2001, **11**, 2887; (c) M.-C. Daniel and D. Astruc, *Chem. Rev*., 2004, **104**, 293.
5. (a) J. Schulz, A. Roucoux, H. Patin, *Chem. Rev*., 2002, **102**, 3757; (b) D. Astruc, F. Lu, J.R. Aranzaes, *Angew. Chem. Int. Ed*., 2005, **44**, 7852; (c) F. Raimondi, G.G. Scherer, R. Kotz, A. Wokaun, *Angew. Chem. Int. Ed*., 2005, **44**, 2190; (c) M. Moreno-Manas, R. Pleixats, *Acc. Chem. Res*., 2003, 36, 638.
6. W. Zhang, H. Qi, L. Li, X. Wang, J. Chen, K. Peng and Z. Wang, *Green Chem.*, 2009, **11**, 1194.
7. A. Balanta, C. Godard, C. Claver, *Chem. Soc. Rev.*, 2011, **40**, 4973.
8. (a) J. S. Beck, J. C. VartUli, W. J. Roth, M. E. Leonowicz, C. T. Kresge, K. D. Schmitt, C. T-W. Chu, D. H. Olson, E. W. Sheppard, S. B. McCullen, J. B. Higgins, and J. L. Schlenkert, *J. Am. Chem. Sot*., 1992, **114***,* 10834; (b) C. T. Kresge, M. E. Leonowicz, W. J. Roth, J. C. Vartuli and J. S. Beck, *Nature*, 1992, **359**, 710.
9. K. Komura, Y. Nakano and M. Koketsu *Green Chem.*, 2011, **13**, 828.
10. (a) C. P. Mehnert, D. W. Weaver, and J. Y. Ying, *J. Am. Chem. Soc*., 1998, **120***,* 12289; (b) A. Papp, G. Galbacsb and A. Molnara, Tetrahedron Lett., 2005, 46, 7725.
11. D. Zhao, Jianglin Feng, Qisheng Huo, Nicholas Melosh, Glenn H. Fredrickson, Bradley F. Chmelka,* Galen D. Stucky, Science, 1998, 279, 548; (b) D. Zhao, Q. Huo, J. Feng, B. F. Chmelka and Galen D. Stucky, *J. Am. Chem. Soc.* **1998,** *120,* 6024.
12. L. Li, J.-l. Shi and J. Yan, *Chem. Commun*., 2004, 1990.
13. P. Han, X. Wang, X. Qiu, X. Ji and L. Gao, J. Mol. Catal. A: Chem., 2007, **272**, 136.

14. N. Kim, M. S. Kwon, C. M. Park and J. Park *Tetrahedron Lett*., 2004, **45**, 7057.
15. B. Basu and S. Paul *Appl. Organometal. Chem*., 2013, **27**, 588.
16. L. Tan, X. Wu, D. Chen, H. Liu, X. Menga and F. Tang, *J. Mater. Chem. A*, 2013, **1**, 10382.
17. (a) A. Corma, H. Garcıa and A. Leyva, *Appl. Catal. A: Gen*., 2002, **236**, 179; (b) H. Bulut, L. Artok and S. Yilmaz, *Tetrahedron Lett*., 2003, **44**, 289; (c) L. Artok and H. Bulut, *Tetrahedron Lett*., 2004, **45**, 3881.
18. M. L. Kantam, S. Roy, M. Roy, B. Sreedhar and B. M. Choudary, *Adv. Synth. Catal*., 2005, **347**, 2002.
19. M-R. Kim and S-H Choi, *J. Nano Mat*., doi:10.1155/2009/302919.
20. F. Amorosoa, S. Colussi, A. D. Zottoa, J. Llorca and A. Trovarelli, J. Mol. Catal. A: Chem., 2010, **315**, 197.
21. L.-S. Zhong, J.-S. Hu, Z.-M. Cui, L.-J. Wan and W.-G. Song,*Chem. Mater*.**,** 2007**, 19***,* 4557.
22. A. Monopoli, A. Nacci, V. Calo, F. Ciminale, P. Cotugno, A. Mangone, L. Carla Giannossa, P. Azzone and N. Cioffi, *Molecules*, 2010, **15**, 4511.
23. N. Pal and A. Bhaumik *Dalton Trans*., 2012, **41**, 9161.
24. (a)S. Bhadra, B. Sreedhar, and B. C. Ranua, *Adv. Synth. Catal*., 2009, **351**, 2369; (b) K. Shimizu, N. Imaiida, K. Kon, S. M. A. H. Siddiki and A. Satsuma, *ACS Catal*., 2013, **3***,* 998; (c) K. Shimizu, K. Kon, W. Onodera, H. Yamazaki and J. Kondo, *ACS Catal*., 2013, **3**, 112; (d) I. W. Davies, L. Matty, D. L. Hughes, and P. J. Reider, *J. Am. Chem. Soc*., 2001**, 123***,* 10139.
25. B. Basu and B. Mandal, *Curr. Org. Chem*., 2011, **15**, 3870.
26. (a) T. Ando, S. J. Brown, J. H. Clark, D. G. Cork, T. Hanafusa, J. Ichihara, J. M. Millar and M. S. Robertson, *J. Chem. Soc., Perkin Trans., II*, 1986, 1133; (b) T. Ando, J. H. Clark, D. G. Cork and T. Kimura, *Bull. Chem. Soc. Jpn*., 1986, **59**, 3281; (c) T. Ando, J. H. Clark, D. G. Cork, T. Hanafusa, J. Ichihara and T. Kimura, *Tetrahedron Lett*., 1987, **28**, 1421; (d) J. H. Clark, *Chem. Rev*., 1980, **80**, 429.
27. G. W. Kabalka, L. Wang, R. M. Pagni, C. M. Hair, V. Namboodiri, *Synthesis*, 2003, 217: (b) D. Villemin and F. Caillot, *Tetrahedron Lett.*, 2001, **42**, 639.
28. B. F. Sels, D. E. De Vos, P. A. Jacobs, *Catal. Rev*., 2001, **43**,443.
29. M. L. Kantama*,* S. Roy, M. Roy , B. Sreedhar, B. M. Choudary, R. L. De, *J. of Mol. Catal. A: Chem*., 2007, **273**, 26.

30. V. Polshettiwar, R. Luque, A. Fihri, H. Zhu, M. Bouhrara and J-M. Basset, *Chem. Rev.* 2011, **111**, 3036.
31. A. J. Amali and R. K. Rana, *Green Chem.*, 2009, **11**, 1781.
32. M. L. Toebes, J. A. van Dillen, K. P. de Jong, *J. Mol. Catal. A: Chem.*, 2001, **173**, 75: (b) P. Albers, R. Burmeister, K. Seibold, G. Prescher, S. F. Parker and D. K. Ross, *J. Catal.*, 1999, **181**, 145.
33. G. Marck, A. Villiger and R. Buchecker, *Tetrahedron Lett.*, 1994, **35**, 3277.
34. T. Tagata and M. Nishida, *J. Org. Chem.*, 2003, **68**, 9412.
35. (a) B. H. Lipshutz, J. A. Sclafani and P. A. Blomgren, *Tetrahedron*, 2000, **56**, 2139; (b) S. Tasler and B. H. Lipshutz *J. Org. Chem.*, 2003, **68**, 1190; (c) B. H. Lipshutz, S. Tasler, W. Chrisman, B. Spliethoff, and B. Tesche *J. Org. Chem*., 2003, **68**, 1177; (d) B. H. Lipshutz, P. A. Blomgren, *J. Am. Chem. Soc*., 1999, **121**, 5819; (e) B. H. Lipshutz and Hirishi Ueda, *Angew. Chem.* **2000**, *112*, 4666; *Angew. Chem., Int. Ed*., 2000, **39**, 4492.
36. B. H. Lipshutz, B. A. Frieman and A. E. Tomaso, *Angew. Chem*., 2006, **118**, 1281; *Angew. Chem. Int. Ed*. 2006, **45**, 1259.
37. B. H. Lipshutz, J. B. Unger, and B. R. Taft, *Org. Lett*., 2007, **9**, 1089.
38. B. H. Lipshutz, D. M. Nihan, E. Vinogradova, B. R. Taft and Z. V. Boskovic, *Org. Lett*., 2008, **10**, 4279.
39. (a) V. Georgakilas, D. Gournis, V. Tzitzios, L. Pasquato, D. M. Guldi and M. Prato, *J. Mater. Chem*., 2007, **17**, 2679; (b) M. S. Dresselhaus, G. Dresselhaus and P. Avouris, Eds. Carbon Nanotubes: Synthesis, Structure, Properties and Applications; Springer: Berlin, 2001.
40. X. Chen, Y. Hou, H. Wang, Y. Cao, and J. He *J. Phys. Chem. C*, 2008, **112**, 8172.
41. (a) A. K. Geim and K. S. Novoselov, *Nat. Mater*., 2007, **6**, 183; (b) Y. W. Zhu, S. Murali, W. W. Cai, X. S. Li, J. W. Suk, J. R. Potts and R. S. Ruoff, *Adv. Mater*., 2010, **22**, 3906; (c) M. J. Allen, V. C. Tung and R. B. Kaner, *Chem. Rev*., 2010, **110**, 132; (d) K. S. Novoselov, A. K. Geim, S. V. Morozov, D. Jiang, Y. Zhang, S. V. Dubonos, I. V. Grigorieva and A. A. Firsov, Science, 2004, **306**, 666.
42. D. R. Dreyer, S. Park, C. W. Bielawski and R. S. Ruoff, *Chem. Soc. Rev*., 2010, **39**, 228: (b) T. Szabo, O. Berkesi, P. Forgo, K. Josepovits, Y. Sanakis, D. Petridis and I. Dekany, *Chem. Mater*., 2006, **18**, 2740.
43. D. R. Dreyer and C. W. Bielawski, *Chem. Sci*., 2011, **2**, 1233.

44. S. Navalon, A. Dhakshinamoorthy, M. Alvaro, and H. Garcia, *Chem. Rev*., 2014, **114**, 6179.
45. (a) M. Scheuermann, L. Rumi, P. Steurer, W. Bannwarth and R. Mulhaupt, *J. Am. Chem. Soc*., 2009, **131**, 8262; (b) H. Bai, C. Li and G. Shi, *Adv. Mater*., 2011, **23**, 1089.
46. G. M. Scheuermann, L. Rumi, P. Steurer, W. Bannwarth, and R. Mulhaupt J. Am. Chem. Soc., 2009, **131**, 8262.
47. (a) J. Zhu, G. Zeng, F. Nie, X. Xu, S. Chen, Q. Hana and Xin Wang, *Nanoscale*, 2010, **2**, 988; (b) J. Song, L. Xu, C. Zhou, R. Xing, Q. Dai, D. liu, and H. Song, *ACS Appl. Mater. Interfaces*, 2013, **5**, 12928.
48. A. Kamal, V. Srinivasulu, J. N. S. R. C Murty, N. Shankaraiah, N. Nagesh, T. S. Reddy and A. V. S. Raoa, *Adv. Synth. Catal*., 2013, **355**, 2297.
49. A. Shaabani and M. Mahyari, *J. Mater. Chem. A*, 2013, **1**, 9303.
50. Y-S. Feng, X-Y. Lin, J. Hao and H-J. Xu *Tetrahedron*, 2014, **70**, 5249.
51. L. Yin and J. Liebscher, *Chem. Rev*., 2007, **107**, 133.
52. P. Zheng and W. Zhang, *J. Catal*., 2007, **250**, 324; (b) X. Jiang, G. Wei, X. Zhang, W. Zhang, P. Zhen, F. Wen and L. Shi, *J. Mol. Catal. A: Chem*., 2007, **277**, 102.
53. Y. Li, E. Boone and M. A. El-Sayed, *Langmuir*, 2002, **18**, 4921.
54. T. Teranishi and M. Miyake, *Chem. Mater*., 1998, **10**, 594.
55. G. Liu, M. Hou, J. Song, T. Jiang, H. Fan, Z. Zhang and B. Han, *Green Chem.*, 2010, **12**, 65.
56. J-F. Soulé, H. Miyamura, and S. Kobayashi, *J. Am. Chem. Soc*., 2013, **135**, 10602.
57. (*a*) K. W. Pepper, H. M. Paisley and M. A. Young *J. Chem. Soc*., 1953, 4097; (*b*) R. V. Law, D. C. Sherrington and C. E. Snape, *Macromolecules*, 1996, **29**, 6284.
58. (*a*) S. Pickup, E. D. Blum, W. T. Ford and M. Periyasami, *J. Am. Chem. Soc*., 1986, **108**, 3987; (*b*) T. Balakrishnan and W. T. Ford, *J. Appl. Polym. Sci*., 1982, **27**, 133.
59. R. Quarrell, T. D. Claridge, G. W. Weaver and G. Lowe, *Mol. Divers*., 1996, **4**, 223.
60. C. M. G. Judkins, K. A. Knights, B. F. G. Johnson, Y. R. de Miguel, R. Raja and J. M. Thomas, *Chem. Commun*., 2001, 2624.
61. J. K. Cho, R. Najman, T. W. Dean, O. Ichihara, C. Muller, and M. Bradley, *J. Am. Chem. Soc*. 2006, **128**, 6276.
62. R. Pal, T. Sarkar and S. Khasnobis, *Arkivoc*, 2012, (i) 570.
63. H. W. Gibson and F. C. Bailey, *J. Chem. Soc. Chem. Comm.*, 1977, 815.

64. (a) B. Basu, M. M. H. Bhuiyan, P. Das and I. Hossain, Tetrahedron Lett., 2003, **44**, 8931. (b) B. Basu, P. Das and S. Das, *Mol. Diversity*, 2005, **9**, 259.
65. S. V. Ley, C. Mitchell, D. Pears, C. Ramarao, J. Q. Yu and W. Zhou, *Org.Lett*., 2003, **5**, 4665.
66. (a) B. Basu, S. Das, P. Das and A. K. Nanda, *Tetrahedron Lett*., 2005, **46**, 8591; (b) B. Basu, S. Das, P. Das, B. Mandal, D. Banerjee and F. Almqvist, *Synthesis*, 2009, 1137.

CHAPTER II

1. (a) M. Bodzansky, *Principles of Peptide Synthesis*, Springer, Berlin, 1984, ch. 4; (b) J. C. Bardwell and B. S. Mamathambika, *Annu. Rev. Cell Dev. Biol*., 2008, **24**, 211.
2. (a) C. -S. Jiang, W. E. G. Muller, H. C. Schroder and Y. -W. Guo, *Chem Rev*., 2012, **112**, 2179; (b) S. H. Lee, *Arch. Pharm. Res*., 2009, **32**, 299.
3. (a) P. J. Nieuwenhuizen, J. Reedijk, M. van Duin and W. J. McGill, *Rubb. Chem. Technol*., 1997, **70**, 368; (b) H. L. Fisher, *Ind. Eng. Chem*. **1950**, *42*, 1978.
4. I. Beletskaya and C. Moberg, *Chem. Rev*., 1999, **99**, 3435.
5. J. Lahiri, L. Isaacs, B. A. Grzybowski, J. Carbeck and G. M. Whitesides, *Langmuir*, 1999, **15**, 7186; (b) E. Ostuni, B. A. Grzybowski, M. Mrksich, C. S. Roberts and G. M. Whitesides, *Langmuir*, 2003, **19**, 1861; (b) R. Singhvi, A. Kumar, G. P. Lopez, G. N. Stephanopoulos, D. I. C. Wang, G. M.Whitesides and D. E. Inber, *Science*, 1994, **264**, 696.
6. X. Chen, Y. Zhou, X. Peng and J. Yoon, *Chem. Soc. Rev*., 2010, **39**, 2120.
7. G. K. Jennings and P. E. Laibinis, *J. Am. Chem. Soc.*, 1997**, 119**, 5208.
8. (a) P. Attri, S. Gupta and R. Kumar, *Green Chem. Lett. Rev*., 2012, **5**, 33 and references therein; (b) S. U. Sonavane, M. Chidambaram, J. Almog, Y. Sasson, *Tetrahedron Lett*., 2007, **48**, 6048; (c) M. Kirihara, Y. Asai, S. Ogawa, T. Noguchi, A. Hatano and Y. Hirai, *Synthesis*, 2007, 3286; (d) R. Hunter, M. Caira and N. Stellenboom, *J. Org. Chem*., 2006, **71**, 8268; (e) H. Firouzabad, N. Iranpoor, M. A. Zolfigol, *Synth. Commun*., 1998, **28**, 1179. New York, 1972; Vol. 2, pp 1–95.
9. (a) S. L. S. Leite, V. L. Pardini and V. Hans, *Synth. Commun*., 1990, **20**, 393; (b) Q. T. Do, D. Elothmani, G. L. Guillanton, J. Simonet , *Tetrahedron Lett*., 1997, **38**, 3383.
10. R. G. Guy, in "*The Chemistry of Cyanates and their Thio Derivatives, Part II*", Ed. S. Patai, Wiley, New York, p. 867.

11. C. J. Burns, L. D. Field, J. Morgan, D. D. Ridley and V. Vignevich, *Tetrahedron Lett*., 1990, **40**, 6489.
12. X. Jia, Y. Zhang and X. Zhou, *Tetrahedron Lett*., 1994, **35**, 8833.
13. K. R. Prabhu, A. R. Ramesha and S. Chandrasekaran, *J. Org. Chem*., 1995, **60**, 7142.
14. H. Guo, Z. Zhan and Y. Zhang, *Synth. Commun*., 1997, **27**, 2721.
15. (a) B. Basu, S. Paul and A. K. Nanda, *Green Chem*., 2009, **11**, 1115; (b) B. Basu, S. Paul and A. K. Nanda, *Green Chem*. 2010, **12**, 767; (c) B. Basu, S. Das, P. Das and A. K. Nanda, *Tetrahedron Lett*., 2005, **46**, 8591; (d) B. Basu, S. Das, P. Das, B. Mandal, D. Banerjee and F. Almqvist, *Synthesis*, 2009, 1137.
16. A. R. Kiasat and M. F. Mehrjarde, *Bull. Kor. Chem. Soc*., 2008, **29**, 2346.
17. (a) H. R. Shahbazkia, M. Aminlari and M. *J.* Tavana, *Felin Med. Surg*., 2009, **11**, 305; (b) K. R. Leininger and J. Westley, *J. Biol. Chem*., 1968, **243**, 1892.
18. J. E. Christian, G. L. Jenkins, L. C. Keagle and J. A. Crum, *J. Am. Pharm. Assoc*., 1946, **35**, 328.
19. M. Tajbakhsh, M. M. Lakouraj and M. S. Mahalli, *Monatsh Chem*. 2008, **139**, 1453.
20. W. E. Truce and G. A. Toren, *J. Am. Chem. Soc*., 1954, **76**, 695.
21. U. Firouzabadi, N. Iranpoor and M. Abbasi, *Tetrahedron Lett*., 2010, **51**, 508.
22. W. E. Truce and J. P. Milionis, *J. Am. Chem. Soc*., 1952, **74**, 974.
23. (a) J. Choi and N. M. Yoon, *J. Org. Chem*., 1995, **60**, 3266; (b) I. Atonio and G. Gerolamo, *Gazz. Chim. Ital*., 1960, **90**, 262.
24. R. Hiskey, B. D. Thomas and J. A. Kepler, *J. Org. Chem*., 1964, **29**, 3671.
25. (a) A. G. Zhdanko, A. V. Gulevich and V. G. Nenajdenko, *Tetrahedron*, 2009, **65**, 4692; (b) V. H. Nguyen, H. Nishino, S. Kajikawa and K. Kurosawa, *Tetrahedron*, 1998, **54**, 11445.

CHAPTER III

1. (a) D. J. Procter, *J. Chem. Soc. Perkin Trans* 1., 2000, 835; (b) L. Liu, J. E. Stelmach, S. R. Natarajan, M. –H. Chen, S. B. Singh, C. D. Schwartz, C. E. Fitzgerald, S. J. O'Keefe, D. M. Zaller, D. M. Schmatz, J. B. Doherty, *Bioorg. Med. Chem. Lett*., 2003, **13**, 3979; (c) D. N. Jones, In Comprehensive Organic Chemistry. Barton DH, Ollis DW, Eds. Pergamon: New York, **1979**; Vol. 3.
2. S. W. Kaldor, V. J. Kalish, J. F. Davies, II, B. V. Shetty, J. E. Fritz, K. Appelt, J. A. Burgess, K. M. Campanal, N. Y. Chirgadze, D. K. Clawson, B. A. Dressman, S. D. Hatch, D. A. Khalil, M. B. Kosa, P. P. Lubbehusen, , M. A. Muesing, A. K. Patick, S.

H. Reich, K. S. Su and J. H. Tatlock, *J. Med. Chem*., 1997, **40**, 3979; (b) G. De Martino, M. C. Edler, R. G. La, A. Cosuccia, M. C. Barbera, D. Barrow, R. I. Nicholson, G. Chiosis, A. Brancale, E. Hamel, M. Artico and R. Silvestri, *J. Med. Chem*., 2006**, 49**, 947; (c) G. Liu, J. R. Huth, E. T. Olejniczak, F. Mendoza, S. W. Fesik, T. W. von Geldern, *J. Med. Chem*., 2001, **44**, 1202; (d) S. F. Nielsen, E. Ø. Nielsen, G. M. Olsen, T. Liljefors and D. Peters, *J. Med. Chem*., 2000 **43**, 2217.

3. C. Korth, B. C. H. May, F. E. Cohen and S. B. Prusiner, *Proc Natl. Acad. Sci. U S A.* 2001, **98**, 9836.
4. R. J. S. Hickman, B. J. Christie, R. W. Guy and T. White, *Aust. J. Chem*., 1985, **38**, 899.
5. T. Migita, T. Shimizu, Y. Asami, J. Shiobara, Y. Kato and M. Kosugi, *Bull. Chem. Soc. Jpn*., 1980, **53**, 1385.
6. (a) C. C. Eichman and J. P. Stambuli, *Molecules*, 2011, **16**, 590; (b) P. Guan, C. Cao, Y. Liu, Y. Li, P. He, Q. Chen, G. Liu and Y. Shi, *Tetrahedron Lett*., 2012, **53**, 5987.
7. C. –K. Chen, Y. –W. Chen, C. –H. Lin, H. –P. Lin and C. –F. Lee, *Chem. Commun*., 2010, **46**, 282.
8. Y. C. Wong, T. T. Jayanth and C. H. Cheng, *Org. Lett*., 2006, **8**, 5613.
9. A. Correa, M. Carril and C. Bolm, *Angew. Chem. Int. Ed*., 2008, **47**, 2880.
10. C. S. Lai, H. L. Kao, Y. J. Wang and C. F. Lee, *Tetrahedron Lett*., 2012, **53**, 4365.
11. T. –J. Liu, C. –L. Yi, C. –C. Chan and C. –F. Lee, *Chem Asian J*, 2013, **8**, 1029.
12. V. P. Reddy, A. V. Kumar, K. Swapna and K. P. Rao, *Org. Lett*., 2009, **11**, 1697.
13. (a) Y. J. Chen and H. H. Chen, *Org. Lett*., 2006, **8**, 5609; (b) C. G. Bates, R. K. Gujadhur and D. Venkataraman, *Org. Lett*., 2002, **4**, 2803.
14. (a) T. Sela and A. Vigalok, *Org Lett*., 2014, **16**, 1964; (b) S. Minakata, M. Komatsu, *Chem. Rev*., 2009, **109**, 711; (c) C. J. Li, *Chem. Rev*., 2005, **105**, 3095; (d) Y. Jung and R. A. Marcus, *J. Am. Chem. Soc*., 2007, **129**, 5492; (e) *Organic Reactions in Water*, (Ed.: U. M. Lindström), Blackwell, Oxford, U. K. **2007**; (f) C. –J. Li and L. Chen, *Chem. Soc. Rev*., 2006, **35**, 68.
15. (a) R. S. Schwab, D. Singh, E. E. Alberto, P. Piquini, O. E. D. Rodrigues and A. L. Braga, *Catal. Sci. Technol*., 2011, **1**, 569; (b) S. Jammi, S. Sakthivel, L. Rout, T. Mukherjee, S. Mandal, R. Mitra, P. Saha and T. Punniyamurthy, *J. Org. Chem*., 2009, **74**, 1971; (c) L. Rout, T. K. Sen and T. Punniyamurthy, *Angew. Chem*., 2007, **119**, 5679; *Angew. Chem. Int. Ed*., 2007, **46**, 5583.
16. M. Carril, R. SanMartin, E. Dominguez and I. Tellitu, *Chem. Eur. J*., 2007, **13**, 5100.

17. L. Rout, P. Saha, S. Jammi and T. Punniyamurthy, *Eur. J. Org. Chem*., 2008, 640.
18. W. Y. Wu, J. C. Wang and F. Y Tsai, *Green. Chem*., 2009, **11**, 326.
19. M. -T. Lan, W. –Y. Wu, S. –H. Huang, K. –L. Luo and F. –Y. Tsai, *RSC Adv*., 2011, **1**, 1751.
20. P. Malik and D. Chakraborty, *Appl. Organomet. Chem*., 2012, **26***,* 557.
21. (a) B. Basu, S. Das, P. Das, B. Mandal, D. Banerjee and F. Almqvist, *Synthesis*, 2009, 1137; (b) B. Basu, S. Das, P. Das and A. K. Nanda, *Tetrahedron Lett*., 2005, **46**, 8591.
22. B. Basu, M. M. H. Bhuiyan, P. Das and I. Hossain, *Tetrahedron Lett*., 2003, **44**, 8931.
23. M. A. Dar, S. H. Nam, S. K. Youn and W. B. Kim, *J. Solid State Electrochem.*, 2010, **14**, 1719.
24. K. Bahrami, M. M. Khodaei and A. Nejati, *Green. Chem*., 2010, **12**, 1237.
25. S. Jammi, P. Barua, L. Rout, P. Saha and T. Punniyamurthy, *Tetrahedron Lett*., 2008, **49**, 1484.
26. Structure and Reactivity in Aqueous Solution, ed. C. J. Cramer and D. G. Truhlar ACS, Washington, DC, **1994**.
27. S. Jana, B. Dutta, R. Bera and S. Koner, *Inorg. Chem*., 2008, **47**, 5512.
28. D. Ma, Q. Geng, H. Zhang and Y. Jiang, *Angew. Chem. Int. Ed*., 2010, **49**, 1291.
29. B. Basu, B. Mandal, S. Das and S. Kundu, *Tetrahedron Lett*., 2009, **50**, 5523.
30. F. Y. Kwong and S. L. Buchwald *Org. Lett*., 2002, **4**, 3517.
31. S. Jammi, S. Sakthivel, L. Rout, T. Mukherjee, S. Mandal, Mitra R, P. Saha and T. Punniyamurthy, *J. Org. Chem*., 2009, **74**, 1971.
32. J. R. Campbell, *J. Org. Chem*., 1962, 27, 2207.
33. M. A. Fernandez–Rodriguez, Q. Shen and J. F. Hartwig, *Chem. Eur. J.* **2006**, *12*, 7782.
34. H. L. Kao, C.K. Chen, Y. J. Wang and C.-F. Lee, *Eur. J. Org. C*hem., 2011, 1776.
35. C. M. Suter and H. L. Hansen, *J. Am. Chem. Soc*., 1932, **54**, 4100.

CHAPTER IV

1. (a) W. Yu, M. D. Porosoff and J. G. Chen, *Chem. Rev*., 2012, **112**, 5780; (b) B. L. Cushing, V. L. Kolesnichenko and C. J. O'Connor, *Chem. Rev*., 2004, **104**, 3893; (c) R. Ferrando, J. Jellinek and R. L. Johnston, *Chem. Rev*., 2008, **108**, 845; (4) D. S. Wang and Y. D. Li, *Adv. Mater*., 2011, **23**, 1044; (5) C. T.Campbell, *Annu. Rev. Phys. Chem*., 1990, **41**, 775.
2. M. H. Perez-Temprano, J. A. Casares and P. Espinet, *Chem. – Eur. J*., 2012, **18**, 1864.

3. B. Coq and F. Figueras, *J. Mol. Catal. A: Chem*., 2001, **173**, 117.
4. (a) S.W. Han, Y. Kim and K. J. Kim, *J. Colloid Interface Sci*., 1998, **208**, 272; (b) S. Link, Z. L. Wang and M. A. El-Sayed, *J. Phys. Chem. B*, 1999, **103**, 3529.
5. (a) J. H. Sinfelt. Bimetallic Catalysts, Wiley, New York, 1983; (b) J. H. Sinfelt, *Int. Rev. Phys. Chem*., 1988, 7, 281.
6. J. A. Rodriguez, *Surf. Sci. Rep*., 1996, **24**, 223.
7. I. P. Beletskaya and A. V. Cheprakov, *Chem. Rev*., 2000, **100**, 3009.
8. R. Chinchilla and C. Najera, *Chem. Rev*., 2007, 107, 874.
9. (a) A. L. Casado and P. Espinet, *Organometallics*, 2003, **22**, 1305; (b) G. D. Allred and L. S. Liebeskind, *J. Am. Chem. Soc*., 1996, **118**, 2748.
10. (a) Z.-Y. Shih, C.-W. Wang, G. Xu and H.-T. Chang, *J. Mater. Chem. A*, 2013, 1, 4773; (b) S. V. Myers, A. I. Frenkel and R. M. Crooks, *Chem. Mater*., 2009, 21, 4824; (c) Y. Peng and W.-D. Z. Li, Eur. J. Org. Chem., 2010, 6703; (d) P. Espinet and A. M. Echavarren, *Angew. Chem., Int. Ed*., 2004, **43**, 4704.
11. (a) K. I. Choi and M. A. Vannice, *J. Catal*., 1991, **131**, 36; (b) E. S. Bickford, S. Velu and C. Song, *Catal. Today*, 2005, **99**, 347; (c) B. K. Furlong, J. W. Hightower, T. Y. L. Chan, A. Sarkany and L. Guczi, *Appl. Catal., A*, 1994, **117**, 41.
12. (a) C. Rsini, L. Arrighi, M. C. Herrera Delgado, M. A. Larrubia Vargas, L. J. Alemany, P. Riani, S. Beradinelli, R. Marazza and G. Busca, *Int. J. Hydrogen Energy*, 2006, **31**, 13; (b) C. Rsini, L. Arrighi, L. J. Alemany, R. Marazza and G. Busca, *Catal. Commun*., 2005, **6**, 441; (c) K. Sun, J. Liu, N. K. Nag and N. D. Browning, *J. Phys. Chem. B*, 2002, **106**, 12239; (d) P. R. Subramanian and D. E. J. Laughlin, *J. Phase Equilib*., 1991, **12**, 231; (e) S. Giorgio, C. Chapon and C. R. Henry, *Langmuir*, 1997, **13**, 2279; (f) A. M. Molenbroek, S. Haukka and B. S. Clausen, *J. Phys. Chem. B*, 1998, **102**, 10680; (g) S. Lambert, B. Heinrichs, A. Brasseur, A. Rulmont and J.-P. Pirard, *Appl. Catal. A*, 2004, **270**, 201; (h) G. Mattei, C. Maurizio, C. Sada, P. Mazzoldi, C. de Julian Fernandez, E. Cattaruzza and G. Battaglin, *J. Non-Cryst Solids*, 2004, **345**, 667; (i) V. Sanchez-Escribano, L. Arrighi, P. Riani, R. Marazza and G. Busca, *Langmuir*, 2006, **22**, 9214.
13. Z. Yin, W. Zhou, Y. Gao, D. Ma, C. J. Kiely and X. Bao, *Chem. Eur. J.* 1012, **18**, 4887.
14. Z. Y. Shih, C. –W. Wang, G. Xu and H. –T. Chang, *J. Mater. Chem. A*, 2013, **1**, 4773.
15. J. Müslehiddinoglu, J. Li, S. Tummala and R. Deshpande *Org Process Res Dev*, 2010, **14**, 890.

16. R. K. Ramchandani, B. S. Uphade, M. P. Vinod, R. D. Wakharkar, V. R. Choudhary and A. Sudalai, *Chem. Commun*., 1997, 2071.
17. S.-J. Kim, S.-D. Oh, S. Lee and S. -H. Choi, *J. Ind. Eng. Chem*., 2008, **14**, 449.
18. F. Heshmatpour, R. Abazari and S. Balalaie, *Tetrahedron*, 2012, **68**, 3001.
19. W. Xu, Y. L. Sun, M. H. Guo, W. Q. Zhang, Z. W. Gao, *Chin. J. Org. Chem*., 2013, **33**, 820.
20. B. Basu, S. Das, P. Das, B. Mandal, D. Banerjee and F. Almqvist, *Synthesis*, 2009, 1137.
21. (a) B. Basu, S. Das, P. Das and A. K. Nanda, *Tetrahedron Lett*., 2005, **46**, 8591; (b) B. Basu, P. Das and S. Das, *Mol. Diversity*, 2005, **9**, 259; (c) B. Basu, Md. M. H. Bhuiyan, P. Das and I. Hossain, *Tetrahedron Lett*., 2003, **44**, 8931.
22. R. D. S. Deutsch, A. Siani, P. T. Fanson, H. Hirata, S. Matsumoto, C. T. Williams and M. D. Amiridis, *J. Phys. Chem. C*, 2007, **111**, 4246.
23. S. Chen, H. Zhang, L. Wu, Y. Zhao, C. Huang, M. Ge and Z. Liu, *J. Mater. Chem*., 2012, **22**, 9117.
24. K. Sonogashira, Y. Tohda and N. Hagihara, *Tetrahedron Lett*., 1975, **16**, 4467.
25. (a) R. Chinchilla and C. Najera, *Chem. Soc. Rev*., 2011, **40**, 5084; (b) R. Chinchilla and C. Najera, *Chem. Rev*., 2007, **107**, 874.
26. (a) K. Sonogashira, *J. Organomet. Chem*., 2002, **653**, 46; (b) P. Siemsen, R. C. Livingstone and F. Diederich, *Angew. Chem., Int. Ed*., 2000, **39**, 2632; (c) E. Merkul, D. Urselmann and T. J. J. Muller, *Eur. J. Org. Chem*., 2011, 238.
27. A. Elangovan, Y.-H. Wang and T.-I. Ho, *Org. Lett*., 2003, **5**, 1841.
28. J. Cheng, Y. Sun, F. Wang, M. Guo, J.-H. Xu, Y. Pan and Z. Zhang, J. Org. Chem., 2004, 69, 5428.
29. P. Foley, R. Dicosimo and G. M. Whitesides, *J. Am. Chem. Soc*., 1980, **102**, 6713.
30. D. R. Anton and R. H. Crabtree, *Organometallics*, 1983, **2**, 855.
31. (a) S. Jana, B. Dutta, R. Bera and S. Koner, Inorg. Chem., 2008, 47, 5512; (b) B. Karimi and D. Enders, Org. Lett., 2006, 8, 1237.
32. (a) J. M. Richardson and C. W. Jones, *Adv. Synth. Catal*., 2006, **348**, 1207; (b) H. Erdogan, O. Metin and S. Ozkar, *Phys. Chem. Chem. Phys*., 2009, **11**, 10519.
33. (a) J. A. Widegren and R. G. Finke, *J. Mol. Catal. A: Chem*., 2003, **198**, 317; (b) O. Metin and S. Ozkar, *J. Mol. Catal. A: Chem*., 2008, **295**, 39.
34. B. Basu and S. Paul, *Appl. Organomet. Chem*., 2013, **27**, 588.
35. P. Li, L. Wangand and H. Li, *Tetrahedron*, 2005, **61**, 8633.

36. U. S. Sorensen and E. P. Villar, *Tetrahedron*, 2005, **61**, 2697.

37. O. Akihiro, T. Hisataka and O. Junzo, *Chem. Asian J.*, 2006, **1**, 430.

CHAPTER V

1. (a) T. Mizoroki, K. hlori, and A. Ozaki, *Bull. Chem. Soc. Jap*., 1971, **44**, 581; (b) R. F. Heck and J. P. Nolley Jr, *J . Org. Chem*., 1972, **37**, 2320; (c) N. Miyaura and A. Suzuki, *J. Chem. Soc. Chem. Comm*., 1979, 866.
2. (a) G. Bringmann, S. Rudenauer, T. Bruhn, L. Benson and R. Brun, *Tetrahedron*, 2008, **64**, 5563; (b) Y. D. Wang, M. Dutia, M. B. Floyd, A. S. Prashad, D. Berger and M. Lin, *Tetrahedron*, 2009, **65**, 57; (c) F. Bellina, S. Cauteruccio, A. Di Fiore, C. Marchetti and R. Rossi, *Tetrahedron*, 2008, **64**, 6060; (d) Y. Fang, R. Karisch and M. Lautens, *J. Org. Chem*., 2007, **72**, 1341; (e) X. Yang, X. Dou and K. Mullen, *Chem.–Asian J*., 2008, **3**, 759; (f) J. Kim and T. M. Swager, *Nature*, 2001, **411**, 1030; (g) J. Hassan, M. Sevignon, C. Gozzi, E. Schulz and M. Lemaire, *Chem. Rev*., 2002, **102**, 1359.
3. (a) H. Bonnemann, W. Brijoux, R. Brinkmann, E. Dinjus, T. Joussen and B. Korall, *Angew. Chem., Int. Ed. Engl*., 1991, **30**, 1312; (b) M. T. Reetz and G. Lohmer, *Chem. Commun*., 1996, 1921.
4. (a) N. Hadei, E. A. B. Kantchev, C. J. O'Brien and M. G. Organ, *Org. Lett*., 2005, **7**, 1991; (b) M. Miura, *Angew. Chem., Int. Ed*., 2004, **43**, 2201; (c) I. P. Beletskaya and A. V. Cheprakov, *Chem. Rev.*, 2000**, 100***,* 3009.
5. (a) R. Narayanan, *Molecules*, 2010, **15**, 2124; (b) L. Yin and J. Liebscher, *Chem. Rev*., 2007**, 107**, 133.
6. (a) M. Tobisu, T. Xu, T. Shimasaki, and N. Chatani, *J. Am. Chem. Soc*., 2011, **133**, 19505; (b) D. Zim, V. R. Lando, J. Dupont and A. L. Monteiro, *Org. Lett*., 2001, **3**, 3049; (c) R. J. Kalbasi and N. Mosaddegh, *Bull. Korean Chem. Soc*. 2011, **32**, 2584; (d) M. B. Thathagar, J. Beckers, and G. Rothenberg, *J. Am. Chem. Soc*., 2002, **124**, 11858; (e) S. Lyer, C. Ramesh and A. Ramani, *Tetrahedron lett*., 1997, **38**, 8533; (b) S. Martınez, M. Moreno-Manas, A. Vallribera, U. Schubert, A. Roigc and E. Molinsc *New J. Chem*., 2006, **30**, 1093; (f) W. Zhang, H. Qi, L. Li, X. Wang, J. Chen, K. Peng and Z. Wang, *Green Chem.*, 2009, **11**, 1194; (g) S. Iyer, *J. Organomet. Chem*., 1995, **490**, C27; (h) S. Iyer and V. V. Thakur, *J. Mol. Catal. A: Chem*., 2000, **157**, 275; (i) S. E. Denmark and C. R. Butler, *Chem. Commun*., 2009, 20.
7. S. Cai, D. Wang, Z. Niu and Y. Li *Chinese Journal of Catalysis*, 2013, **34**, 1964.
8. M. T. Reetz, R. Breinbauer and K. Wanninger, *Tetrahedron Lett*., 1996, **37**, 4499.

9. S-B. Wang, W. Zhu, J. Ke, M. Lin, and Y-W. Zhang, *ACS Catal*., 2014, **4**, 2298; (b) F. Heshmatpour , R. Abazari and S. Balalaie *Tetrahedron*, 2012, **68**, 3001; (c) M-R. Kim and S-H Choi, *J. Nano Mat*., doi:10.1155/2009/302919; (d) R. K. Ramchandani, B. S. Uphade, M. P. Vinod, R. D. Wakharkar, V. R. Choudhary and A. Sudalai, *Chem Commun*., 1997, 2071; (e) B. H. Lipshutz, D. M. Nihan, E. Vinogradova, B. R. Taft and Z. V. Boskovic, *Org. Lett.,*2008, **10**, 4279; (f) O. Metin, S. F. Ho, C. Alp, H. Can, M. N. Mankin, M. S. Gültekin, M. Chi, and S. Sun, *Nano Research*, 2013, **6**, 10; (g) L. Tan, X. Wu, D. Chen, H. Liu, X. Menga and F. Tang, *J. Mater. Chem. A*, 2013, **1**, 10382; (h) Y-S. Feng, X-Y. Lin, J. Hao and H-J. Xu, *Tetrahedron*, 2014, **70**, 5249.
10. D. Sengupta, J. Saha, G. De and B. Basu, *J. Mater. Chem. A*, 2014, **2**, 3986.
11. B. Basu, S. Paul and A. K. Nanda, *Green Chem.*, 2009, **11**, 1115.
12. B. Basu, S. Das, P. Das, B. Mandal, D. Banerjee, F. Almqvist, *Synthesis* 2009, 1137.
13. K. Bhowmik, D. Sengupta, B. Basu and G. De, *RSC Adv*., 2014, **4**, 35442.
14. H. Bonin, D. Delbrayelle, P. Demonchaux and E. Gras, *Chem. Commun*., 2010, **46**, 2677.
15. Y. Zhang, M. Wang, P. Li and L. Wang, *Org. Lett*. 2012, **14**, 2206.
16. T. Fukuyama, M. Arai, H. Matsubara and I. Ryu, *J. Org. Chem*., 2004, **69**, 8105.
17. J. Salabert, R. M. Sebastian, A. Vallribera , J. F. Cívicos and C. Najera, *Tetrahedron*, 2013, **69**, 2655.
18. (a) T. Shimasaki, Y. Konno, M. Tobisu and N. Chatani, *Org. Lett*., 2009, **11**, 4890; (b) H. -J. Xu, Y. -Q. Zhao, and X. –F. Zhou, *J. Org. Chem*. 2011, **76**, 8036. (c) Z. -Y. Peng, F-F. Ma, L-F. Zhu, X-M. Xie and Z. Zhang, *J. Org. Chem*., 2009, **74**, 6855; (d) K. Kikukawa, M. Naritomi, G.-X. He, F. Wada, and T. Matsuda, *J. Org. Chem*., 1985, 50, 299.
19. J. C. Roberts and J. A. Pincock, *J. Org. Chem.* 2004, **69**, 4279.
20. T. Jensen, H. Pedersen, B. Bang-Andersen, R. Madsen and M. Jorgensen, *Angew. Chem. Int. Ed*., 2008, **47**, 888.

CHAPTER VI

1. D. R. Dreyer, and C. W. Bielawski, *Chem. Sci*., 2011, **2**, 1233.
2. T. Szabo, E. Tombacz, E. Illes, I. Dekany, *Carbon*, 2006, **44**, 537.
3. H. P. Boehm, A. Clauss, G. Fischer and U. Hofmann, *Fifth Conference on Carbon*; Pergamon: Oxford, 1962; pp 73-80.

4. (a) D. R. Dreyer, H.-P. Jia and C. W. Bielawski, *Angew. Chem., Int. Ed.* 2010, **49**, 6813; b) M. Mirza-Aghayan, E. Kashef-Azar and R. Boukherroub, *Tetrahedron Lett*., 2012 , **53**, 4962; (c) D. R. Dreyer, H. -P. Jia, A. D. Todd, J. Geng and C. W. Bielawski, *Org. Biomol. Chem.*, 2011, **9**, 7292; (d) H. Huang, J. Huang, Y. -M Liu, H.-Y. He, Y. Cao, K. -N. Fan, *Green Chem*., 2012, **14**, 930; (e) H.-P. Jia, D. R. Dreyer, C. W. Bielawski, *Adv. Synth. Catal*., 2011, **353**, 528.
5. D. R. Dreyer, A. D. Todd and C. W. Bielawski, *Chem. Soc. Rev*., 2014, **43**, 5288.
6. F. Liu, J. Sun, L. Zhu, X. Meng, C. Qi, F.-S. Xiao, *J. Mater. Chem*., 2012, **22**, 5495.
7. B. Garg and Y-C. Ling, *Green Materials*, 2012, **1**, 47.
8. S. M. S. Chauhan and S. Mishra, *Molecules*, 2011, **16**, 7256.
9. S. Verma, H. P. Mungse, N. Kumar, S. Choudhary, S. L. Jain, B. Sain and O. P. Khatri, *Chem. Commun*., 2011, **47**, 12673.
10. A. Dhakshinamoorthy, M. Alvaro, P. Concepcion, V. Fornes and H. Garcia, *Chem. Commun.,* 2012, **48**, 5443.
11. A. Dhakshinamoorthy, M. Alvaro, M. Puche, V. Fornes, and H. Garcia *ChemCatChem*, 2012, **4**, 2026.
12. H. Yu, X. Wang, Y. Zhu, G. Zhuang, X. Zhong and J. -G. Wang, *Chem. Phys. Lett*., 2013, **583**, 146.
13. H. Wang, T. Deng, Y. Wang, X. Cui, Y. Qi, X. Mu, X. Hou and Y. Zhu, *Green Chem*., 2013, **15**, 2379.
14. A. Shaabani, M. Mahyari and F. Hajishaabanha, *Res. Chem. Intermed*., 2014, **40**, 2799.
15. S. Eigler, C. Dotzer, F. Hof, W. Bauer and A. Hirsch, *Chem.– Eur. J*., 2013, **19**, 9490.
16. (a) D. R. Dreyer and C. W. Bielawski, *Adv. Funct. Mater*., 2012, **22**, 3247; (b) D. R. Dreyer, K. A. Jarvis, P. J. Ferreira and C. W. Bielawski, *Polym. Chem*., 2012, **3**, 757; (c) B. Konkena and S. Vasudevan, *J. Phys. Chem. Lett*., 2012, **3**, 867.
17. (a) W. S. Hummers and R. E. Offeman, *J. Am. Chem. Soc.*, 1958, **80**, 1339; (b) R. K. Layek, S. Samanta, D. P. Chatterjee and A. K. Nandi, *Polymer*, 2010, **51**, 5846.
18. Q. Zhuo, Y. Ma, J. Gao, P. Zhang, Y. Xia, Y. Tian, X. Sun, J. Zhong and X. Sun, *Inorg. Chem*., 2013, **52**, 3141.
19. A. Dondoni, *Angew. Chem., Int. Ed*., 2008, **47**, 8995.
20. D. R. Dreyer and C. W. Bielawski, *Adv. Funct. Mater*., 2012, **22**, 3247.

21. (a) R. J. Cremlyn, An Introduction to Organosulfur Chemistry, John Wiley and Sons, Chichester, 1996; (b) K. S. Eccles, C. J. Elcoate, S. E. Lawrence and A. R. Maguire, ARKIVOC, 2010, 216; (c) S. Banerjee, J. Das, R. P. Alvarez and S. Santra, *New J. Chem*., 2010, **34**, 302; (d) R. N. Salvatore, R. A. Smith, A. K. Nischwitz and T. Gavin, *Tetrahedron Lett*., 2005, **46**, 8931; (e) J. R. Cabrero-Antonino, A. Leyva-Perez and A. Corma, *Adv. Synth. Catal*., 2012, **354**, 678.
22. K. J. Miller and M. M. Abu-Omar, *Eur. J. Org. Chem*., 2003, 1294.
23. (a) Y.-C. Wu and J. Zhu*, J. Org. Chem.* 2008, **73**, 9522; (b) R. Varala, S. Nuvula and S. R. Adapa, *Bull. Korean Chem. Soc*., 2006, **27**, 1079; (c) S. K. De, *Adv. Synth. Catal*., 2005, **347**, 673; (d) S. K. De, *Tetrahedron Lett*., 2004, **45**, 1035; (e) S. K. De, *Tetrahedron Lett*., 2004, **45**, 2339; (f) N. S. Srivastava, K. Dasgupta and B. K. Banik, *Tetrahedron Lett*., 2003, **44**, 1191; (g) A. Kamal and G. Chouhan, *Tetrahedron Lett*., 2002, **43**, 1341; (h) S. Muthusamy, S. A. Babu and C. Gunanathan, *Tetrahedron*, 2002, **58**, 7897; (i) E. Mondal, P. R. Sahu, G. Bose and A. T. Khan, *Tetrahedron Lett*., 2002, **43**, 2843; (j) S. Muthusamy, S. A. Babu and C. Gunanathan, *Tetrahedron Lett*., 2001, **42**, 359; (k) H. Firouzabadi, N. Iranpoor and H. Hazarkhani, *J. Org. Chem*., 2001, **66**, 7527; (l) J. S. Yadav, B. V. S. Reddy and S. K. Pandey, *Synlett*, 2001, 238; (m) B. Karimi and H. Seradj, *Synlett*, 2000, 805; (n) H. Firouzabadi, N. Iranpoor and B. Karimi, *Synthesis*, 1999, 58; (o) T. Ravindranathan, S. P. Chavan and S. W. Dantale, *Tetrahedron Lett*., 1995, **36**, 2285; (p) P. K. Mandal and S. C. Roy, *Tetrahedron*, 1995, **51**, 7823; (q) V. G. Saraswathy and S. J. Sankararaman, *J. Org. Chem.*, 1994, **59**, 4665; (r) V. Kumar and S. Dev, *Tetrahedron Lett*., 1983, **24**, 1289; (s) B. Burczyk and Z. Kortylewicz, *Synthesis*, 1982, 831; (t) B. S. Ong, *Tetrahedron Lett*., 1980, *21*, 4225; (u) L. F. Fieser, *J. Am. Chem. Soc*., 1954, **76**, 1945; (v) C. Djerassi and M. Gorman, *J. Am. Chem. Soc*., 1953, **75**, 3704; (x) J. W. Ralls, R. M. Dobson and B. Reigel, *J. Am. Chem. Soc*., 1949, **71**, 3320.
24. (a) M. H. Ali and M. G. Gomes, *Synthesis*, 2005, 1326; (b) H. Firouzabadi, N. Iranpoor, A. A. Jafari and M. R. Jafari, *J. Mol. Catal. A: Chem.* 200**6**, **247**, 14; (c) S. Gogoi, J. C. Borah and N. C. Barua, *Synlett*, 2004, 1592; (d) R. Ballini, G. Bosica, R. Maggi, A. Mazzacani, P. Righi and G. Sartori, *Synthesis*, 2001, 1826; (e) T. Aoyama, T. Takido and M. Kodomar, *Synlett*, 2004, 2307; (f) F. Shirini and J. Albadi, *Bull. Korean Chem. Soc*., 2010, **31**, 1119; (g) D. M. Pore, U. V. Desai, R. B. Mane and P. P. Wadgaonkar, *Indian J. Chem.*, 2006, **45B**, 1291; (h) N. Jung, S. D. Ssle,; S. Tjohann and S. Se, *Org. Lett*., 2014, **16**, 1036; (i) B. Shaohu, C. Lu, J. Yongjun and

Y. Jianguo, *Chin. J. Chem*., 2010, **28**, 2119; (j) E. J. Lenardao, E. L. Borges, S. R. Mendes, G. Perin and R. G. Jacob, *Tetrahedron Lett.*, 2008, **49**, 1919.

25. (a) L. K. Papernaya, E. P. Levanova, L. V. Klyba and A. I. Albanov, *Russ. J. Org. Chem*., 2009, **45**, 1036; (b) L. K. Papernaya, E. P. Levanova, E. N. Sukhomazova, A. I. Albanov and E. N. Deryagina, *Russ. J. Org. Chem*., 2005, **41**, 952.
26. S. Eigler and A. Hirsch, *Angew. Che. Int. Ed*., 2014, **53**, 7720.
27. Q. Ding, B. Cao, J. Yuan, X Liu and Y. Peng, *Org. Biomol. Chem.*, 2011, **9**, 748.
28. M. Vafaeezadeh, Z. B. Dizicheh and M. M. Hashemi, *Catal. Commun*., 2013, **41**, 96.
29. D. M. Pore, U. V. Desai, R. B. Mane and P. P. Wadgaonkar, *Indian J. Chem.*, 2006, **45B**, 1291-1295.
30. (a) H. Firouzabadi, N. Iranpoor and H. Hazarkhani, *J. Org. Chem*., 2001, **66**, 7527; (b) M. Prato, U. Quintily, G. Scorrano and A. Sturaro, *Synthesis*, 1982, 679.
31. P. O'Neill and A. F. Hegarty, *J. Org. Chem.*, 1987, **52**, 2114.
32. (a) S. K. De, *Tetrahedron Lett*., 2004, **45**, 2339; (b) S. Muthusamy, S. A. Babu and C. Gunanathan, *Tetrahedron*, 2002, **58**, 7897.

CHAPTER VII

1. (a) P. M. Ajayan and B. I. Yakobson, *Nature*, 2006, **441**, 818; (b) D. A. Dikin, S. Stankovich, E. J. Zimney, R. D. Piner, G. H. B. Dommett, G. Evmenenko, S. T. Nguyen and R. S. Ruoff, *Nature*, 2007, **448**, 457; (c) R. K. Prud'homme, I. A. Aksay, D. H. Adamson, A. A. Abdala, U.S. Patent 092432, 2007; (d) R. Ruoff, *Nat. Nanotechnol.*, 2008, **3**, 10; (e) M. J. McAllister, J. -L. Li, D. H. Adamson, H. C. Schniepp, A. A. Abdala, J. Liu, M. Herrera-Alonso, D. L. Milius, R. Car, R. K. Prud'homme and I. A. Aksay, *Chem. Mater.*, 2007, **19**, 4396.
2. (a) S. Stankovich, D. A. Dikin, G. H. B. Dommett, K. M. Kohlhaas, E. J. Zimney, E. A. Stach, R. D. Piner, S. T. Nguyen and R. S. Ruoff, *Nature*, 2006, **442**, 282; (b) A. K. Geim and K. S. Novoselov, *Nat. Mater*., 2007, **6**, 183; (c) D. Li and R. B. Kaner, *Science*, 2008, **320**, 1170.
3. P. V. Kamat, *J. Phys. Chem. Lett*., 2010, **1**, 520.
4. Y. Gao, D. Ma, C. Wang, J. Guan and X. Bao, *Chem. Commun*., 2011, **47**, 2432.
5. (a) S. Moussa, A. R. Siamaki, B. F. Gupton and M. S. El-Shall, *ACS Catal*., 2012, **2**, 145. (b) H. Goksu, S. F. Ho, O. Metin, K. Korkmaz, A. M. Garcia, M. S. Gultekin and S. Sun, *ACS Catal*., 2014, **4**, 1777.
6. O. C. Compton and S. T. Nguyen, *Small*, 2010, **6**, 711.
7. H. Bai, C. Li and G. Shi, *Adv. Mater*., 2011, **23**, 1089.

8. (a) G. M. Scheuermann, L. Rumi, P. Steurer, W. Bannwarth and R. Mulhaupt, *J. Am. Chem. Soc*., 2009, **131**, 8262; (b) Y. Li, X. Fan, J. Qi, J. Ji, S. Wang, G. Zhang and F. Zhang, *Nano Res*., 2010, **3**, 429; (c) Z. Tang, S. Shen, J. Zhuang and X. Wang, *Angew. Chem., Int. Ed*., 2010, **49**, 4603; (d) A. R. Siamaki, A. E. R. S. Khder, V. Abdelsayed, M. S. El-Shall and B. F. Gupton, *J. Catal*., 2011, **279**, 1; (e) Y. Li, X. B. Fan, J. J. Qi, J. Y. Ji, S. L. Wang, G. L. Zhang and F. B. *Zhang, Mater. Res. Bull*., 2010, **45**, 1413; (f) E. Yoo, T. Okada, T. Akita, M. Kohyama, I. Honma and J. Nakamura, *J. Power Sources*, 2011, **196**, 110; (g) M. Bayati, J. M. Abad, R. J. Nichols and D. J. Schiffrin, *J. Phys. Chem. C*, 2010, **114**, 18439; (h) S. Sharma, A. Ganguly, P. Papakonstantinou, X. Miao, M. Li, J. L. Hutchison, M. Delichatsios and S. Ukleja, *J. Phys. Chem. C*, 2010, 114, 19459; (i) R. Kou, Y. Shao, D. Wang, M. H. Engelhard, J. H. Kwak, J. Wang, V. V. Viswanathan, C. Wang, Y. Lin, Y. Wang, I. A. Aksay and J. Liu, *Electrochem. Commun.*, 2009, **11**, 954.
9. (a) P. Mondal, A. Sinha, N. Salam, A. S. Roy, N. R. Jana and S. M. Islam, *RSC Adv*., 2013, **3**, 5615; (b) S. O. Moussa, L. S. Panchakarla, M. Q. Ho and M. S. El-Shall, *ACS Catal*., 2014, **4**, 535; (c) Z. Ji, X. Shen, G. Zhu, H. Zhou and A. Yuan, *J. Mater. Chem*., 2012, **22**, 3471.
10. (a) X. Chen, H. Ke and G. Zou, *ACS Catal*., 2014, **4**, 379; (b) G. A. Molander and O. A. Argintaru, *Org. Lett*., 2014, **16**, 1904; (c) R. Martin and S. L. Buchwald, *J. Am. Chem. Soc*., 2007, **129**, 3844; (d) S. Lou and G. C. Fu, *J. Am. Chem. Soc*., 2010, **132**, 1264.
11. (a) K. Tamao, K. Sumitani and M. Kumada, *J. Am. Chem. Soc*., 1972, **94**, 4374; (b) R. J. P. Corriu and J. P. Masse, *J. Chem. Soc., Chem. Commun*. 1972, 144a. (c) N. Liu and Z. X. Wang, *J. Org. Chem*., 2011, **76**, 10031.
12. N. Yoshikai, H. Matsuda and E. Nakamura, *J. Am. Chem. Soc*., 2009, **131**, 9590.
13. M. M. Heravi and P. Hajiabbasi, *Monatsh. Chem*., 2012, **143**, 1575.
14. P. Styring , C. Grindon and C. M. Fisher, *Catal. Lett*., 2001*,* **77***,* 219.
15. Nam T. S. Phan, D. H. Brown and P. Styring, *Green Chem*., 2004, **6**, 526.
16. F.-Y.Tsai, B.-N. Lin, M.-J. Chen, C.-Y. Mou and S.-T. Liu, *Tetrahedron*, 2007, **63**, 4304.
17. J. M. Richardson and C. W. Jones, *J. Mol. Catal. A: Chem*., 2009, **297**, 125.
18. S. Tasler and B. H. Lipshutz, *J. Org. Chem*., 2002, **68**, 1190.
19. J.-F. Soule, H. Miyamura, and S. Kobayashi, *J. Am. Chem. Soc*., 2013, **135**, 10602.
20. K. Bhowmik, A. Mukherjee, M. K. Mishra and G. De, *Langmuir*, 2014, **30**, 3209.

21. J. Wang, X. Zhang, Z. Wang, L. Wang and Y. Zhang, *Energy Environ. Sci*., 2012, **5**, 6885.
22. S. H. Wu and D. H. Chen, *J. Colloid Interface Sci*., 2003, **259**, 282.
23. G. Cahiez, C. Chaboche, F. Mahuteau-Betzer and M. Ahr, *Org. Lett*., 2005, **7**, 1943.
24. A. C. Ferrari, J. C. Meyer, V. Scardaci, C. Casiraghi, M. Lazzeri, F. Mauri, S. Piscane, D. Jiang, K. S. Novoselov, S. Roth and A. K. Geim, *Phys. Rev. Lett*., 2006, **97**, 187401.
25. C. Fu, G. Zhao, H. Zhang and S. Li, *Int. J. Electrochem. Sci*., 2014, **9**, 46.
26. E. Alacid and C. Najera, *Org. Lett*., 2008, **10**, 5011.
27. B. Basu, K. Biswas, S. Kundu and S. Ghosh, *Green Chem*., 2010, **12**, 1734.
28. L. Wang and Z. X. Wang, *Org. Lett*., 2007, **9**, 4335.
29. B. Basu, S. Das, P. Das, B. Mandal, D. Banerjee and F. Almqvist, *Synthesis*, 2009, 1137.
30. X. H. Fan and L. M. Yang, *Eur. J. Org. Chem*., 2011, 1467.
31. D. Srimani and A. Sarkar, *Tetrahedron Lett*., 2008, **49**, 6304.

CHAPTER VIII

1. (a) S. Stankovich, D. A. Dikin, G. H. B. Dommett, K. M. Kohlhaas, E. J. Zimney, E. A. Stach, R. D. Piner, S. T. Nguyen and R. S. Ruoff, *Nature*, 2006, **442**, 282; (b) A. A. Balandin, S. Ghosh, W. Z. Bao, I. Calizo, D. Teweldebrhan, F. Miao and C. N. Lau, *Nano Lett*., 2008, **8**, 902; (c) Z. Lee, K. J. Jeon, A. Dato, R. Erni, T. J. Richardson, M. Frenklach and V. Radmilovic, *Nano Lett*., 2009, **9**, 3365; (d) K. P. Loh, Q. L. Bao, G. Eda and M. Chhowalla, *Nat. Chem*., 2010, **2**, 1015; (e) J. Peng, W. Gao, B. K. Gupta, Z. Liu, R. R. Aburto, L. Ge, L. Song, L. B. Alemany, X. Zhan, G. Gao, S. A. Vithayathil, B. A. Kaipparettu, A. A. Marti, T. Hayashi, J. J. Zhu and P. M. Ajayan, *Nano Lett*. 2012, **12**, 844.
2. B. Li, H. Cao, J. Yin, Y. A. Wu and J. H. Warner, *J. Mater. Chem*., 2012, **22**, 1876.
3. H. Bai, C. Li and G. Shi, *Adv. Mater*., 2011, **23**, 1089.
4. (a) P. Zhang, X. Zhang, S. Zhang, X. Lu, Q. Li, Z. Su and G. Wei, *J. Mater. Chem. B*, 2013, **1**, 6525; (b) M. Balcioglu, M. Rana and M. V. Yigit, *J. Mater. Chem. B*, 2013, **1**, 6187; (c) B. Li, H. Cao, J. Shao, M. Qu and J. H. Warner, *J. Mater. Chem*., 2011, **21**, 5069; (d) X. Y. Zhang, H. P. Li, X. L. Cui and Y. H. Lin, *J. Mater. Chem*., 2010, **20**, 2801; (e) S. J. Guo, D. Wen, Y. M. Zhai, S. J. Dong and E. K. Wang, *ACS Nano*, 2010, **4**, 3959.

5. (a) G. M. Scheuermann, L. Rumi, P. Steurer, W. Bannwarth and R. Mulhaupt, *J. Am. Chem. Soc*., 2009, **131**, 8262; (b) A. Kamal, V. Srinivasulu, J. N. S. R. C Murty, N. Shankaraiah, N. Nagesh, T. Srinivasa Reddy, and A. V. Subba Rao, *Adv. Synth. Catal*. 2013, **355**, 2297; (c) N. Zhang, H. Qiu, Y. Liu, W. Wang, Y. Li, X. Wang and Jianping Gao, *J. Mater. Chem*., 2011, **21**, 11080; (d) Y. -S. Feng, X. -Y. Lin, J. Hao and H. -J. Xu *Tetrahedron*, 2014, **70**, 5249.
6. (a) S. W. Kaldor, V. J. Kalish, J. F Davies, II, B. V. Shetty, J. E. Fritz, K. Appelt, J. A. Burgess, K. M. Campanal, N. Y. Chirgadze, D. K. Clawson, B. A. Dressman, S. D. Hatch, D. A. Khalil, M. B. Kosa, P. P. Lubbehusen, M. A. Muesing, A. K. Patick, S. H. Reich, K. S. Su and J. H. Tatlock, *J. Med. Chem*., 1997, **40**, 3979; (b) G. D. Martino, M. C. Edler, G. La Regina, A. Cosuccia, M. C. Barbera, D. Barrow, R. I. Nicholson, G. Chiosis, A. Brancale, E. Hamel, M. Artico and R. Silvestri, *J. Med. Chem*., 2006, 49, 947; (c) G. Liu, J. R. Huth, E. T. Olejniczak, F. Mendoza, S. W. Fesik and T. W. von Geldern, *J. Med. Chem*., 2001, **44**, 1202; (d) S. F. Nielsen, E. Ø. Nielsen, G. M. Olsen, T. Liljefors and D. Peters, *J. Med. Chem*., 2000, **43**, 2217.
7. T. Migita, T. Shimizu, Y. Asami, J. Shiobara, Y. Kato and M. Kosugi, *Bull. Chem. Soc. Jpn*., 1980, **53**, 1385.
8. H. J. Cristau, B. Chabaud, A. Chene and H. Christol, *Synthesis*, 1981, 892.
9. (a) C. C. Eichman and J. P. Stambuli, *Molecules*, 2011, **16**, 590; (b) P. Malik and D. Chakraborty, *Appl. Organomet. Chem*., 2012, **26**, 557; (c) V. P. Reddy, K. Swapna, A. V. Kumar and K. R. Rao, *J. Org. Chem*., 2009, **74**, 3189.
10. Y. Yatsumonji, O. Okada, A. Tsubouchi and T. Takeda, *Tetrahedron*, 2006, **62**, 9981.
11. Y. Zhang, K. C. Ngeow and J. Y. Ying *Org. Lett*., 2007, **9**, 3495.
12. Y.-Q. Cao, Z. Zhang, Y.-X. Guo and G.-Q. Wu, *Synthetic Commun*., 2008, **38**, 1325.
13. S. Jammi, P. Barua, L. Rout, P. Saha and T. Punniyamurthy, *Tetrahedron Lett*., 2008, **49**, 1484.
14. J. Zhang, C. M. Medley, J. A. Krause, and H. Guan, *Organometallics*, 2010, **29**, 6393.
15. P. Guan, C. Cao, Y. Liu, Y. Li, P. He, Q. Chen, G. Liu and Y. Shi, *Tetrahedron Lett*., 2012, **53**, 5987.
16. N. Pal and A. Bhaumik, *Dalton Trans*., 2012, **41**, 9161.
17. (a) B. H. Lipshutz and S. Tasler, *Adv. Synth. Catal*., 2001, **343**, 327; (b) B. H. Lipshutz, B. A. Frieman, C.-T. Lee, A. Lower, D. M. Nihan and B. R. Taft, *Chem. Asian J*., 2006, **1**, 417; (c) J.-F. Soule, H. Miyamura, and S. Kobayashi, *J. Am. Chem. Soc*., 2013, **135**, 10602

18. (a) J. Wang, X. B. Zhang, Z. L. Wang, L. M. Wang and Y. Zhang, *Energy Environ. Sci*., 2012, **5**, 6885; (b) Y. Choi, H. S. Bae, E. Seo, S. Jang, K. H. Park and B. S. Kim, *J. Mater. Chem*., 2011, **21**, 15431.
19. K. Bhowmik, A. Mukherjee, M. K. Mishra and G. De, *Langmuir*, 2014, **30**, 3209.
20. K. Bhowmik, D. Sengupta, B. Basu and G. De, *RSC Adv*., 2014, **4**, 35442.
21. (a) S. Jana, B. Dutta, R. Bera and S. Koner, *Inorg. Chem*., 2008, **47**, 5512; (b) D. Sengupta, J. Saha, G. De and B. Basu, *J. Mater. Chem. A*, 2014, **2**, 3986.
22. B. Basu, B. Mandal, S. Das and S. Kundu, *Tetrahedron Lett*., 2009, **50**, 5523.
23. N. Park, K. Park, M. Jang, and S. Lee, *J. Org. Chem*., 2011, **76**, 4371.
24. J.-H. Cheng, C. Ramesh, H.-L. Kao, Y.-J. Wang, C.-C. Chan, and C.-F. Lee, *J. Org. Chem*., 2012, **77**, 10369.
25. S. Jammi, S. Sakthivel, L. Rout, T. Mukherjee, S. Mandal, Mitra R, P. Saha and T. Punniyamurthy, *J. Org. Chem*., 2009, **74**, 1971.
26. M. A. Fernandez–Rodriguez, Q. Shen and J. F. Hartwig, *Chem. Eur. J.* **2006**, *12*, 7782.
27. W. Y. Wu, J. C. Wang and F. Y Tsai, *Green. Chem*., 2009, **11**, 326.
28. J. R. Campbell, *J. Org. Chem*., 1962, **27**, 2207.
29. J. Nakayama, T. Tajiri and M. Hoshino, *Bull. Chem, Soc. Jpn*., 1986, **59**, 2907.
30. C. M. Suter and H. L. Hansen, *J. Am. Chem. Soc*., 1932, **54**, 4100.

INDEX